ARTICLES PUBLICATS

(Comissió de Doctorat de Juliol del 2003)

Proton Mediated Partial Degradation of *Closo*-dicarbaboranes

C. Viñas,[†] R. Núñez,[†] I. Rojo,[†] F. Teixidor,*[,†] R. Kivekäs,[‡] and R. Sillanpää[§]

Institut de Ciència de Materials de Barcelona, Campus de la UAB, E-08193 Bellaterra, Spain, Department of Chemistry, P.O. Box 55, University of Helsinki, FIN-00014, Finland, and Department of Chemistry, University of Turku, FIN-20014, Finland

Received December 29, 2000

The *o*-carborane, the most intensively studied heteroborane, has an icosahedral structure and possesses tridimensional aromatic character.[1] While typical organic aromatic compounds are characterized by undergoing substitution rather than addition, thus preserving the original backbone structure, this does not take place with *o*-carborane, which upon nucleophilic attack loses B(3) or B(6) to yield the anion $[7,8\text{-}C_2B_9H_{12}]^-$.[2] As a consequence, the original *o*-carborane structure is not retained, which is in marked contrast with conventional aromatic compounds. The $[7,8\text{-}C_2B_9H_{12}]^-$ anion has a C_2B_3 pentagonal face made, which resembles the cyclopentadienyl anion in its coordinating capacity. We have proven earlier that anionic ligands incorporating the fragment $[7,8\text{-}C_2B_9H_{10}]^-$ can be easily produced from the closo precursors upon reaction with a transition metal ion. The necessary requirement for the reaction to take place is that the closo species incorporate coordinating elements, S or P, on the cluster carbon atoms.[3] In addition, this partial degradation was observed only with chelating closo derivatives.

In this paper we demonstrate for the first time that, given the necessary chemical and geometrical arrangements to produce proton chelation, the proton can also induce conversion of the *closo*-C_2B_{10} to the *nido*-C_2B_9 species. For this purpose, we have used an *o*-carborane C-substituted with H^+ scavenger elements, e.g., oxygen. The 1,2-$(PPh_2)_2$-1,2-$C_2B_{10}H_{10}$ closo species[4] (**1**) was adequate as it is a chelating agent that can be oxidized to the corresponding phosphine oxide. Hydrogen peroxide, H_2O_2, recently[5] used to produce *closo*-$[B_{12}(OH)_{12}]^{2-}$, was a suitable oxidizing agent and a source of H^+. Thus it was expected that upon oxidation of the phosphorus atoms, and the possibility to chelate the proton, the closo cluster would progress to the anionic aromatic C_2B_9 cluster liberating one boron atom and overall producing a neutral species. Indeed this is what happened. In a typical experiment 5.56 mL (0.51 mmol) of a 0.1 M solution of H_2O_2 was added to a flask containing 1,2-$(PPh_2)_2$-1,2-$C_2B_{10}H_{10}$ (**1**) (0.1 g, 0.20 mmol) in THF at 0 °C. After stirring for 24 h, H[7,8-$(OPPh_2)_2$-7,8-$C_2B_9H_{10}$], H[**2**], was formed.[6] The reaction is schematically represented in Scheme 1.

Scheme 1. Preparation of H[**2**] by Treatment of 1,2-$(PPh_2)_2$-1,2-$C_2B_{10}H_{10}$ with H_2O_2

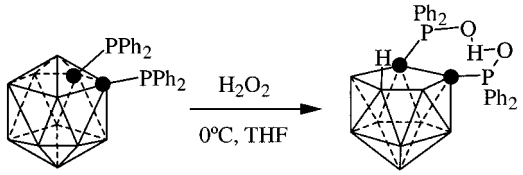

The nido nature of the cluster was clearly demonstrated by the ^{1}H NMR apical proton resonance at δ −2.01, and by the 2:2:1:2:1:1 ^{11}B NMR pattern observed in the range δ −5.6/−33.9 typical for *nido*-C_2B_9 derivatives. The only ^{31}P NMR resonance at δ 47.08 was in agreement with the proposed structure. Furthermore its chemical shift was in agreement with the expected chemical shift for oxidized phosphines.[7]

To ensure that H_2O_2 was the sole agent causing the closo to nido conversion, an alternative sequential process was developed, as schematically indicated in Scheme 2. Oxidation of $[NMe_4][7,8\text{-}(PPh_2)_2\text{-}7,8\text{-}C_2B_9H_{10}]$, $[NMe_4][\mathbf{3}]$,[8] with H_2O_2 was performed in acetone at 0 °C to yield after stirring for 4 h a white solid that corresponds to $[NMe_4][7,8\text{-}(OPPh_2)_2\text{-}7,8\text{-}C_2B_9H_{10}]$, $[NMe_4][\mathbf{2}]$.[9] Extra addition of $[NMe_4]Cl$ increased the yield. Thorough acidification of $[NMe_4][\mathbf{2}]$ in CH_2Cl_2 with HCl gas yielded H[**2**] after previous separation of $[NMe_4]Cl$.[6] Compound $[NMe_4][\mathbf{2}]$ was characterized by ^{1}H and ^{11}B NMR along with chemical analyses.[10] Compounds H[**2**] obtained by both procedures, directly from **1** and from $[NMe_4][\mathbf{3}]$, were identical according to the spectroscopic data.[7]

Notwithstanding these results, the additional H^+ resonance could not be identified in the ^{1}H NMR spectra of H[**2**]. To get a

* E-mail: teixidor@icmab.es.
† Institut de Ciència de Materials de Barcelona.
‡ University of Helsinki.
§ University of Turku.

(1) (a) Grimes, R. N. *Carboranes*; Academic Press: New York, 1970. (b) Grimes, R. N. *Metal Interactions with Boron Clusters*; Plenum: New York, 1982. (c) Olah, G. A.; Prakash, G. K. S.; Williams, R. E.; Field, L. E.; Wade, K. *Hypercarbon Chemistry*; Wiley: New York, 1987. (d) Hawthorne, M. F. *Advaces in Boron Chemistry*; Special Publication No. 201; Royal Society of Chemistry: London, 1997; p 261. (e) Ionov, S. P.; Kuznetsov, N. T. *Russ. J. Coord. Chem.* **2000**, *26*, 325.
(2) (a) Wiesboeck, R. A.; Hawthorne, M. F. *J. Am. Chem. Soc.* **1964**, *86*, 1642. (b) Zakharkin, L. I.; Kalinin, V. N. *Tetrahedron Lett.* **1965**, 407.
(3) (a) Teixidor, F.; Viñas, C.; Abad, M. M.; López, M.; Casabo, J. *Organometallics* **1993**, *12*, 3766. (b) Teixidor, F.; Viñas, C.; Kivekäs, R.; Sillanpää, R.; Casabó, J. *Inorg. Chem.* **1994**, *33*, 2645. (c) Viñas, C.; Abad, M. M.; Teixidor, F.; Sillanpää, R.; Kivekäs, R. *J. Organomet. Chem.* **1998**, *555*, 17.
(4) Alexander, R. P.; Schroder, H. A. *Inorg. Chem.* **1963**, *2*, 1107.
(5) Peymann, T.; Herzog, A.; Knobler, C. B.; Hawthorne, M. F. *Angew. Chem., Int. Ed.* **1999**, *38*, 1062.

(6) H[**2**], method A: To a solution of 1,2-$(PPh_2)_2$-1,2-$C_2B_{10}H_{10}$ (0.1 g, 0.20 mmol) (**1**) in THF at 0 °C was added 5.56 mL (0.51 mmol) of a solution of 0.1 M H_2O_2. The mixture was stirred for 24 h, and a precipitate was formed. The solid was filtered off, washed with water, and dried in vacuo. Compound H[**2**] was obtained (yield: 94%). H[**2**], method B: A solution of $[NMe_4][7,8\text{-}(OPPh_2)_2\text{-}7,8\text{-}C_2B_{10}H_{10}]$, $[NMe_4][\mathbf{2}]$, (1 g, 1.64 mmol) in CH_2Cl_2 (50 mL) was bubbled with a HCl stream for 15 min. A precipitate of $[NMe_4]Cl$ was separated, and the solution was evaporated in vacuo. A white solid was obtained (yield: 97.7%).
(7) Selected spectroscopic and analytical data for H[**2**]: FTIR (KBr, cm^{-1}) ν = 3058, 3012 (C_{ar}−H), 2525 (B−H); ^{1}H{^{11}B} NMR (300.13 MHz, $CDCl_3$, 25 °C, TMS) δ = −2.01 (br s, 1 H, B−H−B), 7.22−7.97 (m, 20 H, C_6H_5); ^{11}B NMR (96.29 MHz, $CDCl_3$, 25 °C, $Et_2O{\cdot}BF_3$) δ = −5.6 (d, 2 B, ^1J(B,H) = 128 Hz), −8.7 (d, 2 B, ^1J(B,H) = 133 Hz), −11.9 (1 B), 16.8 (2 B), −30.2 (d, 1 B, ^1J(B,H) = 123 Hz), −33.9 (d, 1 B, ^1J(B,H) = −147 Hz); ^{31}P{^{1}H} NMR (121.48 MHz, $CDCl_3$, 25 °C, 85% H_3PO_4) δ = 47.08 (s); ^{13}C{^{1}H} NMR (75.47 MHz, $CDCl_3$, 25 °C, TMS) δ = 128.49 (d, ^1J(P,C) = 42 Hz), 132.35 (d, ^1J(P,C) = 21 Hz), 133.20 (d, ^1J(P,C) = 10 Hz), 134.89 (s). $C_{26}H_{31}B_9O_2P_2$: Calcd: C, 58.40; H, 5.84. Found: C, 58.22; H, 5.78.
(8) Teixidor, F.; Viñas, C.; Abad, M. M.; Núñez, R.; Kivekäs R.; Sillanpää, R. *J. Organomet. Chem.* **1995**, *503*, 193.
(9) $[NMe_4][\mathbf{2}]$: To a solution of $[NMe_4][7,8\text{-}(PPh_2)_2\text{-}7,8\text{-}C_2B_{10}H_{10}]$, $[NMe_4][\mathbf{3}]$ (0.5 g, 0.87 mmol) in acetone at 0 °C was added dropwise 12.4 mL (1.24 mmol) of a 0.1 M H_2O_2 solution. The mixture was stirred at room temperature for 4 h, and a white solid was precipitated. The addition of a $[NMe_4]Cl$ aqueous solution increases the precipitation of the solid. The solid was filtered off, washed with water, and dried in vacuo to obtain compound $[NMe_4][\mathbf{2}]$ (yield: 74.1%).

10.1021/ic001477e CCC: $20.00
Published on Web 06/07/2001

Scheme 2. Preparation of H[**2**] Using $[NMe_4][7,8\text{-}(PPh_2)_2\text{-}7,8\text{-}C_2B_9H_{10}]$ as Starting Material

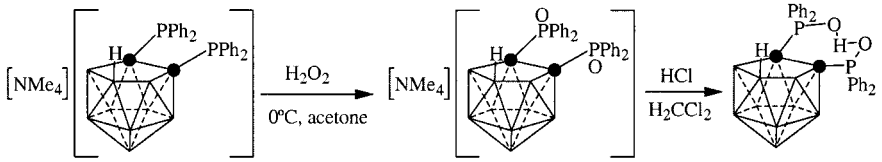

precise structure determination, crystals of H[**2**] were grown. An ethanol solution of this protonated species yielded adequate crystals for X-ray diffraction after standing for 2 months at 4 °C.[11] Figure 1 shows an ORTEP diagram and most relevant distances and angles of H[**2**]. Structure analysis confirmed the expected structure: both phosphorus atoms are oxidized, and the proton between the oxygen atoms balances out the negative charge of the *nido*-carborane cage. The proton lies approximately midway between the oxygen atoms, and the short O(1)···O(2) distance (2.421(4) Å), the O−H distances (1.21(5) Å), and the O−H−O angle (174(4)°) indicate an essentially centrosymmetric linear hydrogen bond. In $[(^iPr_3PO)_2H][I_3]$, which contains a centrosymmetric P−O−H−O−P hydrogen bond, the P−O distance of 1.530(6) Å is comparable with the distances in H[2] but the O···O distance of 2.386 Å is slightly shorter than that in H[**2**].[12]

The only reported structures containing a P−O−H−O−P array are $[(Me_3PO)_2H][AuI_2]$,[13] $[(Ph_3PO)_2H][ICl_4]$,[14] and $[(^iPr)_3PO)_2H][I_3]$[12] and one containing the moiety $PtPPh_2OHOPPh_2Pt$.[15] Surprisingly, none of them is chelating. Thus, H[**2**] is the first fully characterized proton chelated to two P−O moieties. Again, the singularity of the *nido*-$[C_2B_9]^-$ cluster with its intrinsic negative charge has permitted us to report for the first time the chelating P−O−H−O−P motif.

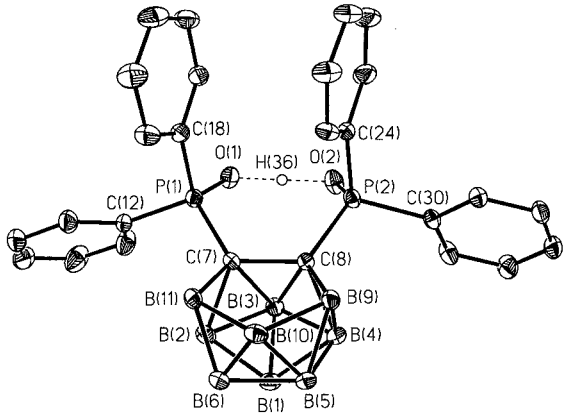

Figure 1. ORTEP drawing of compound H[**2**]. Hydrogen atoms, except H(36), have been omitted. Selected bond distances (Å) and angles (deg): P(1)−O(1) 1.523(3), P(1)−C(7) 1.810(3), P(2)−O(2) 1.534(3), P(2)−C(8) 1.808(3), C(7)−C(8) 1.609(5), O(1)−P(1)−C(7) 112.12(16), O(2)−P(2)−C(8) 112.58(15), C(8)−C(7)−P(1) 122.1(2), C(7)−C(8)−P(2) 121.4(2).

Acknowledgment. This work was supported, in part, by the CICYT (Project MAT98-0921) and European Union Project INCO-COPERNICUS (PL972004). R.K. thanks the Academy of Finland (Project 41519).

Supporting Information Available: Crystallographic data in CIF format. This material is available free of charge via the Internet at http://pubs.acs.org. Additionally, crystallographic data for the structures reported in this paper have been deposited with the Cambridge Data Centre.

IC001477E

(10) Selected spectroscopic and analytical data for $[NMe_4][\mathbf{2}]$: FTIR, (KBr, cm^{-1}) ν = 3019 (C_{ar}−H), 2535 (B−H); $^1H\{^{11}B\}$ NMR (300.13 MHz, ($(CD_3)_2CO$), 25 °C, TMS) δ = −2.01 (br s, 1 H, B−H−B), 3.45 (s, 12 H, CH_3), 7.24−7.92 (m, 20 H, C_6H_5); ^{11}B NMR (96.29 MHz, ($(CD_3)_2CO$), 25 °C, $Et_2O{\cdot}BF_3$) δ = −5.6 (d, 2 B, ^1J(B,H) = 119 Hz), −11.1 (d, 3 B, ^1J(B,H) = 133 Hz), −19.0 (d, 2 B, ^1J(B,H) = 111 Hz), −32.2 (d, 1 B, ^1J(B,H) = 142 Hz), −33.9 (d, 1 B, ^1J(B,H) = 150); $^{31}P\{^1H\}$ NMR (121.48 MHz, ($(CD_3)_2CO$), 25 °C, 85% H_3PO_4) δ = 29.3 (s); $^{13}C\{^1H\}$ NMR (75.47 MHz, ($(CD_3)_2CO$), 25 °C, TMS) δ = 55.1 (s), 126.8 (d, ^1J(P,C) = 37.4 Hz), 129.9 (d, ^1J(P,C) = 26 Hz), 132.4 (d, ^1J(P,C) = 33 Hz), 135.89 (s), 137.2 (d, ^1J(P,C) = 18 Hz), 138.5 (s). $C_{30}H_{42}B_9NO_2P_2$: Calcd: C, 59.27; H, 6.96; N, 2.30. Found: C, 58.95; H, 7.00; N, 2.45.

(11) Crystal structure analysis for H[**2**]: $C_{26}H_{31}B_9O_2P_2$, M = 534.74, triclinic, a = 11.638(3) Å, b = 13.124(3) Å, c = 11.480(3) Å, α = 108.66(2)°, β = 110.25(2)°, γ = 103.25(2)°, V = 1440.1(6) Å^3, T = 294(2) K, space group $P\bar{1}$ (No. 2), Z = 2, λ (Mo Kα)= 0.175 mm^{-1}, 5343 reflections measured, 5069 unique (R_{int} = 0.0293) which were used in all calculations. The final R1(F^2) = 0.0547 (observed data), wR2(F^2) = 0.1110 (observed data). Solution and refinement were by SHELX-97. Non-hydrogen atoms were refined anisotropically. H-atoms were in calculated positions as riding atoms, except H(36), which was refined isotropically with fixed U.

(12) Ruthe, F.; Jones, P. G.; du Mont, W.-W.; Deplano P.; Mercuri, M. L. *Z. Anorg. Allg. Chem.* **2000**, *626*, 1105.

(13) Godfrey, S. M.; Ho, N.; McAuliffe, C. A.; Pritchard, R. G. *Angew. Chem., Int. Ed. Engl.* **1996**, *35*, 2344.

(14) Carmalt, C. J.; Norman, N. C.; Farrugia, L. J. *Polyhedron* **1993**, *12*, 2081.

(15) Liu, L.-K.; Wen, Y.-S.; Lin, I. J. B.; Lai, J. S.; Liu, C. W. *Bull. Inst. Chem. Acad. Sin.* **1990**, *37*, 65.

Chameleonic Capacity of $[3,3'\text{-}Co(1,2\text{-}C_2B_9H_{11})_2]^-$ in Coordination. Generation of the Highly Uncommon S(thioether)−Na Bond

Francesc Teixidor,[†] Josefina Pedrajas,[†] Isabel Rojo,[†,‡] Clara Viñas,*[,†] Raikko Kivekäs,[§] Reijo Sillanpää,[∥] Igor Sivaev,[⊥,#] Vladimir Bregadze,[⊥] and Stefan Sjöberg[#]

Institut de Ciència de Materials de Barcelona (CSIC), Campus de la UAB, E-08193 Bellaterra, Spain, Department of Chemistry, P.O. Box 55, University of Helsinki, FIN-00014, Finland, Department of Chemistry, University of Jyväskylä, FIN-40351, Finland, A. N. Nesmeyanov Institute of Organoelement Compounds, Russian Academy of Sciences, Vavilov Str. 28, 117813 Moscow, Russia, and BMC, Institute of Chemistry, Department of Organic Chemistry, Uppsala University, P.O. Box 599, S-75124 Uppsala, Sweden

Received February 27, 2003

The multiple binding modes of $[3,3'\text{-}Co(1,2\text{-}C_2B_9H_{11})_2]^-$ allow it to adjust to different coordinating or geometric demands. $[3,3'\text{-}Co(1,2\text{-}C_2B_9H_{11})_2]^-$ can behave as a platform on which two types of coordinating moieties exist: the BH's and boron- or carbon-bonded elements with available lone pairs. Until now, no compounds containing Na^+ bonded to thioether ligands were known other than $Na[7,8\text{-}\mu\text{-}\{S(CH_2CH_2O)_3CH_2CH_2S\}\text{-}7,8\text{-}C_2B_9H_{10}]$. The dithioether moiety in the latter compound is preorganized to favor chelation and produces a five-membered ring. This definitely assists in coordination to sodium. To avoid this preorganization and assess the independent strength of the C−S(thioether)−Na bond, the anionic nonpreorganized dithioether $[1,1'\text{-}\mu\text{-}\{S(CH_2CH_2O)_3CH_2CH_2S\}\text{-}3,3'\text{-}Co(1,2\text{-}C_2B_9H_{10})_2]^-$ ligand was synthesized. The two cluster moieties have sufficient accessible rotamers to allow adequate metal coordination, but they do not preorganize. The synthetic procedure leading to $[1,1'\text{-}\mu\text{-}\{S(CH_2CH_2O)_3CH_2CH_2S\}\text{-}3,3'\text{-}Co(1,2\text{-}C_2B_9H_{10})_2]^-$ implied the formation of idealized meso and racemic forms. These forms behave differently toward Na^+. In the meso form coordination to sodium is achieved via the two sulfur (C−S) and three oxygen elements in the exo cluster chain. In the racemic form coordination is achieved via the three oxygen elements in the exo cluster chain, with no thioether participation. The remaining Na^+ coordination sites are filled by oxygen atoms from ancillary ligands. These coordination environments were determined by the crystal structures of $Na[1,1'\text{-}\mu\text{-}\{S(CH_2CH_2O)_3CH_2CH_2S\}\text{-}3,3'\text{-}Co(1,2\text{-}C_2B_9H_{10})_2]\cdot(CH_3)_2CO\cdot CHCl_3\cdot CH_2Cl_2$ (meso form) and $Na[1,1'\text{-}\mu\text{-}\{S(CH_2CH_2O)_3CH_2CH_2S\}\text{-}3,3'\text{-}Co(1,2\text{-}C_2B_9H_{10})_2]\cdot 2(CH_3)_2CO$ (racemic form). Therefore, C−S(thioether)−Na coordination has been demonstrated for the first time with nonpreorganized ligands, although the cluster participation has been found necessary. A situation similar to that obtained with the racemic form of $[1,1'\text{-}\mu\text{-}\{S(CH_2CH_2O)_3CH_2CH_2S\}\text{-}3,3'\text{-}Co(1,2\text{-}C_2B_9H_{10})_2]^-$, having only three coordinating oxygen atoms, is also possible for $[3,3'\text{-}Co(8\text{-}\{O(CH_2CH_2O)_2CH_3\}\text{-}1,2\text{-}C_2B_9H_{10})(1',2'\text{-}C_2B_9H_{11})]^-$. This ligand does not have thioethers, and it was interesting to discover how the $[3,3'\text{-}Co(1,2\text{-}C_2B_9H_{11})_2]^-$ moiety would behave with a low supply of coordination sites in a more flexible $-O-CH_2CH_2-O-CH_2CH_2-O-CH_2CH_3$ arrangement. The structure of $Na[3,3'\text{-}Co(8\text{-}\{O(CH_2CH_2O)_2CH_2CH_3\}\text{-}1,2\text{-}C_2B_9H_{10})(1',2'\text{-}C_2B_9H_{11})]$ shows that the chain contributes three oxygen atoms for coordination to Na^+ and, interestingly, the $[3,3'\text{-}Co(1,2\text{-}C_2B_9H_{11})_2]^-$ moiety provides three extra B−H coordination sites.

Introduction

In 1990 the molecular structure of $Na[7,8\text{-}\mu\text{-}\{S(CH_2CH_2O)_3CH_2CH_2S\}\text{-}7,8\text{-}C_2B_9H_{10}]$ (**1**) was reported[1] featuring the first S(thioether)−Na bond. The macrocyclic ring external to the cluster is pentacoordinated to Na^+ through two sulfur and three oxygen atoms. Surprisingly, and despite the enormous progress in alkali-metal coordination chemistry,[2] compound **1** has remained the unique example of S(thioether)−Na coordination. This may be attributed to the general assumption that thioethers are poor ligands.[3] Monodentate thioether

* To whom correspondence should be addressed. Telefax: Int. Code + 34 93 5805729. E-mail: clara@icmab.es.
[†] Campus de la UAB.
[‡] Enrolled in the Ph.D. program of the UAB.
[§] University of Helsinki.
[∥] University of Jyväskylä.
[⊥] Russian Academy of Sciences.
[#] Uppsala University.

(1) Teixidor, F.; Viñas, C.; Rius, J.; Miravitlles, C.; Casabó, J. *Inorg. Chem.* **1990**, *29*, 149−152.

10.1021/om030135o CCC: $25.00
Publication on Web 07/22/2003

ligands are not efficient metal coordinating agents. At least two thioether moieties performing as a chelating agent are necessary for effective coordination,[4] and even under these circumstances only labile complexes have been produced. However, we have demonstrated that when the sulfur atoms are directly bonded to the anionic 7,8-dicarba-*nido*-undecaborate cluster, then strongly coordinating thioether ligands are produced.[5] The question arises as to why thioether anionic molecules are so strongly coordinating. The *nido*-[C_2B_9]$^-$ anionic cluster may largely be responsible for such an effect.

On the other hand, the unit [3,3′-Co(1,2-$C_2B_9H_{11}$)$_2$]$^-$ has been the object of many studies[6] since its discovery in 1965.[7] Although *closo*-[3,3′-Co(1,2-$C_2B_9H_{11}$)$_2$]$^-$ and *nido*-[7,8-$C_2B_9H_{12}$]$^-$ are very different structurally, these two carborane compounds present some remarkable similarities. There is a negative charge delocalized within the cluster, and the cluster carbon atoms are susceptible to being bonded to coordinating elements such as S and P. Thus, it seems reasonable that [3,3′-Co(1,2-$C_2B_9H_{11}$)$_2$]$^-$ could be a good probe to show that **1** is not a singular compound featuring a rare example of a S(thioether)−Na bond. In contrast to **1**, the [3,3′-Co(1,2-$C_2B_9H_{11}$)$_2$]$^-$ backbone would not be able to take advantage of chelation if the two sulfur atoms were placed on the different [C_2B_9]$^-$ moieties. Since there are several possible rotamers of [3,3′-Co(1,2-$C_2B_9H_{11}$)$_2$]$^-$, a preference for a rotamer orientation involving the S(thioether)−Na bond would provide clear evidence for the strength of the latter.

To reach this goal, it was necessary to synthesize the first polydentate macrocycle incorporating [3,3′-Co(1,2-$C_2B_9H_{11}$)$_2$]$^-$ as a link. Prior to this work only a few small cyclic compounds using three to five atoms as spacers had been synthesized. These are the polymethylene-bridged, aza-, oxa-, and thiaalkane-1,1′-diyl-bridged carbon-linked cobalt bis(dicarbollides) [1,1′-μ-{TsN(CH_2CH_2)$_2$}-3,3′-Co(1,2-$C_2B_9H_{10}$)$_2$]$^-$,[8] [1,1′-μ-(CH_2OCH_2)-3,3′-Co(1,2-$C_2B_9H_{10}$)$_2$]$^-$, and [1,1′-μ-(CH_2SCH_2)-3,3′-Co(1,2-$C_2B_9H_{10}$)$_2$]$^-$.[9] In the receptor reported here, the spacer −(CH_2CH_2O)$_3$$CH_2CH_2$− is bonded to the cobaltacarborane through two thioether groups, one on each "C_2B_9" moiety, thereby providing five coordinating elements: three oxygen and two sulfur atoms.

For comparative purposes a more relaxed noncyclic (also a three-oxygen binding) [3,3′-Co(1,2-$C_2B_9H_{11}$)$_2$]$^-$ ligand and its Na complex have also been synthesized and are reported in this paper. These have been made possible due to the availability of the zwitterionic compound [3,3′-Co(8-$C_4H_8O_2$-1,2-$C_2B_9H_{10}$)(1′,2′-$C_2B_9H_{11}$)] (**2**), which was reported in 1996.[10]

Compound **2** has been shown to be susceptible to nucleophilic attack on the positively charged oxygen atom, e.g. by pyrrolyl,[11] by imide, cyanide, and amines,[12] by phenolate and by dialkyl or diaryl phosphite,[13] and by *N*-alkylcarbamoyldiphenylphosphine oxides,[14] resulting in one anionic species formed by the opening of the dioxane ring. In this paper the opening of the latter ring has been accomplished with [RO]$^-$ sodium salts.

Results and Discussion

I. Synthesis and Characterization of Functionalized Disubstituted Cobaltabis(dicarbollide) Derivatives Incorporating Five Heteroatoms (Two Thioether and Three Ether Groups) in the Exo-Cluster Chain. To prepare the cobaltabis(dicarbollide) starting material, it was first necessary to prepare the *closo*-carborane/thioether−ether−hydrocarbon backbone 1,1′-μ-{S(CH_2CH_2O)$_3$$CH_2CH_2$S}(1,2-$C_2B_{10}H_{11}$)$_2$ (**3**). This species was produced by reaction of 1-SH-1,2-$C_2B_{10}H_{11}$ with K[EtO] and $ClCH_2$(CH_2OCH_2)$_3$$CH_2Cl$. Deboronation of **3** with an excess of KOH in ethanol led to the desired nido species [7,7′-μ-{S(CH_2CH_2O)$_3$$CH_2CH_2$S}-(7,8-$C_2B_9H_{11}$)$_2$]$^{2-}$ (**4**). The nonequivalence of the initial substituents on the [C_2B_9]$^-$ cluster resulted in the isolation of two geometric isomers.

To synthesize the corresponding cobaltabis(dicarbollide) derivative [1,1′-μ-{S(CH_2CH_2O)$_3$$CH_2CH_2$S}-3,3′-Co-(1,2-$C_2B_9H_{10}$)$_2$]$^-$ (**5**), we used a method previously developed in our group.[15] After reaction of [N(CH_3)$_4$]$_2$[7,7′-μ-{S(CH_2CH_2O)$_3$$CH_2CH_2$S}(7,8-$C_2B_9H_{11}$)$_2$] with K[^{t}BuO] and cobalt(II) chloride in 1,2-dimethoxyethane, the solvent was evaporated and the product was extracted with CH_2Cl_2 and NaCl/water, giving Na[**5**]. The reactions are shown in Scheme 1. A racemic mixture and a meso form are possible (Figure 1), but three major bands named **5a**−**c** were separated by preparative TLC.

(2) Some recent references: (a) Danil de Namor, A. F. *Coord. Chem. Rev.* **1999**, *190*−*192*, 283−295. (b) Bandyopadhyay, K.; Liu, H.; Liu, S.-G.; Echegoyen, L. *Chem. Commun.* **2000**, 141−142. (c) Bandyopadhyay, K.; Liu, S.-G.; Liu, H.; Echegoyen, L. *Chem. Eur. J.* **2000**, *23*, 4385−4392. (d) Moore, A. J.; Goldenberg, L.; Bryce, M. R.; Petty, M. C.; Monkman, A. P.; Port, S. N. *Adv. Mater.* **1998**, *10*, 395−395. (e) Tsukube, H.; Mizutani, Y.; Shinoda, S.; Okazaki, T.; Tadokoro, M.; Hori, K. *Inorg. Chem.* **1999**, *38*, 3506−3512. (f) Reinhoudt, D. N. *J. Am. Chem. Soc.* **1998**, *120*, 4652−4657. (f) Flink, S.; van Veggel, F. C. J. M.; Reinhoudt, D. N. *J. Phys. Chem. B* **1999**, *103*, 6515−6520.

(3) (a) Comba, P. *Coord. Chem. Rev.* **2000**, *200*−*202*, 217−245. (b) Bayón, J. C.; Claver, C.; Masdeu-Bultó, A. M. *Coord. Chem. Rev.* **1999**, *193*−*195*, 73−145.

(4) (a) Raper, E. S. *Coord. Chem. Rev.* **1996**, *153*, 199−255. (b) Fourmigué, M.; *Coord. Chem. Rev.* **1998**, *178*−*180*, 823−864. (c) Akrivos, P. D.; Katsikis, H. J.; Koumoutsi, A. *Coord. Chem. Rev.* **1997**, *167*, 95−204.

(5) (a) Teixidor, F.; Casabó, J.; Viñas, C.; Sanchez, E.; Escriche, L. Kivekäs, R. *Inorg. Chem.* **1991**, *30*, 3053−3058. (b) Teixidor, F.; Flores, M. A.; Viñas, C.; Kivekäs, R.; Sillanpää, R. *Angew. Chem.* **1996**, *108*, 2388−2390; *Angew. Chem., Int. Ed. Engl.* **1996**, *35*, 2251−2253.

(6) (a) Plešek, J. *Chem. Rev.* **1992**, *92*, 269−278. (b) Hawthorne, M. F.; Maderna, A.; *Chem. Rev.* **1999**, *99*, 3421−3434. (c) Sivaev, B.; Bregadze, V. I. *Collect. Czech. Chem. Commun.* **1999**, *64*, 783−805.

(7) Hawthorne, M. F.; Young, D. C.; Wegner, P. A. *J. Am. Chem. Soc.* **1965**, *87*, 1818−1819.

(8) Gomez, F. A.; Johnson, S. E.; Knobler, C. B.; Hawthorne, M. F. *Inorg. Chem.* **1992**, *31*, 3558−3567.

(9) Nabakka, J. M.; Harwell, D. E.; Knobler, C. B.; Hawthorne, M. F. *J. Organomet. Chem.* **1998**, *55*, 423−429.

(10) (a) Plešek, J.; Hermanek, S.; Nöth, H.; Franken, A. Preparations and Structures of New [(1,2-$C_2B_9H_{11}$)$_2$-3-Co]$^-$ Derivatives. Ninth International Meeting on Boron Chemistry, Ruprech-Karls-Universität, Heidelberg, Germany, July 14−18, 1996; Poster #82. (b) Plešek, J.; Hermánek, S.; Franken, A.; Cisarova, I.; Nachtigal, C. *Collect. Czech. Chem. Commun.* **1997**, *62*, 47−56. (c) Selucky, P.; Plešek, J.; Rais, J.; Kyrs, M.; Kadlecova, L. *J. Radioanal. Nucl. Chem.* **1991**, *149*, 131−140. (d) Plešek, J.; Stibr, B.; Hermanek, S. *Collect. Czech. Chem. Commun.* **1984**, *49*, 1492−1496.

(11) Llop, J.; Masalles, C.; Viñas, C.; Teixidor, F.; Sillanpää, R.; Kivekäs, R. *J. Chem. Soc., Dalton Trans.* **2003**, 556−561.

(12) (a) Sivaev, I. B.; Starikova, Z. A.; Sjöberg, S.; Bregadze, V. I. *J. Organomet. Chem.* **2002**, *649*, 1−8. (b) Sivaev, I. B.; Sjöberg, S.; Bregadze, V. I., Synthesis of Functional Derivatives of Cobalt Bis(1,2-dicarbollide) Anion for Boron Neutron Capture Therapy. International Conference Organometallic Compounds−Materials of the Next Century, Nizhny Novgorod, Russia, May 29−June 2, 2000, p. 141.

(13) Plešek, J.; Grüner, B.; Heřmánek, S.; Báča, J.; Mareček, V.; Jänchenová, J.; Lhotský, A.; Holub, K.; Selucký, P.; Rais, J.; Císařová, I.; Čáslavský, J. *Polyhedron* **2002**, *21*, 975−986.

(14) Grüner, B.; Plešek, J.; Báča, J.; Císařová, I.; Dozol, J.-F.; Rouquette, H.; Viñas, C.; Selucký, P.; Rais, J. *New J. Chem.* **2002**, *26*, 1519−1527.

(15) Viñas, C.; Pedrajas, J.; Bertrán, J.; Teixidor, F.; Kivekäs, R.; Sillanpää, R. *Inorg. Chem.* **1997**, *36*, 2482−2486.

Scheme 1. Synthesis of *closo*-1,1′-*μ*-{S(CH$_2$CH$_2$O)$_3$-CH$_2$CH$_2$S}(1,2-C$_2$B$_{10}$H$_{11}$)$_2$, *nido*-[7,7′-*μ*-{S(CH$_2$CH$_2$O)$_3$-CH$_2$CH$_2$S}(7,8-C$_2$B$_9$H$_{11}$)$_2$]$^{2-}$, and [1,1′-*μ*-{S(CH$_2$CH$_2$O)$_3$CH$_2$CH$_2$S}-3,3′-Co(1,2-C$_2$B$_9$H$_{10}$)$_2$]$^-$ [a]

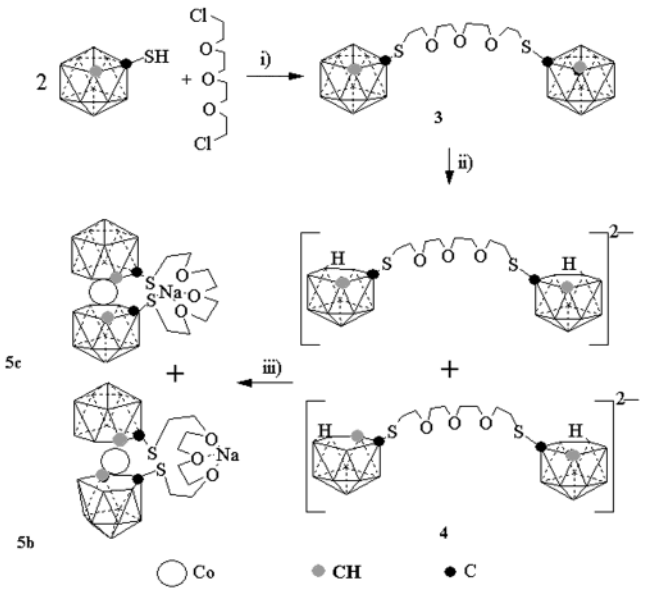

[a] Legend: (i) KOH, EtOH, reflux 2 h; (ii) NMe$_4$OH, EtOH, reflux 4 h; (iii) K[^{t}BuO], CoCl$_2$, 1,2-dimethoxyethane, reflux 24 h, NaCl in the workup.

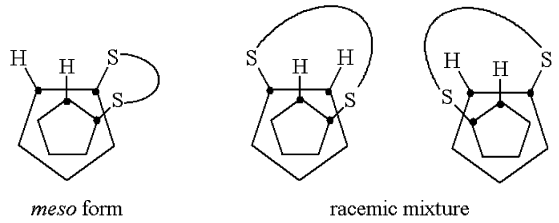

Figure 1. Geometric isomers of the anionic complex **[5]**$^-$ (view from the top of the pentagonal faces).

The ^{1}H NMR spectra of these compounds are very similar, displaying four resonances between 4.36 and 2.90 ppm: two broad singlets corresponding to the hydrogen atoms bonded to the cluster carbon atoms and two multiplet signals that correspond to the methylene units of the exo-cluster chain. The ^{11}B{^{1}H} NMR spectra of compounds **5a**−**c** are similar and appear in the range from +8 to −20 ppm. The ^{13}C{^{1}H} NMR resonances were striking in regard to the cluster carbon atom chemical shifts. Compound **5a** displayed these resonances at 63.89 and 67.73 ppm, compound **5b** at 65.30 and 67.39 ppm, and compound **5c** at 58.27 and 60.58 ppm. Those for **5c** are distinctly different from the first two sets. If comparison of these resonances is made with a similar, albeit nonmacrocyclic, compound, [NMe$_4$][1,1′-(SCH$_2$CH$_3$)$_2$-3,3′-Co(1,2-C$_2$B$_9$H$_{10}$)$_2$], with a cation which is not susceptible to coordination,[15] some sense may be made of these chemical shift values. The cluster ^{13}C{^{1}H} NMR resonances in [NMe$_4$][1,1′-(SCH$_2$CH$_3$)$_2$-3,3′-Co(1,2-C$_2$B$_9$H$_{10}$)$_2$] are observed at 63.84 and 67.00 ppm, values comparable to these found for **5a**,**b**, suggesting that in **5c** the two thioether groups participate in coordination. This is less probable for **5a**,**b**. The ^{13}C{^{1}H} NMR chemical shift difference between **5a**/**5b** and **5c** parallels the electrochemical Fc/Fc$^+$ shift observed in ferrocene (Fc) macrocycles upon coordination to a substrate.[16] In these, the Fc/Fc$^+$ $E_{1/2}$ potential depends on the degree of communication between the receptor and ferrocene sites, communication that could be achieved by directly bonding one of the receptor coordinating sites to the ferrocene fragment.[17] This also takes place in the cobaltacarborane macrocycles described here, where the two coordinating sites in the receptor, the thioether groups, are directly bonded to the cobaltacarborane moiety. As a consequence, the ^{13}C{^{1}H} NMR chemical shift difference between **5c** and **5a**/**5b** can arise via coordination of the macrocycle's S and O atoms to either Na or K in a well-communicated receptor/[3,3′-Co(1,2-C$_2$B$_9$H$_{11}$)$_2$]$^-$ system. Na and K ions coexist in the mother liquor but, as will be shown later, only Na is coordinated. Elemental analyses for **5a** are in agreement with the Na[1,1′-*μ*-{S(CH$_2$CH$_2$O)$_3$CH$_2$-CH$_2$S}-3,3′-Co(1,2-C$_2$B$_9$H$_{10}$)$_2$] formulation but were not decisive for **5b**,**c**. More information about the coordination geometry required a single-crystal X-ray structural information.

Scheme 2. Opening of the Exo-Cluster Dioxanate Ring Reaction by Nucleophilic Attack: Synthesis of Complexes 6−10[a]

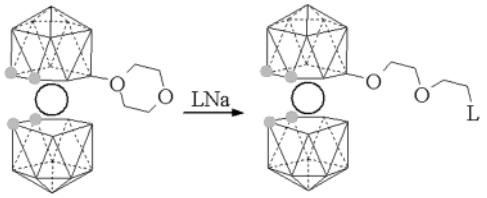

L= OCH$_3$ (**6**); OCH$_2$CH$_3$ (**7**); OCH$_2$CH$_2$OCH$_3$ (**8**); OCH$_2$CH$_2$OCH$_2$CH$_3$ (**9**).

[a] Atoms in gray are CH vertexes; the rest of the vertices in the clusters are BH.

II. Synthesis and Characterization of Functionalized Monosubstituted Cobaltabis(dicarbollide) Derivatives Incorporating Three or Four Ether Groups in the Exo-Cluster Chain. To study the cluster influence on coordination, we synthesized a ligand incorporating the (OCH$_2$CH$_2$)$_2$OR chain and the [3,3′-Co(1,2-C$_2$B$_9$H$_{11}$)$_2$]$^-$ moiety. It was expected that a polyether open chain would allow higher cluster participation in bonding than a polyether macrocycle. With this aim, the anionic species [3,3′-Co(8-{O(CH$_2$CH$_2$O)$_n$R}-1,2-C$_2$B$_9$H$_{10}$)(1′,2′-C$_2$B$_9$H$_{11}$)]$^-$ (n = 2, 3; R = −CH$_3$, −CH$_2$CH$_3$) were synthesized from the zwitterionic [3,3′-Co(8-C$_4$H$_8$O$_2$-1,2-C$_2$B$_9$H$_{10}$)(1′,2′-C$_2$B$_9$H$_{11}$)] (**2**) compounds[10] according to Scheme 2.

Compound **2** was prepared by the reaction of the cobaltabis(dicarbollide) anion with Et$_2$O·BF$_3$ in 1,4-dioxane analogously to the synthesis of the similar derivative of the *closo*-dodecaborate anion [B$_{12}$H$_{11}$O$_2$C$_4$H$_8$]$^-$.[18] This synthesis gives a higher yield (94% compared to

(16) (a) Beer, P. D.; Sikanyika, H.; Blackburn, C. *J. Chem. Soc., Chem. Commun.* **1989**, *23*, 1831−1833. (b) Beer, P. D. *Adv. Inorg. Chem.* **1992**, *39*, 79−157. (c) Beer, P. D. *Adv. Mater.* **1994**, *6*, 607−609. (d) Beer, P. D.; Blackburn, C.; McAleer, J. F.; Sikanyika, H. *Inorg. Chem.* **1990**, *29*, 378−381.

(17) (a) Kaifer, A. E.; Mendoza, S. In *Comprehensive Supramolecular Chemistry*; Gokel, G. W., Ed.; Elsevier Science: Oxford, U.K., 1996; Vol. 1, pp 701−732. (b) Beer, P. D.; Gale, P. A.; Chen, Z.; Drew, M. G. B.; Heath, J. A.; Ogden, M. I.; Powell, H. R. *Inorg. Chem.* **1997**, *36*, 5880−5893. (c) Beer, P. D.; Gale, P. A.; Chen, G. Z. *Coord. Chem. Rev.* **1999**, *185*−*186*, 3−36.

(18) Sivaev, I. B.; Semioshkin, A. A.; Brellochs, B.; Sjöberg, S.; Bregadze, V. I. *Polyhedron* **2000**, *19*, 627−632.

Table 1. Crystallographic Parameters for Na[5b]·2$(CH_3)_2CO$, Na[5c]·$(CH_3)_2CO$·$CHCl_3$·CH_2Cl_2, and Na[7]

	Na[5b]·2$(CH_3)_2CO$	**Na[5c]**·$(CH_3)_2CO$·$CHCl_3$·CH_2Cl_2	Na[7]
empirical formula	$C_{18}H_{48}B_{18}CoNaO_5S_2$	$C_{17}H_{45}B_{18}Cl_5CoNaO_4S_2$	$C_{10}H_{34}B_{18}CoNaO_3$
fw	685.18	831.40	478.87
cryst syst	orthorhombic	monoclinic	monoclinic
space group	*Pna*2$_1$ (No. 33)	*P*2$_1$/*c* (No. 14)	*P*2$_1$/*c* (No. 14)
a (Å)	18.625(2)	15.542(2)	15.0356(4)
b (Å)	10.710(2)	11.393(2)	11.4643(3)
c (Å)	17.715(1)	22.150(2)	14.7322(3)
β (deg)	90	91.266(8)	105.3940(11)
V (Å^3)	3533.7(8)	3921.1(9)	2448.32(10)
Z	4	4	4
T (°C)	21	21	−100
λ (Å)	0.710 69	0.710 69	0.710 73
ρ (g cm^{-3})	1.288	1.408	1.299
μ (cm^{-1})	6.46	9.23	7.32
goodness of fit	1.040	1.104	1.073
R1[a] ($I > 2\sigma(I)$)	0.0552	0.0692	0.0461
wR2[b] ($I > 2\sigma(I)$)	0.1164	0.1734	0.0923
Flack param *x*	0.04(4)		

[a] $R1 = \Sigma||F_o| - |F_c||/\Sigma|F_o|$. [b] $wR2 = \{\Sigma[w(F_o^2 - F_c^2)^2]/\Sigma[w(F_o^2)^2]\}^{1/2}$.

45%) and has a better workup procedure than the one reported earlier.[10b]

The highly nucleophilic character of [RO]$^-$ anions has been used to obtain partially degraded *o*-carborane derivatives.[19] Thus, it was expected that they would have sufficient nucleophilic power to open the exo-cluster aliphatic ring of the zwitterionic [3,3′-Co(8-$C_4H_8O_2$-1,2-$C_2B_9H_{10}$)(1′,2′-$C_2B_9H_{11}$)] derivative of [Co($C_2B_9H_{11}$)$_2$]$^-$ and yield the corresponding salts.

In the present work, sodium salts of [RO]$^-$ (R = $-CH_3$, $-CH_2CH_3$, $-CH_2CH_2OCH_3$, $-CH_2CH_2OCH_2CH_3$) were used as nucleophilic agents. The larger derivatives would provide information about the nucleophilic dependence on the size and on the possibilities to modulate solubility in the resulting ligands. All Na[RO] salts were prepared by dissolving NaOH in the corresponding alcohol. Once the sodium salts had been formed, the addition of the zwitterionic species **2** to the solution of the nucleophilic agent yielded the addition compound in about 45 min. The nucleophilic attack was carried out at room temperature to avoid secondary reactions. Following purification the pure compounds [3,3′-Co(8-{O(CH_2CH_2O)$_2CH_3$}-1,2-$C_2B_9H_{10}$)(1′,2′-$C_2B_9H_{11}$)]$^-$ (**6**), [3,3′-Co(8-{O(CH_2CH_2O)$_2CH_2CH_3$}-1,2-$C_2B_9H_{10}$)(1′,2′-$C_2B_9H_{11}$)]$^-$ (**7**), [3,3′-Co(8-{O(CH_2CH_2O)$_3$-CH_3)-1,2-$C_2B_9H_{10}$)(1′,2′-$C_2B_9H_{11}$)]$^-$ (**8**), and [3,3′-Co(8-{O(CH_2CH_2O)$_3CH_2CH_3$)-1,2-$C_2B_9H_{10}$)(1′,2′-$C_2B_9H_{11}$)]$^-$ (**9**) were obtained. The ^{1}H NMR spectra of these compounds are very similar, displaying four resonances between 4.19 and 3.44 ppm: two broad singlets corresponding to the hydrogen atoms bonded to the cluster carbon atoms, a triplet signal that corresponds to the methylene units to B(8)−O, and a multiplet from the other O−CH_2 groups of the exo-cluster chain. At room temperature the proton resonances for the hydrogen atoms on the two cluster carbon atoms for compound **8** overlap at 4.17 ppm but two singlets are observed at 4.19 and 4.13 ppm at −60 °C, providing the nonequivalency of the two cluster fragments. The ^{1}H{^{11}B} NMR spectra display nine additional signals, in the range 2.96−1.44 ppm, assigned to the B−H exo-cluster hydrogen atoms. The ^{11}B{^{1}H} NMR spectra corresponding to compounds **6**−**9** featured an identical 1:1:1:1:2:4:2:2:2:1:1 pattern ranging from +24 to −28 ppm. The resonance at the lowest field remains a singlet in the ^{11}B NMR spectrum and is assigned to the B(8)-substituted boron atom. The observed ^{11}B NMR pattern reflects the C_s symmetry of the molecules (12 different signals). The boron resonance with relative intensity 4 is due to coincidental overlap of two different resonances with a 2:2 ratio. The MALDI-TOF mass spectrum of **7** displays a signal group centered at *m*/*z* 456.14 corresponding to the anionic fragment **7**.

Table 2. Selected Bond Lengths (Å) for Na[5b]·2$(CH_3)_2CO$

Co3−C1	2.112(9)	S1−C1	1.806(10)
Co3−C2	2.070(8)	S2−C1′	1.792(10)
Co3−B4	2.109(12)	Na−O1	2.344(9)
Co3−B7	2.099(12)	Na−O2	2.366(9)
Co3−B8	2.122(12)	Na−O3	2.403(9)
Co3−C1′	2.129(9)	Na−O4	2.292(12)
Co3−C2′	2.083(10)	Na−O5	2.242(12)
Co3−B4′	2.124(11)	C1−C2	1.629(14)
Co3−B7′	2.121(12)	C1′−C2′	1.631(14)
Co3−B8′	2.133(11)		

III. Coordination Motif to Hard Metal Ions. Ligands **5** and **6**−**9** mostly differ in the additional chelating capacity provided by the −OCH_2CH_2O− units. To learn the effects on coordination, solid-state studies were conducted on the sodium salts of **5b**,**c** and solid and solution studies were conducted on the sodium salt of **7**.

(a) Cluster Participation in Na Coordination in the Presence of the Thioether/Polyether Exo-Cluster Chain. Dissolution of either **Na[5b]** or **Na[5c]** in a CH_2Cl_2/$CHCl_3$/$(CH_3)_2CO$ solvent mixture (initially 2:1:1) yielded blood red single crystals of sufficient quality to allow the crystal structures of **Na[5b]** and **Na[5c]** to be determined from X-ray diffraction data.[20] **Na[5b]** crystallizes out in an enantiomeric space group.

Crystallographic analyses of **Na[5b]**·2$(CH_3)_2CO$ (Tables 1 and 2, Figure 2) and **Na[5c]**·$(CH_3)_2CO$·$CHCl_3$·CH_2Cl_2 (Tables 1 and 3, Figure 3) confirmed that in both compounds the [3,3′-Co(1,2-$C_2B_9H_{11}$)$_2$]$^-$ structural frag-

(19) (a) Warren, L. F.; Hawthorne, M. F. *J. Am. Chem. Soc.* **1964**, *86*, 1642−1643. (b) Hawthorne, M. F.; Wegner, P. A.; Stafford, R. C. *Inorg. Chem.* **1965**, *4*, 1675. (c) Hawthorne, M. F.; Andrews, T. D.; Garret, P. M.; Olsen, F. P.; Reintjes, M.; Tebbe, F. N.; Warren, L. F.; Wegner, P. A.; Young, D. C. *Inorg. Syn.* **1967**, *10*, 91-.

(20) Sheldrick, G. M. SHELX-97; University of Göttingen, Göttingen, Germany, 1997.

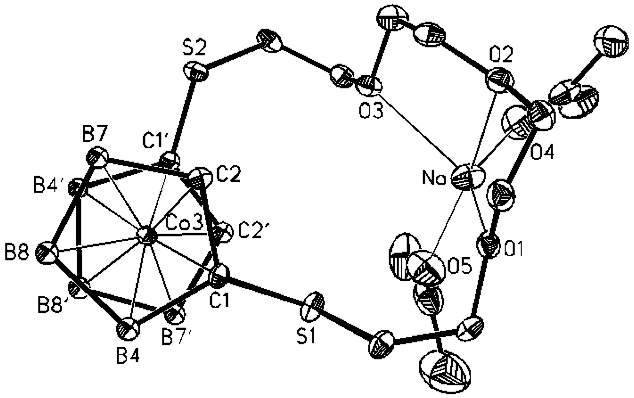

Figure 2. Simplified molecular structure of **Na[5b]**·2$(CH_3)_2CO$. Noncoordinated boron atoms are omitted.

Table 3. Selected Bond Lengths (Å) for Na[5c]·$(CH_3)_2CO$·$CHCl_3$·CH_2Cl_2

Co3−C1	2.070(6)	S1−Na	2.893(3)
Co3−C2	2.131(6)	S2−Na	2.900(3)
Co3−B4	2.107(8)	S1−C2	1.805(6)
Co3−B7	2.128(7)	S2−C1′	1.804(6)
Co3−B8	2.142(7)	Na−O1	2.353(5)
Co3−C1′	2.131(6)	Na−O2	2.421(5)
Co3−C2′	2.072(6)	Na−O3	2.393(5)
Co3−B4′	2.119(7)	Na−O4	2.249(6)
Co3−B7′	2.098(7)	C1−C2	1.640(8)
Co3−B8′	2.144(7)	C1′−C2′	1.661(8)

ment is a part of the macrocycle, but the fragments are made of different geometric isomers. Connections to the sulfur atoms on the organic fragment take place via one cluster carbon atom on each dicarbollyl moiety. The flexible macrocyclic chain in **Na[5b]** is coordinated by three oxygen atoms to Na^+, and two oxygen atoms from two acetone molecules complete the pentacoordination around Na^+. The coordination geometry of Na^+ is a distorted trigonal bipyramid. The short Na−O(acetone) distances suggest that acetone ligands are quite tightly bonded to the sodium cation.

As expected from the $^{13}C\{^1H\}$ NMR data for **Na[5c],** the structure found for this complex is different from that of **Na[5b]**. The coordination number for the Na^+ cation is 6, and the flexible macrocyclic chain coordinates to Na^+ through all five of its donor atoms, including the two thioether S atoms. The sixth coordination position is occupied by the oxygen atom of one acetone, completing a pentagonal-pyramidal structure. One chlorine atom of the dichloromethane solvate is at a distance of 3.399(4) Å from the sodium. This distance is too long to be considered bonding to the Na^+ ion.

The two structures are markedly different, especially considering the site around Na^+, and the cobaltabis(dicarbollide) rotamers are also different. In both structures, **Na[5b]** and **Na[5c]**, the dicarbollide ligands adopt a staggered conformation with all four cluster carbon atoms in a cisoid disposition. Thus, the projection of one of the two carbon atoms from one dicarbollide into the C_2B_3 plane of the second dicarbollide lies between the two cluster carbon atoms. This can be understood if we assume that the more stable rotamers are those where the more electronegative cluster elements are facing the same side of the dicarbollide moiety. We have also observed this phenomenon in mixed pyrrolyl/dicarbollide Co(III) complexes,[21] where the nitrogen projection on the C_2B_3 face bisects the

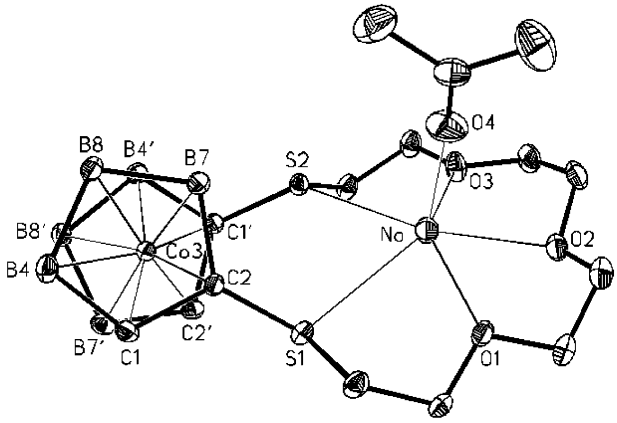

Figure 3. Simplified molecular structure of **Na[5c]**·$(CH_3)_2CO$·$CHCl_3$·CH_2Cl_2. Noncoordinated boron atoms and chloroform and dichloromethane molecules are omitted.

C_c-C_c bond (C_c is cage carbon). This has also been reported for other molecules incorporating [3,3′-Co(1,2-$C_2B_9H_{11})_2]^-$ structural fragments.[22] There are major differences between the backbone conformations in **Na[5b]** and **Na[5c]** that may be described by the torsion angles through the centers of Co-coordinated C_2B_3 faces (marked c and c′). Thus the C1−c−c′−C1′ torsion angles have values of −97.2(5) and −118.4(3)° for **Na[5b]** and **Na[5c]**, while the values for C2−c−c′−C1′ torsion angles are −27.7(6) and −48.6(3)°. The differences in both cases are ca. 21°. A more pronounced difference between **Na[5b]** and **Na[5c]** is, however, the different conformations of the organic flexible spacer $-S(CH_2CH_2O)_3CH_2CH_2S-$, resulting from its distinct connections to the [3,3′-Co(1,2-$C_2B_9H_{11})_2]^-$ moiety. These correspond to the idealized racemic and meso forms, respectively (Figure 1). The meso **Na[5c]** form exhibits a considerably shorter S···S distance (3.510(2) Å), than for the racemic **Na[5b]** (4.951(4) Å); hence, a type of spatial chelating site "SCCS" with a S···S distance comparable to that found in **1** (3.371 Å) is formed.[1] Consequently in **Na[5c]** both sulfur atoms have structural conditions suitable for chelating the metal, in contrast to **Na[5b]**. Ligand **5** provides five coordinating sites in the meso isomer and only three in the racemic one. The coordinated metal binds the solvent in order to fulfill its coordination requirement.

With the structure **Na[5c]** we have shown that other examples of S(thioether)−Na coordination are possible and that it is not necessary to have a preorganized S···S disposition, as was the case in Na[7,8-μ-{S-$(CH_2CH_2O)_3CH_2CH_2S$}-7,8-$C_2B_9H_{10}$], in order to get S(thioether)−Na coordination. The only reported ex-

(21) (a) Lamrani, M.; Gómez, S.; Viñas, C.; Teixidor, F.; Sillanpää, R.; Kivekäs, R. *New J. Chem.* **1996**, *20*, 909−912. (b) Teixidor, F.; Gómez, S.; Lamrani, M.; Viñas, C.; Sillanpää, R.; Kivekäs, R. *Organomatallics* **1997**, *16*, 1278−1283. (c) Gómez, S.; Viñas, C.; Lamrani, M.; Teixidor, F.; Kivekäs, R.; Sillanpää, R. *Inorg. Chem.* **1997**, *36*, 3565−3567. (d) Llop, J.; Viñas, C.; Teixidor, F.; Victori, L.; Kivekäs, R.; Sillanpää, R. *Organometallics* **2001**, *19*, 4024−4030. (e) Llop, J.; Viñas, C.; Teixidor, F.; Victori, L.; Kivekäs, R.; Sillanpää, R. *Organometallics* **2002**, *21*, 355−361. (f) Llop, J.; Viñas, C.; Teixidor, F.; Victori, L.; Kivekäs, R.; Sillanpää, R. *Inorg. Chem.* **2002**, *41*, 3347−3352. (g) Sillanpää, R.; Llop, J.; Viñas, C.; Teixidor, F.; Kivekäs, R. *Acta Crystallogr.* **2001**, *C57*, 900−901.

(22) (a) Petrina, A.; Malý, K.; Petrícek, V.; Subrtová, V.; Línek, A.; Hummel, L. *Z. Kristallogr.* **1981**, *154*, 217−226. (b) Chamberlin, R. M.; Scott, B. L.; Melo, M. M.; Abney, K. D. *Inorg. Chem.* **1997**, *36*, 809−817.

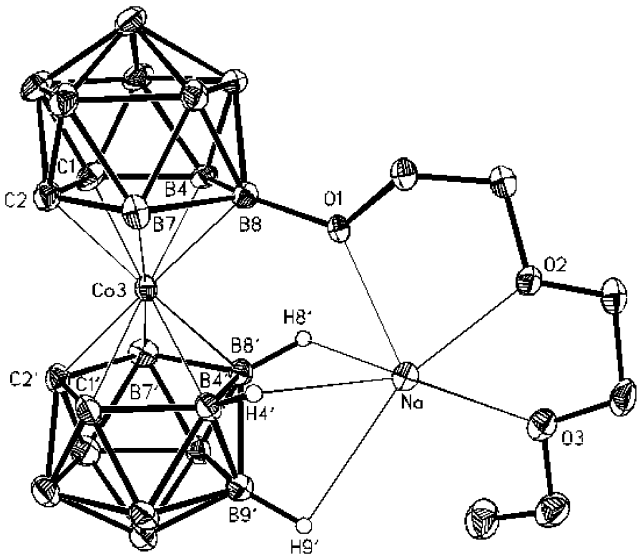

Figure 4. Molecular structure of **Na[7]**.

Table 4. Selected Bond Lengths (Å) for Na[7]

Co3−C1	2.037(3)	Na−O1	2.357(2)
Co3−C2	2.044(3)	Na−O2	2.287(3)
Co3−B4	2.080(3)	Na−O3	2.407(2)
Co3−B7	2.098(3)	Na−H4′	2.368
Co3−B8	2.132(4)	Na−H8′	2.448
Co3−C1′	2.041(3)	Na−H9′	2.867
Co3−C2′	2.049(3)	O1−B8	1.433(4)
Co3−B4′	2.080(3)	C1−C2	1.622(4)
Co3−B7′	2.104(3)	C1′−C2′	1.603(4)
Co3−B8′	2.114(3)		

amples of S(thioether)−Na bonds are restricted to thioether sulfur bonded to negatively charged carboranes via the cluster carbon atoms. The cluster seems to play a role in facilitating the bonding. Also, S(thioether)−Na bonding has been possible with the assistance of coordinating entities associated with the $ROCH_2CH_2OCH_2CH_2OR$ group, as present in **1** and **5**. In this regard we were interested in investigating how the [3,3′-Co(1,2-$C_2B_9H_{11}$)$_2$]$^-$ cluster incorporating the $ROCH_2CH_2OCH_2CH_2OR$ group, but with an absence of −S−, would behave toward Na coordination.

(b) Cluster Participation in Na Coordination in the Presence of the Polyether Exo-Cluster Chain. 1. Coordination in the Solid State. Crystallization by slow diffusion of hexane into a saturated dichloromethane solution of **Na[7]** at controlled temperature (4 °C) afforded air- and moisture-insensitive orange plate-shaped monocrystals suitable for X-ray analysis. An X-ray diffraction study of **Na[7]** confirmed the proposed structure. A drawing of the compound is shown in Figure 4, and selected bond lengths and angles are listed in Table 4.

In the absence of the two S(thioether) moieties present as in **Na[5b]** and **Na[5c]**, the Na^+ coordinates three B−H groups: B4−H4, B8−H8, and B9−H9. It is of note that the B4···Na, B8···Na, and B9···Na contacts are short with distances of 2.857(4), 2.895(4), and 3.141(4) Å. Overall, the number of sodium short contacts is 6 in **Na[7],** one contact less than in **Na[5c]**. The coordination geometry is not typical for 6-coordination. This is due to a rigid ligand and the fact that coordinative saturation and bond directionality for Na^+ are far less significant factors than in many transition-element complexes. A short cluster B−H···Na interaction was reported recently in a [3,3′-Co(1,2-$C_2B_9H_{11}$)$_2$]$^-$ derivative. The X-ray crystal structure of Na[8-$(OCH_2CH_2)_2OC_6H_4$-2-OCH_3-3,3′-Co(1,2-$C_2B_9H_{10}$)(1′,2′-$C_2B_9H_{11}$)][13] shows that the Na presents six short contacts: four Na−O contacts derived from the four oxygen atoms of the ligand, one Na−O contact derived from an ancillary water molecule, and a B8′−H contact with a Na−H distance of 2.23(3) Å. This H···Na distance is clearly shorter than the ones reported in this paper for B4H4···Na, B8H8···Na, and B9H9···Na bonds (2.368, 2.448, and 2.867 Å). The above description supports our earlier statement that boron clusters, if required, involve themselves in coordination to satisfy the metal's requirements.

2. Coordination in Solution. Although definitive evidence for B−H···Na^+ interactions in the solid state is given by the X-ray analysis of the sodium salt of **7**, no proof of its existence in solution has been found in the $^1H\{^{11}B\}$ NMR spectrum at room temperature. We have run low-temperature experiments with the aim of freezing out the more stable rotamers and fixing specific B−H···Na^+ interactions.

Variable-temperature $^1H\{^{11}B\}$ NMR spectra recorded in the range 22 to −80 °C using dichloromethane as a solvent are shown in Figure 5. There is a high dependence of the chemical shift of one B−H signal on temperature. This B−H resonance becomes broader and shifts to lower fields as the temperature decreases. At room temperature the signal is a well-defined singlet. With a decrease in temperature, the signal becomes a very broad singlet. These spectroscopic data are in agreement with intramolecular B−H···Na^+ interactions, most probably corresponding to those observed in the solid state (Figure 4). The NMR data above −70 °C could be explained either by the rapid exchange between the available geometric rotamers, providing different B−H···Na^+ interactions, or by a progressive increase in the number of molecules whose B−H···Na^+ interactions have been replaced by coordinating solvent molecules.

IV. Role of the Electron-Rich Atom (O) Directly Bonded to a Cluster Boron Atom. It has been proven that anionic clusters containing electron-rich exo-cluster substituents (S or P) dissipate electron density into the electron-rich element. [5,23] This element becomes a strong Lewis base and a very good coordinating ligand.[5,24] Most probably the oxygen atom in the B(8)−O bond in **6**−**9** can play the same role as S and P atoms, dissipating the negative charge and becoming a strong Lewis base. Thus, the anionic species can coordinate to a Lewis acid through the oxygen atom at the B(8) position. This coordination, shown in Chart 1, could easily be formed in an almost irreversible reaction upon contact with protons from an acidic medium. A high pK_a acid is generated due to the strong basicity of the B−O group and the existence of a second oxygen atom that can also

(23) (a) Teixidor, F.; Núñez, R.; Viñas, C.; Sillanpää, R.; Kivekäs, R. *Inorg. Chem.* **2001**, *40*, 2587−2594.

(24) (a) Teixidor, F.; Flores, M. A.; Viñas, C.; Kivekäs, R.; Sillanpää, R. *J. Am. Chem. Soc.* **2000**, *122*, 1963−1973. (b) Teixidor, F.; Romerosa, A.; Viñas, C.; Rius, J.; Miravitlles, C.; Casabó, J. *J. Chem. Soc., Chem. Commun.* **1991**, 192−193. (c) Teixidor, F.; Ayllón, J. A.; Viñas, C.; Rius, J.; Miravitlles, C.; Casabó, J. *J. Chem. Soc., Chem. Commun.* **1992**, 1279−1280. (d) Teixidor, F.; Casabó, J.; Romerosa, A. M.; Viñas, C.; Rius, J.; Miravitlles, C. *J. Am. Chem. Soc.* **1991**, *113*, 9895−9896.

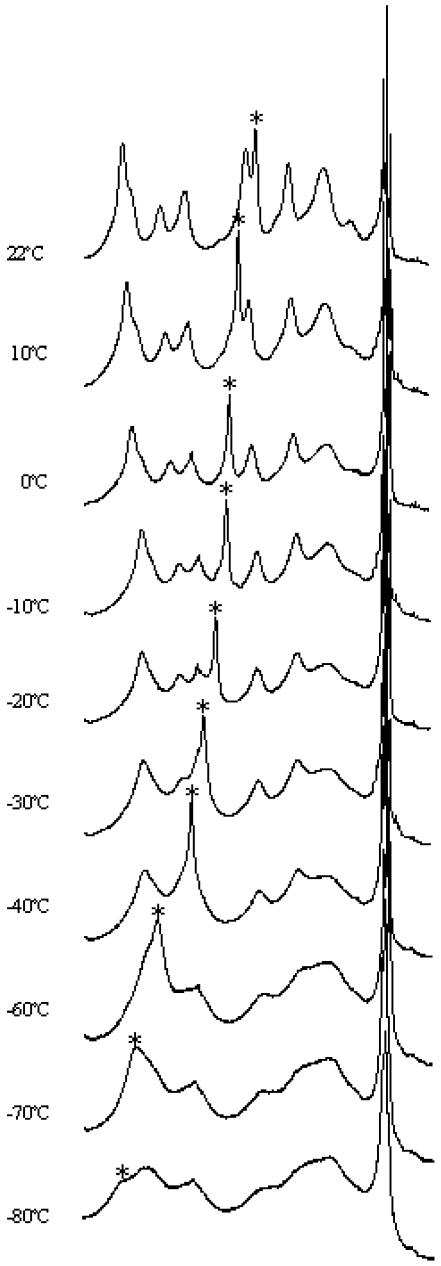

Figure 5. $^{1}H\{^{11}B\}$ NMR spectra of **7** in dichloromethane for **Na[7]** as a function of temperature. The asterisks denote signals corresponding to H atoms from intramolecular B−H···Na^{+} interactions.

Chart 1. Suggested Species Formed by Coordination of the Oxygen Atom in Addition Compounds with Lewis Acids (A)

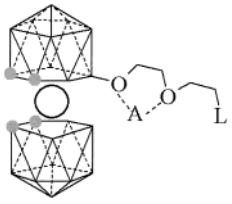

interact with a Lewis acid (A), forming a O···A···O interaction.

Matrix-assisted laser desorption/ionization (MALDI)[25] supports, although does not confirm, the special nucleophilic character of the B−O unit. MALDI is widely used for mass spectrometric analysis of large, nonvolatile biomolecules; e.g., peptides, proteins, oligonucleotides, and oligosaccharides.[26] Synthetic polymers of high molecular weight, fullerene derivatives, and synthetically prepared dendrimers have also been studied by MALDI-MS. The possible ion formation mechanisms in MALDI spectrometry are primary and secondary. "Primary" ionization refers to generation of the first ions from neutral molecules in the sample. "Secondary" mechanisms are those which lead to ions that are not directly generated by primary processes. In the mass spectrum, the products of primary and secondary processes are both usually observed. One attractive mechanism different from the former ones is that the ions observed in MALDI mass spectra are already present in the solid sample and are merely liberated by the laser pulse. This mechanism is potentially most relevant for molecules that form strong metal ion complexes such as crown ethers, ionophores, and metal-binding proteins.[27] Under these circumstances, the larger the ions, the easier the separation. Compounds **6**−**9** fulfill these requirements and were studied by the MALDI-MS technique at the negative ion mode without the use of matrixes. The lack of matrixes aids the interpretation of the primary and secondary mechanisms. We understand as a "primary" mechanism the separation of the anionic cobaltabis(dicarbollide) derivatives from the bonded sodium cation. The "secondary" mechanism can give some clues about the nucleophilic character of the electron-rich oxygen atom directly bonded to the cluster B(8) boron atom. Figure 6 shows the MALDI-TOF-MS spectrum of compound **7** as a representative example. Peaks with

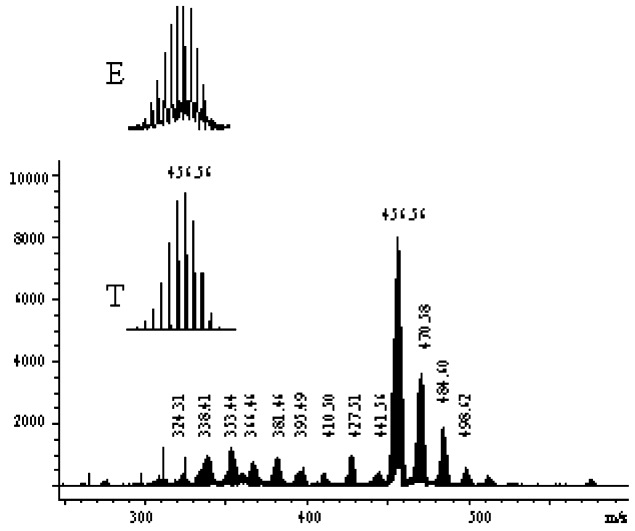

Figure 6. MALDI-TOF mass spectrum obtained for the anionic compound **7** (T = calculated, E = experimental).

(25) (a) Karas, M.; Hillenkamp, F. *Anal. Chem*. **1988**, *60*, 2299. (b) Karas, M.; Bachmann, D.; Hillenkamp, F. *Anal. Chem*. **1985**, *57*, 2935. (c) Tanaka, K.; Waki, H.; Ido, Y.; Akita, S.; Yoshida, Y.; Yoshida, T. *Rapid Commun. Mass Spectrom*. **1988**, *2*, 151.

(26) (a) Overberg, A.; Hassenbürger, A.; Hillenkamp, F. Laser Desorption Mass Spectrometry. Part II: Performance and Applications of Matrix-Assisted Laser Desorption/Ionization of Large Biomolecules. In *Mass Spectrometry in the Biological Sciences: A Tutorial*; Gross, M. L., Ed.; Kluwer: Dordrecht, The Netherlands, 1992; p 181. (b) Caprioli, R. M.; Malorni, A.; Sidona, G. *Mass Spectrometry in Biomolecular Sciences*, NATO ASI Ser. C, Vol. 475; Kluwer: Dordrecht, The Netherlands, 1996. (c) Chapman, J. R. *Protein and Peptide Análisis by Mass Spectrometry*. Methods Mol. Biol.., Vol. 61; Humana Press: Totowa, NJ, 1996.

(27) Lehmann, W. D. *Massenspektrometrie in der Biochemie Spektrum*; Akadademischer Verlag: Heidelberg, Germany, 1996.

ion masses higher than the molecular ion peak at *m*/*z* 456.56 (M) are observed at *m*/*z* 470.58, 484.60, and 498.62, with intensities decreasing in this order. These peaks correspond to (M + CH_2), (M + CH_2CH_2), and (M + $CH_2CH_2CH_2$), respectively. Peaks with ion masses lower than the molecular peak are observed at *m*/*z* 441.56 (M − CH_3) and 427.51 (M − CH_2CH_3). It appears that part of the polyether chain in some molecules is transferring methylene groups to like molecules, thereby increasing their molecular weight by 14 or 15. These peaks can be interpreted as an electrophilic reaction between like anions. This is also observed in compounds **6**−**9** and has been noted previously[28] for R = −OCH_2-$CH_2OCH_2CH_2$-pyr (pyr = pyrrolyl, indolyl, carbazolyl). This indicates that the CH_2 supplier is the initial −$OCH_2CH_2OCH_2CH_2$− fragment and not the ring-opening nucleophile. Our interpretation is that the nucleophilic B−O group enhances the CH_2 trapping. There are several structures that can accommodate this CH_2 increment. Work is underway to see if this could be a synthetic procedure for cobaltabis(dicarbollide) methyl derivatives.

Conclusion

This work demonstrates the extraordinary chameleonic capacity of [3,3′-Co(1,2-$C_2B_9H_{11}$)$_2$]$^-$ toward coordination of a metal ion, Na^+. No other examples of S(thioether)−Na coordination besides Na[7,8-*μ*-{S-$(CH_2CH_2O)_3CH_2CH_2S$}-7,8-$C_2B_9H_{10}$] are known. Extra coordination sites are filled with the oxygen atoms of the macrocycle or from solvent molecules. Given that there are fewer oxygen coordinating sites accessible, the [3,3′-Co(1,2-$C_2B_9H_{11}$)$_2$]$^-$ fragment supplies B−H moieties to fulfill the metal's coordination demands. The [3,3′-Co(1,2-$C_2B_9H_{11}$)$_2$]$^-$ enhances the coordinating capacity of X in B−X moieties (X = O, S, P), converting a weakly coordinating element, thioether, into a good nucleophile or an ether oxygen into a strong nucleophile. The availability of B−H groups and their geometrical distribution offers an unusual way of satisfying the metal's demand.

Experimental Section

Instrumentation. Elemental analyses were performed using a Carlo Erba EA1108 microanalyzer. IR spectra were recorded from KBr pellets on a Shimadzu FTIR-8300 spectrophotometer. The ^{1}H NMR, ^{1}H{^{11}B} NMR (300.13 MHz), ^{11}B NMR (96.29 MHz), and ^{13}C{^{1}H} NMR (75.47 MHz) spectra were recorded with a Bruker ARX 300 instrument equipped with the appropriate decoupling accessories. Chemical shift values for ^{11}B NMR spectra were referenced to external BF_3·OEt_2, and those for ^{1}H, ^{1}H{^{11}B}, and ^{13}C{^{1}H} NMR spectra were referenced to $Si(CH_3)_4$. Chemical shifts are reported in units of parts per million downfield from the reference, and all coupling constants are reported in Hertz. The mass spectra were recorded in the negative ion mode using a Bruker Biflex MALDI-TOF-MS (N_2 laser; λ_{exc} 337 nm (0.5 ns pulses); voltage ion source 20.00 kV (Uis1) and 17.50 kV (Uis2)).

Materials. Experiments were carried out, except when noted, under a dry, oxygen-free dinitrogen atmosphere using standard Schlenk techniques, with some subsequent manipulation in the open laboratory. EtOH was dried over molecular sieves and deoxygenated prior to use. 1,2-Dimethoxyethane and 1,4-dioxane were distilled from sodium benzophenone before use. Other solvents were reagent grade. All organic and inorganic salts were Fluka or Aldrich analytical reagent grade and were used as received. 1-SH-1,2-$C_2B_{10}H_{11}$ was prepared according to the literature.[29]

Synthesis of [3,3′-Co(8-$C_4H_8O_2$-1,2-$C_2B_9H_{10}$)(1′,2′-$C_2B_9H_{11}$)] (2). To 0.90 g (2.0 mmol) of Cs[3,3′-Co(1,2-$C_2B_9H_{11}$)$_2$] in 100 mL of 1,4-dioxane was added 2.0 mL (16.0 mmol) of Et_2O·BF_3 and the reaction mixture heated at reflux under an N_2 atmosphere for 5 h. The solution was cooled to room temperature, filtered, and evaporated to dryness. The residue was taken up in dichloromethane and passed through a layer of silica using dichloromethane as the eluent. The eluate was evaporated in vacuo, giving 0.76 g (94%) of orange solid, for which the ^{1}H and ^{11}B NMR spectra were identical with those of an authentic sample prepared according to the literature.[10b]

Synthesis and Isolation of 1,1′-*μ*-{S($CH_2CH_2O)_3$-CH_2CH_2S}-(1,2-$C_2B_{10}H_{11}$)$_2$ (3). To a stirred solution of KOH (0.48 g, 8.51 mmol) in EtOH was added 1.50 g (8.51 mmol) of 1-SH-1,2-$C_2B_{10}H_{11}$. The mixture was stirred at room temperature for 30 min, and then bis[2-(2-chloroethoxy)ethyl] ether (0.98 g, 4.26 mmol) was added. The solution was refluxed for 2 h. After removal of the solvent, the residue was extracted with water and diethyl ether. The organic phase was washed with a KOH solution and dried over anhydrous magnesium sulfate. The solvent was removed, and the yellow residue was purified by column chromatography using ethyl acetate as the mobile phase (R_f = 0.875). Yield: 1.7 g (78%). ^{1}H NMR ($(CD_3)_2CO$): *δ* 3.93 (s, 2H, C_c-*H*), 3.69−3.62 (m, 12H, CH_2O), 3.10 (t, ^3J(H,H) = 7, 4H, CH_2O). ^{13}C{^{1}H} NMR ($(CD_3)_2CO$): *δ* 74.66 (C_c−H), 71.27 (C_c−H), 70.34 (*C*H_2O), 69.22 (*C*H_2O), 68.16 (*C*H_2O), 37.00 (S*C*H_2). ^{11}B NMR ($(CD_3)_2CO$): *δ* −1.3 (d, ^1J(B,H) = 156, 1B, B(9)), −4.7 (d, ^1J(B,H) = 148, 1B, B(12)), −8.6 (d, ^1J(B,H) = 143, 4B), −12.2 (d, ^1J(B,H) = 163, 4B). IR (cm^{-1}): *ν* 3067, 3041 (C_c−H), 2942, 2869 (C−H), 2599 (B−H), 1119 (C−O). Anal. Calcd for $C_{12}H_{38}B_{20}O_3S_2$: C, 28.22; H, 7.50; S, 12.55. Found: C, 28.61; H, 7.42; S, 12.17.

Synthesis and Isolation of [N($CH_3)_4]_2$[7,7′-*μ*-{S-($CH_2CH_2O)_3CH_2CH_2$S}(7,8-$C_2B_9H_{11}$)$_2$] (4). To a stirred solution of **3** (0.40 g, 0.78 mmol) in 15 mL of EtOH was added 1.08 g (11.86 mmol) of NMe_4OH (in MeOH at 25%). The solution was refluxed for 4 h. A white precipitate appeared after cooling with ice. The solid was collected by filtration and washed with water and petroleum ether. Yield: 0.37 g (91%). ^{1}H NMR ($CDCl_3$): *δ* 3.66−3.57 (m, 12H, CH_2O), 3.44 (s, 24H, N(C$H_3)_4$), 3.13−2.99 (m, 2H, SCH_2), 2.71−2.62 (m, 2H, SCH_2), −2.81 (br s, 2H, B−*H*−B). ^{13}C{^{1}H} NMR ($CDCl_3$): *δ* 71.17 (*C*H_2O), 70.19 (*C*H_2O), 70.01 (*C*H_2O), 55.25 (N(*C*$H_3)_4$), 35.67 (S*C*H_2). ^{11}B NMR ($CDCl_3$): *δ* −9.5 (d, ^1J(B,H) = 77, 1B), −10.2 (d, ^1J(B,H) = 72, 1B), −14.5 (d, ^1J(B,H) = 251, 1B), −17.0 (d, ^1J(B,H) = 134, 3B), −21.8 (d, ^1J(B,H) = 152, 1B), −32.6 (d, ^1J(B,H) = 131, 1B), −36.2 (d, ^1J(B,H) = 143, 1B). IR (cm^{-1}): *ν* 3045 (C_c−H), 2916, 2867 (C−H), 2531 (B−H), 1480 (δ(C−H)$_{alkyl}$), 1116, 1083 (C−O). Anal. Calcd for $C_{20}H_{62}B_{18}$-$N_2O_3S_2$: C, 37.68; H, 9.80; N, 4.39; S, 10.06. Found: C, 37.48; H, 9.44; N, 4.18; S, 9.16.

Synthesis and Isolation of [1,1′-*μ*-{S($CH_2CH_2O)_3$-CH_2CH_2S}-3,3′-Co(1,2-$C_2B_9H_{10}$)$_2$]$^-$ ([5]$^-$). To 30 mL of dimethoxyethane containing 0.27 g (0.42 mmol) of **4** were added 1.12 g (8.64 mmol) of $CoCl_2$ and 0.96 g (8.64 mmol) of K[^{t}BuO]. The mixture was refluxed for 24 h. The solvent was evaporated, and a CH_2Cl_2/H_2O mixture was added, along with an excess of NaCl and a few drops of 1 M HCl. A red organic layer was obtained along with a brown solid in the CH_2Cl_2/H_2O interlayer. The organic layer was separated and dried over anhydrous magnesium sulfate. The solvent was removed, and the residue was purified by successive preparative TLC in silica gel/gypsum using CH_2Cl_2/CH_3CN (10:1) as eluent. Three bands were separated: **5a** (R_f = 0.05), **5b** (R_f = 0.08),

(28) Llop, J.; Masalles, C.; Viñas, C.; Teixidor, F.; Sillanpää, R.; Kivekäs, R. *J. Chem. Soc., Dalton Trans.* **2003**, 556−561.
(29) Viñas, C.; Benakki, R.; Teixidor, F.; Casabó, J. *Inorg. Chem.* **1995**, *34*, 3844−3845.

and **5c** (R_f = 0.24). The brown solid from the interlayer was treated with an acidic aqueous solution and CH_2Cl_2, to produce a red-orange organic layer. After drying, separation was performed as above to produce the same set of bands. The combined yield were as follows: **5a**, 51%, 0.125 g; **5b**, 20%, 0.057 g; **5c**, 11%, 0.038 g. **Na[5]** (**5a**): ^{1}H NMR ($(CD_3)_2CO$): δ 4.36 (s, 1H, C_c−*H*), 4.28 (s, 1H, C_c−*H*), 4.03−3.63 (m, 12H, C*H*$_2$O), 3.18−3.13 (m, 4H, SC*H*$_2$). ^{13}C{^{1}H} NMR ($(CD_3)_2CO$): δ 69.68 (*C*H$_2$O), 67.73 (*C*$_c$−H), 63.89 (*C*$_c$−H), 37.59 (S*C*H$_2$). ^{11}B NMR ($(CD_3)_2CO$): δ 8.1 (d, ^1J(B,H) = 50), 1.0, −2.1, −6.1, −7.4, −15.1 (d, ^1J(B,H) = 88). IR (cm^{-1}): ν 3029 (C_c−H), 2824, 2868 (C−H), 2553 (B−H), 1082 (C−O). Anal. Calcd for $C_{12}H_{36}B_{18}CoNaO_3S_2$: C, 25.35; H, 6.32; S, 11.27. Found: C, 25.73; H, 6.11; S, 11.18. **Na[5]**·2($CH_3)_2CO$ (**5b**): ^{1}H NMR ($(CD_3)_2CO$): δ 4.15 (s, 2H, C_c−*H*), 3.78−3.56 (m, 12H, C*H*$_2$O), 3.29−2.90 (m, 4H, SC*H*$_2$), 2.90 (s, 12H, (C*H*$_3$)$_2$CO). ^{13}C{^{1}H} NMR ($(CD_3)_2$-CO): δ 70.46 (*C*H$_2$O), 70.27 (*C*H$_2$O), 69.65 (*C*H$_2$O), 67.39 (*C*$_c$−H), 65.30 (*C*$_c$−H), 37.59 (S*C*H$_2$). ^{11}B NMR ($(CD_3)_2CO$): δ 7.9 (d, ^1J(B,H) = 141, 2B), 0.6 (d, ^1J(B,H) = 141, 2B), −3.1 (d, ^1J(B,H) = 129, 2B), −4.1 (d, ^1J(B,H) = 111, 4B), −7.2 (d, ^1J(B,H) = 143, 2B), −11.7 (d, ^1J(B,H) = 154, 2B). −15.7 (d, ^1J(B,H) = 153, 2B), −20.4 (d, ^1J(B,H) = 154, 2B). IR (cm^{-1}): ν 3030 (C_c−H), 2931, 2900 (C−H), 2554 (B−H), 1108, 1082 (C−O). Anal. Calcd for $C_{18}H_{48}B_{18}CoNaO_5S_2$: C, 31.55; H, 7.06; S, 9.36. Found: C, 31.08; H, 6.86; S, 8.85. **Na[5]**·($CH_3)_2CO$·$CHCl_3$·CH_2Cl_2 (**5c**): ^{1}H NMR ($(CD_3)_2CO$): δ 4.16 (s, 1H, C_c−*H*), 3.93 (s, 1H, C_c−*H*), 3.89−3.46 (m, 12H, C*H*$_2$O), 3.31−2.97 (m, 4H, SC*H*$_2$), 2.91 (s, 6H, (C*H*$_3$)$_2$CO). ^{13}C{^{1}H} NMR ($(CD_3)_2CO$): δ 70.51 (*C*H$_2$O), 69.94 (*C*H$_2$O), 69.67 (*C*H$_2$O), 60.58 (*C*$_c$−H), 58.27 (*C*$_c$−H), 38.31 (S*C*H$_2$), 37.54 (S*C*H$_2$). ^{11}B NMR ($(CD_3)_2CO$): δ 6.3 (d, ^1J(B,H) = 122, 2B), 0.9 (d, ^1J(B,H) = 145, 2B), −2.9 (d, ^1J(B,H) = 139, 3B), −4.4 (d, ^1J(B,H) = 144, 1B), −6.8 (d, ^1J(B,H) = 104, 6B), −12.6 (d, ^1J(B,H) = 177, 2B), −15.8 (d, ^1J(B,H) = 119, 1B), −17.3 (d, ^1J(B,H) = 126, 1B). IR (cm^{-1}): ν 2970, 2931, 2868 (C−H), 2561 (B−H), 1110, 1082 (C−O). Anal. Calcd for $C_{17}H_{45}B_{18}Cl_5CoNaO_4S_2$: C: 24.56; H, 5.45; S, 7.71. Found: C, 24.28; H, 5.66; S, 8.05.

Synthesis and Isolation of the Sodium Salt of [3,3′-Co(8-{O(CH$_2$CH$_2$O)$_2$CH$_3$}-1,2-C$_2$B$_9$H$_{10}$)(1′,2′-C$_2$B$_9$H$_{11}$)]$^-$ (6). A 60 mL portion of deoxygenated CH_3OH containing 68.4 mg (1.22 mmol) of NaOH was stirred for 45 min. Then 500 mg (1.22 mmol) of [8-(OCH$_2$CH$_2$)$_2$-3,3′-Co(1,2-C$_2$B$_9$H$_{10}$)(1′,2′-C$_2$B$_9$H$_{11}$)] (**2**) was added. The mixture was stirred for 15 min, and then this was evaporated to dryness in vacuo. Purification by thin-layer chromatography (silica gel, dichloromethane/ethanol (9:1)) yielded analytically pure **6**. Yield: 555 mg (98%). ^{1}H NMR ($(CD_3)_2CO$): δ 4.10 (br s, 2H, C_c−*H*), 4.04 (br s, 2H, C_c−*H*), 3.99 (br s, 2H, OC*H*$_2$), 3.68 (t, ^3J(H,H) = 4, 6H, OC*H*$_2$), 3.45 (s, 3H, C*H*$_3$), 3.20−1.44 (br m, 17H, B−*H*). ^{1}H{^{11}B} NMR ($(CD_3)_2CO$): δ 4.10 (br s, 2H, C_c−*H*), 4.04 (br s, 2H, C_c−*H*), 3.99 (t, ^3J(H,H) = 4, 2H, OC*H*$_2$), 3.68 (t, ^3J(H,H) = 4, 6H, OC*H*$_2$), 3.45 (s, 3H, C*H*$_3$), 3.20 (br s, 1H, B−*H*), 2.99 (br s, 3H, B−*H*), 2.74 (br s, 3H, B−*H*), 2.13 (br s, 2H, B−*H*), 1.96 (br s, 2H, B−*H*), 1.70 (br s, 1H, B−*H*), 1.64 (br s, 2H, B−*H*), 1.54 (br s, 2H, B−*H*), 1.44 (br s, 1H, B−*H*). ^{13}C{^{1}H} NMR ($(CD_3)_2$-CO): δ 71.69 (O*C*H$_2$), 70.62 (O*C*H$_2$), 69.87 (O*C*H$_2$), 69.00 (O*C*H$_2$), 57.87 (*C*H$_3$), 52.55 (*C*$_c$−H), 47.17 (*C*$_c$−H). ^{11}B NMR ($(CD_3)_2CO$): δ 23.8 (s, 1B, B(8)), 8.0 (d, ^1J(B,H) = 137, 1B), 2.5 (d, ^1J(B,H) = 139, 1B), −1.5 (d, ^1J(B,H) = 146, 1B), −3.9 (d, ^1J(B,H) = 130, 2B), −5.1 (d, ^1J(B,H) = 123, 2B), −5.8 (d, ^1J(B,H) = 143, 2B), −8.2 (d, ^1J(B,H) = 142, 2B), −15.9 (d, ^1J(B,H) = 152, 2B), −19.2 (d, ^1J(B,H) = 159, 2B), −21.2 (d, ^1J(B,H) = 158, 1B), −27.2 (d, ^1J(B,H) = 157, 1B). IR (cm^{-1}): ν 3034 (C_c−H), 2932, 2883, 2839 (C_{alkyl}−H), 2573, 2544, 2534 (B−H), 1099, 1049 (C−O and ν_{as}(C−O−C)), 1454, 1365 (δ(C_{alkyl}−H)), 1296, 750 (γ(C_{alkyl}−H)). Anal. Calcd for $C_9H_{32}B_{18}CoNaO_3$: C, 23.25; H, 6.94. Found: C, 23.52; H, 7.33. MALDI-TOF (*m*/*z*): 442.54 (M; 100%), 456.54 (M + CH_2; 76%), 470.54 (M + CH_2CH_2; 47%), 427.50 (M − CH_3; 18%), 411.51 (M − OCH_3; 35%), 397.48 (M − CH_2OCH_3; 47%), 382.47 (M − $CH_2CH_2OCH_3$; 49%), 367.46 (M − $OCH_2CH_2OCH_3$; 58%), 353.46 (M − $CH_2OCH_2CH_2OCH_3$; 60%), 339.44 (M − CH_2CH_2-$OCH_2CH_2OCH_3$; 61%), 324.43 (M − $OCH_2CH_2OCH_2CH_2OCH_3$; 60%).

Synthesis and Isolation of the Sodium Salt of [3,3′-Co(8-{O(CH$_2$CH$_2$O)$_2$CH$_2$CH$_3$}-1,2-C$_2$B$_9$H$_{10}$)(1′,2′-C$_2$B$_9$H$_{11}$)]$^-$ (7). This compound was prepared by utilizing the same procedure as for **6**, but in deoxygenated CH_3CH_2OH. Yield: 572 mg (98%). ^{1}H NMR (CD_2Cl_2): δ 3.81 (br s, 2H, OC*H*$_2$), 3.71−3.61 (m, 10H: 8H, OC*H*$_2$; 2H, C_c−*H*), 3.49 (br s, 2H, C_c−*H*), 2.96−1.47 (br m, 17H, B−*H*), 1.23 (t, ^3J(H,H) = 7, 3H, C*H*$_3$). ^{1}H{^{11}B} NMR (CD_2Cl_2): δ 3.81 (t, ^3J(H,H) = 4, 2H, OC*H*$_2$), 3.71−3.61 (m, 10H: 8H, OC*H*$_2$; 2H, C_c−*H*), 3.49 (br s, 2H, C_c−*H*), 2.96, 2.90 (br s, 4H, B−*H*), 2.71 (br s, 1H, B−*H*), 2.54 (br s, 2H, B−*H*), 2.15 (br s, 2H, B−*H*), 2.09 (br s, 2H, B−*H*), 1.87 (br s, 2H, B−*H*), 1.64 (br s, 3H, B−*H*), 1.47 (br s, 1H, B−*H*), 1.23 (t, ^3J(H,H) = 7, 3H, C*H*$_3$). ^{13}C{^{1}H} NMR (CD_2Cl_2): δ 71.71 (O*C*H$_2$), 69.17 (O*C*H$_2$), 68.95 (O*C*H$_2$), 68.32 (O*C*H$_2$), 67.39 (O*C*H$_2$), 51.08 (*C*$_c$−H), 47.50 (*C*$_c$−H), 14.67 (*C*H$_3$). ^{11}B NMR (CD_2Cl_2): δ 26.9 (s, 1B, B(8)), 6.4 (d, ^1J(B,H) = 133, 1B), 1.9 (d, ^1J(B,H) = 141, 1B), −1.1 (d, ^1J(B,H) = 150, 1B), −5.7 (d, ^1J(B,H) = 134, 6B), −7.5 (d, ^1J(B,H) = 174, 2B), −16.1 (d, ^1J(B,H) = 161, 2B), −17.9 (d, ^1J(B,H) = 164, 2B), −20.9 (d, ^1J(B,H) = 162, 1B), −28.0 (d, ^1J(B,H) = 144, 1B). IR (cm^{-1}): ν 3038 (C_c−H), 2980, 2912, 2874 (C_{alkyl}−H), 2554, 2534 (B−H), 1121, 1105, 1082, 1075 (C−O and ν_{as}(C−O−C)), 1454, 1348 (δ(C_{alkyl}−H)), 1248, 748 (γ(C_{alkyl}−H)). Anal. Calcd for $C_{10}H_{34}B_{18}CoNaO_3$: C, 25.08; H, 7.16. Found: C, 25.01; H, 7.27. MALDI-TOF (*m*/*z*): 456.56 (M; 100%), 470.58 (M + CH_2; 46%), 484.60 (M + CH_2CH_2; 23%), 498.62 (M + $CH_2CH_2CH_2$; 7%), 441.56 (M − CH_3; 7%), 427.51 (M − CH_2CH_3; 17%), 410.50 (M − OCH_2CH_3; 5%), 395.49 (M − $CH_2OCH_2CH_3$; 7%), 381.46 (M − $CH_2CH_2OCH_2CH_3$; 11%), 366.46 (M − $OCH_2CH_2OCH_2CH_3$; 10%), 353.44 (M − $CH_2OCH_2CH_2OCH_2CH_3$; 15%), 338.41 (M − $CH_2CH_2OCH_2CH_2OCH_2CH_3$; 11%), 324.31 (M − OCH_2CH_2-$OCH_2CH_2OCH_2CH_3$; 5%).

Synthesis and Isolation of the Sodium Salt of [3,3′-Co(8-{O(CH$_2$CH$_2$O)$_3$CH$_3$}-1,2-C$_2$B$_9$H$_{10}$)(1′,2′-C$_2$B$_9$H$_{11}$)]$^-$ (8). This compound was prepared using the same procedure as for **6**, but in deoxygenated $CH_3OCH_2CH_2OH$. Yield: 595 mg (96%). ^{1}H NMR ($(CD_3)_2CO$): δ 4.17 (br s, 4H, C_c−*H*), 3.75 (br s, 2H, OC*H*$_2$), 3.65−3.54 (m, 10H, OC*H*$_2$), 3.35 (s, 3H, C*H*$_3$), 2.94−1.46 (br m, 17H, B−*H*). ^{1}H NMR ($(CD_3)_2CO$, −60 °C)): δ 4.19 (br s, 2H, C_c−*H*), 4.13 (br s, 2H, C_c−*H*), 3.75 (br s, 2H, OC*H*$_2$), 3.65−3.54 (m, 10H, OC*H*$_2$), 3.35 (s, 3H, C*H*$_3$), 2.94−1.46 (br m, 17H, B−*H*). ^{1}H{^{11}B} NMR ($(CD_3)_2CO$): δ 4.17 (br s, 4H, C_c-*H*), 3.75 (t, ^3J(H,H) = 4, 2H, OC*H*$_2$), 3.65−3.54 (m, 10H, OC*H*$_2$), 3.35 (s, 3H, C*H*$_3$), 2.94 (br s, 3H, B−*H*), 2.84 (br s, 1H, B−*H*), 2.71 (br s, 3H, B−*H*), 2.05 (br s, 2H, B−*H*), 1.87 (br s, 2H, B−*H*), 1.64 (br s, 3H, B−*H*), 1.55 (br s, 2H, B−*H*), 1.46 (br s, 1H, B−*H*). ^{13}C{^{1}H} NMR ($(CD_3)_2CO$): δ 71.27 (O*C*H$_2$), 69.68 (O*C*H$_2$), 69.46 (O*C*H$_2$), 68.60 (O*C*H$_2$), 58.12 (*C*H$_3$), 52.88 (*C*$_c$−H), 46.76 (*C*$_c$−H). ^{11}B NMR ($(CD_3)_2CO$): δ 24.4 (s, 1B, B(8)), 6.5 (d, ^1J(B,H) = 137, 1B), 1.6 (d, ^1J(B,H) = 141, 1B), −1.6 (d, ^1J(B,H) = 153, 1B), −3.9 (d, ^1J(B,H) = 158, 2B), −6.0 (d, ^1J(B,H) = 150, 2B), −6.4 (d, ^1J(B,H) = 132, 2B), −7.9 (d, ^1J(B,H) = 139, 2B), −16.3 (d, ^1J(B,H) = 153, 2B), −19.5 (d, ^1J(B,H) = 158, 2B), −21.3 (d, ^1J(B,H) = 167, 1B), −27.6 (d, ^1J(B,H) = 160, 1B). IR (cm^{-1}): ν 3042 (C_c−H), 2932, 2903, 2874 (C_{alkyl}−H), 2573, 2538 (B−H), 1161, 1094, 1057 (C−O and ν_{as}(C−O−C)), 1470, 1350 (δ(C_{alkyl}−H)), 1252, 748 (γ(C_{alkyl}−H)). Anal. Calcd for $C_{11}H_{36}B_{18}CoNaO_4$: C, 25.96; H, 7.13. Found: C, 25.83; H, 7.24. MALDI-TOF (*m*/*z*): 499.58 (M; 100%), 514.60 (M + CH_3; 49%), 528.61 (M + CH_2CH_3; 13%), 456.53 (M − OCH_2CH_2; 5%), 442.52 (M − $CH_2OCH_2CH_2$; 4%), 428.50 (M − $CH_2CH_2OCH_2CH_2$; 3%), 383.46 (M − $CH_2CH_2OCH_2CH_2OCH_2$-CH_2; 4%), 354.44 (M − $CH_2OCH_2CH_2OCH_2CH_2OCH_2CH_2$; 4%), 340.42 (M − $CH_2CH_2OCH_2CH_2OCH_2CH_2OCH_2$ CH_2; 20%), 324.41 (M − $OCH_2CH_2OCH_2CH_2OCH_2CH_2$ OCH_2CH_2; 17%).

Synthesis and Isolation of the Sodium Salt of [3,3′-Co(8-{O(CH$_2$CH$_2$O)$_3$CH$_2$CH$_3$}-1,2-C$_2$B$_9$H$_{10}$)(1′,2′-C$_2$B$_9$H$_{11}$)]$^-$ (9). This compound was prepared using the same

procedure as for **6** but in deoxygenated $CH_3CH_2OCH_2CH_2OH$. Yield: 611 mg (96%). ^{1}H NMR ($(CD_3)_2CO$): δ 4.19 (br s, 2H, C_c−*H*), 4.16 (br s, 2H, C_c−*H*), 3.69−3.44 (m, 14H, O*CH*$_2$), 2.91−1.37 (br m, 17H, B−*H*), 1.15 (t, ^3J(H,H) = 6, 3H, *CH*$_3$). ^{1}H{^{11}B} NMR ($(CD_3)_2CO$): δ 4.19 (br s, 2H, C_c−*H*), 4.16 (br s, 2H, C_c−*H*), 3.69−3.44 (m, 14H, O*CH*$_2$), 2.91 (br s, 3H, B−*H*), 2.72 (br s, 1H, B−*H*), 2.68 (br s, 3H, B−*H*), 2.02 (br s, 2H, B−*H*), 1.81 (br s, 2H, B−*H*), 1.63 (br s, 1H, B−*H*), 1.54 (br s, 2H, B−*H*), 1.46 (br s, 2H, B−*H*), 1.37 (br s, 1H, B−*H*). ^{13}C{^{1}H} NMR ($(CD_3)_2CO$): δ 71.80 (O*CH*$_2$), 70.22 (O*CH*$_2$), 70.02 (O*CH*$_2$), 69.96 (O*CH*$_2$), 69.41 (O*CH*$_2$), 68.47 (O*CH*$_2$), 66.05 (O*CH*$_2$), 53.38 (*C*$_c$−H), 46.56 (*C*$_c$−H), 14.62 (*CH*$_3$). ^{11}B NMR ($(CD_3)_2CO$): δ 24.4 (s, 1B, B(8)), 5.9 (d, ^1J(B,H) = 128, 1B), 1.3 (d, ^1J(B,H) = 140, 1B), −1.6 (d, ^1J(B,H) = 186, 1B), −3.7 (d, ^1J(B,H) = 166, 2B), −6.3 (d, ^1J(B,H) = 139, 6B), −16.4 (d, ^1J(B,H) = 145, 2B), −19.5 (d, ^1J(B,H) = 152, 2B), −21.2 (d, ^1J(B,H) = 115, 1B), −27.5 (d, ^1J(B,H) = 135, 1B). IR (cm^{-1}): ν 3038 (C_c−H), 2922, 2870 (C_{alkyl}−H), 2557 (B−H), 1097 (C−O and ν_{as}(C−O−C)), 1454, 1348 (δ(C_{alkyl}−H)), 1248, 748 (γ(C_{alkyl}−H)). Anal. Calcd for $C_{12}H_{38}B_{18}CoNaO_4$: C, 27.56; H, 7.32. Found: C, 27.55; H, 7.26. MALDI-TOF (*m*/*z*): 500.56 (M; 100%), 514.58 (M + CH_2; 62%), 528.60 (M + CH_2CH_2; 16%), 383.45 (M − $CH_2CH_2OCH_2CH_2OCH_2CH_3$; 5%), 367.45 (M − $OCH_2CH_2OCH_2CH_2OCH_2CH_3$; 4%), 353.43 (M − CH_2OCH_2-$CH_2OCH_2CH_2OCH_2$ CH_3; 4%), 339.41 (M − $CH_2CH_2OCH_2CH_2$-$OCH_2CH_2OCH_2CH_3$; 14%), 323.41(M − OCH_2 $CH_2OCH_2CH_2$-$OCH_2CH_2OCH_2CH_3$; 11%).

X-ray Diffraction Studies. X-ray Structure Determinations of Na[5b]·2$(CH_3)_2$CO, Na[5c]·$(CH_3)_2$CO·$CHCl_3$·CH_2Cl_2, and Na[7]. Single-crystal data collections for **Na[5b]**·2$(CH_3)_2$CO and **Na[5c]**·$(CH_3)_2$CO·$CHCl_3$·CH_2Cl_2 were performed at room temperature on a Rigaku AFC5S diffractometer using graphite-monochromated Mo Kα radiation, while a crystal of **Na[7]** was measured on a Nonius KappaCCD diffractometer at −100 °C. Totals of 3213, 6912, and 4774 unique reflections were collected for **Na[5b]**·2$(CH_3)_2$CO, **Na[5c]**·$(CH_3)_2$CO·$CHCl_3$·CH_2Cl_2, and **Na[7]**, respectively.

The structures were solved by direct methods and refined on F^2 by the SHELXL97 program.[20] For **Na[5b]**·2$(CH_3)_2$CO, boron atoms were refined with isotropic displacement parameters, but other non-hydrogen atoms were refined with anisotropic displacement parameters. **Na[5b]**·2$(CH_3)_2$CO crystallizes in a noncentrosymmetric space group, and the absolute configuration of **Na[5b]**·2$(CH_3)_2$CO was determined by refinement of the Flack *x* parameter. For **Na[5c]**·$(CH_3)_2$CO·$CHCl_3$·CH_2Cl_2 and **Na[7]**, all non-hydrogen atoms were refined with anisotropic displacement parameters. For all structures, the hydrogen atoms were treated as riding atoms using the SHELX97 default parameters.

Acknowledgment. This work was supported by the MCyT (Grant No. MAT01-1575) and the INTAS (Grant No. 99-00806).

Supporting Information Available: Tables giving detailed crystallographic data, atomic positional and thermal displacement parameters, and bond distances and angles for Na[1,1′-μ-{$S(CH_2CH_2O)_3CH_2CH_2S$}-3,3′-Co(1,2-$C_2B_9H_{10})_2$]·2$(CH_3)_2$CO (**Na[5b]**·2$(CH_3)_2$CO), Na[1,1′-μ-{$S(CH_2CH_2O)_3$-CH_2CH_2S}-3,3′-Co(1,2-$C_2B_9H_{10})_2$]·$(CH_3)_2$CO·$CHCl_3$· CH_2Cl_2 (**Na[5c]**·$(CH_3)_2$CO·$CHCl_3$·CH_2Cl_2), and Na[3,3′-Co(8-{$O(CH_2$-$CH_2O)_2CH_2CH_3$}-1,2-(1,2-$C_2B_9H_{10}$)(1′,2′-$C_2B_9H_{11}$)] **(Na[7])**. This material is available free of charge via the Internet at http://pubs.acs.org.

OM030135O

Relevance of the Electronegativity of Boron in η^5-Coordinating Ligands: Regioselective Monoalkylation and Monoarylation in Cobaltabisdicarbollide $[3,3'\text{-}Co(1,2\text{-}C_2B_9H_{11})_2]^-$ Clusters

Isabel Rojo,[a] Francesc Teixidor,*[a] Clara Viñas,[a] Raikko Kivekäs,[b] and Reijo Sillanpää[c]

Abstract: Regioselective monoalkylation and monoarylation in cobaltabisdicarbollide clusters has been achieved starting from $Cs[8\text{-}I\text{-}3,3'\text{-}Co(1,2\text{-}C_2B_9H_{10})(1',2'\text{-}C_2B_9H_{11})]$ by cross-coupling reactions between a B–I fragment and an appropriate Grignard reagent in the presence of a Pd catalyst and CuI. A considerable number of monoalkylated and monoarylated derivatives have been synthesized, which allowed study of the influence of boron in metallocene-type ligands and the effect of alkyl and aryl substituents on boron in boron anionic clusters. Experimental data from UV/Vis spectroscopy, $E_{1/2}$ measurements, and X-ray diffraction analysis, and supported by EHMO and ab initio analyses, indicate that the participation of metal d orbitals in the HOMO is less than that in typical metallocene complexes. This can be explained in terms of the lower electronegativity of boron compared to carbon. Related to this is the –I character of alkyl groups when bonded to boron in boron anionic clusters, contrary to the common belief that alkyl groups are generally electron-releasing moieties.

Keywords: cobalt · B–C coupling · charge transfer · cross-coupling · isolobal relationship

Introduction

The cyclopentadienyl ligand, $[C_5H_5]^-$, produces "half-sandwich" and "sandwich" compounds, metallocenes that occur widely in contemporary organometallic chemistry. It is usually assumed that for generic metallocenes the six lowest orbitals are based mainly on the contributions of the $[C_5H_5]^-$ orbitals and that the next five MOs have little or no bonding character.[1] This orbital diagram can be modulated on going to substituted $[C_5H_5]^-$ derivatives. In this sense, the pentamethylcyclopentadienyl, $[C_5Me_5]^-$ or Cp*, is one of the best known, allowing the isolation of Cp* complexes for which $[C_5H_5]^-$ analogues are unknown or are kinetically unstable.[2] The methyl groups on Cp* are electron-releasing, and this results in more electron density at the metal than in the analogous $[C_5H_5]^-$ complexes. Accordingly, electrochemical measurements indicate that Cp* complexes are more easily oxidized than the $[C_5H_5]^-$ analogues by approximately 0.5 V.[1] Other examples of $[C_5H_5]^-$ derivatives include C_5Me_4H,[3] C_5H_4Me,[4] and the important class of indenyl complexes.[5] More profound changes are obtained by replacing a carbon by nitrogen, as in the structurally analogous pyrrolyl anion $[NC_4H_4]^-$.[6] Similarly to $[C_5H_5]^-$, more stable ligand molecular orbitals are generated, due to the higher electronegativity of nitrogen.[7, 8] In this case, the nonbonding character of the metal d orbitals should be even more enhanced than that in $[C_5H_5]^-$ metallocenes. The question that arises is whether this situation can be reversed. We hypothesized that the incorporation of the less electronegative boron in the ring should produce a different situation.

Recently, alkyl substitution on boron in boron clusters has become a subject of renewed interest. Alkylations with different degrees of alkyl incorporation have been performed on $[B_{12}H_{12}]^{2-}$,[9] $[CB_{11}H_{11}]^-$,[10] $p\text{-}C_2B_{10}H_{12}$,[11] $m\text{-}C_2B_{10}H_{12}$,[12]

[a] Dr. F. Teixidor, I. Rojo,[+] Dr. C. Viñas
Institut de Ciència de Materials de Barcelona (C.S.I.C.)
Campus de la U.A.B., 08193 Bellaterra (Spain)
Fax: +34 (9)-3-5805729
E-mail: teixidor@icmab.es

[b] R. Kivekäs
Department of Chemistry, P.O. Box 55
University of Helsinki
00014 Helsinki (Finland)

[c] R. Sillanpää
Department of Chemistry, University of Jyväskylä
40351 Jyväskylä (Finland)

[+] I. Rojo
Isabel Rojo is enrolled in the Ph.D. program of the UAB.

Supporting information for this article is available on the WWW under http://www.chemeurj.org or from the author: ^1H and $^{13}C\{^1H\}$ NMR spectra for compounds $[\mathbf{2}]^- - [\mathbf{9}]^-$.

 DOI: 10.1002/chem.200304970

and *o*-$C_2B_{10}H_{12}$.[13] Except in the case of *o*-carborane, alkylation procedures have been directed towards permethylation by using strong methylating agents such as MeI/$AlCl_3$[12] or CF_3SO_3Me.[11, 14] In the case of *o*-carborane, selective alkylations/arylations at positions 9, 12 or 3 have been successfully achieved from the corresponding iodo derivatives.[15] However, the derivative chemistry of the most extensively studied of the anionic borate clusters, the cobaltabisdicarbollide [3,3′-Co(1,2-$C_2B_9H_{11}$)$_2$]$^-$ ([**1**]$^-$), remains very much unexplored.[16] The fundamental reason for this is the synthetic strategy leading to these derivatives. Two basic substitutions may occur on [**1**]$^-$, on either carbon or boron. With few exceptions,[17] substitutions on carbon have been achieved at a very early stage on the starting *o*-carborane,[18] and therefore [**1**]$^-$ has not been used as starting material. Substitution on boron has been achieved under Friedel–Crafts conditions[19] or with strong alkylating agents.[20] Consequently, regioselective substitutions have not been possible, and specific derivatives could only be obtained after careful separations of complex mixtures. Very recently, the facile, high-yielding preparation of the zwitterionic 8-dioxanate derivative [8-$C_4H_8O_2$-3,3′-Co(1,2-$C_2B_9H_{10}$)(1′,2′-$C_2B_9H_{11}$)][21] has facilitated the preparation of many derivatives of [**1**]$^-$ by nucleophilic ring opening.[22] An alternative starting material is [8-OH-3,3′-Co(1,2-$C_2B_9H_{10}$)(1′,2′-$C_2B_9H_{11}$)]$^-$.[23] Besides these remarkable compounds, there are the readily available halogeno derivatives of [**1**]$^-$.[24] In this regard, regiospecific syntheses of 8-I and 8,8′-I_2[25] have been described, but no 8-alkyl/aryl derivatives have been reported. As mentioned by Bregadze in 1992,[26] halogeno derivatives appear to be inert towards substitution reactions, although Hawthorne and co-workers have recently shown that starting from [3,3′-Co(8,9,12-I_3-1,2-$C_2B_9H_8$)$_2$]$^-$ it is possible to achieve the hexasubstitution of [**1**]$^-$.[27] This opened up the possibility of achieving monosubstitution from [8-I-3,3′-Co(1,2-$C_2B_9H_{10}$)(1′,2′-$C_2B_9H_{11}$)]$^-$ ([**2**]$^-$). Figure 1 shows the numbering of the vertices for compound [**2**]$^-$.

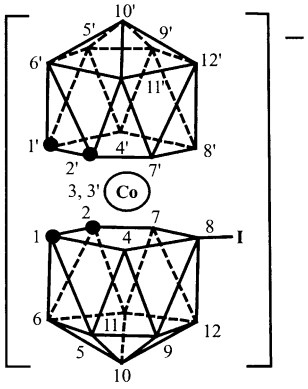

Figure 1. Numbering of the vertices for [8-I-3,3′-Co(1,2-$C_2B_9H_{10}$)(1′,2′-$C_2B_9H_{11}$)]$^-$ ([**2**]$^-$).

In this report, we describe how the latter compound, [**2**]$^-$, can be a suitable starting material for regiospecifically obtaining alkyl and aryl derivatives of [**1**]$^-$ and, with the compounds in hand, how we were able to study the effect of alkyl or aryl substitution on their electronic properties.

Results

Modified synthesis of Cs[8-I-3,3′-Co(1,2-$C_2B_9H_{10}$)(1′,2′-$C_2B_9H_{11}$)] (Cs[2]): Matel and co-workers[25] reported a method whereby [**1**]$^-$ could be quantitatively converted into the corresponding B8-monoiodinated compound ([**2**]$^-$). However, during our investigation we found that on applying the same procedure a mixture of the starting compound [**1**]$^-$ and the desired product [**2**]$^-$ was obtained. Therefore, we have slightly modified the reported procedure so as to obtain [**2**]$^-$ as a pure compound (see Experimental Section). Under our new reaction conditions, we were able to increase the yield from 84% in the reported reaction to 95%, and our work-up procedure is shorter.

Palladium-catalyzed B–C cross-coupling reactions on Cs[8-I-3,3′-Co(1,2-$C_2B_9H_{10}$)(1′,2′-$C_2B_9H_{11}$)] with Grignard reagents: We were interested in checking whether the cross-coupling methodology that can be successfully used at the antipodal, B9, and/or B12 *o*-carborane positions[15a,b] of 9,12-I_2-1,2-$C_2B_{10}H_{10}$ and 12-I-1,2-$C_2B_{10}H_{11}$, at the B3 vertex of 3-I-1,2-$C_2B_{10}H_{11}$, and at B8, B9, and B12[27] of the [3,3′-Co(8,9,12-I_3-$C_2B_9H_8$)$_2$]$^-$ could also be applied at the single B8 vertex of [8-I-3,3′-Co(1,2-$C_2B_9H_{10}$)(1′,2′-$C_2B_9H_{11}$)]$^-$. Successful B–C coupling reaction was achieved by using Cs[8-I-3,3′-Co(1,2-$C_2B_9H_{10}$)(1′,2′-$C_2B_9H_{11}$)] (Cs[**2**]) as the starting compound. The B–I unit was transformed into a B–R vertex by using a Grignard reagent in the presence of a palladium catalyst and copper(I) iodide as a cocatalyst.[15a] In a typical experiment, the Cs[**2**] salt was dissolved in THF and treated with the Grignard reagent at low temperatures (Scheme 1). A range of temperatures between −84 and 0 °C was typically investigated. A

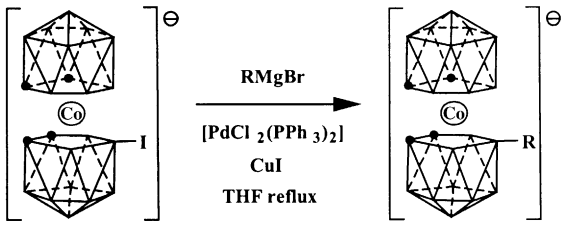

R = I ([**2**]$^-$)
R = Methyl ([**3**]$^-$)
R = Ethyl ([**4**]$^-$)
R = Phenyl ([**5**]$^-$)
R = Biphenyl ([**6**]$^-$)
R = Anthracenyl ([**7**]$^-$)
R = 4-Butylphenyl ([**8**]$^-$)
R = 2-Phenylethyl ([**9**]$^-$)

Scheme 1.

brown precipitate formed; the mixture was then allowed to warm to room temperature, whereupon the palladium catalyst and CuI were added in a single portion. A period of reflux, ranging from a few minutes to several hours, followed by work-up, yielded the desired compounds. The reaction provided good to very good yields of all the compounds (between 76 and 95%). The reaction seems to be quite general, once the optimal conditions in terms of temperature

and reaction time have been found. The versatility of the reaction has been explored by producing B8–alkyl (methyl [**3**]$^-$, ethyl [**4**]$^-$), B8–aryl (phenyl [**5**]$^-$, biphenyl [**6**]$^-$, anthracenyl [**7**]$^-$), combined aryl/alkyl (4-butylphenyl ([**8**]$^-$)), and combined alkyl/aryl (2-phenylethyl ([**9**]$^-$)) derivatives. Thus, it can be considered a general reaction for the regioselective generation of 8-alkyl or 8-aryl derivatives of compound [**1**]$^-$.

The Pd-catalyzed coupling of [**2**]$^-$ with Grignard reagents described here is proposed to follow the mechanistic pathway previously proposed for the similar Pd-catalyzed coupling of Grignard reagents with *B*-iodocarborane derivatives.[15a, 28] In these earlier reports, it was said that diminished yields are observed in reactions in which the intermediate in the catalytic cycle is capable of β-hydrogen elimination. If this were the case, low coupling yields would have been expected with ethylmagnesium bromide, but the corresponding product was obtained in reasonably good yield (80%). However, β-hydrogen elimination may account for the unsuccessful preparations of [8-CH_2=$CHCH_2$-3,3′-Co(1,2-$C_2B_9H_{10}$)-(1′,2′-$C_2B_9H_{11}$)]$^-$, [8-Cl$(CH_2)_3$-3,3′-Co(1,2-$C_2B_9H_{10}$)(1′,2′-$C_2B_9H_{11}$)]$^-$, [8-CH_2=$CH(CH_2)_3$-3,3′-Co(1,2-$C_2B_9H_{10}$)(1′,2′-$C_2B_9H_{11}$)]$^-$, and [8-Me$(CH_2)_9$-3,3′-Co(1,2-$C_2B_9H_{10}$)(1′,2′-$C_2B_9H_{11}$)]$^-$. Attempts to synthesize these compounds were made by reacting the cesium salt of [**2**]$^-$ with allylmagnesium bromide or with the corresponding Grignard reagents of 1-chloro-3-iodopropane, 5-bromopentene, and 1-bromodecane, respectively. The nature of [**3**]$^-$–[**9**]$^-$ has been corroborated by elemental analysis, MS, IR, and ^{1}H, ^{1}H{^{11}B}, ^{13}C{^{1}H}, ^{11}B, and ^{11}B{^{1}H} NMR spectroscopies, and where appropriate, for [*n*Bu_4N][**3**], [Me_4N][**8**], and [Me_4N][**9**], by X-ray crystal structure determination.

NMR spectral considerations

Qualitative description of the ^{11}B NMR spectra: The sensitivity of the electron distribution in carboranes to the presence of substituents has long been apparent.[29] For icosahedral carborane derivatives of 1-R-1,2-*closo*-$C_2B_{10}H_{11}$, ^{11}B NMR studies have shown that the chemical shifts of the cage boron atoms vary with the substituent R,[30] particularly that at the boron atom opposite to the point of attachment of the substituent, the "antipodal atom".[30b, 31] In this work, we report compounds with a substituent on the B8 atom of cobaltabisdicarbollide and the influence of this substituent on the ^{11}B chemical shift.

The ^{11}B{^{1}H} NMR data of [**1**]$^-$, [**2**]$^-$, and all of the monosubstituted compounds prepared in this work are shown in Table 1. The spectra can be interpreted considering the ^{11}B{^{1}H} NMR spectra of [**1**]$^-$ and [**2**]$^-$, the latter also being derived from [**1**]$^-$. The ^{11}B{^{1}H} NMR spectrum of [**1**]$^-$ displays five resonances in the range $\delta = +6.5$ to $\delta = -22.7$ with a 2:2:8:4:2 pattern, in agreement with an averaged C_{2v} symmetry. The ^{11}B NMR chemical shifts of compound [**1**]$^-$ were assigned with the aid of a 2D ^{11}B{^{1}H}-^{11}B{^{1}H} COSY experiment and correspond to B(8,8′), B(10,10′), B(4,4′,7,7′,9,9′,12,12′), B(5,5′,11,11′), and B(6,6′) from low to high field.[32] Incorporation of one iodine atom at position B8 lowers the symmetry to C_s, maintaining only one symmetry plane and rendering the two dicarbollide moieties non-equivalent. Therefore, the ^{11}B{^{1}H} NMR spectrum of [**2**]$^-$ displays ten resonances in the range $\delta = +6.5$ to $\delta = -23.1$, with a 1:1:1:2:*5*:2:2:2:1:1 pattern. The resonance in italics integrating as five corresponds to the B–I signal, which overlaps with four B–H signals.

Substitution of iodine by alkyl and aryl groups maintains the same C_s symmetry and therefore the observed pattern is almost the same. In Table 1, the B–C resonance is shown in italics. The rather complex ^{11}B{^{1}H} spectra of [3,3′-Co(1,2-$C_2B_9H_{11})_2$]$^-$ derivatives with a B8–C bond consist of one set of signals for each carborane ligand moiety, one perturbed by B–C substitution and the second almost unchanged compared to that of parent unsubstituted anion [**1**]$^-$. Only when no peak coincidence overlap was found could the positions be assigned

Table 1. ^{11}B{^{1}H} NMR spectra [ppm] of B8-monosubstituted derivatives of [3,3′-Co(1,2-$C_2B_9H_{11})_2$]$^-$. Within each column, the number of boron atoms shown in the first entry (the parent compound) is preserved. An asterisk (*) is used to denote where one of the two boron atoms should be accounted for in the following column. Figures in italics relate to the resonances due to B–R (R ≠ H). The numbers in parentheses denote coupling constants ^1J(B,H) in Hertz.

Compound	δ^{11}B Integration											
[**1**]	**6.5** 2		**1.4** 2		**–6.0** 8		**–17.2** 4		**–22.7** 2			
[**2**]$^-$	**6.5** 1	**3.5** 1	**1.3** 1	**–1.7** 2*	***–4.8*** *5*	**–5.4** 2	**–16.0** 2	**–17.5** 2	**–20.9** 1	**–23.1** 1		
	(138)	(154)	(157)	(151)	(135)	(140)	(145)	(147)	(186)	(188)		
[**3**]$^-$	***16.6*** *1*	**7.6** 1	**0.6** 2		**–3.5** 2	**–4.7** 4	**–6.2** 2	**–17.3** 2	**–17.8** 2	**–22.3** 1	**–25.3** 1	
		(142)	(140)		(138)	(120)	(138)	(144)	(148)	(172)	(169)	
[**4**]$^-$	***19.0*** *1*	**7.8** 1	**1.2** 2		**–4.7** 6		**–5.7** 2	**–16.7** 4		**–21.6**	**–24.4** 1	
		(140)	(137)		(107)		(118)	(149)		(183)	(178)	
[**5**]$^-$	***13.3*** *1*	**5.7** 1	**2.5** 2		**–2.8** 2	**–4.6** 4	**–6.1** 2	**–16.6** 2	**–17.9** 2	**–21.2** 1	**–22.3** 1	
		(134)	(127)		(168)	(148)	(141)	(138)	(135)	(121)	(130)	
[**6**]$^-$	***13.3*** *1*	**6.2** 1	**2.6** 2		**–2.7** 2	**–4.3** 4	**–5.9** 2	**–16.5** 2	**–17.7** 2	**–21.1** 1	**–22.2** 1	
		(155)	(132)		(147)	(143)	(149)	(92)	(136)	(104)	(156)	
[**7**]$^-$	***11.3*** *1*	**5.3** 1	**2.2** 1	**1.4** 1	**–2.8** 2	**–4.7** 4	**–6.2** 2	**–16.9** 4		**–20.8** 2		
		(138)	(103)	(118)	(184)	(143)	(140)	(151)		(158)		
[**8**]$^-$	***11.8*** *1*	**3.7** 1	**1.1** 1	**0.7** 1	**–4.2** 2	**–6.2** 4	**–7.7** 2	**–18.3** 2	**–19.5** 2	**–22.5** 1	**–23.9** 1	
		(137)	(136)	(136)	(154)	(146)	(145)	(139)	(141)	(145)	(122)	
[**9**]$^-$	***16.3*** *1*	**6.5** 1	**2.5** 2		**–6.0** 6		**–7.1** 2	**–18.3** 4		**–23.4** 1	**–25.8** 1	
		(137)	(136)		(146)		(145)	(139)		(145)	(122)	

on the basis of cross-peaks in the $^{11}B\{^1H\}$-$^{11}B\{^1H\}$ COSY experiments. The resonance at $\delta = +16.6$ is not split into a doublet in the ^{11}B NMR spectrum of compound $[\mathbf{3}]^-$, indicating that this resonance corresponds to the B–Me vertex (Figure 2). Once the B8 resonance was known, the two-dimensional $^{11}B\{^1H\}$-$^{11}B\{^1H\}$ COSY NMR spectrum proved helpful for the assignment of the remaining peaks.[33]

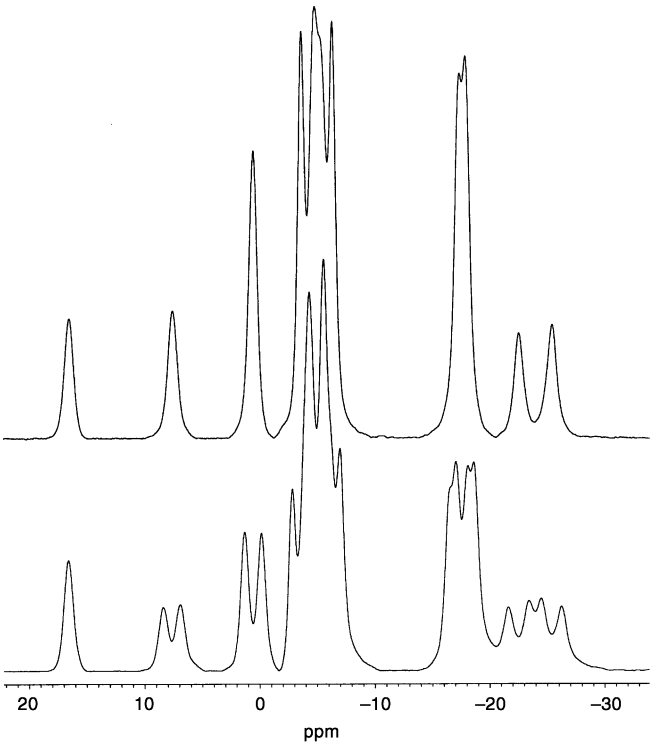

Figure 2. $^{11}B\{^1H\}$ and ^{11}B NMR spectra of $[n\mathrm{Bu_4N}][8\text{-Me-}3,3'\text{-Co}(1,2\text{-}C_2B_9H_{10})(1',2'\text{-}C_2B_9H_{11})]$.

Figure 3 shows the $^{11}B\{^1H\}$ NMR and $^{11}B\{^1H\}$-$^{11}B\{^1H\}$ COSY NMR spectra of compound $[\mathbf{3}]^-$, with the assignments deduced from the off-diagonal resonances. A stick representation of the chemical shifts and relative intensities in the $^{11}B\{^1H\}$ NMR spectra of compounds $[\mathbf{1}]^-$ and $[\mathbf{3}]^-$ is shown in Figure 4. Compared with compound $[\mathbf{1}]^-$, compound $[\mathbf{3}]^-$ shows a 10 ppm deshielding at B8, the vertex bonded to the methyl group, and a 2.5 ppm deshielding at the B4 and B7 positions, these being adjacent to B8. There is also a shielding effect of 2.6 ppm at B6, which is the antipodal vertex to B(8). Table 2 shows the boron NMR data for compounds $[\mathbf{1}]^-$ and $[\mathbf{3}]^-$.

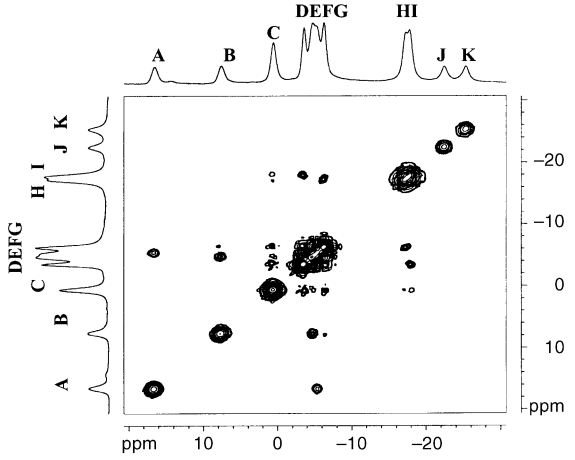

Figure 3. The $^{11}B\{^1H\}$-$^{11}B\{^1H\}$ 2D COSY NMR spectrum of $[n\mathrm{Bu_4N}][8\text{-Me-}3,3'\text{-Co}(1,2\text{-}C_2B_9H_{10})(1',2'\text{-}C_2B_9H_{11})]$. The resonance marked **A** corresponds to B8, **B** to B8′, **C** to B(10,10′), **D** to B(4,7), **E** to B(4′,7′), **F** to B(8,12), **G** to B(9′,12′), **H** to B(5′,11′), **I** to B(5,11), and **J** and **K** to B6 and B6′.

Table 2. $^{11}B\{^1H\}$ NMR chemical shifts [ppm] for compounds $Cs[3,3'\text{-}Co(1,2\text{-}C_2B_9H_{11})_2]$ and $[n\mathrm{Bu_4N}][8\text{-Me-}3,3'\text{-Co}(1,2\text{-}C_2B_9H_{10})(1',2'\text{-}C_2B_9H_{11})]$. $\Delta\delta$ are the differences between the chemical shift of $[n\mathrm{Bu_4N}][8\text{-Me-}3,3'\text{-Co}(1,2\text{-}C_2B_9H_{10})(1',2'\text{-}C_2B_9H_{11})]$ and that of the same vertex in $Cs[3,3'\text{-Co}(1,2\text{-}C_2B_9H_{11})_2]$.

Boron atom	$[\mathbf{1}]^-$	$[\mathbf{3}]^-$	$\Delta\delta$
B8	6.5	16.6	$16.6-(6.5)=+\mathbf{10.1}$
B8′	6.5	7.6	$7.6-(6.5)=+1.1$
B10,B10′	1.4	0.6	$0.6-(1.4)=-0.8$
B4,B7	−6.0	−3.5	$-3.5-(-6.0)=+\mathbf{2.5}$
B4′,B7′	−6.0	−4.7	$-4.7-(-6.0)=+1.3$
B9,B12	−6.0	−4.7	$-4.7-(-6.0)=+1.3$
B9′,B12′	−6.0	−6.2	$-6.2-(-6.0)=-0.2$
B5′,B11′	−17.2	−17.3	$-17.3-(-17.2)=-0.1$
B5,B11	−17.2	−17.8	$-17.8-(-17.2)=-0.6$
B6′	−22.7	−22.4	$-22.4-(-22.7)=+0.3$
B6	−22.7	−25.3	$-25.3-(-22.7)=-\mathbf{2.4}$

Qualitative description of ^1H and $^{13}C\{^1H\}$ NMR spectra: In agreement with the symmetry, the ^1H and $^{13}C\{^1H\}$ NMR spectra exhibit two slightly different C–H carborane signals ($C_{cluster}$–H) due to the substituted and the unsubstituted cage for $[\mathbf{2}]^- - [\mathbf{9}]^-$ (Table 3), and one C–H carborane signal for $[\mathbf{1}]^-$. They also display resonances attributable to the R groups at the expected positions.

Table 3. Chemical shift values [ppm] of the hydrogen and carbon cluster atoms in the ^1H and $^{13}C\{^1H\}$ NMR spectra of B(8)-monosubstituted derivatives of $[3,3'\text{-Co}(1,2\text{-}C_2B_9H_{11})_2]^-$.

Compound	δ $^{13}C\{^1H\}$ NMR	δ ^1H NMR
$[\mathbf{1}]^-$	51.03	3.94 (brs, 4H)
$[\mathbf{2}]^-$	59.34	4.54 (brs, 2H)
	49.16	4.29 (brs, 2H)
$[\mathbf{3}]^-$	51.03	4.08 (brs, 2H)
	49.87	3.87 (brs, 2H)
$[\mathbf{4}]^-$	50.55	4.10 (brs, 2H)
	49.25	3.88 (brs, 2H)
$[\mathbf{5}]^-$	54.03	4.58 (brs, 2H)
	49.76	3.76 (brs, 2H)
$[\mathbf{6}]^-$	53.75	4.60 (brs, 2H)
	49.76	3.87 (brs, 2H)
$[\mathbf{7}]^-$	53.07	4.52 (brs, 2H)
	47.82	3.08 (brs, 2H)
$[\mathbf{8}]^-$	54.40	4.60 (brs, 2H)
	49.78	3.73 (brs, 2H)
$[\mathbf{9}]^-$	50.42	4.12 (brs, 2H)
	49.14	3.92 (brs, 2H)

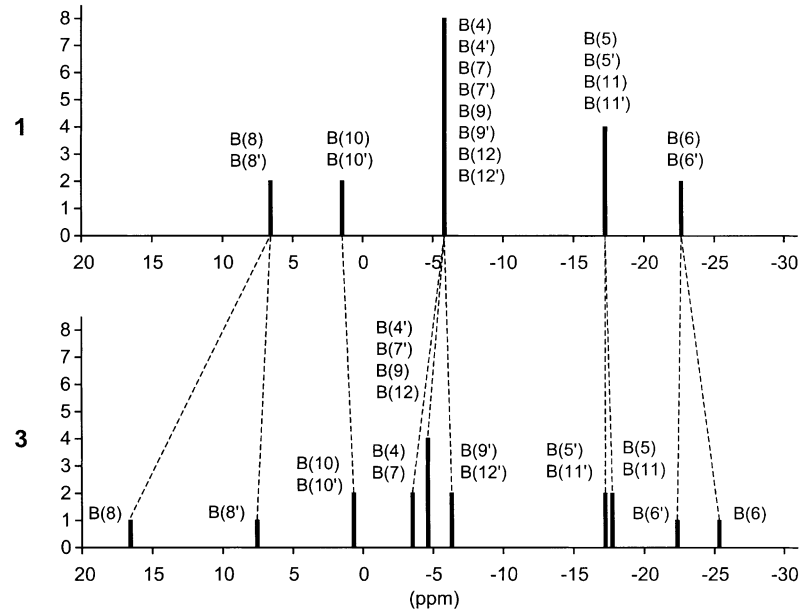

Figure 4. Stick representation of the chemical shifts and relative intensities in the $^{11}B\{^1H\}$ NMR spectra of compounds $[\mathbf{1}]^-$ and $[\mathbf{3}]^-$. Lines join equivalent positions in the two compounds.

Molecular and crystal structures of $[\mathbf{3}]^-$, $[\mathbf{8}]^-$, and $[\mathbf{9}]^-$: Suitable single crystals of $[\mathbf{3}]^-$ were obtained by slow evaporation of the solvents from a solution in $CHCl_3$/hexane. In the case of $[\mathbf{8}]^-$, crystals were obtained by slow concentration of a solution in CH_2Cl_2/acetone, while $[\mathbf{9}]^-$ was similarly crystallized from a mixture of CH_2Cl_2/EtOH/acetone.

The structures of $[\mathbf{3}]^-$, $[\mathbf{8}]^-$, and $[\mathbf{9}]^-$ are presented in Figures 5–7, respectively. Crystallographic data for $[n\mathrm{Bu_4N}][\mathbf{3}]$, $[\mathrm{Me_4N}][\mathbf{8}]$, and $[\mathrm{Me_4N}][\mathbf{9}]$ are given in Table 4,

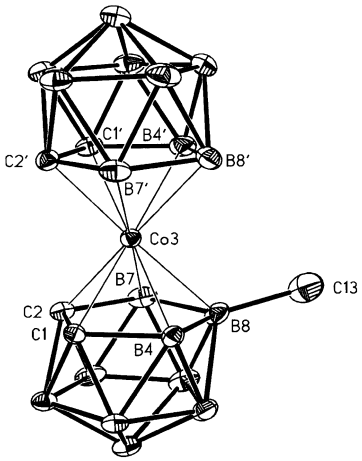

Figure 5. Drawing of $[\mathbf{3}]^-$ with 30% thermal displacement ellipsoids.

and selected bond lengths and angles are listed in Tables 5–7, respectively. Crystallographic analyses confirmed the expected B(8)-substituted cobaltabisdicarbollide structures for each compound. In each compound, the B10-Co3-B10′ jack-knife angle (see Figure 1) is close to 180° [174.98(7)–178.86(5)°] and the Co3–B8 distance is slightly longer than the Co3–C_c distances (C_c is the cluster carbon atom).

In each compound, the two five-membered coordinating sites are in a staggered conformation. The rotamers of $[\mathbf{3}]^-$ and $[\mathbf{9}]^-$ (defined by two cobaltabisdicarbollide moieties) are similar, but that of $[\mathbf{8}]^-$ is different. In $[\mathbf{3}]^-$ and $[\mathbf{9}]^-$, C2′ is oriented between C1 and C2 and thus the cluster carbon atoms of the non-substituted dicarbollide cage are oriented away from the B8 atom bearing the substituent, while in $[\mathbf{8}]^-$ B8 is oriented between C1′ and C2′. The former conformation has been observed in most cases,[22e, 34] while the latter conformation has been found in complex $[\mathbf{5}]^-$, which also bears a phenyl substituent at B8.[21] In

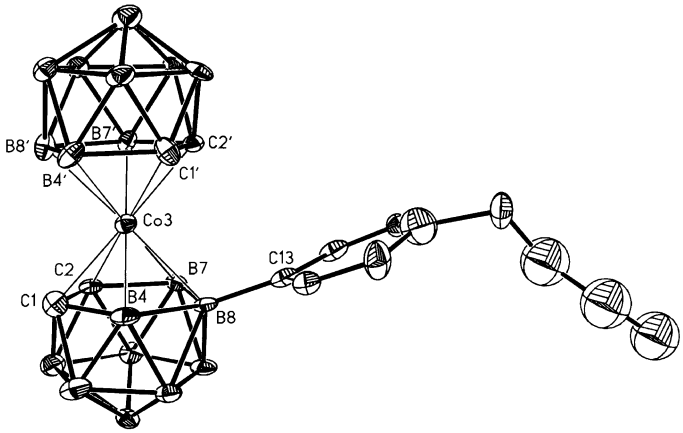

Figure 6. Drawing of $[\mathbf{8}]^-$ with 20% thermal displacement ellipsoids.

$[\mathbf{3}]^-$ and $[\mathbf{9}]^-$, the Co3-B8-C13 angles are 121.1(2) and 122.6(3)°, respectively. On the other hand, the Co3-B8-C13 angle in $[\mathbf{8}]^-$ is 114.37(13)°, which is comparable with the corresponding value of 116.9° in $[\mathbf{5}]^-$. It seems that in $[\mathbf{8}]^-$ the phenyl group at B8 is oriented towards the cobalt atom and the upper belt. Thus, the reason for the unusual rotamer may be a weak interaction between the metal atom and the phenyl group, and/or a weak interaction between the hydrogens at C1′ and C2′ and the phenyl carbon atoms.

The C1–C2 and C1′–C2′ bond lengths in $[\mathbf{3}]^-$ and $[\mathbf{9}]^-$ are similar (about 1.615 Å; see Table 5 and Table 7), but in $[\mathbf{8}]^-$ (Table 6) the corresponding distances are 1.662(3) and 1.599(3) Å, respectively. The B8–C13 distance in $[\mathbf{8}]^-$ is 1.652(3) Å, while that in $[\mathbf{5}]^-$ is 1.577(5) Å.[21] The elongated distance in the former is possibly due to the long attached alkyl group.

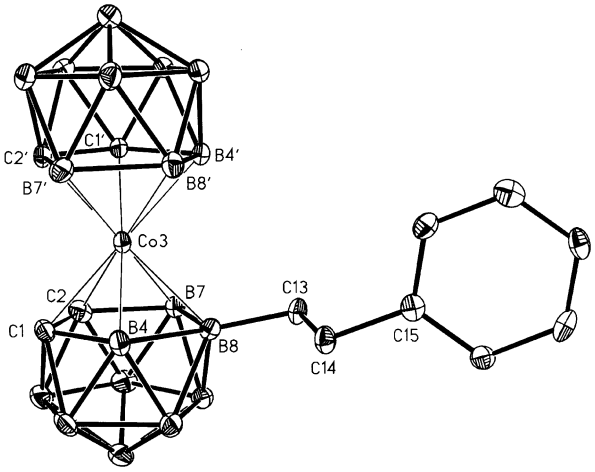

Figure 7. Drawing of $[\mathbf{9}]^-$ with 30% thermal displacement ellipsoids.

Table 4. Crystallographic data and structural refinement details for compounds $[n\mathrm{Bu_4N}][\mathbf{3}]$, $[\mathrm{Me_4N}][\mathbf{8}]$, and $[\mathrm{Me_4N}][\mathbf{9}]$.

	$[n\mathrm{Bu_4N}][\mathbf{3}]$	$[\mathrm{Me_4N}][\mathbf{8}]$	$[\mathrm{Me_4N}][\mathbf{9}]$
empirical formula	$C_{21}H_{60}B_{18}CoN$	$C_{18}H_{46}B_{18}CoN$	$C_{16}H_{42}B_{18}CoN$
formula weight	580.21	530.07	502.02
crystal system	monoclinic	monoclinic	orthorhombic
space group	$P2_1/n$ (no. 14)	Cc (no. 9)	$P2_12_12_1$ (no. 19)
a [Å]	14.7523(2)	18.6079(8)	13.8955(3)
b [Å]	10.8299(2)	17.6746(9)	13.9474(3)
c [Å]	22.2034(3)	9.9608(4)	14.4267(3)
β [°]	103.2283(7)	112.942(3)	90
V [Å^3]	3453.22(9)	3016.8(2)	2795.98(10)
Z	4	4	4
T [°C]	−100	−100	−100
λ [Å]	0.71073	0.71073	0.71073
ρ [g cm^{-3}]	1.116	1.167	1.193
μ [cm^{-1}]	5.13	5.81	6.24
goodness-of-fit	0.997	1.058	1.032
$R1$[a] $[I > 2\sigma(I)]$	0.0465	0.0778	0.0462
$wR2$[b] $[I > 2\sigma(I)]$	0.1133	0.2042	0.0876
Flack parameter x	–	0.31(7)	0.171(19)

[a] $R1 = \Sigma\,||F_o| - |F_c||/\Sigma\,|F_o|$. [b] $wR2 = \{\Sigma[w(F_o^2 - F_c^2)^2]/\Sigma[w(F_o^2)^2]\}^{1/2}$.

Table 5. Selected bond lengths [Å] and angles [°] for $[n\mathrm{Bu_4N}][\mathbf{3}]$.

Co3 – C1	2.032(2)
Co3 – C2	2.039(3)
Co3 – C1′	2.048(3)
Co3 – C2′	2.040(3)
Co3 – B8	2.144(3)
Co3 – B8′	2.125(3)
C1 – C2	1.619(4)
B8 – C13	1.684(5)
C1′ – C2′	1.615(4)
Co3-B8-C13	121.1(2)
B4-B8-C13	120.6(3)
B7-B8-C13	130.8(3)

Table 6. Selected bond lengths [Å] and angles [°] for $[\mathrm{Me_4N}][\mathbf{8}]$.

Co3 – C1	2.009(3)
Co3 – C2	1.9901(18)
Co3 – C2′	2.024(2)
Co3 – C1′	2.066(2)
Co3 – B8′	2.160(2)
Co3 – B8	2.170(2)
C1 – C2	1.662(3)
B8-C13	1.652(3)
C1′ – C2′	1.599(3)
Co3-B8-C13	114.37(13)
B4-B8-C13	124.66(18)
B7-B8-C13	121.02(18)

Table 7. Selected bond lengths [Å] and angles [°] for $[\mathrm{Me_4N}][\mathbf{9}]$.

Co3 – C1	2.026(3)
Co3 – C2	2.041(4)
Co3 – C2′	2.051(4)
Co3 – C1′	2.053(3)
Co3 – B8	2.152(4)
Co3 – B8′	2.124(4)
C1 – C2	1.615(5)
B8 – C13	1.599(5)
C1′ – C2′	1.614(4)
Co3-B8-C13	122.6(3)
B4-B8-C13	128.0(3)
B7-B8-C13	124.7(3)

Discussion

Through a B – C coupling reaction it has been possible to cleanly and regioselectively generate monoalkyl and monoaryl derivatives of cobaltabisdicarbollide at the B8 position in good to high yield. Previous to this work, only one of the compounds presented, $[\mathrm{Me_4N}][8\text{-}C_6H_5\text{-}3,3'\text{-}Co(1,2\text{-}C_2B_9H_{10})(1',2'\text{-}C_2B_9H_{11})]$ ($[\mathbf{5}]^-$), had been reported, which was obtained as a by-product and consequently in low yield.[21] The synthetic procedure reported here provides access to a large number of monoalkyl and monoaryl derivatives of $[\mathbf{1}]^-$ and permits systematic study of their electronic properties.

^{11}B chemical shift dependence: Table 1 displays the ^{11}B resonances of $[\mathbf{1}]^- - [\mathbf{9}]^-$. The top row shows the resonances of the parent species $[\mathbf{1}]^-$. As a consequence of the lower symmetry of $[\mathbf{2}]^- - [\mathbf{9}]^-$, the columns become split into two or three, but in such a way that the average of the weighted individual contributions remains very close to the entry in the top row. One clear exception relates to the B – C resonances shown in the first column and the B – I resonance, which is masked by other resonances, in the column with the entry −6.0 in the top row. The constancy of the averaged column values can be interpreted in terms of the perturbation originating from the alkyl or aryl substitution not producing long-range effects, although local effects on the *ipso* boron atom are important, giving rise to a 10 – 13 ppm shift to lower field for alkyl substituents, and a 5 – 7 ppm shift for the aryl analogues. Without exception, the ^{11}B resonance of the B–R moiety (R = alkyl, aryl) is shifted to lower field. If we consider that only the σ_d contribution is relevant in determining the position of the NMR signal, since the chemical shifts of $[\mathbf{1}]^-$ are taken as references, the conclusion would be that the -C(alkyl) groups have a −I influence on boron.[35] The same is true for the local effect created by the -C(aryl) groups,

although for these it is less pronounced. The methyl carbon can only withdraw electron density from the boron, whereas an additional mechanism is available to the aromatic ring, whereby electron density is transferred to a ψ* orbital on the cluster, thereby partly compensating for the loss of local electron density on boron due to the carbon σ bond (see Figure 8). Contrary to the common belief that alkyl groups are electron-releasing, we stress here that they are electron-withdrawing when attached to boron in boron clusters. The following experimental and discussion sections are set out to support this hypothesis.

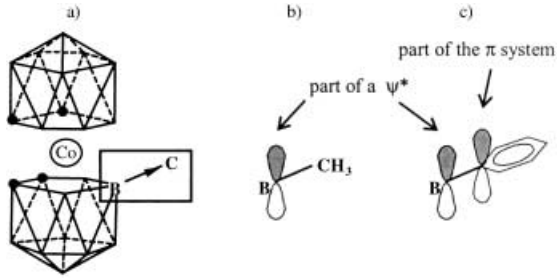

Figure 8. a) Polarization effect of B–C *exo*-cluster bond due to the higher electronegativity of C. When the organic group bonded to the boron atom possesses a double bond (vinyl or aryl group) or a lone pair, a π back-donation to a cluster antibonding ψ* orbital takes place due to orbital overlap as shown in c). This is not possible when the organic group is an alkyl group as in b).

Cyclic voltammetric studies: Only one coupled reduction/oxidation process has been observed for complexes $[\mathbf{1}]^- - [\mathbf{9}]^-$ within the range of potentials studied (-2.5 to -1.0 V, referenced to Fc^+/Fc, which was taken as zero). The reduction current wave is caused by the reduction process "$Co^{III} \rightarrow Co^{II}$";[36] the reverse oxidation process is also observed. Figure 9 shows the cyclic voltammogram of $[\mathbf{9}]^-$ as a

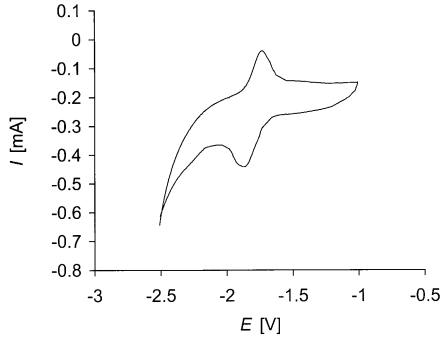

Figure 9. Cyclic voltammogram of compound $[\mathbf{9}]^-$, recorded in acetonitrile containing 0.1 M tetrabutylammonium perchlorate as supporting electrolyte at a scan rate of 100 mV s^{-1}. Potential values are referenced to the Fc^+/Fc couple.

representative example. A conceivable oxidation process beyond the reoxidation of Co^{II} for complexes $[\mathbf{1}]^- - [\mathbf{9}]^-$ was not observed in the range of electrode potentials investigated. Table 8 lists reduction potentials E_{red}, ΔE values ($\Delta E = E_{red} - E_{ox}$), and $E_{1/2}$ ($E_{1/2} = (E_{red} + E_{ox})/2$) for complexes $[\mathbf{1}]^- - [\mathbf{9}]^-$. $E_{1/2}$ is the half-wave potential associated with the Co^{III}/Co^{II} redox process. Among the $E_{1/2}$ values listed, three distinct groupings can be discerned; those of the aryl-substituted derivatives near -1.73 V ($[\mathbf{5}]^-$, $[\mathbf{6}]^-$, $[\mathbf{7}]^-$, $[\mathbf{8}]^-$), those of the non-aryl-substituted derivatives near -1.84 V ($[\mathbf{1}]^-$, $[\mathbf{3}]^-$, $[\mathbf{4}]^-$, $[\mathbf{9}]^-$), and the distinct potential of the iodo derivative ($[\mathbf{2}]^-$) ($E_{1/2} = -1.58$). A simple explanation would be to consider that an electron-releasing substituent R at the π perimeter of the dicarbollide ligand would cause a higher electron density at the Co^{III} center and make it more difficult to reduce, whereas electron-withdrawing groups at the periphery would decrease the reduction overpotential as compared with the parent complex $[\mathbf{1}]^-$. We do not believe that this simple explanation is the right one. It could be satisfactory if $[\mathbf{1}]^-$ was the definitive reference point, with the half-wave potentials $E_{1/2}$ for +I substituents above and those for −I substituents below its potential. However, this is not the case. A more realistic grouping can be made by considering one group of compounds with aromatic substituents ($[\mathbf{5}]^-$, $[\mathbf{6}]^-$, $[\mathbf{7}]^-$, $[\mathbf{8}]^-$) and a second group made up of the alkyl- ($[\mathbf{3}]^-$, $[\mathbf{4}]^-$, $[\mathbf{9}]^-$) and hydrogen-substituted $[\mathbf{1}]^-$. Compound $[\mathbf{2}]^-$ is treated separately. This encouraged us to study the electronic spectra of $[\mathbf{1}]^- - [\mathbf{9}]^-$ and to see if a property existed that differentiated the two sets of compounds. An initial inconvenience that we found was the broadness of the UV/Vis bands, which precluded observation of the individual features of interest.

Table 8. Data obtained from cyclic voltammetry studies in acetonitrile. The $[Fe(C_5H_5)_2]^+/[Fe(C_5H_5)_2]$ couple was taken as the zero reference.

Compound	$E_{1/2}$ [V]	ΔE [V]	E_{red} [V]
$[\mathbf{1}]^-$	−1.83	0.24	−1.95
$[\mathbf{2}]^-$	−1.58	0.27	−1.71
$[\mathbf{3}]^-$	−1.90	0.29	−2.04
$[\mathbf{4}]^-$	−1.81	0.16	−1.89
$[\mathbf{5}]^-$	−1.74	0.23	−1.85
$[\mathbf{6}]^-$	−1.77	0.32	−1.93
$[\mathbf{7}]^-$	−1.67	0.26	−1.83
$[\mathbf{8}]^-$	−1.74	0.21	−1.84
$[\mathbf{9}]^-$	−1.81	0.15	−1.88

UV/Vis spectra: Hawthorne and co-workers[37] have reported that the UV/Vis spectrum of $[\mathbf{1}]^-$ in methanol consists of four absorptions at 216, 293, 345, and 445 nm, which is essentially in agreement with that subsequently reported by Matel and co-workers[25] with one absorption band ($\lambda_{max} = 287$ nm, $\varepsilon \approx 30000$ L cm^{-1} mol^{-1}). The visible spectrum was interpreted by Cerný and co-workers[38] on the basis of ligand field theory.

We have recorded the UV/Vis spectrum of $[\mathbf{1}]^-$ in acetonitrile, as this is the solvent used in the cyclic voltammetry studies, and although the spectrum is rather similar to those already reported, there are some discrepancies in the positions of the maxima and their absorption coefficients, which indicates that these values are strongly dependent on how the absorption (A) is measured. We used the same solvent for all the complexes. The spectra did not show well-defined peaks, which made comparing them difficult; see, for instance, the spectrum of compound **7** shown in Figure 10. To

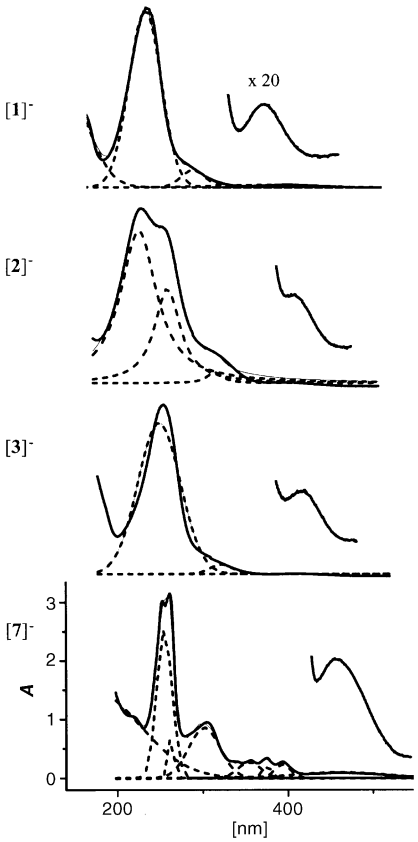

Figure 10. UV/Vis spectra (solid lines) of some selected compounds, from top to bottom $[\mathbf{1}]^-$, $[\mathbf{2}]^-$, $[\mathbf{3}]^-$, and $[\mathbf{7}]^-$, and the results of line fitting with gaussians (dashed lines). The expanded sections on the right show the absorption near 445 nm amplified 20 times.

overcome this problem, a line-fitting analysis was performed.[39] The results obtained are shown in Figure 10 for the parent compound $[\mathbf{1}]^-$, as well as for the B8–I $[\mathbf{2}]^-$, B8–alkyl $[\mathbf{3}]^-$, and B8–aryl $[\mathbf{7}]^-$ derivatives as representative examples. The full set of data is shown in Table 9. As can be seen in Figure 10, the deconvolution with Gaussians permitted discernment of the sub-band positions and the retrieval of λ_{max} and ε data that would otherwise have been impossible. The goodness-of-fit (R^2) of all the spectra was between 0.999 and 0.991. Therefore, relevant comparisons can be made. It can readily be observed that absorptions near 281, 337, and 445 nm, present in the spectrum of $[\mathbf{1}]^-$, are in fact present in all the spectra with comparable ε values. These absorptions are therefore attributed to the $[3,3'\text{-}Co(1,2\text{-}C_2B_9H_{11})_2]^-$ moiety. A second set of absorptions can be ascribed to the aromatic substituents by comparison with the UV/Vis spectrum of the fragment alone; for example, anthracene has two characteristic absorptions at 253 and 375 nm[40] and we observe these bands at 255 and 375 nm in the spectrum of $[\mathbf{7}]^-$. These bands due to the substituents appear at $\lambda < 270$ nm in most of the spectra. Finally, a set of absorptions is observed that cannot be assigned to either of the aforementioned individual fragments, the cluster and the R substituent, and that therefore must be attributed to their interaction. These absorptions appear at around $\lambda = 320$ nm and are only present in the spectra of compounds $[\mathbf{2}]^-$, $[\mathbf{5}]^-$, $[\mathbf{6}]^-$, $[\mathbf{7}]^-$, and $[\mathbf{8}]^-$, and not in those of compounds $[\mathbf{1}]^-$, $[\mathbf{3}]^-$, $[\mathbf{4}]^-$, and $[\mathbf{9}]^-$. Therefore, these absorptions are only found when R contains lone pairs as in $[\mathbf{2}]^-$ or π electrons as in $[\mathbf{5}]^-$, $[\mathbf{6}]^-$, $[\mathbf{7}]^-$, and $[\mathbf{8}]^-$.

The influence of boron: There are similarities and differences between $[Co(C_5H_5)_2]^+$ and compound $[\mathbf{1}]^-$. Both compounds obey the 18 e$^-$ rule, the cobalt is in a +3 oxidation state in both, and 1 e$^-$ reduction should involve the partial filling of the LUMO (see Figure 11). The differences between

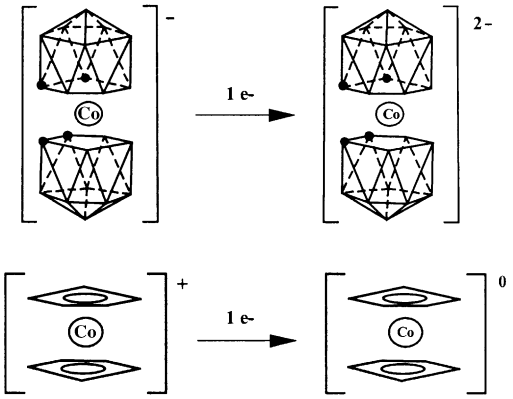

Figure 11. Schematic representations of the 1 e$^-$ reduction processes for compounds $[Co(C_2B_9H_{11})_2]^-$ ($[\mathbf{1}]^-$) and $[Co(C_5H_5)_2]^+$.

$[Co(C_5H_5)_2]^+$ and $[\mathbf{1}]^-$ relate to their charge, their color, and consequently their electronic spectra. While $[Co(C_5H_5)_2]^+$ is yellow-green, $[\mathbf{1}]^-$ is orange. Absorptions in the visible region are found at 404 nm for $[Co(C_5H_5)_2]^+$ and at 445 nm for $[\mathbf{1}]^-$, the former being more energetic than the latter.[38, 41] On the other hand, it is clear that $[C_2B_9H_{11}]^{2-}$ is more effective at

Table 9. UV/Vis spectra for compounds $[\mathbf{1}]^- - [\mathbf{9}]^-$ in acetonitrile. λ positions [nm] and ε values [L cm^{-1} mol^{-1}] are reported and were calculated following line-fitting analysis.

Compound	λ (ε)						
$[\mathbf{1}]^-$	207 (11.698)		281 (27.264)		337 (2.642)		445 (392)
$[\mathbf{2}]^-$			287 (26.604)	320 (9.151)	375 (3.113)		452 (375)
$[\mathbf{3}]^-$			289 (20.943)		362 (2.415)		450 (324)
$[\mathbf{4}]^-$			293 (24.622)		355 (2.075)		450 (313)
$[\mathbf{5}]^-$	223 (13.962)		287 (21.887)	319 (8.207)	366 (3.113)		452 (321)
$[\mathbf{6}]^-$		251 (25.943)*	251 (25.943)*	322 (2.642)	378 (2.075)		450 (377)
$[\mathbf{7}]^-$	214 (9.906)	255 (59.762)	262 (22.381)	320 (2.238)	354 (6.429)	375 (5.000), 393 (5.476)	454 (2.143)
$[\mathbf{8}]^-$	228 (16.981)	272 (10.472)	294 (26.698)	320 (9.340)	379 (3.396)		452 (311)
$[\mathbf{9}]^-$			290 (22.736)		368 (3.132)		452 (371)

stabilizing the highest cobalt oxidation state,[42] Co^{III}, than $[C_5H_5]^-$, and makes its reduction to Co^{II} more difficult. Thus, $E_{1/2}$ values are found at -1.25 V for $[Co(C_5H_5)_2]^+$ and -1.83 V for $[\mathbf{1}]^-$, the second requiring more energy.[43] The mismatch between the electrochemical and visible data led us to think that the redox processes were not parallel in $[Co(C_5H_5)_2]^+$ and $[\mathbf{1}]^-$, suggesting that the participating frontier orbitals did not have the same origin.

The dicarbollide $[C_2B_9H_{11}]^{2-}$ anion has been considered as being isolobal with $[C_5H_5]^-$.[44] Both coordinate in a η^5 manner and produce a rich organometallic chemistry.[16] The main reported differences concern the inward orientation of the open face orbitals in $[C_2B_9H_{11}]^{2-}$, and its capacity to stabilize higher oxidation states. All of the above data led us to think that there are more profound but undetected differences as a consequence of the presence of boron in the coordinating face. Boron is much less electronegative than carbon (2.0 vs 2.5), the difference being the same as that between carbon and nitrogen (2.5 vs 3.0). Consequently, this should differentiate the orbital energies and their capacity to interact with a common metal in the same oxidation state.[8] If a fragment molecular orbital (FMO) analysis is performed on the interactions of $[C_5H_5]^-$ and $[C_2B_9H_{11}]^{2-}$ orbitals with those of a common Co^{III} ion, it is logical to assume that the energy of the HOMO in the ligand fragment should be higher (less negative) in $[C_2B_9H_{11}]^{2-}$ than in $[C_5H_5]^-$, the reason being that there are more boron atoms or comparatively fewer electronegative elements. Therefore, the chances that the HOMO of $[\mathbf{1}]^-$ is, in essence, a Co^{III} d orbital are less than in the case of $[Co(C_5H_5)_2]^+$. At the extreme, the HOMO may not have any contribution from the metal d orbitals. Common thinking is that the HOMO of organometallic complexes is, in essence, a metal d orbital[1] and therefore the $18\,e^-$ rule is mostly obeyed. In a similar way, the LUMO in an organometallic complex is usually thought to be mostly contributed by a metal d orbital. However, this is so because common ligands are invariably made of carbon, or more electronegative elements than carbon. Boron, being to the left of carbon in the Periodic Table, apports fundamental differences.

Influence of the substituents at the cluster B8 position: As stated above, a careful analysis of the line shape in the UV/Vis spectra of $[\mathbf{2}]^-$, $[\mathbf{5}]^-$, $[\mathbf{6}]^-$, $[\mathbf{7}]^-$, and $[\mathbf{8}]^-$ indicated an extra absorption band not attributable to $[\mathbf{1}]^-$ nor to the substituent. This band, near 320 nm, was only observed in the species with direct B8–aryl or B8–I bonds. Interestingly, those compounds having the band near 320 nm ($[\mathbf{2}]^-$, $[\mathbf{5}]^-$–$[\mathbf{8}]^-$) are also those that are more prone to reduction.

To understand the easier reduction of the aryl as compared to the alkyl derivatives of $[\mathbf{1}]^-$, it is necessary to know the origin of the 320 nm band. It is neither due to $[\mathbf{1}]^-$ nor to the aromatic fragment, but to synergy between them. Indeed, this is what is found in the extended Hückel molecular orbital (EHMO) analysis of $[\mathbf{5}]^-$, as shown schematically in Figure 12 for just a few orbitals, including the frontier orbitals. It can clearly be seen that the HOMO is purely due to the cluster fragment, while the LUMO is mostly due to the LUMO+2 of the aromatic fragment, in accord with the UV spectrum and with the notion that the redox processes are not parallel in

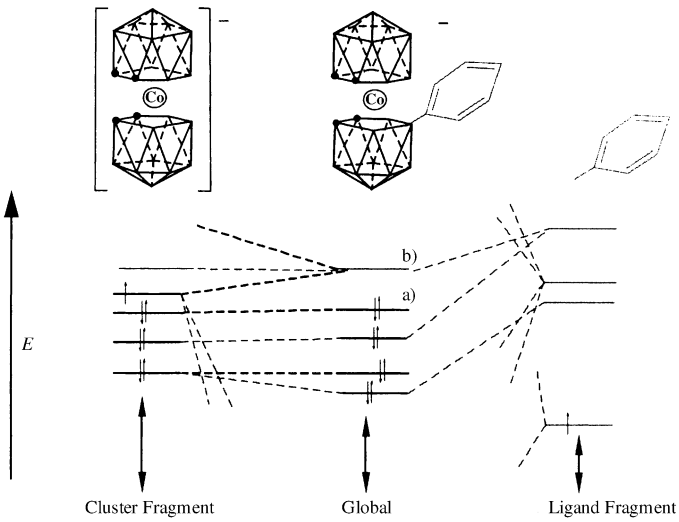

Figure 12. Fragment orbital analysis of $[\mathbf{5}]^-$ showing only relevant frontier orbitals and the contribution of the fragment orbitals. In this approach, the HOMO (a) is purely derived from the cluster fragment and the LUMO (b) contains a significant contribution from orbitals based on the ligand fragment.

$[Co(C_5H_5)_2]^+$ and $[\mathbf{1}]^-$. The $E_{1/2}$ values for the aryl-substituted species can now be nicely interpreted, considering that the HOMO–LUMO gap is diminished in the aryl-substituted compounds as compared to that in $[\mathbf{1}]^-$, thus requiring a less cathodic potential for the reduction to proceed.

On incorporation of boron into the coordinating carbocycle, that is, on going from $[C_5H_5]^-$ to the C_2B_3 open face in $[C_2B_9H_{11}]^{2-}$, there is a greater energy mismatch between the relevant orbitals on the ligand and on the metal that generate the frontier orbital in the complex, the net effect of which is that the orbital overlap is no longer very efficient. The participation of the metal orbitals in the molecular frontier orbitals is less, or, in other words, the contribution from the ligand orbitals in the frontier orbitals is larger. Therefore, besides the influence of the central metal ion on the energy of the molecular orbitals, it seems clear that the relative contribution from the boron-containing ligands in the more relevant frontier orbital features is large, contrary to what is assumed for conventional η^5 ligands.

Comparison of the structures of $[\mathbf{3}]^-$ and $[\mathbf{5}]^-$ offers relevant information concerning the participation of the metal d orbitals in frontier orbitals. Wagner and co-workers[45] studied the α^* dip angle, defined as the angle between the center of gravity of the substituted cyclopentadienyl ring, the *ipso* carbon atom, and the exocyclic carbon atom (or boron), in order to measure the degree of substituent bending in ferrocenyl carbocations and borylferrocene. The larger the value of α^*, the greater the interaction between the filled d-type orbitals at the metal and the empty p orbital at boron (or carbon). The same strategy can also be used to assess the possibility of interaction between cobalt d orbitals and the π aromatic system in the compounds described herein, for instance in $[\mathbf{5}]^-$. Wagner reported α^* values of about 18° in $[Fe(C_5H_5)(BR_2\text{-}C_5H_4)]$. In conventional metallocenes, the reference point is practically zero. However, substituents on $[7,8\text{-}C_2B_9H_{11}]^{2-}$ derivatives already present a natural dip angle

and therefore in sandwich metallaboranes it is necessary to base discussion on $\Delta\alpha^*$, the reference value being provided by the experimental α^* value found for $[\mathbf{3}]^-$, which is 16.3°. The value of α^* for $[\mathbf{5}]^-$ is 20.7°, and thus $\Delta\alpha^*$ is 4.4°, which suggests that there is a degree of interaction, albeit minor, between the d orbitals on the metal and orbitals of suitable symmetry on the aryl moiety.

ab initio Interpretation: All the above interpretations based on experimental observations are supported by ab initio calculations[46] on $[\mathbf{1}]^-$, $[\mathbf{2}]^-$, $[\mathbf{3}]^-$, $[\mathbf{5}]^-$, $[\mathbf{8}]^-$, and $[\mathbf{9}]^-$. Calculations have been performed on these because geometrical parameters are either presented in this paper ($[\mathbf{3}]^-$, $[\mathbf{8}]^-$, and $[\mathbf{9}]^-$) or are available elsewhere ($[\mathbf{1}]^-$,[47] $[\mathbf{5}]^-$,[21] and $[\mathbf{2}]^-$[48]). A single-point calculation at the HF/3-21 G level was performed on all of them, with the exception of $[\mathbf{2}]^-$, in the case of which all atoms were computed with the 3-21 G basis set but the iodine was computed at 6 G*. To reduce computational time, the butyl group in $[\mathbf{8}]^-$ was converted into an ethyl group by simply replacing the terminal -CH_2CH_3 moiety by a hydrogen. The new C–H distance was set at the average of the two remaining C–H lengths. No other approximations were made. Table 10 displays the HOMO and LUMO energies, the LUMO and HOMO energy gap, and the $E_{1/2}$ potential value, as also reported in Table 8. The compounds are ordered with respect to their reduction potentials. Compound $[\mathbf{3}]^-$ is the most difficult to reduce and compound $[\mathbf{2}]^-$ is the most easily reducible. Interestingly, the $E_{1/2}$ column fully parallels the HOMO energy column. This was, in principle, unexpected as, according to Koopman's theorem, this property would be related to the $Co^{III} \rightarrow Co^{IV}$ process. A good matching with the LUMO–HOMO gap column related to the $Co^{III} \rightarrow Co^{II}$ process was also found. The only discrepancies are found for $[\mathbf{9}]^-$ and $[\mathbf{5}]^-$, which have practically identical LUMO–HOMO values but a 70 mV difference in $\Delta E_{1/2}$. It is possible that a larger basis set would account for these differences.

Table 10. Relationship of frontier orbitals energy and redox potential.

Compound	E_{HOMO}	E_{LUMO}	$\Delta E_{(HOMO\text{-}LUMO)}$	$E_{1/2}$ [V]
$[\mathbf{3}]^-$	– 6.46939	5.283453	– 11.752843	– 1.90
$[\mathbf{1}]^-$	– 6.246414	5.453047	– 11.699461	– 1.83
$[\mathbf{9}]^-$	– 6.14250	5.136343	– 11.278843	– 1.81
$[\mathbf{5}]^-$	– 5.727132	5.563548	– 11.29068	– 1.74
$[\mathbf{8}]^-$	– 5.550179	5.47337	– 11.023549	– 1.74
$[\mathbf{2}]^-$	– 5.479989	5.503018	– 10.983007	– 1.58

Looking at the spatial disposition of the HOMO and LUMO for $[\mathbf{2}]^-$, $[\mathbf{5}]^-$, and $[\mathbf{8}]^-$, it is clear that the HOMO is centered on the lone pair or π electron containing substituent (I, Ph) and that the LUMO is a metal d orbital (see Figure 13 for a representation of the HOMO and LUMO for $[\mathbf{5}]^-$). Therefore, the LUMO–HOMO gap is the result of the combined effect of the two molecular fragments, as evidenced experimentally by UV/Vis spectroscopy and studied by line-fitting analysis. Inspection of the spatial disposition of the orbitals also reveals that the frontier orbitals are not the same

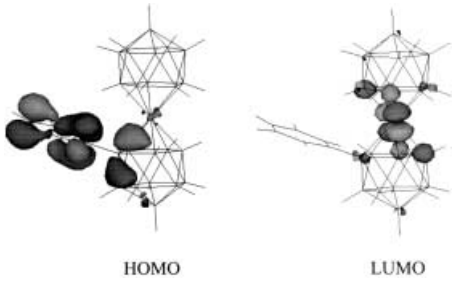

Figure 13. Representation of the HOMO and LUMO for $[\mathbf{5}]^-$.

in the two sets of compounds. For $[\mathbf{1}]^-$, $[\mathbf{3}]^-$, and $[\mathbf{9}]^-$, the LUMOs have the same origin, but it is not a d orbital; the d orbitals mostly participate in LUMO+1 and LUMO+2. On the contrary, the HOMOs are different, a d orbital in $[\mathbf{1}]^-$, a cluster spread molecular orbital in $[\mathbf{3}]^-$, and a π orbital on the phenyl fragment in $[\mathbf{9}]^-$.

We have differentiated two sets of compounds through the presence or absence of an aromatic ring. Nevertheless, it is possible that the sequential energy destabilization of the HOMO shown in Table 10 on going from the alkyl through the aryl $[3,3'\text{-}Co(1,2\text{-}C_2B_9H_{11})_2]^-$ derivatives to the iodo derivative may be related to the $-I$ character of the methyl group when bonded to boron. One electronegative element causes a greater stabilization of one filled orbital. According to Table 10, the HOMO of $[\mathbf{3}]^-$ is the most stabilized, while that of $[\mathbf{2}]^-$ is the most destabilized. All else being equal, this supports our concept of a –I methyl group. The effect of the phenyl group, although very similar, is mitigated by electron back-donation to the boron. The case of the iodo derivative ($[\mathbf{2}]^-$) can easily be explained considering that iodine has an Allred–Rochow electronegativity of 2.2 compared to 2.5 for carbon and that the back-donation effect is large due to the high polarizability of the iodine lone pairs.

Conclusion

Regioselective monoalkylation and monoarylation in cobaltabisdicarbollide clusters has been successfully accomplished by cross-coupling reactions between a B–I fragment and an appropriate Grignard reagent in the presence of a Pd catalyst and CuI. This has facilitated the preparation of a considerable number of monoalkylated and monoarylated derivatives, which, in turn, has permitted study of the influence of boron in metallocene-type ligands and the effect of alkyl and aryl substituents on boron in boron anionic clusters. Experimental data from UV/Vis spectroscopy, $E_{1/2}$ measurements, and X-ray diffraction analysis, and supported by EHMO and ab initio analyses, indicate that the participation of metal d orbitals in the HOMOs of these complexes is less than that in typical metallocene complexes. This can be explained as a consequence of the lower electronegativity of boron as compared to carbon. Related to this is the –I character of alkyl groups when bonded to boron in boron anionic clusters, contrary to the common belief that alkyl groups are generally electron-donating groups. Alkyl groups are donating towards elements of equal or greater electronegativity, but boron is less

electronegative. Relevant to this discussion is the accepted negative character of the methyl group in MeLi as a result of $\chi_{Li} = 1.0$ and $\chi_C = 2.5$.

Experimental Section

General considerations: Elemental analyses were performed using a Carlo Erba EA 1108 microanalyzer. IR spectra were recorded from samples in KBr pellets on a Shimadzu FTIR-8300 spectrophotometer. UV/Vis spectroscopy was carried out with a Cary 5E spectrophotometer using 0.1 cm cuvettes. The concentration of the complexes was 1×10^{-3} mol L^{-1}. ^{1}H and ^{1}H{^{11}B} NMR (300.13 MHz), ^{13}C{^{1}H} NMR (75.47 MHz), and ^{11}B NMR (96.29 MHz) spectra were recorded with a Bruker ARX 300 instrument equipped with the appropriate decoupling accessories. Chemical shift values for ^{11}B NMR spectra are referenced to external $BF_3 \cdot OEt_2$, and those for ^{1}H, ^{1}H{^{11}B}, and ^{13}C{^{1}H} NMR spectra are referenced to $SiMe_4$. Chemical shifts are reported in units of parts per million downfield from the reference signal, and all coupling constants are reported in Hertz.

Unless otherwise noted, all manipulations were carried out under a dinitrogen atmosphere using standard vacuum line techniques. THF was distilled from sodium/benzophenone prior to use. EtOH was dried over molecular sieves and deoxygenated prior to use. The cesium salt of compound [**1**]$^-$ was supplied by Katchem Ltd. (Prague) and was used as received. All other reagents were obtained commercially and were used as purchased. Bis(triphenylphosphine)palladium dichloride[49] was synthesized according to the literature.

Electrochemical measurements were performed in a standard double-compartment three-electrode cell. Ag/AgCl/[nBu$_4$N]Cl (0.1 M in MeCN) was used as a reference electrode. A 4 mm^2 platinum plate and a platinum wire were used as working and counter electrode, respectively. All measurements were performed in acetonitrile with 0.1 M tetrabutylammonium perchlorate as supporting electrolyte. Cyclic voltammograms were recorded at a scan rate of 100 mV s^{-1}. The mass spectra were recorded in negative-ion mode using a Bruker Biflex MALDI-TOF MS [N_2 laser; λ_{exc} 337 nm (0.5 ns pulses); voltage ion source 20.00 kV (Uis 1) and 17.50 kV (Uis 2)].

Synthesis of Cs[8-I-3,3′-Co(1,2-C$_2$B$_9$H$_{10}$)(1′,2′-C$_2$B$_9$H$_{11}$)] (Cs[2]): Iodine (1.67 g, 6.58 mmol) was added to a solution of Cs[**1**] (1.5 g, 3.28 mmol) in EtOH (20 mL). The reaction mixture was left to stand overnight at room temperature and was then heated under reflux for 2.5 h. The excess iodine was decomposed by the addition of a solution of Na_2SO_3 (0.66 g, 5.26 mmol) in water (16 mL) and the resulting mixture was boiled for 5 min. The mixture was concentrated until the precipitation of an orange solid. This was filtered off, washed with water and petroleum ether, and dried in vacuo (1.82 g, 95 %). ^{1}H{^{11}B} NMR (300 MHz, [D$_6$]acetone, 25 °C, TMS): $\delta = 4.54$ (brs, 2H; C$_c$–H), 4.29 (brs, 2H; C$_c$–H), 3.04 (brs, 2H; B–H), 2.59 (brs, 2H; B–H), 2.46 (brs, 4H; B–H), 1.93 (brs, 4H; B–H), 1.84 (brs, 1H; B–H), 1.77 (brs, 2H; B–H), 1.70 (brs, 2H; B–H); IR (KBr): $\tilde{\nu} =$ 3040, 3032 (C$_c$–H), 2574, 2542, 2500 (B–H), 1138, 1099, 1016, 976, 617, 773, 750 cm^{-1}; MALDI-TOF MS: m/z (%): 449.3 (100) [M^+], 323.5 (47) [$M^+ -$ I]; elemental analysis calcd (%) for C$_4$H$_{21}$B$_{18}$CoCsI: C 8.25, H 3.63; found: C 8.35, H 3.50.

Synthesis of [nBu$_4$N][8-Me-3,3′-Co(1,2-C$_2$B$_9$H$_{10}$)(1′,2′-C$_2$B$_9$H$_{11}$)] ([nBu$_4$N][3]): A solution of Cs[**2**] (1.0 g, 1.72 mmol) in THF (100 mL) was treated with methylmagnesium bromide (2.29 mL, 3.0 M in diethyl ether; 6.88 mmol) at −84 °C, forming a brown precipitate. The mixture was allowed to warm to room temperature, and then [PdCl$_2$(PPh$_3$)$_2$] (0.14 g, 0.21 mmol) and CuI (0.049 g, 0.26 mmol) were added. The mixture was refluxed for 20 h. Twenty drops of water were then added to quench the excess Grignard reagent, and the solvent was removed in vacuo. The residue was extracted with dichloromethane (3 × 30 mL) and the remaining black insoluble material was discarded. The solvent was removed and water (30 mL) was added to the yellow residue. This was extracted with diethyl ether (3 × 30 mL), and the combined organic layers were dried over anhydrous magnesium sulfate. The solvent was removed, the product was redissolved in hot water (50 mL), and [nBu$_4$N]Cl · H$_2$O (0.96 g, 3.44 mmol) was added to precipitate the product. The precipitate was collected by filtration and dried in vacuo (0.91 g, 91 %). ^{1}H{^{11}B} NMR (300 MHz, [D$_6$]acetone, 25 °C, TMS): $\delta = 4.08$ (brs, 2H; C$_c$–H), 3.87 (brs, 2H; C$_c$–H), 3.44 (t, ^3J(H,H) = 8 Hz, 8H; N(CH$_2$CH$_2$CH$_2$CH$_3$)$_4$), 2.93 (brs, 2H; B–H), 2.73 (brs, 2H; B–H), 2.65 (brs; B–H), 1.96 (brs; B–H), 1.91 (brs; B–H), 1.68 (brs; B–H), 1.79 (q, ^3J(H,H) = 8 Hz, 8H; N(CH$_2$CH$_2$CH$_2$CH$_3$)$_4$), 1.58 (brs; B–H), 1.42 (h, ^3J(H,H) = 7 Hz, 8H; N(CH$_2$CH$_2$CH$_2$CH$_3$)$_4$), 0.98 (t, ^3J(H,H) = 7 Hz, 12H; N(CH$_2$CH$_2$CH$_2$CH$_3$)$_4$), 0.59 (brs, 3H; B–Me); IR (KBr): $\tilde{\nu} =$ 3055 (C$_c$–H), 2962, 2922, 2873 (C$_{alkyl}$–H), 2554 (B–H), 1465, 1436, 1383 (δ(C–H)$_{alkyl}$), 1100, 1098 (B–C), 973 (υ_{as}(C–N)), 718, 694 (γ(C–H)), 535 cm^{-1}; MALDI-TOF MS: m/z (%): 338.6 (100) [M^+]; elemental analysis calcd (%) for C$_{21}$H$_{60}$B$_{18}$CoN: C 43.47, H 10.42, N 2.41; found: C 43.15, H 10.50, N 2.57.

Synthesis of [Me$_4$N][8-Et-3,3′-Co(1,2-C$_2$B$_9$H$_{10}$)(1′,2′-C$_2$B$_9$H$_{11}$)] ([Me$_4$N][4]): A solution of ethylmagnesium bromide (3.0 M in diethyl ether; 0.46 mL, 1.37 mmol) was added dropwise to a stirred solution of Cs[**2**] (200 mg, 0.34 mmol) in THF (50 mL) at 0 °C. The mixture was set aside at room temperature for 2 h and then [PdCl$_2$(PPh$_3$)$_2$] (10 mg, 0.01 mmol) and CuI (2 mg, 0.01 mmol) were added in a single portion. The brown solution was refluxed for 20 min and a grey solid was filtered off and discarded. After removal of the solvent, diethyl ether (20 mL) was added to the residue and the excess Grignard reagent was destroyed by the slow addition of dilute HCl. The organic phase was separated, and the aqueous layer was extracted with diethyl ether (3 × 20 mL). The combined organic layers were washed with water (3 × 20 mL) and dried over anhydrous magnesium sulfate. The solvent was removed. The residue was dissolved in the minimum volume of EtOH and an aqueous solution containing an excess of [Me$_4$N]Cl was added, resulting in the formation of a precipitate. This was filtered off, washed with water and petroleum ether, and dried in vacuo (117 mg, 80 %). ^{1}H{^{11}B} NMR (300 MHz, [D$_6$]acetone, 25 °C, TMS): $\delta = 4.10$ (brs, 2H; C$_c$–H), 3.88 (brs, 2H; C$_c$–H), 3.42 (s, 12H; Me$_4$N), 3.06 (brs, 2H; B–H), 2.90 (brs, 2H; B–H), 2.71 (brs, 2H; B–H), 2.64 (brs, 1H; B–H), 1.94 (brs, 2H; B–H), 1.86 (brs, 2H; B–H), 1.64 (brs, 2H; B–H), 1.57 (brs, 4H; B–H), 1.18 (q, ^3J(H,H) = 8 Hz, 2H; CH_2CH$_3$), 0.87 (t, ^3J(H,H) = 8 Hz, 3H; CH$_2$CH_3); IR (KBr): $\tilde{\nu} =$ 3038 (C$_c$–H), 2941, 2922, 2862 (C$_{alkyl}$–H), 2544, 2513 (B–H), 1481 (δ(C–H)$_{alkyl}$), 947 (υ_{as}(C–N)), 743, 719 cm^{-1} (B–C); MALDI-TOF MS: m/z (%): 352.5 (100) [M^+]; elemental analysis calcd (%) for C$_{10}$H$_{38}$B$_{18}$CoN: C 28.20, H 8.99, N 3.29; found: C 28.18, H 9.05, N 3.27.

Synthesis of [Me$_4$N][8-C$_6$H$_5$-3,3′-Co(1,2-C$_2$B$_9$H$_{10}$)(1′,2′-C$_2$B$_9$H$_{11}$)] ([Me$_4$N][5]): Similarly, Cs[**2**] (200 mg, 0.34 mmol) in THF (50 mL) and a solution of phenylmagnesium bromide (1.0 mL; 1.37 mmol), prepared from magnesium turnings (0.67 g, 27.56 mmol) and bromobenzene (1.5 mL, 14.27 mmol), were reacted at 0 °C in THF (10 mL). After 30 min at room temperature, [PdCl$_2$(PPh$_3$)$_2$] (10 mg, 0.01 mmol) and CuI (2 mg, 0.01 mmol) were added. The brown solution was heated under reflux for 2 h. Work-up and purification as described above gave [Me$_4$N][**5**] (150 mg, 92 %). ^{1}H{^{11}B} NMR (300 MHz, [D$_6$]acetone, 25 °C, TMS): $\delta = 7.32 - 7.01$ (m, 5H; C$_6$H$_5$), 4.58 (brs, 2H; C$_c$–H), 3.76 (brs, 2H; C$_c$–H), 3.42 (s, 12H; Me$_4$N), 3.12 (brs, 2H; B–H), 2.91 (brs, 2H; B–H), 2.85 (brs, 4H; B–H), 2.77 (brs, 2H; B–H), 1.93 (brs, 2H; B–H), 1.79 (brs, 4H; B–H), 1.75 (brs, 1H; B–H); IR (KBr): $\tilde{\nu} =$ 3028 (C$_c$–H), 2961, 2874 (C$_{aryl/alkyl}$–H), 2554, 2536, 2473 (B–H), 1479 (δ(C–H)$_{alkyl}$), 947 (υ_{as}(C–N)), 742, 704 cm^{-1} (B–C); MALDI-TOF MS: m/z (%): 400.8 (100) [M^+]; elemental analysis calcd (%) for C$_{14}$H$_{38}$B$_{18}$CoN: C 35.48, H 8.08, N 2.96; found: C 35.30, H 8.00, N 2.93.

Synthesis of [Me$_4$N][8-C$_{12}$H$_9$-3,3′-Co(1,2-C$_2$B$_9$H$_{10}$)(1′,2′-C$_2$B$_9$H$_{11}$)] ([Me$_4$N][6]): Similarly, Cs[**2**] (200 mg, 0.34 mmol) in THF (50 mL) and a solution of biphenylmagnesium bromide (1.37 mmol), prepared from magnesium turnings (67 mg, 2.75 mmol) and 4-bromobiphenyl (0.32 g, 1.37 mmol), were reacted at 0 °C in THF (6.0 mL). After 30 min at room temperature, [PdCl$_2$(PPh$_3$)$_2$] (10 mg, 0.01 mmol) and CuI (2 mg, 0.01 mmol) were added. The brown solution was refluxed for 2 d. Work-up and purification as described above gave [Me$_4$N][**6**] (180 mg, 95 %). ^{1}H{^{11}B} NMR (300 MHz, [D$_6$]acetone, 25 °C, TMS): $\delta = 7.66 - 7.35$ (m, 5H; C$_{12}$H$_9$), 4.60 (brs, 2H; C$_c$–H), 3.87 (brs, 2H; C$_c$–H), 3.36 (s, 12H; Me$_4$N), 3.18 (brs, 2H; B–H), 2.95 (brs, 1H; B–H), 2.82 (brs, 2H; B–H), 2.63 (brs, 1H; B–H), 2.18 (brs, 1H; B–H), 2.04 (brs, 4H; B–H), 1.77 (brs, 4H; B–H), 1.53 (brs, 2H; B–H); IR (KBr): $\tilde{\nu} =$ 3028 (C$_c$–H), 2961, 2922, 2866 (C$_{aryl/alkyl}$–H), 2559 (B–H), 1481 (δ(C–H)$_{alkyl}$), 945 (υ_{as}(C–N)), 740, 700 cm^{-1} (B–C); MALDI-TOF MS: m/z (%): 476.6 (100) [M^+]; elemental analysis calcd (%) for C$_{20}$H$_{42}$B$_{18}$CoN: C 43.67, H 7.70, N 2.55; found: C 43.50, H 7.60, N 2.50.

Synthesis of Cs[8-$C_{14}H_9$-3,3′-Co(1,2-$C_2B_9H_{10}$)(1′,2′-$C_2B_9H_{11}$)] (Cs[7]): Similarly, Cs[**2**] (100 mg, 0.17 mmol) in THF (25 mL) was treated with a solution of anthracenylmagnesium bromide (1.37 mmol), prepared from magnesium turnings (67 mg, 2.75 mmol) and 9-bromoanthracene (0.35 g, 1.37 mmol) in THF (24 mL) at 0 °C. After 30 min at room temperature, [$PdCl_2(PPh_3)_2$] (10 mg, 0.01 mmol) and CuI (2 mg, 0.01 mmol) were added. The brown solution was heated under reflux for 41 h. Some drops of water were added to destroy the excess Grignard reagent and the solid was filtered off and discarded. The solution was concentrated, causing the precipitation of a red solid, which was collected by filtration and dried in vacuo (83 mg, 76 %). $^1H\{^{11}B\}$ NMR (300 MHz, [D_6]acetone, 25 °C, TMS): $\delta = 9.40$, 8.53, 8.24, 8.05, 7.88, 7.51, 7.32, 6.95 (m, 9H; $C_{14}H_9$), 4.52 (brs, 2H; C_c–H), 3.82 (brs, 4H; B–H), 3.15 (brs, 1H; B–H), 3.08 (brs, 2H; C_c–H), 2.71 (brs, 2H; B–H), 2.63 (brs, 2H; B–H), 2.58 (brs, 2H; B–H), 1.95 (brs, 1H; B–H), 1.58 (brs, 2H; B–H), 1.11 (brs, 2H; B–H), 0.71 (brs, 1H; B–H); IR (KBr): $\tilde{\nu} = 3047$ (C_c–H), 2970 (C_{aryl}–H), 2559 (B–H), 727 cm^{-1} (B–C); MALDI-TOF MS: *m*/*z* (%): 501.7 (100) [M^+]; elemental analysis calcd (%) for $C_{18}H_{30}B_{18}CoCs$: C 34.16, H 4.78; found: C 34.26, H 4.80.

Synthesis of [Me_4N][8-C_6H_4*n*Bu-3,3′-Co(1,2-$C_2B_9H_{10}$)(1′,2′-$C_2B_9H_{11}$)] ([Me_4N][8]): Similarly, Cs[**2**] (200 mg, 0.34 mmol) in THF (40 mL) was treated with a solution of 4-butylphenylmagnesium bromide (1.37 mmol), prepared from magnesium turnings (67 mg, 2.75 mmol) and 1-bromo-4-butylbenzene (0.24 mL, 1.37 mmol) in THF (6 mL) at 0 °C. After 30 min at room temperature, [$PdCl_2(PPh_3)_2$] (96 mg, 0.04 mmol) and CuI (26 mg, 0.04 mmol) were added. The reaction mixture was refluxed for 5 min and was left at room temperature overnight. Work-up and purification as described above gave [Me_4N][**8**] (170 mg, 93 %). $^1H\{^{11}B\}$ NMR (300 MHz, [D_6]acetone, 25 °C, TMS): $\delta = 7.21$ (d, $^3J(H,H) = 8$, 2H, C_6H_4), 6.92 (d, $^3J(H,H) = 8$, 2H, C_6H_4), 4.60 (brs, 2H, C_c–H), 3.73 (brs, 2H, C_c–H), 3.42 (s, 12H, Me_4N), 3.11 (brs, 2H, B–H), 2.86 (brs, 2H, B–H), 2.80 (brs, 2H, B–H), 2.50 (t, $^3J(H,H) = 8$, 2H, $CH_2CH_2CH_2CH_3$), 1.92 (brs, 2H, B–H), 1.74 (brs, 2H, B–H), 1.71 (brs, 2H, B–H), 1.54 (c, $^3J(H,H) = 8$, 2H, $CH_2CH_2CH_2CH_3$), 1.50 (brs, 3H, B–H), 1.41 (brs, 2H, B–H), 1.30 (h, $^3J(H,H) = 7$, 2H, $CH_2CH_2CH_2CH_3$), 0.89 (t, $^3J(H,H) = 7$, 2H, $CH_2CH_2CH_2CH_3$); IR (KBr): $\tilde{\nu} = 3038$ ($C_{cluster/aryl}$–H), 2951, 2928, 2856 (C_{alkyl}–H), 2534 (B–H), 1479 (δ(C–H)$_{alkyl}$), 947 (υ_{as}(C–N)), 742, 702 cm^{-1} (B–C); elemental analysis calcd (%) for $C_{18}H_{46}B_{18}CoN$: C 40.78, H 8.75, N 2.64; found: C 40.69, H 8.68, N 2.67.

Synthesis of [Me_4N][8-$C_2H_4C_6H_5$-3,3′-Co(1,2-$C_2B_9H_{10}$)(1′,2′-$C_2B_9H_{11}$)] ([Me_4N][9]): Similarly, Cs[**2**] (200 mg, 0.34 mmol) in THF (15 mL) was treated with a solution of 2-phenylethylmagnesium bromide (1.37 mmol), prepared from magnesium turnings (67 mg, 2.75 mmol) and (2-bromoethyl)benzene (0.19 mL, 1.37 mmol) in THF (6 mL) at 0 °C. After 30 min at room temperature, [$PdCl_2(PPh_3)_2$] (96 mg, 0.04 mmol) and CuI (26 mg, 0.04 mmol) were added. The reaction mixture was refluxed for 15 min and was left at room temperature overnight. Work-up and purification as described above gave [Me_4N][**9**] (140 mg, 81 %). $^1H\{^{11}B\}$ NMR (300 MHz, [D_6]acetone, 25 °C, TMS): $\delta = 7.18$ (m(a), C_6H_5), 4.12 (brs, 2H, C_c–H), 3.92 (brs, 2H, C_c–H), 3.37 (s, 12H, Me_4N), 2.95 (brs, 2H, B–H), 2.82 (brs, 2H, B–H), 2.72 (brs, 2H, B–H), 2.08 (t, $^3J(H,H) = 3$, 2H, CH_2), 1.91 (brs, 3H, B–H), 1.60 (brs, 8H, B–H), 1.40 (t, $^3J(H,H) = 3$, 2H, CH_2); IR (KBr): $\tilde{\nu} =$ 3028 ($C_{cluster/aryl}$–H), 2922, 2854 (C_{alkyl}–H), 2602, 2554, 2523 (B–H), 1479 (δ(C–H)$_{alkyl}$), 943 (υ_{as}(C–N)), 762, 706 cm^{-1} (B–C); elemental analysis calcd (%) for $C_{16}H_{42}B_{18}CoN$: C 38.28, H 8.43, N 2.79; found: C 37.98, H 8.33, N 2.82.

X-ray crystallography: Single-crystal data collections for [nBu$_4$N][**3**], [Me_4N][**8**], and [Me_4N][**9**] were performed at −100 °C on an Enraf-Nonius KappaCCD diffractometer using graphite-monochromated $Mo_{K\alpha}$ radiation. A total of 6075, 4403, and 5083 unique reflections were collected for [nBu$_4$N][**3**], [Me_4N][**8**], and [Me_4N][**9**], respectively. The structures were solved by direct methods and refined against F^2 using the SHELXL97 program.[50] For all structures, the hydrogen atoms were treated as riding using the SHELXL97 default parameters. For [nBu$_4$N][**3**], all non-hydrogen atoms were refined with anisotropic displacement parameters.

In the case of [Me_4N][**8**], for the butyl chain connected to the phenyl group only the vicinal carbon atom of the latter could be clearly located in the Fourier map. In the vicinity of this carbon, a bulky volume with an electron density of just below 1.0 e Å^{-3} was found, indicating that neither of the other three carbon atoms of the butyl chain occupies a defined position, and that the chain does not have a fixed orientation in the solid state. Possible positions of the three "missing" atoms of the butyl chain were assumed and the chain was refined by applying DFIX restraints and a fixed isotropic thermal displacement parameter of 0.2 Å^{-2} for the three terminal carbon atoms. The $[Me_4N]^+$ ion is disordered with the central nitrogen occupying one position but each of the methyl groups split between two positions. The disordered methyl carbons of the $[Me_4N]^+$ ion and the three terminal carbon atoms of the butyl chain were refined with isotropic displacement parameters, but the remaining non-hydrogen atoms were refined with anisotropic displacement parameters. [Me_4N][**8**] crystallizes in a non-centrosymmetric space group, and its absolute configuration was determined by refinement of the Flack *x* parameter. [Me_4N][**8**] has a lot of pseudo symmetry, as a result of which it can also be refined in the centrosymmetric space group *C*2/*c*, but this results in higher *R* values and a chemically unrealistic 1D structure.

For [Me_4N][**9**], the $[Me_4N]^+$ ion is disordered showing rotational disorder about the N–C21 bond. The three disordered carbon atoms of the $[Me_4N]^+$ ion were refined with isotropic displacement parameters, but the remaining non-hydrogen atoms were refined with anisotropic displacement parameters. [Me_4N][**9**] crystallizes in a non-centrosymmetric space group, and its absolute configuration was determined by refinement of the Flack *x* parameter.

CCDC-206027, -206028, and -206029, [nBu$_4$N][8-Me-3,3′-Co(1,2-$C_2B_9H_{10}$)(1′,2′-$C_2B_9H_{11}$)], ([nBu$_4$N][**3**]), [Me_4N][8-C_6H_4*n*Bu-3,3′-Co(1,2-$C_2B_9H_{10}$)(1′,2′-$C_2B_9H_{11}$)], ([Me_4N][**8**]), and [Me_4N][8-$C_2H_4C_6H_5$-3,3′-Co(1,2-$C_2B_9H_{10}$)(1′,2′-$C_2B_9H_{11}$)], ([Me_4N][**9**]) contain the supplementary crystallographic data for this paper. These data can be obtained free of charge via www.ccdc.cam.ac.uk/conts/retrieving.html (or from the Cambridge Crystallographic Data Centre, 12 Union Road, Cambridge CB2 1EZ, UK; fax: (+44) 1223-336033; or deposit@ccdc.cam.uk).

Acknowledgement

We thank ENRESA for partial support of this research, as well as MCyT (MAT01–1575) and the Generalitat de Catalunya 2001/SGR/00337.

[1] a) N. J. Long, *Metallocenes: An Introduction to Sandwich Complexes*, Blackwell Science, **1998**; b) A. Togni, R. L. Halterman, *Metallocenes: Synthesis-Reactivity-Applications*, Wiley-VCH, New York, **1998**.
[2] a) J. Ebels, R. Pietschnig, S. Kotila, A. Dombrowski, E. Niecke, M. Nieger, H. M. Schiffner, *Eur. J. Inorg. Chem.* **1998**, 331; b) P. Jutzi, *Comm. Inorg. Chem.* **1987**, *6*, 123.
[3] M. M. Conejo, R. Fernández, E. Gutiérrez-Puebla, A. Monge, C. Ruiz, E. Carmona, *Angew. Chem.* **2000**, *112*, 2025; *Angew. Chem. Int. Ed.* **2000**, *39*, 1949.
[4] G. Rossetto, P. Zanella, G. Carta, R. Bertani, D. Favretto, G. M. Ingo, *Appl. Organomet. Chem.* **1999**, *13*, 509.
[5] D. Zargarian, *Coord. Chem. Rev.* **2002**, 102, 157.
[6] a) N. Kuhn, *Bull. Soc. Chim. Belg.* **1990**, *99*, 707; b) N. Kuhn, G. Henkel, S. Stubenrauch, *Angew. Chem.* **1992**, *104*, 766; *Angew. Chem. Int. Ed. Engl.* **1992**, *31*, 778; c) N. Kuhn, M. Köckerling, S. Stubenrauch, D. Bläser, R. Boese, *J. Chem. Soc. Chem. Commun.* **1991**, 1368.
[7] a) C. Janiak, N. Kuhn, R. Gleiter, *J. Organomet. Chem.* **1994**, *475*, 223; b) N. Kuhn, G. Henkel, J. Kreutzberg, S. Stubenrauch, C. Janiak, *J. Organomet. Chem.* **1993**, *456*, 97.
[8] T. A. Albright, J. K. Burdett, M. H. Whangbo, *Orbital Interactions in Chemistry*, Wiley-Interscience, New York, **1985**, pp. 219.
[9] T. Peymann, C. B. Knobler, M. F. Hawthorne, *J. Am. Chem. Soc.* **1999**, *121*, 5601.
[10] a) B. T. King, Z. Janousek, B. Grüner, M. Trammell, B. C. Noll, J. Michl, *J. Am. Chem. Soc.* **1996**, *118*, 3313; b) D. Stasko, C. A. Reed, *J. Am. Chem. Soc.* **2002**, *124*, 1148; c) M. J. Ingleson, M. F. Mahon, N. J. Patmore, G. D. Ruggiero, A. S. Weller, *Angew. Chem.* **2002**, *114*, 3846; *Angew. Chem. Int. Ed.* **2002**, *41*, 3694.
[11] W. Jiang, C. B. Knobler, M. D. Mortimer, M. F. Hawthorne, *Angew. Chem.* **1995**, *107*, 1470; *Angew. Chem. Int. Ed. Engl.* **1995**, *34*, 1332.
[12] A. Herzog, A. Maderna, G. N. Harakas, C. B. Knobler, M. F. Hawthorne, *Chem. Eur. J.* **1999**, *5*, 1212.
[13] a) L. I. Zakharkin, A. I. Kovredou, V. A. Ol'shevskaya, Zh. S. Shaugumbekova, *J. Organomet. Chem.* **1982**, *226*, 217; b) J. Li, C. M.

Logan, M. Jones, *Inorg. Chem.* **1991**, *30*, 4866; c) G. Barberà, F. Teixidor, C. Viñas, R. Sillanpää, R. Kivekäs, *Eur. J. Inorg. Chem*. **2003**, 1511.
[14] B. T. King, B. C. Noll, A. J. McKinley, J. Michl, *J. Am. Chem. Soc.* **1996**, *118*, 10902.
[15] a) Z. Zheng, W. Jiang, A. A. Zinn, C. B. Knobler, M. F. Hawthorne, *Inorg. Chem.* **1995**, *34*, 2095; b) W. Jiang, C. B. Knobler, C. E. Curtis, M. D. Mortimer, M. F. Hawthorne, *Inorg. Chem.* **1995**, *34*, 3491.
[16] I. B. Sivaer, V. I. Bregadze, *Collect. Czech. Chem. Commun.* **1999**, *64*, 783.
[17] R. M. Chamberlin, B. L. Scott, M. M. Melo, K. D. Abney, *Inorg. Chem.* **1997**, *36*, 809.
[18] C. Viñas, J. Pedrajas, J. Bertran, F. Teixidor, R. Kivekäs, R. Sillanpää, *Inorg. Chem.* **1997**, *36*, 2482; b) C. Viñas, S. Gomez, J. Bertran, F. Teixidor, J. F. Dozol, H. Rouquette, *Chem. Commun.* **1998**, 191; c) C. Viñas, S. Gomez, J. Bertran, F. Teixidor, J. F. Dozol, H. Rouquette, *Inorg. Chem.* **1998**, *37*, 3640; d) C. Viñas, J. Bertran, S. Gomez, F. Teixidor, J. F. Dozol, H. Rouquette, R. Kivekäs, R. Sillanpää, *J. Chem. Soc. Dalton Trans.* **1998**, 2849.
[19] J. N. Francis, M. F. Hawthorne, *Inorg. Chem.* **1971**, *10*, 594.
[20] a) J. Plesek, S. Hermánek, K. Base, L. J. Todd, W. F. Wright, *Collect. Czech. Chem. Commun.* **1976**, *41*, 3509; b) Z. Janousek, J. Plesek, S. Hermánek, K. Base, L. J. Todd, W. F. Wright, *Collect. Czech. Chem. Communn.* **1981**, *46*, 2818.
[21] J. Plesek, S. Hermánek, A. Franken, I. Císarová, C. Nachtigal, *Collect. Czech. Chem. Commun.* **1997**, *62*, 47.
[22] a) I. B. Sivaev, Z. A. Starikova, S. Sjöberg, V. I. Bregadze, *J. Organomet. Chem.* **2002**, *649*, 1; b) P. Selucky, J. Plesek, J. Rais, J. M. Kyrs, L. Kadlecova, *J. Radioanal. Nucl. Chem.* **1991**, *149*, 131; c) J. Plesek, B. Grüner, S. Hermánek, J. Báca, V. Marecek, J. Jänchenová, A. Lhotský, K. Holub, P. Selucký, J. Rais, I. Císarová, J. Cáslavský, *Polyhedron* **2002**, *21*, 975; d) B. Grüner, J. Plesek, J. Báca, I. Císarová, J. F. Dozol, H. Rouquette, C. Viñas, P. Selucký, J. Rais, *New J. Chem.* **2002**, *26*, 1519; e) J. Llop, C. Masalles, C. Viñas, F. Teixidor, R. Sillanpää, R. Kivekäs, *J. Chem. Soc. Dalton Trans.* **2003**, 556; f) F. Teixidor, J. Pedrajas, I. Rojo, C. Viñas, R. Kivekäs, R. Sillanpää, I. Sivaev, V. Bregadze, S. Sjöberg, *Organometallics*, in press .
[23] a) J. Plesek, B. Grüner, J. Báca, J. Fusek, I. Císarová, *J. Organomet. Chem.* **2002**, *649*, 181; b) J. Plesek, B. Grüner, I. Císarová, J. Báca, P. Selucký, J. Rais, *J. Organomet. Chem.* **2002**, *657*, 59.
[24] a) P. K. Hurlburt, R. L. Miller, K. D. Abney, T. M. Foreman, R. J. Butcher, S. A. Kinkead, *Inorg. Chem.* **1995**, *34*, 5215; b) L. Matel, R. Cech, F. Macásek, S. Hermánek, J. Plesek, *Radiochem. Radioanal. Lett.* **1978**, *35*, 241; c) T. E. Paxson, M. K. Kaloustian, G. M. Tom, R. J. Wiersema, M. F. Hawthorne, *J. Am. Chem. Soc.* **1972**, *94*, 4882; d) J. C. Fanning, L. A. Huff, W. A. Smith, A. S. Terell, L. Yasinsac, L. J. Todd, S. A. Jasper, D. J. McCabe, *Polyhedron* **1995**, *14*, 2893.
[25] L. Matel, F. Macásek, P. Rajec, S. Hermánek, J. Plesek, *Polyhedron* **1982**, *1*, 511.
[26] V. I. Bregadze, *Chem. Rev.* **1992**, *92*, 209.
[27] M. D. Mortimer, C. B. Knobler, M. F. Hawthorne, *Inorg. Chem.* **1996**, *35*, 5750.
[28] W. Jiang, D. E. Harwell, M. D. Mortimer, C. B. Knobler, M. F. Hawthorne, *Inorg. Chem.* **1996**, *35*, 4355.
[29] R. N. Grimes, *Carboranes*, Academic Press, New York, **1970**.
[30] a) S. Hermanek, J. Plesek, B. Stibr, V. Grigor, *J. Chem. Soc. Chem. Commun.* **1977**, 561; b) F. Teixidor, C. Viñas, R. W. Rudolph, *Inorg. Chem.* **1986**, *25*, 3339.
[31] a) S. Hermanek, V. Gregor, B. Stibr, J. Plesek, Z. Janousek, V. A. Antonovich, *Collect. Czech. Chem. Commun.* **1976**, *41*, 1492; b) V. I. Stanko, T. A. Babushkina, T. P. Klimova, Y. U. Goltyapin, A. I. Klimova, A. M. Vasilev, A. M. Alymov, V. V. Khrapov, *Zh. Obshch. Khim.* **1976**, *46*, 1071.
[32] Z. Janousek, J. Plesek, S. Hermanek, K. Base, L. J. Todd, W. F. Wright, *Collect. Czech. Chem. Commun*. **1981**, *46*, 2818.
[33] a) D. Reed, *J. Chem. Res.* **1984**, 198; b) T. L. Venable, W. C. Hutton, R. N. Grimes, *J. Am. Chem. Soc.* **1984**, *106*, 29.
[34] a) L. Borodinsky, E. Sinn, R. N. Grimes, *Inorg. Chem.* **1982**, *21*, 1686; b) C. Viñas, J. Bertran, S. Gomez, F. Teixidor, J. F. Dozol, H. Rouquette, R. Kivekäs, R. Sillanpää, *J. Chem. Soc. Dalton Trans.* **1998**, 2849.
[35] C. Viñas, G. Barberà, J. M. Oliva, F. Teixidor, A. J. Welch, G. M. Rosair, *Inorg. Chem.* **2001**, *40*, 6555.
[36] Formally, we are assuming a Co^{III}/Co^{II} couple, although later molecular orbital analyses are indicative of the strong participation of ligand-based orbitals.
[37] M. F. Hawthorne, D. C. Young, T. D. Andrews, D. V. Howe, R. L. Pilling, A. D. Pitts, M. Reintjes, L. F. Warren Jr., P. A. Wegner, *J. Am. Chem. Soc.* **1968**, *90*, 879.
[38] V. Cerný, I. Pavlík, E. Kustková-Maxová, *Collect. Czech. Chem. Communn.* **1976**, *41*, 3232.
[39] Fitting analysis was performed using the Origin 6.0 program, 1991–1999, Microcal (TM) Software, Inc., Northampton (USA).
[40] a) B. S. Furniss, A. J. Hannaford, P. W. G. Smith, A. R. Tatchell, *Textbook of Practical Organic Chemistry*, Longman Scientific & Technical **1989**, p. 392; b) A. J. Gordon, R. A. Ford, *The Chemist's Companion: A Handbook of Practical Data, Techniques and References*, Wiley, **1972**, p. 216.
[41] Y. S. Sohn, D. N. Hendrickson, H. B. Gray, *J. Am. Chem. Soc.* **1971**, *93*, 3603.
[42] R. M. Wing, *J. Am. Chem. Soc.* **1967**, *89*, 5599.
[43] a) W. E. Geiger, D. Brennan, *Inorg. Chem.* **1982**, *21*, 1963; b) W. E. Geiger, *J. Am. Chem. Soc.* **1974**, *96*, 2632.
[44] a) M. F. Hawthorne, *Acc. Chem. Res.* **1968**, *1*, 281; b) L. F. Warren Jr., M. F. Hawthorne, *J. Am. Chem. Soc.* **1968**, *90*, 4823.
[45] A. Appel, F. Jäkle, T. Priermeier, R. Schmid, M. Wagner, *Organometallics* **1996**, *15*, 1188.
[46] Hyperchem Release 7 for Windows (Hypercube Inc.).
[47] L. Borodinsky, E. Sinn, R. N. Grimes, *Inorg. Chem.* **1982**, *21*, 1686.
[48] P. Sivy, A. Preisinger, O. Baumgartner, F. Valach, B. Koren, L. Matel, *Acta Crystallogr. Sect. C* **1986**, *42*, 30.
[49] J. R. Blackburn, R. Nordberg, F. Stevie, R. G. Albrigde, M. M. Jones, *Inorg. Chem.* **1970**, *9*, 2374.
[50] G. M. Sheldrick, SHELXL97, University of Göttingen (Germany), **1997**.

Received: March 20, 2003 [F4970]

Methylation and de-methylation in cobaltabisdicarbollide derivatives.

Isabel Rojo,[a,1] Francesc Teixidor,[a] Raikko Kivekäs,[b] Reijo Sillanpää,[c] Clara Viñas[a *].

[a] *Institut de Ciència de Materials de Barcelona (CSIC), Campus de la U.A.B., E-08193 Bellaterra, Spain. Telefax: Int. Code + 34 93 5805729.* [b] *Department of Chemistry, P.O. Box 55, University of Helsinki, FIN-00014, Finland.* [c] *Department of Chemistry, University of Jyväskylä, FIN-40351, Finland.*

RECEIVED DATE (automatically inserted by publisher); E-mail: clara@icmab.es

Introduction

Since its discovery,[1] the chemistry of cobaltabisdicarbollide anion, [3,3'-Co(1,2-$C_2B_9H_{11})_2$]$^-$, [**1**]$^-$, has been prevalent within the boron cluster literature, and it continues to be a subject of intense study.[2] Halogen substituted derivatives such as [8,8',9,9',12,12'-X_6-3,3'-Co(1,2-$C_2B_9H_8)_2$]$^-$, (X= Cl, Br, I), [8,8'-X_2-3,3'-Co(1,2-$C_2B_9H_{10})_2$]$^-$, (X= Cl, Br, I), have been synthesized but, with some exceptions, they have not been considered suitable starting materials[3] to produce derivatives of [**1**]$^-$. Recently Hawthorne et al.[4] have reported the synthesis of [3,3'-Co(8,9,12-$(CH_3)_3$-1,2-$C_2B_9H_8)_2$]$^-$ starting from [8,8',9,9',12,12'-I_6-3,3'-Co(1,2-$C_2B_9H_8)_2$]$^-$, which opens a route to hexasubstituted derivatives of [**1**]$^-$. Also, B(8)-O derivatives of [3,3'-Co($C_2B_9R_3H_8)_2$]$^-$ are available through [8-$C_4H_8O_2$-3,3'-Co(1,2-$C_2B_9H_{10}$)(1',2'-$C_2B_9H_{11}$)] which was reported in 1996.[5] This dioxanate compound is susceptible to nucleophilic attack on the positively charged oxygen atom, e.g. by pyrrolyl,[6] imide, cyanide or amines,[7] phenolate, dialkyl or diarylphosphite[8] and N-alkylcarbamoyldiphenylphosphine oxides[9] resulting in one anionic species as a consequence of the opening of the dioxane ring. But mono or di B(8)-R (R= alkyl) substituted derivatives of [**1**]$^-$ have not yet been reported. In this work we report on the application of a modified Kumada reaction[10] to produce B-C bonds for the di-substituted cobaltabisdicarbollide derivatives. Molecules containing B-C and B-O bonds are also generated and, interestingly, a high yield oxo-de-methylation is observed for the first time in cluster boron chemistry.

Results and Discussion

Caesium 8,8'-diiodocobaltabisdicarbollide, Cs[**2**], was prepared by a modification of the original synthesis by Mátel et al.[3a] employing ICl instead of I_2. The procedure is much more simple and permits the isolation of Cs[**2**] with an easy purification step (Scheme 1). This method provides a rapid and reliable synthesis of multigram quantities of [**2**]$^-$ in an overall yield of 98%.

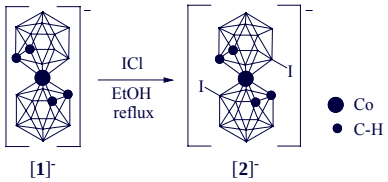

Scheme 1. Preparation of caesium 8,8'-diiodocobaltabisdicarbollide, Cs[**2**].

The reaction involves refluxing a mixture of Cs[**1**] and ICl in ethanol (10 h) to obtain a solution containing Cs[**2**] and the excess of ICl. After destroying the latter with Na_2SO_3, pure Cs[**2**] is obtained concentrating the solution from which a crystalline orange solid separates.

Dimethyl substitution of [**1**]$^-$ at the 8, 8' positions was achieved by B-C cross coupling reaction employing a modified Kumada reaction (Scheme 2). Addition of 5 equivalents of methylmagnesium bromide to a cooled (0°C) solution of Cs[**2**] in THF, followed by a catalytic amount of [$PdCl_2(PPh_3)_2$] and CuI and reflux for 5 h gave a mixture of compounds according to ^{11}B-NMR. Following evaporation of the THF, the residue was extracted with acidic water and diethyl ether. After chromatography on silica with AcOEt, four different bands were separated. Two of these accounted for more than 90% of the collected masses, and have been the ones studied. These bands correspond to Cs[8,8'-$(CH_3)_2$-3,3'-Co(1,2-$C_2B_9H_{10})_2$], Cs[**3**], and to Cs[8-CH_3-8'-OH-3,3'-Co(1,2-$C_2B_9H_{10})_2$], Cs[**4**]. For the specific conditions utilized in this preparation, the ratio of Cs[**3**]/Cs[**4**] is 2/1. This coupling reaction was repeated for 2, 15 and 30 hours refluxing time. Although minor variations in the ratio of Cs[**3**]/Cs[**4**] were observed, these were attributed to differences in the working up method and not to the transformation of [**3**]$^-$ into [**4**]$^-$. The chemical stability of Cs[**3**] towards Grignard derivatives was further proven by adding methylmagnesium bromide to a cooled (0°C) solution of Cs[**3**] in THF (ratio 5:1), followed by a catalytic amount of [$PdCl_2(PPh_3)_2$] and CuI and reflux for 5 h. The ^{11}B-NMR of the reaction crude indicated that [**3**]$^-$ remained unaltered.

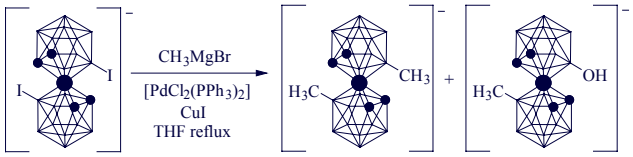

Scheme 2. 8,8'-dimethyl substitution of [**1**]$^-$ by B-C cross coupling reaction.

Similarly, the chemical stability of [**3**]$^-$ towards iodine was proven by adding the latter to a solution of Cs[**3**] in EtOH (ratio 2:1) and reflux for 2h. Again the ^{11}B-NMR of the reaction crude confirmed that [**3**]$^-$ remained unaltered.

The same coupling procedure has been utilized to produce Cs[8,8'-$(CH_3CH_2)_2$-3,3'-Co(1,2-$C_2B_9H_{10})_2$], Cs[**5**], and Cs[8-CH_3CH_2)-8'-OH-3,3'-Co(1,2-$C_2B_9H_{10})_2$], Cs[**6**], with ethyl magnesium bromide instead of methylmagnesium bromide. The dependence of the Cs[**5**]/Cs[**6**] ratio is comparable to the [**3**]$^-$ and [**4**]$^-$ analogues.

Reaction of Cs[**4**] with I_2 in refluxing ethanol (2 h) leads through an unprecedented oxo-de-methylation process to a solution containing [8,8'-μ-O-3,3'-Co(1,2-$C_2B_9H_{10})_2$]$^-$ [**7**]$^-$ (Scheme 3). Pure Cs[**7**] is obtained in 47% yield after concentrating the solution, and eluting the residue with AcOEt in a SiO_2 column.

[1] Isabel Rojo is enrolled in the PhD program of the UAB.

The necessity of I_2 was proven by refluxing Cs[**4**] in EtOH for 2h. In these experimental conditions unaltered Cs[**4**] was obtained. The relevance of the alkyl group in the oxo-de-alkylation reaction was studied by reacting Cs[**6**] with I_2 in the same experimental conditions as for Cs[**4**]. For R=Et no reaction was observed.

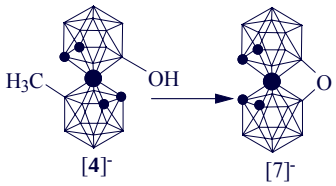

Scheme 3. Schematic representation of the oxo-de-methylation process.

Full structural elucidation of [**3**]$^-$ was obtained with an X-ray diffraction study of [PPN][**3**], (PPN= bis(triphenylphosphoranylidene)ammonium) (Figure 1, Table 1). [PPN][**3**] was produced dissolving the orange solid Cs[**3**] in the minimum amount of EtOH and a solution of [PPN]Cl in EtOH/water was added, resulting in the precipitation of [PPN][**3**]. This was filtered off, washed with water and petroleum ether and dried in vacuum. Crystals suitable single-crystal data collection were obtained by slow evaporation of an ethanol/ acetone solution of the compound.

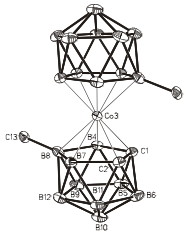

Figure 1. Schematic drawing of [**3**]$^-$ with 20% thermal displacement ellipsoids.

Table 1. Crystallographic Parameters for [PPN][**3**].

empirical formula	$C_{42}H_{56}B_{18}CoNP_2$
fw	890.33
cryst. syst.	monoclinic
cryst. habit, color	block, red
space group	*C*2/*c*
a (Å)	30.9930(7)
b (Å)	8.9763(2)
c (Å)	18.5724(5)
β (deg)	115.9374(11)
V (Å^3)	4646.44(19)
Z	4
T (ºC)	-100
λ (Å)	0.71073
ρ (g cm^{-3})	1.273
μ (cm^{-1})	4.72
goodness-of-fit[a] on F^2	1.039
R^b [$I>2\sigma(I)$]	0.0478
wR^c [$I>2\sigma(I)$]	0.1027

[a] $S = [\Sigma w(F_o^2 - F_c^2)^2]/(n-p)^{1/2}$; [b] $R = \Sigma||F_o| - |F_c||/\Sigma|F_o|$; [c] $wR = \{\Sigma[w(F_o^2 - F_c^2)^2]/\Sigma[w(F_o^2)^2]\}^{1/2}$

Asymmetric unit of [PPN][**3**] consists of half of [8,8'-$(CH_3)_2$-3,3'-Co(1,2-$C_2B_9H_{10})_2$]$^-$ or [**3**]$^-$ complex unit, with the metal occupying at inversion center, and half of [PPN]$^+$ ion, with the nitrogen atom at 2-fold axis. Thus the methyl groups of the centrosymmetric [**3**]$^-$ moiety as well as the cage carbons lie on opposite sides of the complex moiety. Crystallographic parameters for [PPN][**3**] are presented in Table 1, and selected bond lengths and angles are listed in Table 2. A drawing of [**3**]$^-$ is shown in Figure 1.

Table 2. Selected Bond Lengths (Å) and Angles (deg) for [PPN][**3**].

Co(3)-C(1)	2.017(3)	P-N	1.5787(12)
Co(3)-C(2)	2.017(3)	C(13)-B(8)-Co(3)	117.5(3)
Co(3)-B(4)	2.087(3)	C(13)-B(8)-B(4)	124.9(3)
Co(3)-B(7)	2.101(4)	C(13)-B(8)-B(7)	124.3(3)
Co(3)-B(8)	2.159(4)	P-N-P[d]	146.9(2)
C(1)-C(2)	1.645(4)	[d] Equivalent position –*x*, *y*, -*z*+1/2	
B(8)-C(13)	1.488(6)		

The clusters for [PPN][**3**] have the expected near-icosahedral geometry with the lengths of the differing types of connectivities standing in the expected sequence C-C < C-B < B-B, the magnitude of these connectivities being comparable to these determined for [**1**]$^-$.[6,8,9] A notable exception is the short B-C bond of the B(8)-Me *exo*-cluster group, which is 1.488(6) Å. For ex. in [8,8',9,9',12,12'-$(CH_3)_6$-3,3'-Co(1,2-$C_2B_9H_8)_2$]$^-$,[4] the shortest B-Me bond length in a similar chemical environment is 1.679(12) Å.

Characterization of the remaining synthesized compounds has been done mostly with ^{11}B-NMR and MALDI-TOF mass spectra. The ^{11}B-NMR spectrum of derivatives of Cs[**1**] is the result of the addition of the two individual halves, as schematised in Figure 2.[11] As an example, the ^{11}B{^{1}H}-NMR of Cs[8-CH_3-3,3'-Co(1,2-$C_2B_9H_{10}$)(1',2'-$C_2B_9H_{11}$)] is the addition of the ^{11}B{^{1}H}-NMR of Cs[**1**] plus Cs[**3**]. The spectrum of the first displays resonances at ppm, 6.5(1), 1.4(1), -6.0(4), -17.2(2) and -22.7(1) and the spectrum of Cs[**3**] at ppm 14.9(1), 1.0(1), -4.0(4), -17.4(2) and -24.2(1). The spectrum of Cs[8-CH_3-3,3'-Co(1,2-$C_2B_9H_{10}$)(1',2'-$C_2B_9H_{11}$)] should then be very close to 14.9(1), 6.5(1), 1.4(1), 1.0(1), -4.0(4), -6.0(4), -17.2(2), -17.4(2), -22.7(1), and -24.2(1). The experimental spectrum of Cs[8-CH_3-3,3'-Co(1,2-$C_2B_9H_{10}$)(1',2'-$C_2B_9H_{11}$)][12] consists of bands at 16.6(1), 7.6(1), 0.6(2), -3.5(2), -4.7(2), -5.2(2), -6.2(2), -17.3(2), -17.8(2), -22.4(1) and -25.3(1). We have tested this method with other available examples and it works extremely well. It is therefore a remarkable tool to assist in the structural elucidation of derivatives of [**1**]$^-$ mainly when other techniques like COSY, GIAO are not applicable. The ^{11}B-NMR of Cs[**4**] displays resonances at 23.7(1), 13.1(1), 0.3(1), -2.5(1), -4.2(4), -5.7(2), -6.9(2), -17.6(2), -19.8(2), -24.1(1), -28.4(1). If resonances attributable to the expected participant component Cs[**3**] are removed, the spectrum is left with the resonances of the unknown fragment, 23.7(1), -2.5(1), -5.7(2), -6.9(2), -19.8(2) and -28.4(1). The 1:1:2:2:2:1 pattern is consistent with a $\mathbf{C}_s$ fragment symmetry, and the high chemical shift value at 23.7 strongly supports assignment to B(8)-OH. The synthesis of Cs[8,8'-$(OH)_2$-3,3'-Co(1,2-$C_2B_9H_{10})_2$] had been produced by the reductive acetoxylation of Cs[**1**].[13] The reported NMR displays resonances at 25.8(1), -4.6(1), -5.6(2), -8.6(2), -19.8(2), and -29.6(1). The matching with the non-methyl moiety of Cs[**4**] is excellent, proving the Cs[8-CH_3-8'-OH-3,3'-Co(1,2-$C_2B_9H_{10})_2$] nature of Cs[**4**]. Its atomic composition was elucidated by comparison of the highest mass peak envelop found near 354 m/z in the MALDI-TOF mass spectrum with the simulated peak for $B_{18}CoC_5OH_{24}$ corresponding to the formula of [**4**]$^-$. A similar reasoning was applied for the structural elucidation of Cs[**5**] and Cs[**6**].

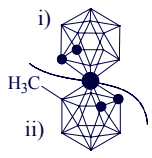

Figure 2. The ^{11}B-NMR spectrum of [8-(CH_3)-3,3'-Co(1,2-$C_2B_9H_{10}$)(1,2-$C_2B_9H_{11}$)]$^-$ is the result of the addition of the two individual halves: i) + ii).

Compound [**7**]$^-$ was characterized by MALDI-TOF mass spectrometry, and by comparison of the ^{11}B-NMR spectrum with reported data.[14] Compound Cs[**7**] had been earlier synthesized by reaction of Cs[**1**] with paraformaldehyde and H_2SO_4 in acetic anhydride (19.7 % yield). The structure had been initially[14] reported to correspond to [8,8'-μ-OCH_3-3,3'-Co(1,2-$C_2B_9H_{10})_2$] but a later X-ray diffraction[15] analysis confirmed it to be Cs[8,8'-μ-O-3,3'-Co(1,2-$C_2B_9H_{10})_2$].

Conclusions

The synthesis of [**3**]$^-$-[**6**]$^-$ has shown that the modified Kumada reaction can be applied to produce B-C bonds for di-substituted cobaltabisdicarbollide metallacarboranes. For the reaction to proceed and avoid unreacted di-iodo starting material a high ratio (2.5:1) of the Grignard reagent per iodine in [**2**]$^-$ has to be used. When the ratio is lowered to 1.25:1 a large proportion of unreacted starting material is recovered. This suggest that other reactions consuming CH_3MgBr or CH_3CH_2MgBr take place besides the formation of the B-CH_3 or B-CH_2CH_3 moieties. The syntheses of [**4**]$^-$ and [**6**]$^-$ are explained through unknown intermediates shown as [**"4"**]$^-$ in Figure 3 that upon hydrolysis produce the hydroxy derivative. The [**"4"**]$^-$ intermediate does not derive from [**3**]$^-$ as was proven earlier when discussing the stability of [**3**]$^-$ towards Grignard reagents. It must be formed in parallel to [**3**]$^-$. It is remarkable the unprecedented de-methylation process found for [**4**]$^-$ to yield [**7**]$^-$, and the fact that a de-ethylation did not happen with [**6**]$^-$.

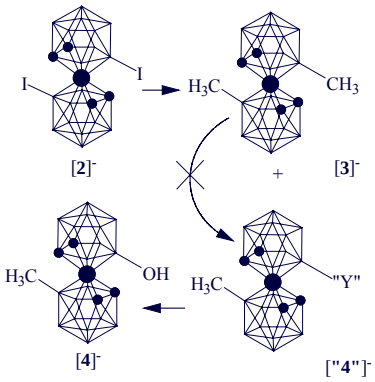

Figure 3. From diiodine to hydroxymethyl showing the intermediate precursor of the latter. The crossed arrow indicates that [**"4"**]$^-$ does not have its origin in [**3**]$^-$.

Experimental Section

General Considerations. Elemental analyses were performed using a Carlo Erba EA1108 microanalyzer. IR spectra were recorded from KBr pellets on a Shimadzu FTIR-8300 spectrophotometer. The mass spectra were recorded in the negative ion mode using a Bruker Biflex MALDI-TOF-MS [N_2 laser; λ_{exc} 337 nm (0.5 ns pulses); voltage ion source 20.00 kV (Uis1) and 17.50 kV (Uis2)]. ^{1}H and ^{1}H{^{11}B} NMR (300.13 MHz), ^{13}C{^{1}H} NMR (75.47 MHz), and ^{11}B NMR (96.29 MHz) spectra were recorded with a Bruker ARX 300 instrument equipped with the appropriate decoupling accessories. All NMR spectra were recorded from CD_3COCD_3 solutions at 25 ºC. Chemical shift values for ^{11}B NMR spectra were referenced to external $BF_3{\cdot}OEt_2$, and those for ^{1}H, ^{1}H{^{11}B}, and ^{13}C{^{1}H} NMR spectra were referenced to $Si(CH_3)_4$. Chemical shifts are reported in units of parts per million downfield from reference, and all coupling constants are reported in Hertz.

All reactions were performed under an atmosphere of dinitrogen employing standard Schlenk techniques. Column chromatography was performed on Matrix silica 60 (0.040-0.063 mm). Methylmagnesium bromide and ethylmagnesium bromide were obtained from Aldrich as 3.0 M solution in diethyl ether. THF was distilled from sodium benzophenone prior to use. EtOH was dried over molecular sieves and deoxygenated prior to use. Cesium salt of compound **1** was supplied by Katchem Ltd. (Prague) and used as received. All other reagents were obtained from commercial sources and used as purchased. Bis-(triphenylphosphine)palladium dichloride[16] was synthesized according to the literature.

Synthesis of Cs[8,8'-I_2-3,3'-Co(1,2-$C_2B_9H_{10})_2$] (Cs[2]). Iodine monochloride (3.0 g, 18.48 mmol) was added to a solution of Cs[3,3'-Co(1,2-$C_2B_9H_{11})_2$)] (3.92 g, 8.58 mmol) in 80 mL of EtOH. The reaction mixture was refluxed for 10 hours. The excess of iodine monochloride was descomposed by addition of 1.68 g (13.34 mmol) of Na_2SO_3 in 40 mL of water and the whole solution was boiled for 5 min. The solvent was concentrated until the precipitation of an orange solid. This was filtered off and washed with water and petroleum ether. The solid was dried in vacuo. Yield: 5.99 g (98 %). Anal. Calcd for $C_4H_{20}B_{18}CoCsI_2$: C: 6.78, H: 2.85 %. Found: C: 7.00, H: 2.83 %. IR ν (cm^{-1}): 3039 (C_c-H), 2592, 2563, 2530 (B-H), 978, 772. ^{1}H-NMR δ: 4.40 (br s, 4H, C_c-*H*), 3.22-1.82 (br m, 16H, B-*H*). ^{1}H{^{11}B}-NMR δ: 4.40 (br s, 4H, C_c-*H*), 3.22 (br s, 4H, B-*H*), 3.06 (br s, 2H, B-*H*), 2.59 (br s, 4H, B-*H*), 2.12 (br s, 2H, B-*H*), 1.82 (br s, 4H, B-*H*). ^{13}C{^{1}H}-NMR δ: 60.07 (s, C_c-H). ^{11}B-NMR δ: 3.6 (d, ^{1}J(B,H)= 144, 2B), -2.5 (d, ^{1}J(B,H)= 144, 8B), -4.4 (s, 2B, B(8,8')), -16.2 (d, ^{1}J(B,H)= 159, 4B), -21.7 (d, ^{1}J(B,H)= 171, 2B). MALDI-TOF-MS: (m/z) = 575.4 (M), 449.5 (M-I), 322.5 (M-2I).

Synthesis of Cs[8,8'-$(CH_3)_2$-3,3'-Co(1,2-$C_2B_9H_{10})_2$] (Cs[3]) and Cs[8-CH_3-8'-OH-3,3'-Co(1,2-$C_2B_9H_{10})_2$] (Cs[4]). A solution of Cs[8,8'-I_2-3,3'-Co(1,2-$C_2B_9H_{10})_2$] (200 mg, 0.28 mmol) in THF (12 mL) was treated with methylmagnesium bromide (0.47 mL, 1.4 mmol) (3.0 M in diethyl ether) at 0ºC, forming a brown precipitate. The mixture was left to room temperature for 30 min and then [$PdCl_2(PPh_3)_2$] (7.9 mg, 0.01 mmol) and CuI (2.2 mg, 0.01 mmol) were added in a single portion. The brown solution was refluxed for 5 hours. The grey solid was discarded by filtration. After removal of the solvent, 20 mL of diethyl ether was added. This was extracted three times with 20 mL of diluite HCl (60 mL of water containing 0.15 mL of concentrated HCl). The organic layer was separated and dried over anhydrous magnesium sulfate. The solvent was removed and the residue was flash-cromatographed over silica gel using as eluent ethyl acetate. Two main bands were separated: [**3**]$^-$ (R_f = 0.15) and [**4**]$^-$(R_f = 0.26). The yield were for Cs[**3**] 67 %, 91 mg, and for Cs[**4**] 33 %, 45.3 mg.

Cs[3]: Anal. Calcd for $C_6H_{26}B_{18}CoCs$: C: 14.87, H: 5.41 %. Found: C: 14.80, H: 5.38 %. IR ν (cm^{-1}): 3048 (C_c-H), 2922, 2831 (C_{alkyl}-H), 2535 (B-H), 747 (B-C), 1373, 1307, 1101, 976. ^{1}H-NMR δ: 4.17 (br s, 4H, C_c-*H*), 0.31 (br s, 6H, CH_3), 2.56-1.60 (br m, 16H, B-*H*). ^{1}H{^{11}B}-NMR δ: 4.17 (br s, 4H, C_c-*H*), 2.56 (br s, 4H, B-*H*), 1.85 (br s, 4H, B-*H*), 1.60 (br s, 8H, B-*H*), 0.31 (s, 6H, CH_3). ^{13}C{^{1}H}-NMR δ: 51.23 (s, C_c-H) 9.17, 8.40, 7.65, 6.86 (br q, B-*C*H_3). ^{11}B-NMR δ: 14.9 (s, 2B, B(8,8')), 1.0 (d, ^{1}J(B,H)= 141, 2B, B(10,10')), -4.0 (d, ^{1}J(B,H)= 141, 8B, B(4,4',7,7',9,9',12,12')), -17.4 (d, ^{1}J(B,H)= 153, 4B, B(5,5',11,11')), -24.2 (d, ^{1}J(B,H)= 167, 2B, B(6,6')). MALDI-TOF-MS: (m/z) = 352.7 (M).

Cs[4]: Anal. Calcd for $C_5H_{24}B_{18}CoCsO$: C: 12.34, H: 4.97 %. Found: C: 12.31, H: 4.95 %. IR ν (cm^{-1}): 3047 (BO-H), 3039 (C_c-H), 2922, 2834 (C_{alkyl}-H), 2573, 2528 (B-H), 747, 725 (B-C), 1077, 973. ^{1}H-NMR δ: 4.27 (br s, 2H, C_c-*H*), 4.00 (br s, 2H, C_c-*H*), 0.26 (br s, 3H, CH_3), 2.83-1.41 (br m, 16H, B-*H*). ^{1}H{^{11}B}-

NMR δ: 4.27 (br s, 2H, C_c-*H*), 4.00 (br s, 2H, C_c-*H*), 2.83 (br s, 1H, B-*H*), 2.75 (br s, 2H, B-*H*), 2.59 (br s, 4H, B-*H*), 1.95 (br s, 2H, B-*H*), 1.79 (br s, 2H, B-*H*), 1.57, 1.53 (br s, 4H, B-*H*), 1.41 (br s, 1H, B-*H*), 0.26 (br s, 3H, C*H*$_3$). ^{13}C{^{1}H}-NMR δ: 53.01 (s, C_c-H), 48.27 (s, C_c-H), 8.49, 7.87, 6.82, 6.16 (br q, B-*C*H$_3$). ^{11}B-NMR δ: 23.7 (s, 1B, B(8)), 13.1 (s, 1B, B(8')), 0.3 (d, ^{1}J(B,H)= 146, 1B, B(10')), -2.5(d, ^{1}J(B,H)= 157, 1B, B(10)), -4.2 (d, ^{1}J(B,H)= 144, 4B, B(4',7',9',12')), -5.7 (d, ^{1}J(B,H)= 135, 2B, B(9,12)), -6.9 (d, ^{1}J(B,H)= 121, 2B, B(4,7)), -17.6 (d, ^{1}J(B,H)= 163, 2B, B(5',11')), -19.8 (d, ^{1}J(B,H)= 167, 2B, B(5,11)), -24.1 (d, ^{1}J(B,H)= 167, 1B, B(6')), -28.4 (d, ^{1}J(B,H)= 171, 1B, B(6)). MALDI-TOF-MS: (m/z) = 354.5 (M).

Synthesis of Cs[8,8'-(CH$_3$CH$_2$)$_2$-3,3'-Co(1,2-C$_2$B$_9$H$_{10}$)$_2$] (Cs[5]) and Cs[8-CH$_3$CH$_2$-8'-OH-3,3'-Co(1,2-C$_2$B$_9$H$_{10}$)$_2$] (Cs[6]). A solution of Cs[8,8'-I$_2$-3,3'-Co(1,2-C$_2$B$_9$H$_{10}$)$_2$] (200 mg, 0.28 mmol) in THF (12 mL) was treated with ethylmagnesium bromide (0.47 mL, 1.4 mmol) (3.0 M in diethyl ether) at 0ºC, forming a brown precipitate. The mixture was left to room temperature for 30 min and then [PdCl$_2$(PPh$_3$)$_2$] (7.9 mg, 0.01 mmol) and CuI (2.2 mg, 0.01 mmol) were added in a single portion. The brown solution was refluxed for 6 hours. The grey solid was discarded by filtration. After removal of the solvent, 20 mL of diethyl ether was added. This was extracted three times with 20 mL of diluite HCl (60 mL of water containing 0.15 mL of concentrated HCl). The organic layer was separated and dried over anhydrous magnesium sulfate. The solvent was removed and the residue was flash-cromatographed over silica gel using as eluent ethyl acetate. Two main bands were separated: [**5**]$^-$ (R_f = 0.11) and [**6**]$^-$(R_f = 0.22). The yield were for Cs[**5**] 62 %, 90 mg, and for Cs[**6**] 31 %, 45 mg.

Cs[5]: Anal. Calcd for $C_8H_{30}B_{18}CoCs$: C: 18.74, H: 5.90 %. Found: C: 18.52, H: 5.80 %. IR ν (cm^{-1}): 3039 (C_c-H), 2961, 2922, 2854 (C_{alkyl}-H), 2562 (B-H), 747 (B-C), 1378, 1299, 1139, 980. ^{1}H-NMR δ: 4.23 (br s, 4H, C_c-*H*), 1.31 (br m, 4H, C*H*$_2$), 0.85 (br m, 6H, C*H*$_3$), 2.60-1.61 (br m, 16H, B-*H*). ^{1}H{^{11}B}-NMR δ: 4.23 (br s, 4H, C_c-*H*), 2.78 (br s, 2H, B-*H*), 2.62 (br s, 4H, B-*H*), 1.95 (br s, 2H, B-*H*), 1.80 (br s, 2H, B-*H*), 1.61 (br s, 4H, B-*H*), 1.51 (br s, 2H, B-*H*), 1.31 (br m, 4H, C*H*$_2$), 0.85 (br m, 6H, C*H*$_3$). ^{13}C{^{1}H}-NMR δ: 51.14 (s, C_c-H), 18.90 (s, CH$_2$*C*H$_3$). ^{11}B-NMR δ: 16.8 (s, 2B, B(8,8')), 1.0 (d, ^{1}J(B,H)= 133, 2B), -4.4 (d, ^{1}J(B,H)= 111, 4B), -5.5 (d, ^{1}J(B,H)= 118, 4B), -17.2 (d, ^{1}J(B,H)= 148, 4B), -24.0 (d, ^{1}J(B,H)= 177, 2B). MALDI-TOF-MS: (m/z) = 380.7 (M).

Cs[6]: Anal. Calcd for $C_6H_{26}B_{18}CoCsO$: C: 14.39, H: 5.23 %. Found: C: 14.30, H: 5.19 %. IR ν (cm^{-1}): 3039 (C_c-H), 2961, 2922, 2867 (C_{alkyl}-H), 2560 (B-H), 743, 724 (B-C), 1099, 979. ^{1}H-NMR δ: 4.35 (br s, 2H, C_c-*H*), 4.04 (br s, 2H, C_c-*H*), 1.34 (br m, 2H, C*H*$_2$), 0.93 (br m, 3H, C*H*$_3$), 2.78-1.51 (br m, 16H, B-*H*). ^{13}C{^{1}H}-NMR δ: 53.36 (s, C_c-H), 47.90 (s, C_c-H). ^{11}B-NMR δ: 23.4 (s, 1B), 14.3 (s, 1B), 0.3 (d, ^{1}J(B,H)= 141, 1B), -2.3 (d, ^{1}J(B,H)= 157, 1B), -4.1 (d, ^{1}J(B,H)= 179, 2B), -5.8 (d, ^{1}J(B,H)= 137, 4B), -6.7 (d, ^{1}J(B,H)= 100, 2B), -17.5 (d, ^{1}J(B,H)= 155, 2B), -20.0 (d, ^{1}J(B,H)= 157, 2B), -23.7 (d, ^{1}J(B,H)= 166, 1B), -28.3 (d, ^{1}J(B,H)= 166, 1B). MALDI-TOF-MS: (m/z) = 367.6 (M).

Synthesis of Cs[8,8'-μ-O-3,3'-Co(1,2-C$_2$B$_9$H$_{10}$)$_2$], Cs[7]. To a solution of Cs[8-CH$_3$-8'-OH-3,3'-Co(1,2-C$_2$B$_9$H$_{10}$)$_2$] (76 mg, 0.16 mmol) in EtOH (5 mL) was added 80 mg (0.31 mmol) of iodine. The orange solution was refluxed for 2 hours. The solvent was removed and the residue was purified over silica gel using ethyl acetate as eluent. A red band corresponding to Cs[**7**] was obtained (R_f = 0.71). Yield: 47 %, 34.5 mg. Anal. Calcd for $C_4H_{20}B_{18}CoCsO$: C: 10.21, H: 4.28 %. Found: C: 10.01, H: 4.12 %. IR ν (cm^{-1}): 3039 (C_c-H), 2573, 2540 (B-H), 1378, 1261, 1037. ^{1}H-NMR δ: 3.76 (br s, 4H, C_c-*H*), 3.99-1.29 (br m, 16H, B-*H*). ^{1}H{^{11}B}-NMR δ: 3.99 (br s, 4H, B-*H*), 3.76 (br s, 4H, C_c-*H*), 2.13 (br s, 2H, B-*H*), 1.88 (br s, 4H, B-*H*), 1.58 (br s, 4H, B-*H*), 1.29 (br s, 2H, B-*H*). ^{13}C{^{1}H}-NMR δ: 45.24 (s, C_c-H). ^{11}B-NMR δ: 17.5 (s, 2B, B(8,8')), -1.5 (d, ^{1}J(B,H)= 149, 2B, B(10,10')), -8.0 (s, ^{1}J(B,H)= 143, 4B, B(4,4',7,7')), -9.4 (d, ^{1}J(B,H)= 137, 4B, B(9,9',12,12')), -14.2 (d, ^{1}J(B,H)= 160, 4B, B(5,5',11,11')), -25.9 (d, ^{1}J(B,H)= 163, 2B, B(6,6')). MALDI-TOF-MS: (m/z) = 338.6 (M).

X-ray diffraction studies.

Single-crystal data collection [PPN][8,8'-(CH$_3$)$_2$-3,3'-Co(1,2-C$_2$B$_9$H$_{10}$)$_2$] or [PPN][**3**] was performed at –100ºC on an Enraf Nonius Kappa CCD diffractometer using graphite monochromatized Mo Kα radiation. A total of 7161 reflections were collected giving 4091 unique reflections [R_{int} = 0.0521]. The structure were solved by direct methods and refined on F^2 by the SHELXL97 program.[17] Non-hydrogen atoms were refined anisotropic thermal displacement parameters but hydrogen atoms were treated as riding atoms using the SHELX97 default parameters.

Acknowledgment. We thank ENRESA for the partial support of this research and MCyT (MAT01-1575), and Generalitat de Catalunya 2001/SGR/00337.

Supporting Information Available: Tables listing detailed crystallographic data, atomic positional and thermal displacement parameters, and bond lengths and angles for [PPN][8,8'-(CH$_3$)$_2$-3,3'-Co(1,2-C$_2$B$_9$H$_{10}$)$_2$] ([PPN][**3**]). This material is available free of charge via the Internet at http://pubs.acs.org.

(1) Hawthorne, M. F.; Young, D.C.; Wegner, P. A. *J. Am. Chem. Soc.* **1965**, *87*, 1818.
(2) See the review: Sivaev I.B., Bregadze V. I. *Collect. Czech. Chem. Commun.* **1999**, *64*, 783.
(3) a) Matel, L.; Macásek, F.; Rajec, P.; Hermánek, S.; Plesek, J. *Polyhedron* **1982**, *1*, 511. b) Matel, L.; Cech, R.; Macásek, F.; Hermánek; S.; Plesek, J. *Radiochem. Radioanal. Lett.* **1978**, *35*, 241. c) Hawthorne, M.F.; Young, D.C.; Andrews, T.D.; Hove, D.V.; Pilling, R.L.; Pitts, A.D.; Reinjes, M.; Warren, L.F.; Wegner, P.A. *J. Am. Chem. Soc.* **1968**, *90*, 879. d) Fanning, J.C.; Huff, L.A.; Smith, W.A.; Terrell, A.S., Yasinsac, L., Todd L.J.; Jasper, S.A Jr.; McCabe, D.J. *Polyhedron* **1995**, *14*, 2893.
(4) Mortimer, M.D., Knobler, C.B.; Hawthorne, M.F. *Inorg. Chem.* **1996**, *35*, 5750.
(5) a) Plesek, J.; Hermanek, S.; Nöth H.; Franken, A. Preparations and Structures of New [(1,2-C$_2$B$_9$H$_{11}$)$_2$-3-Co]$^-$ Derivatives, Ninth International Meeting on Boron Chemistry, Ruprech-Karls-Universität, Heidelberg, Germany, July 14-18, **1996**, Poster #82. b) Plesek, J.; Hermánek, S.; Franken, A.; Cisarova I.; Nachtigal, C. *Collect. Czech. Chem. Commun.* **1997**, *62*, 47. c) Selucky, P.; Plesek, J.; Rais, J.; Kyrs M.; Kadlecova, L. *J. Radioanal. Nucl. Chem.* **1991**, *149*, 131. d) Plesek, J.; Stibr B.; Hermanek, S. *Coll. Czech. Chem. Commun.* **1984**, *49*, 1492.
(6) Llop, J.; Masalles, C.; Viñas, C.; Teixidor, F.; Sillanpää, R.; Kivekäs, R. *Dalton Transactions*, **2003**, 556.
(7) a) Sivaev, I. B.; Starikova, Z. A.; Sjöberg S.; Bregadze, V. I. *J. Organomet. Chem.*, **2002**, *649*, 1. b) Sivaev, I. B.; Sjöberg S.; Bregadze, V. I., Synthesis of Functional Derivatives of Cobalt Bis(1,2-dicarbollide) Anion for Boron Neutron Capture Therapy, International Conference Organometallic Compounds - Materials of the Next Century, Nizhny Novgorod, Russia, May 29-June 2, **2000**.
(8) Plešek, J.; Grüner, B.; Heřmánek, S.; Báča, J.; Mareček, V.; Jänchenová, J.; Lhotský, A.; Holub, K.; Selucký, P.; Rais, J.; Císařová I.; Čáslavský, J. *Polyhedron* **2002**, *21*, 975.
(9) Grüner, B.; Plešek, J.; Báča, J.; Císařová, I.; Dozol, J.-F.; Rouquette, H.; Viñas, C.; Selucký, P.; Rais, J. *New J. Chem.* **2002,** *26***,** 1519.
(10) a) Tamao, K.; Sumitani, K.; Kumada, M. *J. Am. Chem. Soc.* **1972**, *94*, 4374. b) Hayashi, T.; Konishi, M.; Kobori, Y.; Kumada, M.; Higuchi, T.; Hirotsu, K. *J. Am. Chem. Soc.* **1984**, *106*, 158. c) Yamamura, M.; Moritani, I.; Murahashi, S. *J. Organomet. Chem.* **1975**, *23*, C39.
(11) Rojo, I. Doctoral Thesis. Universitat Autonoma de Barcelona, **2003**.
(12) Rojo, I.; Teixidor, F.; Viñas, C.; Kivekäs, R.; Sillanpää, R. *Chem.-Eur. J.* **2003**, submitted.
(13) Plesek, J.; Grüner, B.; Báca, J.; Fusek, J.; Císarová, I. *J. Organom. Chem.* **2002**, *649*, 181.
(14) Plesek, J.; Hermánek, S.; Base, K.; Todd, L. J.; Wright, W. F. *Collect. Czech. Chem. Commun.* **1976**, *41*, 3509.
(15) Petrina, A.; Petrícek, V.; Malý, K.; Subrtová, V.; Línek, A.; Hummel, L. Z. Kristallogr. **1981**, *154*, 217.
(16) Blackburn, J.R.; Nordberg, R.; Stevie, F.; Albrigde, R.G.; Jones, M.M. *Inorg. Chem.* **1970**, *9*, 2374.
(17) Sheldrick, G. M. SHELX97. University of Göttingen, Germany, **1997.**

Generation of bridging alkene and conjugated dialkenes on the [3,3'-Co(1,2-$C_2B_9H_{11})_2]^-$ platform exclusively generated from alkynes. The unique hydroboration role of [3,3'-Co(1,2-$C_2B_9H_{11})_2]^-$

Isabel Rojo,[#,†] Francesc Teixidor,[#] Raikko Kivekäs,[§] Reijo Sillanpää,[&] Clara Viñas*[,#]

[#] *Institut de Ciència de Materials de Barcelona (CSIC), Campus de la U.A.B, 08193 Bellaterra, Spain;* [§] *Department of Chemistry, P.O. Box 55, University of Helsinki, FIN-00014, Finland;* [&] *Department of Chemistry, University of Jyväskylä, FIN-40351, Finland.*

E-mail: clara@icmab.es

The cobaltabis(dicarbollide) anion, [3,3'-Co(1,2-$C_2B_9H_{11})_2]^-$, [**1**]$^-$, first synthesized by Hawthorne and co-workers,[1] has proven to be very valuable in many areas of applied research.[2] Our group has focused on the synthesis of carbon substituted derivatives[3] of [**1**]$^-$ and recently has begun to explore its derivatives on boron.[4] In this paper we report on the unprecedented metal mediated transformation of an alkyne into a B,B' bridging alkene. The ene formation can be associated with the cooperative effect of a B-I and a B-H geometrically placed on an adequate platform, and to their electronic properties. In addition, the synthesis of a conjugated dialkene derivative of [**1**]$^-$ is described. Although examples of metal mediated dialkene formation exist,[5] the novelty reported in this paper, in addition of being the first announced in a (hetero)borane cluster, is that it is generated only from an alkyne (trimethylsilylacetylene), contrarily to the usual case where an alkyne and an alkene are needed. This has been possible through the singular capacity of a B-H to produce hydroboration.

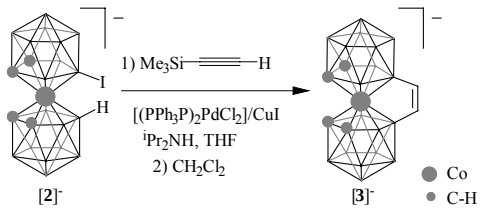

Scheme 1. Preparation of the alkene-linked cobaltabisdicarbollide, [**3**]$^-$.

The 8-monoiodinated derivative, Cs[3,3'-Co(8-I-1,2-$C_2B_9H_{10}$)(1',2'-$C_2B_9H_{11}$)], Cs[**2**],[4,6] is obtained from Cs[**1**] and is used as the starting material for the preparation of the alkene-linked cobaltabis(dicarbollide). Reaction of Cs[**2**] with trimethylsilylacetylene in the presence of [$PdCl_2(PPh_3)_2$]/CuI and diisopropylamine in refluxing THF leaves, after removing the solvent and stirring with CH_2Cl_2, an insoluble red solid, Cs[**3**] (Scheme 1). ^{1}H-NMR of Cs[**3**] indicates the absence of the -$SiMe_3$ group. This was unexpected as removal of -$SiMe_3$ requires the use of specific reagents, e.g Bu_4NF.[7] The ^{11}B-NMR displays a pattern 1:3:2:2:1 ranging from +26.0 to -25.4 ppm, which suggests that in Cs[**3**] both dicarbollide moieties are symmetry related if the resonance of intensity 3 is due to the coincidental overlap of two resonances (1+2). The two moieties could have been equivalent if two alkynyl groups, one in each moiety, had been introduced. This was not the case although Grimes and co-workers have recently reported that the reaction of [Cp*Co(5-I-1,2-Et_2-1,2-$C_2B_3H_4$)][8] with trimethylsilylacetylene using similar catalyst set as the one for Cs[**3**] and diethylamine as solvent led to a mixture of trimethylsilylalkynyl mono and disubstituted metallacarboranes, the latter being produced in 58% yield. In Grimes example the disubstitution had taken place in contiguous boron atoms at the same carborane ligand moiety. Relevant information about the structure of [**3**]$^-$ was obtained from the Matrix Assisted Laser Desorption Ionization mass spectrum (MALDI-TOF) in the negative mode. An envelop was observed near 348.6 m/z which precisely corresponds to the calculated envelop for [μ-8,8'-C_2H_2-3,3'-Co(1,2-$C_2B_9H_{10})_2]^-$, [**3**]$^-$. This formula would be in agreement with the NMR spectroscopic data. The formation of Cs[**3**] can be described considering that an ethylene group generated from an alkyne bridges two equivalent sites of the precursor leaving the original structure practically unaffected. An X-ray diffraction study of Cs[**3**] confirmed the formulation (Figure 1).[9] The ethene bridge with a C13-C13' distance of 1.325(5) Å strongly determines the mutual orientation of the carborane moieties. Consequently, the C_2B_3 faces coordinated to Co are tilted by 7.1(2)º from parallel orientation and B8 and B8' are closer, deviating 11º from ideal eclipsed conformation.

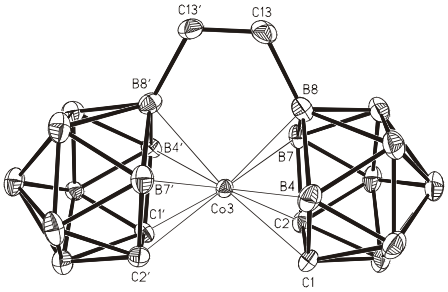

Figure 1. Structure of the anion of Cs[**3**]. Thermal ellipsoids are drawn at the 50% probability level.

In an attempt to learn on the required reacting sites on [**1**]$^-$ for the ethene bridging reaction to proceed, two reactions were conducted: i) Cs[3,3'-Co(8-I-1,2-$C_2B_9H_{10})_2$], Cs[**4**] having two B(8)-I units, was reacted with trimethylsilylacetylene, ii) Cs[**1**] with two B(8)-H was also reacted with the alkyne. In both cases

† Isabel Rojo is enrolled in the UAB PhD Program.

the reaction conditions were the same as for the synthesis of Cs[**3**]. No reaction was observed in either case. This implies that the two non-equivalent groups B(8)-I and B(8')-H are complementary and necessary for the alkyne insertion. Likewise the role of the trimethylsilyl group was assessed performing the reaction of [**2**]$^-$ with acetylene, phenylacetylene, methyl propargyl ether and propargyltrimethylsilane and no reaction was observed. Why does this reaction then take place?. We interpret the reaction as shown in Figure 2. Initially a B-C coupling takes place, which is shifted to the reagents side (step i). This could explain the absence of dicarbollide alkyne derivatives with any of the alkynes tested. For the particular case of trimethylsilylacetylene the polarizable C-Si bond should facilitate hydroboration by the B(8)-H (step ii). Upon the formation of the alkene, the =***C***BSi carbon becomes electron-rich and susceptible to electrophilic attack. This fact plus the bulkyness of the -$SiMe_3$ groups and the electropositive character of Si provide a pathway for a hydrodesilylation process leading to the bridging alkene (step iii).

This reaction finds no parallel in alkyne organic or organometallic chemistry but some similarities can be found in the enyne metathesis first described by Katz.[10] In Katz's original example a conjugated dialkene is generated, in which one of the two ene groups bridges the 2,2' positions in biphenyl to yield 9-vinylphenantrene. Conceptually phenantrene and [**3**]$^-$ are alike. They are formally generated from biphenyl and [**1**]$^-$ respectively, upon the addition of a C=C moiety. This could have been just a geometrical curiosity but it provided some hints about the reactivity of iodocosane, [**2**]$^-$, as we describe next.

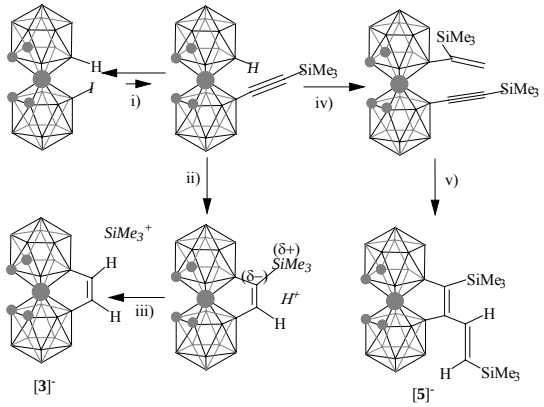

Figure 2. Possible paths of the reaction between [**2**]$^-$ and trimethylsilylacetylene.

The reaction leading to Cs[**3**] was not quantitative. After removal of Cs[**3**] and evaporation of H_2CCl_2, the MALDI-TOF analysis of the solid revealed several peak envelops proving that its composition was complex. The two largest envelops corresponded one to unreacted [**1**]$^-$ and the second to a derivative of [**1**]$^-$ that is the result of fusing two trimethylsilyl moieties, [**5**]$^-$ (Figure 2). An optimization of the reaction conditions has been done to improve the yield of the latter. In this way proton sponge, triethylamine, diethylamine, diisopropylamine and butyllithium have been used as base, and diisopropylamine and THF as solvent. Room temperature and refluxing conditions or a combination of both have also been tested. Finally, different ratios of the alkyne vs. [**2**]$^-$ have been studied. The nature of the final products do not vary much with the different conditions, but the reaction at room temperature in which diisopropylamine is used both as a base and as solvent produces [**5**]$^-$ in largest quantity. We consider that the pathway proposed for [**3**]$^-$ is also valid for [**5**]$^-$. Once the boron-carbon bond formation has taken place, step i) in Figure 2, an alternative route to step ii) is possible that is indicated as step iv). Both ii) and iv) steps are based on a hydroboration. For ii) the hydroboration on the triple bond is intramolecular while for iv) the hydroboration is intermolecular. It has been known that hydroboration of alkynylsilanes proceed with opposite regiochemistry to put the boron on the carbon bonded to silicon.[11] We have not found exception to this observation; both steps ii) and iv) are in agreement with this observation. Following step iv) an alkene group is generated in the molecule which adds to the already present alkyne. In the presence of the "Pd" catalyst an enyne metathesis[12] catalytic cycle leading to the formation of the cobaltabisdicarbollide conjugated dialkene takes place, which is a reasonable product of enyne metathesis.[13] The spectroscopic data are in agreement with this formulation. The MALDI-TOF simulation of the peak corresponding to [**5**]$^-$ matches the experimental one observed at 518.5 m/z. The ^{1}H-NMR of [**5**]$^-$ shows in addition to other resonances two doublets at 6.68 and 5.95 ppm with J(H,H)= 21 Hz which are indicative of alkene protons in a *trans* disposition. The non-equivalency of the two dicarbollide moieties in [**5**]$^-$ is clear from the 1:1:1:1:4:2:2:4:2 ^{11}B-NMR pattern spectra.

Acknowledgment. We thank CICYT for MAT01-1575, Generalitat de Catalunya for 2001/SGR/00337 and CIEMAT for supporting this research.

Supporting Information Available. Synthetic and characterization details for Cs[**3**] and Cs[**5**]; and X-ray structure details (pdf) and crystallographic data (CIF) for Cs[**3**]. This material is available free of charge via the Internet http://pubs.acs.org.

Notes and references

1 Hawthorne, M.F.; Andrews, T.D. *J. Chem. Soc., Chem. Comm.* **1965**, 443.

2 a) Hawthorne, M.F.; Maderna, A. *Chem. Rev.* **1999**, *99*, 3421. b) Grüner, B.; Plešek, J.; Báca, J.; Císarová, I.; Dozol, J.F.; Rouquette, H.; Viñas, C.; Selucký, P.; Rais, J. *New J. Chem.* **2002**, *26*, 1519. c) Masalles, C.; Borrós, S.; Viñas, C.; Teixidor, F. *Adv. Mater.* **2002**, *14*, 449.

3 a) Viñas, C.; Gómez, S.; Bertran, J.; Teixidor, F.; Dozol, J.F.; Rouquette, H. *Chem. Comm.* **1998**, 191

4 Rojo, I.; Teixidor, F.; Viñas, C.; Kivekäs R.; Sillanpää R. *Chem-Eur. J.*, **2003**, in press.

5 a) Layton, M.E.; Morales, C.A.; Shair, M.D. *J. Am. Chem. Soc., Comm.* **2002**, *123*, 5. b) Delas, C.; Urabe, H.; Sato, F. *J. Am. Chem. Soc.* **2001**, *123*, 7937. c) Sheng, Y.H.; Wu Y.D. *J. Am. Chem. Soc.* **2001**, *123*, 6662. d) Chao, K.C.; Rayabarapu, D.K.; Wang, C.C.; Cheng, C.H. *J. Org. Chem.* **2001**, *66(26)*, 8804. e) Bunz, U.H.F.; Kloppenburg, L. *Angew. Chem. Int. Ed.* **1999**, *38*, 4.

6 Matel, L.; Macásek, F.; Rajec, P.; Heřmánek, S.; Plešek, J. *Polyhedron* **1982**, *1*, 511.

7 Pudelski, J.K.; Callstrom, M.R. *Organometallics* **1994**, *13*, 3095.

8 Malaba, D.; Sabat, M.; Grimes, R.N. *Eur J. Inorg. Chem.* **2001**, 2557.

9 Crystal data. Cs[**3**]: $C_6H_{22}B_{18}CoCs$, *FW* = 480.66, orthorhombic, $Pc2_1n$ (no. 33), a = 7.17310(10), b = 9.54050(10), c = 27.2413(4) Å, V = 1864.26(4) Å^3, T = 173 K, Z = 4, $R(F)$ = 0.0297, $wR(F^2)$ = 0.0569.

10 Katz, T.J.; Sivavec, T.M. *J. Am. Chem. Soc.* **1985**, *107*, 737.

11 a) Hassner, A.; Soderquist, J.A. *J. Organomet. Chem.* **1977**, *C1*, 131. b) Zweifel, G.; Backlund, S.J. *J. Am. Chem. Soc.* **1977**, *99*, 3184.

12 a) Trost, B.M.; Krische, M.J. *Synlett* **1997**, 1. b) Fürstner, A.; Szillat, H.; Gabor, B.; Mynott, R. *J. Am. Chem. Soc.* **1998**, *120*, 8305. c) Chatani, N.; Furukawa, N.; Sakurai, H.; Murai, S. *Organometallics* **1996**, *15*, 901.

13 a) Renaud, J.; Graf, C.D.; Oberer, L. *Angew. Chem., Int. Ed.* **2000**, *39*, 3101. b) Stragies, R.; Schuster, N.; Blechert, S. *Angew. Chem., Int. Ed.* **1997**, *36*, 2518.

Polypyrrole Overoxidation Resistance Improvement with Weakly Coordinating Cobaltabisdicarbollide Doping Complexes.

S. Gentil, I. Rojo, C. Viñas, F. Teixidor*

Institut de Ciència de Materials de Barcelona (ICMAB/CSIC), Campus de la UAB, 08193 Bellaterra, Spain

RECEIVED DATE (automatically inserted by publisher); E-mail: teixidor@icmab.es

The overoxidation resistance of electropolymerized polypyrroles doped with $[Co(C_2B_9H_{11})_2]^-$ derivatives bearing different substituents was studied. The investigations were performed using Low Scan Voltammetry techniques, and SEM images were recorded for selected samples. Results show that modifications of the nude cobaltabisdicarbollide peanut shape leading to bulkier derivatives cause a faster overoxidation of the material. Introduction of bulky groups on the dicarbollide moieties of $[Co(C_2B_9H_{11})_2]^-$ lowers the good three-dimensional packing possibility of the PPy threads and the capacity of the $B_{cluster}$-H bonds to compensate positive charges of PPy bipolarons. Additionally, overoxidation resistance improvement is also attributable to the redistribution of electron density in the doping agent. This is achieved by incorporating electron-withdrawing groups in the $[Co(C_2B_9H_{11})_2]^-$ cluster. In this way, polypyrrole doped with $[3,3'\text{-}Co(8\text{-}(CH_2CH_2O)_3\text{-}CH_3\text{-}1,2\text{-}C_2B_9H_{10})(1',2'\text{-}C_2B_9H_{11})]^-$ is more resistant to overoxidation than PPy doped with $[8,8'\text{-}\mu(1'',2''\text{-}C_6H_4)\text{–}3,3'\text{-}Co(\text{-}1,2\text{-}C_2B_9H_{10})_2]^-$ or $[Co(C_2B_9H_{11})_2]^-$.

1. Introduction

In the past decades, intensive investigations have been carried out on intrinsic conducting polymers because of the large practical application possibilities of these promising materials in many fields.[1,2] Among those conjugated double bond polymers, polypyrroles (PPy) have attracted much attention and have been recognized for their interesting applications as sensors,[3-11] coatings,[12,13] fuel cells[14,15] among others. It is well established that for conventional uses, PPy stability at a definite potential or a long-term stability for repetitive oxidation-reduction cycling are needed. Rapid degradation in water or air at high oxidative potential[16-21] or reversibility losses when oxidation-reduction sequences are applied to the material[22-24] are the major limitations of PPy for commercial and industrial developments. PPy chemical stability limit is known to be the overoxidation limit of the material, beyond which conducting material properties are definitely lost. The overoxidation stability highly depends on the PPy doping anion nature[25-27] and in the experimental conditions applied to the material. Therefore, during overoxidation, nucleophiles like OH^- attack the polymer cationic sites, generating hydroxyl groups.[28] This process is subsequently followed by the carbonyl-bond formation, the disruption of the conjugated double-bond system[18,28-33] and polymer doping anion losses. Such degradation processes have been characterized by *in-situ* FTIR studies,[28,30-34] impedance spectroscopy,[35] UV/vis experiments[28,29] and microcalorimetric measurements.[19]

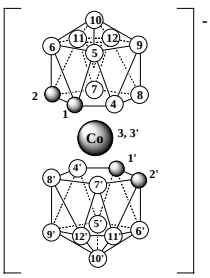

$[\mathbf{1}]^-$

Chart 1

In recent publications of our group, we have reported the use of the high chemically resistant, weakly coordinating cobaltabisdicarbollide $[Co(C_2B_9H_{11})_2]^-$ $[\mathbf{1}]^-$ anion as a doping agent (chart 1).[27,36] It gives a much better overoxidation capacity than, as far as we are aware, any other anions studied to date. Overoxidation threshold resistance is determined to be at 1270 mV for polypyrrole doped with $[\mathbf{1}]^-$ (PPy/[**1**])[27] while overoxidation thresholds in the 800 to 1000 mV range are reported for PPy synthesized in the same experimental conditions, but with common doping anions such as perchlorate $[ClO_4]^-$, hexafluorophosphate $[PF_6]^-$, or dodecylbenzene sulfonate $[DBS]^-$.[27,29] The PPy/[**1**] overoxidation resistance is also better than with $[CB_{11}H_{12}]^-$ and $[B_{10}Cl_{10}]^{2-}$ doped polypyrroles. The $[CB_{11}H_{12}]^-$ and $[B_{10}Cl_{10}]^{2-}$ anions, in similarity to $[\mathbf{1}]^-$, also have a cluster structure with the negative charge delocalised through the whole molecule. The PPy/$[CB_{11}H_{12}]$ and PPy/$[B_{10}Cl_{10}]$ materials are stable up to 1090 and 890 mV, respectively.[37] To date, no derivative compounds of $[\mathbf{1}]^-$ had produced an overoxidation resistance better than the parent compound. Halogen substitutions at the B(8), B(9) and B(12) positions of $[\mathbf{1}]^-$ (Chart 1) yield the hexachloro $[3,3'\text{-}Co(8,9,12\text{-}Cl_3\text{-}1,2\text{-}C_2B_9H_8)_2]^-$ or hexabromo $[3,3'\text{-}Co(8,9,12\text{-}Br_3\text{-}1,2\text{-}C_2B_9H_8)_2]^-$ derivatives that reduce the overoxidation potential threshold from 1270 mV to 1180 mV and 1100 mV, respectively.[37]

Chart 2

We have hypothesized that the high degradation resistance generated by $[\mathbf{1}]^-$ had to be related to the anion shape, to the

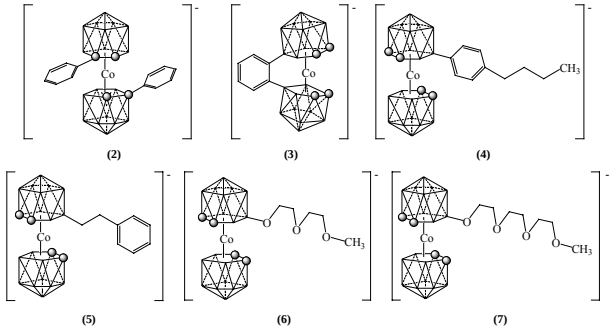

availability of BH's, and their orientations and interactions with the polypyrrole strands. To support this, we have studied in the present work, the overoxidation of PPy doped with different derivatives of [**1**]$^-$ represented in Chart 2. [3,3'-Co(1-C_6H_5-1,2-$C_2B_9H_{10})_2]^-$ [**2**]$^-$ was selected as an example of cluster carbon substituted compound, and [8,8'-μ(1",2"-C_6H_4)–3,3'-Co(-1,2-$C_2B_9H_{10})_2]^-$ [**3**]$^-$ for its rigidness and its more voluminous shape. [3,3'-Co(8-(1"-(4"-C_4H_9)-C_6H_4)-1,2-$C_2B_9H_{10}$)(1',2'-$C_2B_9H_{11}$)]$^-$ [**4**]$^-$, [3,3'-Co(8-(1"-(4"-C_6H_5)-C_2H_4)-1,2-$C_2B_9H_{10}$)(1',2'-$C_2B_9H_{11}$)]$^-$ [**5**]$^-$ were chosen for their similar volume but opposite electronic effects, and [3,3'-Co(8-$(CH_2CH_2O)_2$-CH_3-1,2-$C_2B_9H_{10}$)(1',2'-$C_2B_9H_{11}$)]$^-$ [**6**]$^-$ and [3,3'-Co(8-$(CH_2CH_2O)_3$-CH_3-1,2-$C_2B_9H_{10}$)(1',2'-$C_2B_9H_{11}$)]$^-$ [**7**]$^-$ for their capacity to trap protons from the solution or to coordinate alkaline and other hard metal ions, hence to compensate positive charges.[38] PPy electrochemical polymerization and overoxidation threshold potentials with compounds [**1**]$^-$-[**7**]$^-$ are reported and discussed in the paper.

2. Experimental Section

Solvents and Reagents. Acetonitrile was purchased from Aldrich and distilled prior to its use. Pyrrole was purified by distillation and stored under nitrogen at 0ºC in dark. The cobaltabisdicarbollide cesium salt, Cs[Co($C_2B_9H_{11})_2$], Cs[**1**] was obtained from Katchem and used as received. The cobaltabisdicarbollide derivatives NMe_4[3,3'-Co(1-C_6H_5-1,2-$C_2B_9H_{10})_2$], NMe_4[**2**],[39] NMe_4[8,8'-μ(1",2"-C_6H_4)–3,3'-Co(-1,2-$C_2B_9H_{10})_2$], NMe_4[**3**],[40] Cs[3,3'-Co(8-(1"-(4"-C_4H_9)-C_6H_4)-1,2-$C_2B_9H_{10}$)(1',2'-$C_2B_9H_{11}$)], Cs[**4**],[41] Cs[3,3'-Co(8-(1"-(4"-C_6H_5)-C_2H_4)-1,2-$C_2B_9H_{10}$)(1',2'-$C_2B_9H_{11}$)], Cs[**5**],[41] Na[3,3'-Co(8-$(CH_2CH_2O)_2$-CH_3-1,2-$C_2B_9H_{10}$)(1',2'-$C_2B_9H_{11}$)], Na[**6**],[41] Na[3,3'-Co(8-$(CH_2CH_2O)_3$-CH_3-1,2-$C_2B_9H_{10}$)(1',2'-$C_2B_9H_{11}$)], Na[**7**],[41] were synthesized as reported in the literature.

Electrochemical Procedures. All electrolyte solutions for polypyrrole (PPy) film preparation were deoxygenated by bubbling nitrogen gas before use. All electrochemical experiments were done using an EG&G Princeton Applied Research model 273A potentiostat-galvanostat. Electropolymerizations were performed in dry CH_3CN in a double-compartment, three electrode cells with a 3 mm diameter glassy carbon plate and a 10 cm platinum wire as working and counter electrodes respectively. Potentials are reported with respect to Ag/AgCl (0.1 M tetrabutyl ammonium chloride in CH_3CN) reference electrode. 0.1 M pyrrole and $3.5*10^{-2}$ M doping anion (1% water) solutions were used. Polypyrrole films were grown using both galvanostatic (with a constant current of 0.5 mA during 225s) and cyclic voltammetry (at 100 mV/s from –1000 to 2000 V, 30 scans) techniques. Overoxidation resistance measurements were carried out in a single-compartment cell on the galvanostatically electropolymerized polypyrroles, by scanning the voltage at a low rate (0.5 mV/s, 0-2000 mV vs. Ag/AgCl 10% KCl H_2O) in a 0.1 M NaCl distilled water solution, after a careful electrode washing with CH_3CN and distilled water.

Electron Microscopy. A Hitachi S530 scanning electron microscope (SEM) was used to examine the PPy morphology.

3. Results and Discussion

3.1. Electrochemical growing properties of the doped polypyrroles. Doped PPy materials were generated both by galvanostatic and cyclic voltammetry (CV) techniques. During the galvanostatic process, identical behaviour of all PPy/[**1**]-PPy/[**7**] doped materials is found. Classical anodic peak and plateau wave with a growth potential value of 1600 mV occur in the chronopotentiograms.

When CV methods are employed for the PPy growth, similar CV shapes that reflect the doped PPy structure properties[27,42] are registered for the seven doping anions. Differences are found, however, for the intensity data. The PPy/[**4**] CV growth after thirty sequential scans is shown in Figure 1, as a representative example.

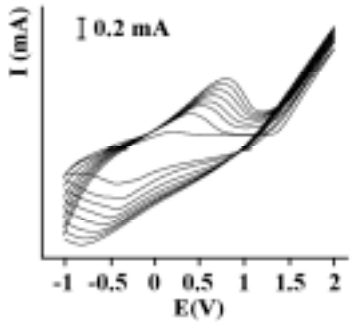

Figure 1. Sequential cyclic voltammetry for the electropolymerization of PPy/[**4**] in CH_3CN at 100 mV.s^{-1} from –1000 to 2000 mV. From the 2nd to the 30th scan, every fourth is recorded for a better clarity.

For all PPy/[**1**]-PPy/[**7**], the first anodic scan show a strong wave with an onset potential corresponding to the pyrrole ring oxidation. After every new cycle, the continuous growth of reversible oxidation-reduction well-resolved waves indicate the film formation and demonstrate the conducting nature of the formed material. When common doping anions such as $[ClO_4]^-$ or $[PF_6]^-$ are used, cyclovoltammograms do not present so well-defined semi-cycles. Because of their hydrophobicity, low mobility and large size properties, derivatives of [**1**]$^-$ are not expelled from the polymer matrix and reversible redox processes occur. While the number of scans increase, both anodic and cathodic peak positions are shifted to a more positive and negative potential respectively. Usual trace-crossing[43-46] is observed for all scans. After reaching the switching potential at 2000 mV, a higher current is observed in the immediate reverse scan. This intensity trace-crossing has been explained[43] by the contribution of free pyrrole monomer molecules present in the newly generated polymer layer.

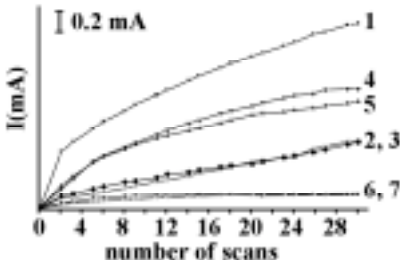

Figure 2. Anodic wave current intensity vs. number of scans for : ■ (**1**), × (**2**), ♦ (**3**), ▼ (**4**), ▲ (**5**), + (**6**), ● (**7**).

Figure 2 depicts the CV intensity of the anodic peak current vs. the number of scans for PPy/[**1**]-PPy/[**7**]. The CV anodic peak current values tend to increase with the number of scans, but as it is seen in figure 2, it is strongly influenced by the ionic size of the dopant, the nature of the side chain on the cluster B(8) atom and by the increasing electrical resistance of the deposit. The more conductive material is obtained with [**1**]$^-$. When the cluster boron B(8) is bonded to an alkyl chain [**5**]$^-$ or an aryl one [**4**]$^-$, the same growing speed and conductivity behaviour of the PPy film is observed, however, oxidative current values are 33% less than for PPy/[**1**]. Bulky and rigid anionic compounds [**2**]$^-$ and [**3**]$^-$ produce intensity values even smaller. Finally, CV intensities for derivatives of [**1**]$^-$, B-O bonded compounds [**6**]$^-$ and [**7**]$^-$, are one order smaller than for PPy/[**1**]. This last result is in agreement with PPy- [3,3'-Co(8-C_4H_4N-$(CH_2)_2$-O-$(CH_2)_2$-O-1,2-$C_2B_9H_{10}$)(1',2'-$C_2B_9H_{11}$)], a self-doped copolypyrrole[42] whose current intensity was far from the normal [**1**]$^-$ doped material.

3.2. Overoxidation Stability, Relationship between the doped PPy overoxidation results and the structure of the doping anions. Overoxidation measurements were made using a slow linear sweep voltammetry (LSV) technique in NaCl solution at 0.5 mV.s^{-1} from 0 to 1800 mV with regard to Ag/AgCl and are reported in Figure 3 for the PPy/[**1**]-PPy/[**7**]. As it was recently reported, PPy/[**1**] displays a peak at 1270 mV on the LSV plots, which is consistent to a high overoxidation resistance of the material.[27,47] This overoxidation threshold is almost 300 mV larger than other values obtained for PPy doped with common anions. Taking into account that PPy electrical properties highly depend on the doping anion properties like charge, anion shape regularity, ionic radius, hydrophobicity or hydrophilicity and on the interaction strength of the anionic species with the polymer matrix,[48-51] our interpretation of the excellent overoxidation stability of the PPy/[**1**] material is related to the three-dimensional peanut shape of the doping anion and its capacity to continuously compensate, through the three-dimensional disposition of the BH's, the positive polarons. Simple calculations[52] show that the distance between the farthest two carbon atoms of the PPy polarons is near 12.3 Å, which is relatively close to the H-B(10)…B(10')-H $[Co(C_2B_9H_{11})_2]^-$ axial distance[53] (10.2 Å including the two hydrogen atoms). Therefore, the use of [**1**]$^-$ gives the possibility of a fully intercalated structure of the polymeric network. On the contrary, the $[CB_{11}H_{12}]^-$ anion is spherical (with a diameter of 5.6 Å including the farthest two hydrogen atoms)[54] and its use can lead to a disruption of the layered space structure arrangement, leading to a lower observed overoxidation resistance. The "spherical" counter-ions such as $[ClO_4]^-$ or $[PF_6]^-$ testify in favour of such reasoning.

The anion [**1**]$^-$ is also considered to be a weakly coordinating anion, an useful spectator anion in making organometallic compounds to be used in catalysis,[55-58] efficient in extracting nuclear wastes,[39,53,59-62] in supramolecular chemistry[63] and in stabilizing cations.[38,64] For the last property, cluster BH bonds interact freely with the cation. Cation/BH interactions have been described in the literature[58,64,65] involving principally the B(8), B(9), B(12) sites that are identified as the site of maximum electron density in the cage. Nevertheless, in some examples, B(7)[38] and B(10)[65] were found to interact with the cation positive charge, demonstrating the diverse coordination possibilities of $[Co(C_2B_9H_{11})_2]^-$. It seems therefore that PPy positive charge interactions with cluster BH bonds appear to be a favourable combination for increasing the overoxidation capacity of the material. Consequently, when B(8), B(9) and B(12) atoms are Br or Cl substituted, cation/BH interactions disappear or are lessened, the typical $[Co(C_2B_9H_{11})_2]^-$ peanut shape is modified, and a drop of overoxidation potential is found.[37] The two hexachloro and hexabromo cobaltabisdicarbollide derivatives are thus less protecting. Similar behaviour but more dedicated to metal coordination was already reported by Xie *et al*. for cobaltabisdicarbollide derivatives with silver salts.[64]

In Figure 3, the LSV experiments corresponding to PPy/[**1**]-PPy/[**7**] are represented. All display well-defined peaks but major shifts of the peak maximum are observed. The rigid [**2**]$^-$ and [**3**]$^-$ dopants produce less overoxidation resistant materials, displaying LSV peaks at 1210 and 1150 mV, respectively. Compound [**4**]$^-$ produces similar overoxidation resistance than the classical [**1**]$^-$ at 1270 mV. Finally, PPy/[**5**], PPy/[**6**], PPy/[**7**], present threshold waves at 1330, 1410, 1450 mV, respectively, which are at more anodic potentials than PPy/[**1**]. The PPy/[**7**] potential shift value of 180 mV as compared with PPy/[**1**] implies that [**7**]$^-$ is the more overoxidation stabilizing anion tested in our experimental conditions and reported so far in the $[Co(C_2B_9H_{11})_2]^-$ family and in the literature.

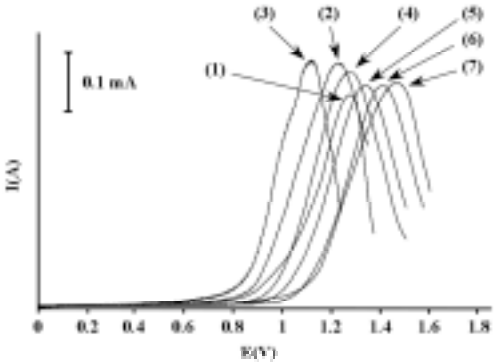

Figure 3. Overoxidation current vs. applied potential for PPy/[**1**-**7**].

It also may be observed that compounds [**2**]$^-$-[**4**]$^-$ bearing aryl groups directly bonded to the cluster atoms produce polypyrrole materials with similar or less overoxidation resistance than [**1**]$^-$ whereas other cluster substituents (alkyl or alkoxy) [**5**]$^-$-[**7**]$^-$ improve the overoxidation performance of the materials. This aspect is in agreement with the fact that a low charge density anion can enhance the chemical stability of the PPy.[27] Aryl groups withdraw electron density from the cluster but in the same time, compensate the lost of electron density by back-donation.[66] Other chains, even the alkyl one, only remove electron density from the cluster, therefore producing a lower delocalised charge in the whole carborane cage.

The [**3**]$^-$ doping anion is the one that shows the most defective overoxidation property. In [**3**]$^-$, the phenyl ring bridging both cluster fragments at B(8) and B(8') positions, is perpendicular to the planes of the ligand coordinating C_2B_3 faces. The H- B(8) and H-B(8'), the two sites with more electron density in [**1**]$^-$, should interact with the moving positive charges of the PPy wires. Due to benzene substitution in [**3**]$^-$, this is not possible. This, along with the very bulky resulting shape of the anion, clearly limit any compact three-dimensional PPy network formation. When the two phenyl rings of [**2**]$^-$ are bonded to the cluster carbon atoms, similar but more mobile anion shape is obtained and all

cation/BH interactions are possible. Consequently, the PPy/[**2**] overoxidation potential threshold value is half way between this of PPy/[**1**] and this of PPy/[**3**]. Compounds [**4**]$^-$-[**7**]$^-$ present the same geometrical characteristics, but differ on the substituents. One of the dicarbollide fragments in the complexes is free of substituents while the second complex moiety is substituted in the B(8) position. In the nude dicarbollide ligand, B-H bonds can interact with the moving positive charge in the PPy wires. Therefore, differences among PPy/[**4**]-PPy/[**7**] overoxidation resistances, can only arise from the electron-withdrawing strength of the chain substituents, and from the capacity of hard oxygen donor atoms to compensate the moving polarons, since the volume of these [**4**]$^-$-[**7**]$^-$ anions and their shape is similar. The introduction of oxygen atom at position eight of the dicarbollide moiety results in a significant redistribution of electron density in the cluster, part of the charge being accumulated in the B(8)-O oxygen atom, therefore overall producing a cluster with lower charge density than [**1**]$^-$. LSV overoxidation results (Figure 3) are in direct correlation with the previous considerations, PPy/[**6**] and PPy/[**7**] being the best overoxidation resistant material. The alkoxy organic groups of complexes [**6**]$^-$ and [**7**]$^-$ can also participate in the compensation of the PPy positive charges by electrostatic interactions in a similar way as oxygen atoms of [3,3'-Co(8-X-$(CH_2CH_2O)_2$-1,2-$C_2B_9H_{10}$)(1',2'-$C_2B_9H_{11}$)] coordinate to Na or hard cations.[39,59,61,62,67]

3.3. Electron Microscopy Observation. Figure 4 shows micrographs of the best and the worst overoxidation resistant materials, PPy/[**7**] (Figure 4B) and PPy/[**3**] (Figure 4C) respectively, and PPy/[**1**] material that was used as reference (Figure 4A). Although PPy/[**1**] SEM images have already been reported,[36] a different view is reported for clarity. Figure 4A shows a rough and reasonably homogeneous surface in which can be seen the typical empty vesicles already reported.[36] The micrograph for PPy/[**7**] shows a relatively more homogeneous and more compact surface than PPy/[**1**], whereas in the PPy/[**3**] image, a less homogeneous, less compact, less cohesive and more irregular layer is observed. Expectedly, this last structure arrangement is less dense and therefore OH^-, or other degradation species, should find less resistance to attack the polymer chain, leading to an increase of the overoxidation degradation rate and to a less anodic LSV experiment peak.

Conclusions

As a conclusion, the overoxidation resistance properties of polypyrrole were evaluated for six new cobaltabisdicarbollide complex doping anions that could be easily sorted by their geometrical characteristics. In this way, three groups of two doping agents each could be produced (see Chart 2) : [**2**]$^-$-[**3**]$^-$, [**4**]$^-$-[**5**]$^-$, and [**6**]$^-$-[**7**]$^-$. Although there are noticeable differences in each group, the group components reasonably behave in the same way when acting as doping agents. For instance, concerning the PPy growth rate, three clear different behaviours, in addition to PPy/[**1**] are observed (see Figure 2). Those different behaviour correspond well with the three groups defined above, to say PPy/[**2**], PPy/[**3**] in the first group, PPy/[**4**], PPy/[**5**] in a second group and PPy/[**6**] and PPy/[**7**] in a third group. In a similar way the same three groups can be generated in the LSV experiments leading to determine the overoxidation threshold. In doing this grouping, it is found that the expected electronic opposite effects in [**4**]$^-$ and [**5**]$^-$ were found not to be determinant for PPy overoxidation resistance.

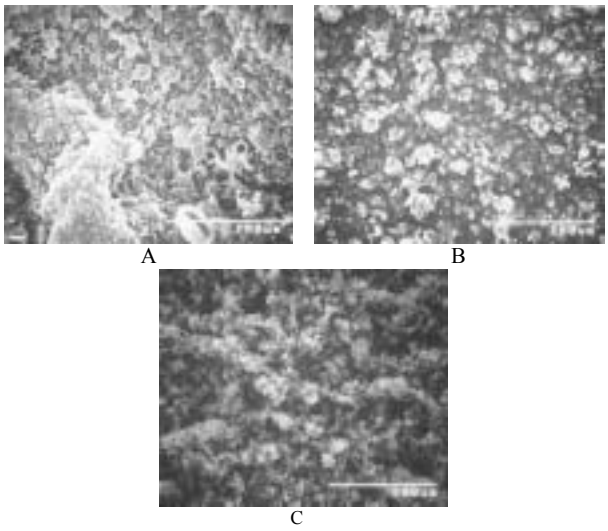

Figure 4. SEM images of electropolymerized PPy/(1) : A, PPy/(7) : B, PPy/(3) : C.

It is also found that for all PPy/[**1**]$^-$-PPy/[**7**]$^-$ materials, low scan voltammetry experiments present a peak corresponding to the overoxidation threshold potential value. This potential is characteristic of the material and highly depends on the nature of the substituents on the carborane cluster cage. The results obtained indicate that polypyrrole overoxidation resistance is enhanced with anions having lower charge density. For the particular case of the excellent $[Co(C_2B_9H_{11})_2]^-$ anions, this is proven by the influence of substituents able to withdraw negative charge from the cluster. These substituents lower the overall charge of the cluster, hence the charge density, a parameter that is believed to be strongly influential in the polypyrrole overoxidation resistance. Additionally, a steric and anion shape influence is very relevant. The $[Co(C_2B_9H_{11})_2]^-$ anion has a peanut shape that allows a good interstitial packing and a three-dimensional distribution of the B-H units ready to compensate the polarons. The less availability of B-H units in the doping agents induces a less favourable overoxidation threshold in the material. Contrarily, the existence of extra hard coordinating elements in the external chains induces a more favourable overoxidation threshold. Bulky derivatives of this shape alter the packing type, expectedly producing less dense material, therefore facilitating penetration of hostile and degradating anions.

Acknowledgment. This work was supported by MCyT (MAT01-1575 project). S. G. thanks the French Ministry of Foreign Affairs, for a "Lavoisier" post-doctoral grant. Assistance of CNM in recording the SEM images is sincerely appreciated.

Notes and references

(1) Sadki, S.; Schottland, P.; Brodie, N.; Sabouraud, G. *Chem. Soc. Rev.* **2000**, *29*, 283.
(2) Wang, L.-X.; Li, X.-G.; Yang, Y.-L. *Reactive & Func. Pol.* **2001**, *47*, 125.
(3) Vidal, J. C.; Garcia, E.; Castillo, J. R. *Anal. Chim. Acta* **1999**, *385*, 213.
(4) Campbell, T. E.; Hodgson, A. J.; Wallace, G. G. *Electroanalysis* **1999**, *11*, 215.

(5) Kincal, D.; Kamer, A.; Child, A. D.; Reynold, J. R. *Synth. Met.* **1998**, *92*, 53.
(6) Kemp, N. T.; Flanagan, G. U.; Kaiser, A. B.; Trodahl, H. J.; Chapman, B.; Partridge, A. C.; Buckley, R. G. *Synth. Met.* **1999**, *101*, 434.
(7) Sun, B.; Fitch, P. G. *Electroanalysis* **1997**, *9*, 494.
(8) Ogura, K.; Shiigi, H.; Nakayama, M. *J. Electrochem. Soc.* **1996**, *143*, 2925.
(9) Nicolas, M.; Fabre, B.; Simonet, J. *Chem. Commun.* **1999**, *17*, 1881.
(10) Barisci, J. N.; Murray, P.; Small, C. J.; Wallace, G. G. *Electroanalysis* **1996**, *8*, 330.
(11) Arrignan, D. W. M.; Lowens, M. J. *Electroanalysis* **1999**, *11*, 647.
(12) Iroh, J. O.; Williams, C. *Synth. Met.* **1999**, *99*, 1.
(13) Su, W.; Iroh, J. O. *Synth. Met.* **1998**, *95*, 159.
(14) Qi, Z.; Pickup, P. G. *Chem. Commun.* **1998**, 15.
(15) Qi, G.; Lefebvre, M. C.; Pickup, P. G. *J. Electroanal. Chem.* **1998**, 9.
(16) Bull, R. A.; Fan, F. F.; Bard, A. J. *J. Electrochem. Soc.* **1982**, *129*, 1009.
(17) Beck, F.; Braun, P.; Oberst, M. *Ber. Busenges. Phys. Chem.* **1987**, *91*, 967.
(18) Ge, H.; Qi, G.; Kang, E.; Neoh, K. G. *Polymer* **1994**, *35*, 504.
(19) Mostany, J.; Scharifker, B. R. *Electochim. Acta* **1997**, *42*, 291.
(20) Schlenoff, J. B.; Xu, H. *J. Electrochem. Soc.* **1992**, *139*, 2397.
(21) Wernet, W.; Wegner, G. *Makroml. Chem.* **1987**, *188*, 1465.
(22) Tamm, J.; Alumaa, a.; Hallik, A.; Sammelselg, v. *J. Electroanal. Chem.* **1998**, *448*, 25.
(23) Smela, E. *Adv. Mater.* **1999**, 1343.
(24) Sansinena, J. M.; Olazabal, V.; Otero, T. F.; Dafonseca, C. N. P.; Depaoli, M. A. *Chem. Commun.* **1997**, 2217.
(25) Tang, H.; Kitani, A.; Shiotani, M. *Electochim. Acta* **1996**, *41*, 1561.
(26) Lippe, J.; Holze, R. *J. Electroanal. Chem.* **1992**, *339*, 411.
(27) Massalles, C.; Borros, S.; Viñas, C.; Teixidor, F. *Adv. Mater.* **2000**, *12*, 1199.
(28) Ghosh, S.; Bowmaker, G. A.; Cooney, R. P.; Seakins, J. M. *Synth. Met.* **1998**, *95*, 63.
(29) Lewis, T. W.; Wallace, G. G.; Kim, C. Y.; Kim, D. Y. *Synth. Met.* **1997**, *84*, 403.
(30) Mazeikiene, R.; Malinauskas, A. *Poly. Deg. Stab.* **2002**, *75*, 255.
(31) Malitesta, C.; Losito, I.; Sabbatini, L.; Zambonin, P. G. *J. Electron. Spectrosc.* **1995**, *76*, 629.
(32) Christensen, P. A.; Hamnett, A. *Electochim. Acta* **1991**, *36*, 1263.
(33) Rodríguez, I.; Scharifker, B. R.; Mostany, J. *J. Electroanal. Chem.* **2000**, *491*, 117.
(34) Li, Y.; Qian, R. *Electochim. Acta* **2000**, *45*, 1721.
(35) Mostany, J.; Scharifker, B. R. *Synth. Met.* **1997**, *87*, 179.
(36) Massalles, C.; Borros, S.; Viñas, C.; Teixidor, F. *Adv. Mater.* **2002**, *14*, 449.
(37) Massalles, C. *URL, Doctoral Thesis.* **2002**.
(38) Llop, J.; Massalles, C.; Teixidor, F.; Viñas, C.; Sillanpää, R.; Kivekäs, R. *J. Chem. Soc., Dalton Trans.* **2003**, *4*, 556.
(39) Viñas, C.; Bertran, J.; Gomez, S.; Teixidor, F.; Dozol, J.-F.; Rouquette, H.; Kivekäs, R.; Sillanpää, R. *J. Chem. Soc., Dalton Trans.* **1998**, 2849.
(40) Shelly, K.; Knobler, C. B.; Hawthorne, M. F. *New J. Chem.* **1988**, *12*, 317.
(41) Rojo, I. **2003**, *Unpublished results*.
(42) Massalles, C.; Llop, J.; Viñas, C.; Teixidor, F. *Adv. Mater.* **2002**, *14*, 826.
(43) Zhou, M.; Heinze, J. *Electochim. Acta* **1999**, *44*, 1733.
(44) Noftle, D. E.; Pletcher, D. *J. Electroanal. Chem.* **1987**, *227*, 229.
(45) Downard, A. J.; Pletcher, D. *J. Electroanal. Chem.* **1986**, *206*, 139.
(46) Downard, A. J.; Pletcher, D. *J. Electroanal. Chem.* **1986**, *206*, 147.
(47) Gentil, S.; Friang, A.; Viñas, C.; Teixidor, F. *Submitted* **2003**.
(48) Levi, M. D.; Lopez, C.; Vieil, E.; Vorotyntsev, A. *Electochim. Acta* **1997**, *42*, 757.
(49) Mohammad, F. *Synth. Met.* **1999**, *99*, 149.
(50) Kiani, M. S.; Mitchell, G. R. *Synth. Met.* **1992**, *42*, 203.
(51) Cheung, K. M.; Bloor, D.; Stevens, G. C. *Journal of Materials Science* **1990**, *25*, 3814.
(52) *Hyperchem 5.0 package*, *(Version 5.0, Hypercube Inc.)*.
(53) Viñas, C.; Gomez, S.; Bertran, J.; Barron, J.; Teixidor, F.; Dozol, J.-F.; Rouquette, H.; Kivekäs, R.; Sillanpää, R. *J. Organomet. Chem.* **1999**, *581*, 188.
(54) King, B. T.; Noll, B. C.; Michl, J. *Collec. Czech. Chem. Commun.* **1999**, *64*, 1001.
(55) Hlatky, G. G.; Turner, H. W.; Eckman, R. R. *J. Am. Chem. Soc.* **1989**, *111*, 2728.
(56) Hlatky, G. G.; Turner, H. W.; Eckman, R. R. *Organometallics* **1992**, *11*, 1413.
(57) Grossman, R. B.; Doyle, R. A.; Buchwald, S. L. *Organometallics* **1991**, *10*, 1501.
(58) Yang, X.; King, W.; Sabat, M.; Marks, T. J. *Organometallics* **1993**, *12*, 4254.
(59) Grüner, B.; Plešek, J.; Báca, J.; Císarová, I.; Dozol, J.-F.; Rouquette, H.; Viñas, C.; Selucký, P.; Rais, J. *New J. Chem.* **2002**, *26*, 1519.
(60) Viñas, C.; Gomez, S.; Bertran, J.; Teixidor, F.; Dozol, J.-F.; Rouquette, H. *Inorg. Chem.* **1998**, *37*, 3640.
(61) Plešek, J.; Grüner, B.; Hermánek, S.; Báca, J.; Marecek, V.; Jänchenová, J.; Lhotský, A.; Holub, K.; Selucký, P.; Rais, J.; Císarová, I.; Cáslavský, J. *Polyhedron* **2002**, *21*, 975.
(62) Plešek, J.; Grüner, B.; Císarová, I.; Báca, J.; Selucký, P.; Rais, J. *J. Organomet. Chem.* **2002**, *657*, 59.
(63) Hardie, M. J.; Raston, C. L. *Angew. Chem. Int. Ed. Engl.* **2000**, *39*, 3835.
(64) Tsang, C.-W.; Sun, J.; Xie, Z. *J. Organomet. Chem.* **2000**, *613*, 99.
(65) Chetcuti, P. A.; Hofherr, W.; Liégard, A.; Rihs, G.; Rist, G. *Organometallics* **1995**, *14*, 666.
(66) Llop, J.; Viñas, C.; Teixidor, F.; Flores, M. A.; Oliva, J. M.; Kivekäs, R.; Sillanpää, R. *J. Organomet. Chem.* **2002**, *657*, 232.
(67) Grüner, B.; Bonnetot, B.; Mongeot, H. *Collec. Czech. Chem. Commun.* **1997**, *62*, 1185.

A cobaltabisdicarbollide geometrical anionic BINAP analogue. Its synthesis and coordinating habits.

Isabel Rojo,[#] Francesc Teixidor,[#] Clara Viñas,[#]* Raikko Kivekäs,[§] Reijo Sillanpää[&]

[#] *Institut de Ciència de Materials de Barcelona (CSIC), Campus de la U.A.B, 08193 Bellaterra, Spain;* [§] *Department of Chemistry, P.O. Box 55, University of Helsinki, FIN-00014, Finland;* [&] *Department of Chemistry, University of Jyväskylä, FIN-40351, Finland.*

RECEIVED DATE (automatically inserted by publisher); E-mail: clara@icmab.es

Introduction

Today synthesizing enantiomerically pure compounds is a very significant endeavour to develop pharmaceuticals, agrochemicals and flavours. Enantioselectivitites can be achieved with both C_1- and C_2- symmetric ligands, utilizing chirality at carbon, chirality on a donor atom (e.g. phosphorus), axial chirality or planar chirality. In 1968 W.S. Knowles[1] and L. Horner,[2] independently, reported the first homogeneously catalyzed hydrogenation of olefins with chiral monodentate tertiary phosphine-Rh complexes (C_1- symmetry ligand). Later Kagan[3] devised DIOP, a C_2- symmetry ligand that represented a major breakthrough in the area. In 1980 Noyori published the synthesis of BINAP (2,2'-bis(diphenylphophanyl)-1,1'-binaphtyl which is an axially dissymmetric C_2- ligand able to perform strong steric and electronic influences on transition-metal complexes. It has found extensive applications in asymmetric catalysis.[4] Since then thousands of chiral ligands and their transition metal complexes have been reported[5] and many of them are known to be highly effective in the asymmetric formation of C-H, C-C, C-O and C-N bonds, etc. Great many of them ressemble very much BINAP and are obtained in racemic form to be later resolved to produce the enantiomeric atropisomers. One example of these is BiPHEP that is represented along with BINAP and [3,3'-Co(1-PPh_2-1,2-$C_2B_9H_{10})_2]^-$ ([**2**]$^-$) in figure 1. While chiral atropisomeric biaryl diphosphines such as BINAP, BIPHEMP, and MeO-BIPHEP are very effective ligands for many asymmetric reactions,[6,7] sometimes they are not efficient for certain substrates due to the lack of ligand rigidity. Introducing a bridge with variable length to link the diaryl groups has been proposed[8] to make rigid ligands with tunable bite angles.[9] Ferrocenyl phosphine ligands, see figure 1, have also been deviced.[10] Chiral ligands of the latter are produced introducing a single substituent.

We had a number of reasons for wishing to prepare metallacarboranyl diphosphines: the rapidly developing field of cobaltabisdicarbollide chemistry provides a pool of unprecedented backbones that may be used to stabilize and/or elaborate any chosen metal centre;[11] to prove that although metallaboranes may look esoteric their stability and reactivity motivates to consider them; to provide the first intrinsically anionic diphosphines in opposition to sulfonated BINAP,[12] for instance; and finally to show how the metal orientation with regard to the swinging axis can be modulated.

We have not done efforts to separate the racemic mixture. Our aim in presenting this work has been to show the possibilities of these ligands, derivatives of [3,3'-Co(1,2-$C_2B_9H_{11})_2]^-$ ([**1**]$^-$), their versatility and their coordinating capacity.

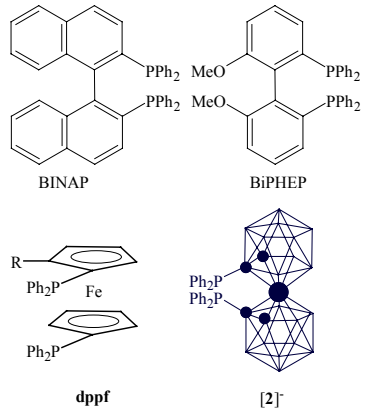

Figure 1. Representation of BINAP, BiPHEP, a diphenyl phosphino ferrocene (**dppf**) and [3,3'-Co(1-PPh_2-1,2-$C_2B_9H_{10})_2]^-$ ([**2**]$^-$).

Results

1. Synthesis of [3,3'-Co(1-PPh_2-1,2-$C_2B_9H_{10})_2]^-$, [2]$^-$.

The desired anionic diphosphine may be prepared conveniently by metallation of [3,3'-Co(1,2-$C_2B_9H_{11})_2]^-$, with *n*-BuLi followed by simple reaction with chlorodiphenylphosphine in 1,2-dimethoxyethane (DME) as a solvent. A red solid corresponding to Li[**2**] spontaneously separates from the solution which is filtered in the air. The M[**2**] (M= NMe_4 or Cs) salts are produced by dissolving Li[**2**] in ethanol and adding an aqueous solution of [NMe_4]Cl or CsCl. Solids corresponding to the M[**2**] (M= NMe_4 or Cs) stoichiometry separate well and can be collected by filtration. The formula for [**2**]$^-$ was proven by the mass spectrum obtained by Matrix Assisted Laser Desorption Ionization (MALDI-TOF). Full agreement between the experimental and calculated pattern was obtained. The ^{11}B-, ^{1}H- and ^{31}P-NMR spectra of M[**2**] are in accord with the proposed structure shown in figure 1. The ^{11}B-NMR of Li[**2**] displays a 1:1:2:2:1:1:1 pattern in the range 9.1 to –20.0 ppm indicative of a *closo* species with all boron atoms in non-equivalent vertexes. The resonances of intensity 2 shall be attributed to the coincidental overlap of two absorptions of intensity 1. The former pattern is consistent with a cluster carbon single substitution in each dicarbollide moiety. In agreement with this, the ^{31}P-NMR shows only one resonance at 23.48 ppm. Finally, the ^{1}H-NMR displays a group of resonances between 7.76 and 7.31 ppm corresponding to aromatic protons and one resonance at 4.37 ppm corresponding to the $C_{cluster}$-***H***, (C_c-***H***), in a ratio

20:2. The absence of other peaks in this very informative region, 4-4.8 ppm, indicated that either the racemic or the *meso* form had been generated, but not the two. These two geometrical isomers could be produced in the reaction, and would present a similar ^{11}B-NMR pattern according to the expected $\boldsymbol{C}_2$ or $\boldsymbol{C}_s$ symmetry, respectively. Therefore a crystal structure determination was necessary to elucidate which one of the two possible isomers had been generated. However, the ^{13}C-NMR of Li[**2**] in the $\boldsymbol{C}_c$-R region already brought important hints about which isomer had been produced. This ^{13}C-NMR excerpt spectrum is shown in figure 2.

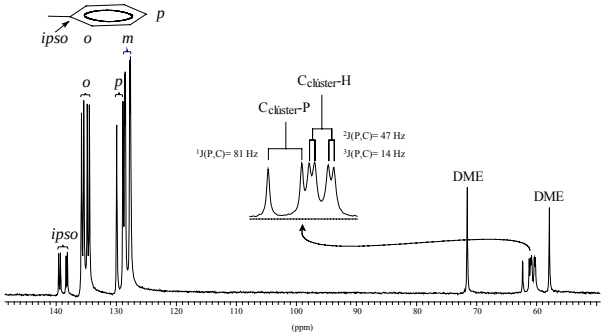

Figure 2. The ^{13}C-NMR spectrum of [**2**]$^-$ with a more detailed view of the $C_{cluster}$-R (R= H or P) region.

The spectrum shows one resonance at 61.41 ppm with a ^{1}J(C,P)= 81 Hz and a doublet of doublets centered at 60.22 ppm with ^{2}J(C,P)= 47 Hz and ^{3}J(C,P)= 14 Hz. Interestingly, the two observed resonances $\boldsymbol{C}_c$-P and $\boldsymbol{C}_c$-H do not present the same splitting pattern with phosphorus. Diagram in figure 3 provides information on the reasons for the splitting dissimilarity of both C_c atoms.

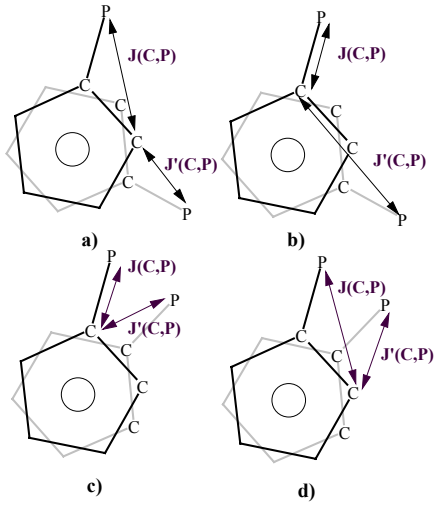

Figure 3. Projection of the pentagonal faces in [**2**]$^-$ (with cobalt in the centre of symmetry). Figures a) and b) correspond to the racemic mixture while figures c) and d) correspond to the *meso* isomer.

J(C,P) stands for the C coupling with the P in the common dicarbollide moiety while J'(C,P) stands for the C coupling with P in the non-common dicarbollide moiety. Figures a) and b) correspond to the racemic mixture while figures c) and d) correspond to the *meso* isomer. Figures b) and c) refer to the ^{13}C resonance for C_c-P while figures a) and d) stand for the ^{13}C resonance of C_c-H. The ratio J(C,P) vs J'(C,P), represented by the arrows lengths is similar in c) and d), therefore a similar splitting patterns would be expected for C_c-P and C_c-H in the *meso* form. The J(C,P) and J'(C,P) discrepancy is very accentuated in the racemic mixture, figures a) and b) in figure 3, the $\boldsymbol{C}_{cluster}$-H having the more similar J and J' values and being subjected then to higher splitting. This would justify the observed pattern in the ^{13}C-NMR of [**2**]$^-$ and prompted us to postulate that the racemic isomer had been generated.

X-ray diffraction. Crystals of [NMe_4][**2**] suitable for an X ray diffraction study were obtained by slow evaporation of a solution of the material in acetone and measured at ambient temperature on a Rigaku AFC5S diffractometer. A total of 7438 unique reflections were collected. The structure was solved by direct methods and refined on F^2 by the SHELXL97 program.[13] The hydrogen atoms were treated as riding atoms using the SHELX97 default parameters. For [NMe_4][**2**], all non-hydrogen atoms were refined with anisotropic displacement parameters. Tables 1 and 2 shows respectively crystallographic data and structural refinement details and selected interatomic distances and angles for [NMe_4][**2**].

Table 2. Selected Interatomic Distances (Å) and Angles (deg) for [NMe_4][**2**].

Co3-C1	2.157(5)	C1'-Co3-C1	135.07(17)
Co3-C2	2.072(4)	P1-C1-Co3	108.3(2)
Co3-B8	2.116(6)	C2-C1-P1	114.4(3)
Co3-C1'	2.147(4)	B4-C1-P1	128.2(3)
Co3-C2'	2.094(4)	P2-C1'-Co3	111.3(2)
Co3-B8'	2.122(6)	C2'-C1'-P2	122.9(3)
P1-C1	1.896(5)	B4'-C1'-P2	120.8(3)
P2-C1'	1.893(4)	B10-Co3-B10'	173.84(14)
C1-C2	1.650(6)		
C1'-C2'	1.612(6)		

A straightforward refinement revealed a sandwich structure, in which the C–PPh_2 moieties are in a *cisoid* disposition showing that the anion corresponds to one of the enantiomers of the racemic form, figure 4.

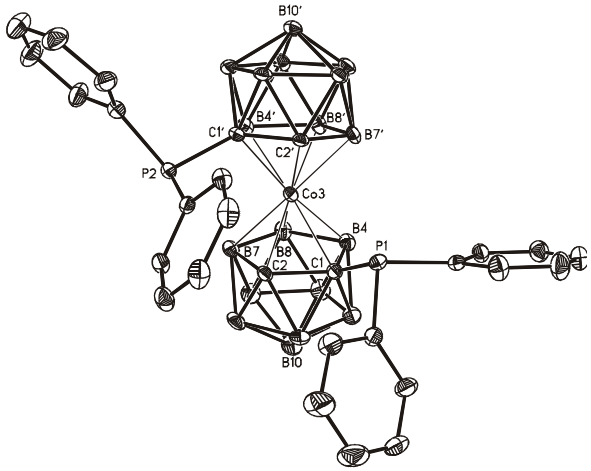

Figure 4. Drawing of anion of [NMe_4][**2**] with 20% thermal displacement ellipsoids.

2. Coordinating capacity.

Two types of metal ions have been studied to assess the coordinating capacity of [**2**]$^-$. Firstly, group 11 elements (Ag, Au) for their tendency to offer lower coordination numbers than other transition metal ions which would provide information on the real chelating predisposition of [**2**]$^-$; secondly transition metal ions of well recognized catalytic importance.

With group 11 elements (Ag, Au)

Treatment of [NMe_4][**2**] with one equivalent of [$MClPPh_3$] (M=Ag, Au) for 0.5 h. in refluxing ethanol afforded complexes [$M(PPh_3)$(**2**)] (**3**, M=Ag; **4**, M=Au) in 71 and 98% yield, respectively, as shown in figure 5.

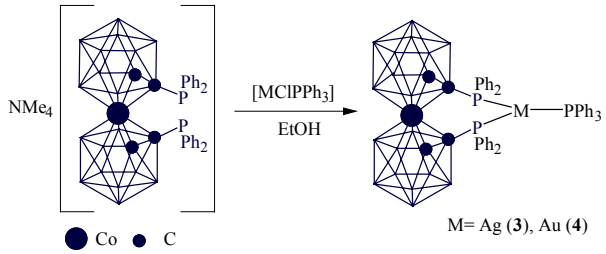

Figure 5. Scheme reaction between ligand [NMe_4][**2**] and [$MClPPh_3$] (M=Ag (**3**), Au (**4**)). Non-specified vertexes are BH's.

Similarly, treatment of [NMe_4][**2**] with one equivalent of [$AgClO_4$] at ambient temperature overnight in ethanol/acetone (10/3) afforded [Ag(acetone)(**2**)] (**5**) in 88% yield, see figure 6.

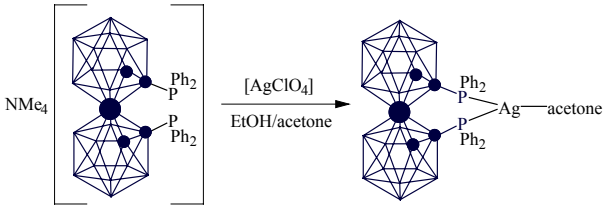

Figure 6. Scheme reaction between ligand [NMe_4][**2**] and [$AgClO_4$].

The molecular structure of **4** in solution was derived from the ^{31}P- and ^{11}B-NMR spectra in d_6-acetone. Interestingly, the spectra were observed better at -60ºC than at room temperature. The ^{11}B-NMR spectra displayed a 1:1:2:2:1:1:1 pattern, in agreement with a C_2 symmetry, in the range 10.0 to -19.4 ppm. The ^{31}P-NMR is simple, showing two sets of resonances: a doublet at 73.61 ppm with ^{2}J(P,P)=146 Hz and a triplet at 45.06 ppm with the same J value. This is in full agreement with Au being trigonally coordinated as shown in figure 5.

More complex is the structural elucidation or behaviour of **3** in solution. In principle a molecular structure such as this for **4** would be expected also in accord with the molecular structure of [Ag{7,8-$(PPh_2)_2$-7,8-$C_2B_9H_{10}$}(PPh_3)][14] where there is a chelating anionic carboranyl diphosphine ligand in which the two phosphorus atoms are in adjacent positions in the same dicarbollide moiety. The ^{31}P-NMR for **3** is, however, relatively simple with two absorptions at δ= 43.50 ppm and 42.81 ppm, and a third one at δ= 32.89 ppm. Each absorption is in fact made of two doublets result of the J(^{31}P,^{109}Ag) and J(^{31}P,^{107}Ag) couplings. Therefore and quite surprising is the fact that no J(P,P) couplings are observed contrarily to [Ag{7,8-$(PPh_2)_2$-7,8-$C_2B_9H_{10}$}(PPh_3)] where all possible cross couplings were found. Of notice is the fact that the two resonances, alghough very similar, at δ= 43.50 ppm and 42.81 ppm, indicate that the two phosphorus in [**2**]$^-$ are non-equivalent. The spectrum is shown in figure 7. This singular behaviour motivated the synthesis of **5**. The ^{31}P-NMR of **5** is very simple with only one resonance at δ= 46.01 ppm consisting of two doublets due to the J(^{31}P,^{109}Ag) and J(^{31}P,^{107}Ag) couplings.

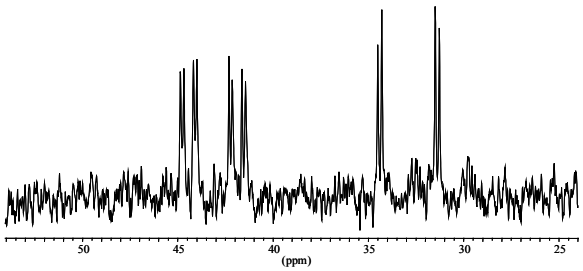

Figure 7. The ^{31}P-NMR spectrum of **3**.

The chemical shifts of the chelating phosphorus atoms in Ag coordinated to [**2**]$^-$ both in **3** and in **5** are very similar which is indicative of a similar surrounding in both complexes although in **3** they are non-equivalent. The only explanation for **3** is that there is not a trigonal coordination around Ag which implies the existence of an extra ancillary ligand that presumably could be the acetone. The existence of this fourth coordinating ligand would render the molecule asymmetric, and no longer the two phosphorus atoms would be equivalent. Also, this tetrahedral environment could be the justification for the lack of phosphorus cross-couplings observed in the ^{31}P-NMR. The ambiguity of the situation induced to grow crystals to unambiguously determine the chelating habit of [**2**]$^-$.

X-ray Single-Crystal Structures of 3, 4 and 5. Single crystals of **3**, **4** and **5** suitable for X-ray structure analysis were obtained from EtOH/acetone (**3**) or from acetone (**4** and **5**) at 22 °C after several days. Compound **3** crystallises in the space group C2/c. Compounds **4** and **5** in $P2_1/n$ (no. 14). Single-crystal data collection for **3**·$OCMe_2$, **4** and **5** were performed at –100ºC on an Enraf Nonius KappaCCD diffractometer using graphite monochromatized Mo Kα radiation. A total of 9571, 8850 and 8990 unique reflections were collected for **3**·$OCMe_2$, **4** and **5**, respectively.

The structures were solved by direct methods and refined on F^2 by the SHELXL97 program.[15] For all structures, the hydrogen atoms were treated as riding atoms using the SHELX97 default parameters. For **3**·$OCMe_2$, one of the phenyl groups connected to P3 and the non-coordinated acetone solvent are disordered both assuming two orientations. The disordered groups were refined as rigid groups and non-hydrogen atoms of the groups were refined with isotropic thermal displacement parameters. Rest of the non-hydrogen atoms were refined with anisotropic displacement parameters. For **4** and **5** all non-hydrogen atoms were refined with anisotropic displacement parameters.

ORTEP plots of the three complexes are shown in figures 8, 9 and 10. Tables 3, 4 and 5 contain selected bond distances and angles for **3**-**5** and crystallographic data and structural refinement details are shown in Table 1.

Both **3** and **5** can be viewed tetrahedrally coordinated, with three short contacts and one long contact. The long contact in **5** is due to Ag-H12' (2.17 Å) and in **3** is due to Ag-O in acetone (2.91 Å). Two of the short contacts are due to the two phosphorus atoms from [**2**]$^-$ and the third by PPh_3 (**3**) or acetone (**5**). In **4**, Au is tricoordinated to three phosphorus, two being provided by [**2**]$^-$ and the third by PPh_3. The trigonal coordination of Au is further

proven by the fact that Au is only 0.0648(5) Å above the plane defined by the three phosphorus atoms. Likewise, the tetrahedral nature of Ag both in **3** and **5** is proven by the distance of Ag to the plane defined by the three closest atoms, in **3** these are the P atoms (Ag distance to the plane = 0.3147 Å), and in **5** they are the two P atoms and the O in acetone (Ag distance to the plane = 0.49690(8) Å).

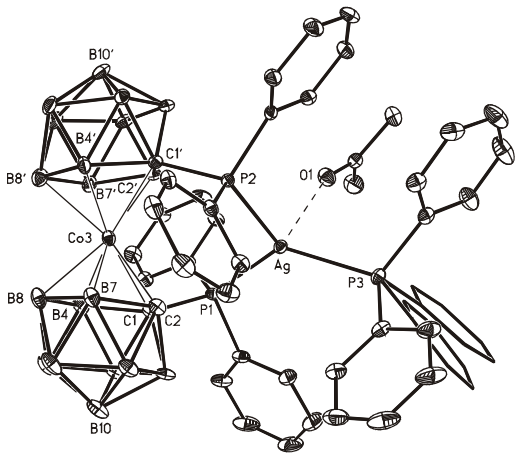

Figure 8. Drawing of **3** with 20% thermal displacement ellipsoids. Only skeletons of the two orientations of the disordered phenyl group are shown.

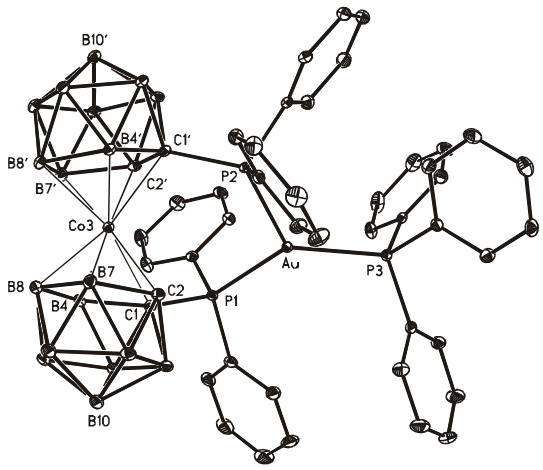

Figure 9. Drawing of **4** with 20% thermal displacement ellipsoids.

The three crystal structures clearly demonstrate the chelating capacity of the two phosphorus atoms in [**2**]$^-$. Although the phosphorus atoms are well separated in [NMe_4][**2**] as shown by the torsion angle C1-*c*-*c*'-C1' (= -102.3º) where c and c' are the centres of the pentagons, is smaller in the complexes, -77.6º, -54.4º and -76.4º for **3**, **4** and **5**, respectively. Figure 11 shows a top view of [**2**]$^-$ and **3**-**5** focusing on the influence of the metal in the cobaltabisdicarbollide rotamer produced. Interestingly, **4** and **5**, although having a similar metal coordination, display a large difference in . On the contrary, **3** and **5**, both Ag complexes, display values almost identical despite having the immediate metal surrounding distinct. This implies that it is the metal covalent radius the factor prevailing in determining the rotational degree of the ligand. The longer the M-P radius the larger is. In this regard M-P distances diminish following the sequence **3**>**5**>**4**, which is the same trend observed for , and for the P···P distance in coordinated [**2**]$^-$ which is 4.206 Å in **3**, 4.196 Å in **5**, and 3.837 Å in **4**.

Table 3. Selected Interatomic Distances (Å) and Angles (deg) for **3**·$OCMe_2$.

Ag-P1	2.5507(9)	P2-Ag-P1	111.21(3)
Ag-P2	2.5470(10)	P3-Ag-P1	129.99(3)
Ag-P3	2.4713(10)	P3-Ag-P2	114.09(3)
Ag-O1	2.906(3)	C1'-Co3-C1	123.05(14)
Co3-C1	2.156(4)	C1-P1-Ag	103.79(11)
Co3-C2	2.113(4)	C1'-P2-Ag	108.87(11)
Co3-B8	2.153(5)	P1-C1-Co3	112.97(17)
Co3-C1'	2.158(3)	C2-C1-P1	115.1(2)
Co3-C2'	2.096(4)	B4-C1-P1	131.3(3)
Co3-B8'	2.158(5)	P2-C1'-Co3	111.77(17)
P1-C1	1.878(4)	C2'-C1'-P2	114.9(2)
P2-C1'	1.878(4)	B4'-C1'-P2	129.9(3)
C1-C2	1.634(5)	B10-Co3-B10'	173.71(11)
C1'-C2'	1.626(5)		

Table 4. Selected Interatomic Distances (Å) and Angles (deg) for **4**.

Au-P1	2.3662(8)	P2-Au-P1	107.00(3)
Au-P2	2.4076(8)	P3-Au-P1	133.08(3)
Au-P3	2.3467(8)	P3-Au-P2	119.69(3)
Co3-C1	2.187(3)	C1'-Co3-C1	115.85(11)
Co3-C2	2.073(3)	P1-C1-Co3	117.10(15)
Co3-B8	2.138(4)	C2-C1-P1	118.6(2)
Co3-C1'	2.163(3)	B4-C1-P1	128.8(2)
Co3-C2'	2.060(3)	P2-C1'-Co3	114.63(15)
Co3-B8'	2.154(4)	C2'-C1'-P2	122.0(2)
P1-C1	1.874(3)	B4'-C1'-P2	124.5(2)
P2-C1'	1.878(3)	B10-Co3-B10'	171.13(8)
C1-C2	1.662(4)		
C1'-C2'	1.653(4)		

Table 5. Selected Interatomic Distances (Å) and Angles (deg) for **5**.

Ag-O	2.3895(17)	O-Ag-P1	114.68(5)
Ag-P1	2.4894(6)	O-Ag-P2	118.65(5)
Ag-P2	2.4933(6)	P1-Ag-P2	114.746(19)
Co3-C1	2.153(2)	C1'-Co3-C1	122.51(8)
Co3-C2	2.095(2)	C1-P1-Ag	104.47(7)
Co3-B8	2.153(3)	C1'-P2-Ag	107.19(7)
Co3-C1'	2.172(2)	P1-C1-Co3	113.96(11)
Co3-C2'	2.103(2)	C2-C1-P1	114.01(14)
Co3-B8'	2.150(3)	B5-C1-P1	118.40(14)
P1-C1	1.882(2)	B4-C1-P1	132.75(17)
P2-C1'	1.880(2)	B6-C1-P1	105.05(14)
C1-C2	1.631(3)	C37-O-Ag	134.76(18)
C1'-C2'	1.622(3)	P2-C1'-Co3	112.52(11)
		B10-Co3-B10'	174.16(5)

Table 1. Crystallographic Data and Structural Refinement Details for Compounds [NMe_4][**2**], **3**·$OCMe_2$, **4** and **5**.

	[NMe_4][**2**]	**3**·$OCMe_2$	**4**	**5**
empirical formula	$C_{32}H_{52}B_{18}CoNP_2$	$C_{52}H_{67}AgB_{18}CoO_2P_3$	$C_{46}H_{55}AuB_{18}CoP_3$	$C_{31}H_{46}AgB_{18}CoOP_2$
formula weight	766.20	1178.35	1151.29	858.00
crystal system	monoclinic	monoclinic	monoclinic	monoclinic
space group	$P2_1/n$ (no. 14)	C2/c	$P2_1/n$ (no. 14)	$P2_1/n$ (no. 14)
a (Å)	12.705(2)	39.7263(5)	11.15040(10)	12.8241(2)
b (Å)	12.1215(18)	12.5412(2)	18.2288(2)	19.1948(5)
c (Å)	27.988(7)	23.5531(3)	24.9604(2)	16.9761(4)
β (deg)	101.416(16)	95.3792(10)	97.0350(10)	108.1789(14)
V (Å^3)	4225.0(14)	11682.8(3)	5035.22(8)	3970.19(15)
Z	4	8	4	4
T (ºC)	21	-100	-100	-100
λ (Å)	0.71069	0.71073	0.71073	0.71073
ρ (g cm^{-3})	1.205	1.340	1.519	1.435
μ (cm^{-1})	5.08	7.41	33.70	10.20
goodness-of-fit	0.996	1.010	1.015	1.034
$R1$[a] [$I>2\sigma(I)$]	0.0603	0.0434	0.0253	0.0313
$wR2$[b] [$I>2\sigma(I)$]	0.1379	0.0867	0.0488	0.0672

[a] $R1 = \Sigma|| F_o| - |F_c||/\Sigma|F_o|$
[b] $wR2 = \{\Sigma[w(F_o^2-F_c^2)^2]/\Sigma[w(F_o^2)^2]\}^{1/2}$

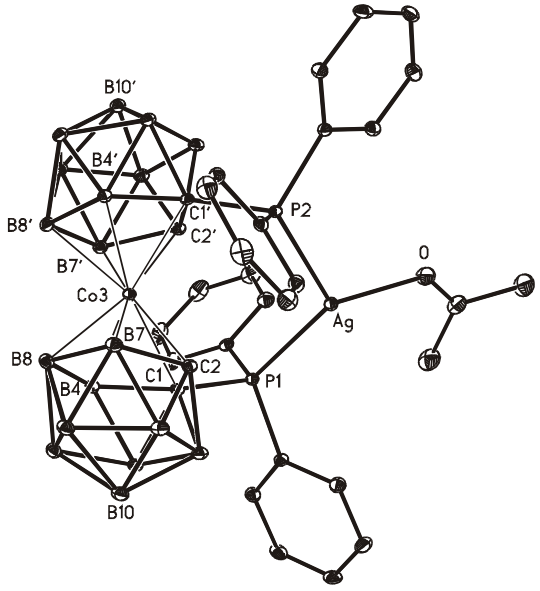

Figure 10. Drawing of **5** with 20% thermal displacement ellipsoids.

With catalytically important elements (Rh and Pd)

We also investigated the reaction of [NMe_4][**2**] with [Rh(μ-Cl)(cod)]$_2$. Complex [NMe_4][Rh(**2**)$_2$] (**6**) was obtained after stirring 2:0.5 mixtures of the starting materials in methylene chloride at ambient temperature overnight. Complex **6** was isolated in 85% yield as brown powdery solid, which is partially soluble in acetone. The different resonances in the ^{11}B-NMR spectra overlap greatly precluding to provide a definitive pattern. The resonances are observed between δ = 7.5 and -19.5 ppm. The ^{31}P-NMR spectra show a doublet at δ = 85.16 ppm with $^1J(P,^{103}Rh)$ = 205 Hz, in agreement with a structure in which the ligand symmetry in the complex has been preserved suggesting that the Rh surrounding is square-planar. The phosphorus strong chelating capacity towards Rh was checked by mixing [NMe_4][**2**] with [RhCl(PPh_3)$_3$] in ethanol at reflux for 1h. The resulting complex was again [NMe_4][Rh(**2**)$_2$] (**6**) in 87% yield. The stability of **6** in acetone was proven by ^{11}B-NMR and ^{31}P-NMR. After several months no noticeable changes had been observed in the spectra.

The reaction of [NMe_4][**2**] with [$PdCl_2(PPh_3)$]$_2$ in refluxing ethanol for 1 hour yielded a brown complex with the stoichiometry [PdCl(**2**)(PPh_3)] (**7**). Complex **7** is sparingly soluble in acetone. The ^{31}P-NMR spectra shows three sets of resonances at δ = 60.39, 54.02 and 30.37 ppm, which indicate the non-equivalency of the two binding phosphorus in (**2**). Resonance at 60.39 ppm corresponds to the PPh_2 trans to PPh_3 and appears as a doublet of doublets with the coupling constants: $^2J(P_{PPh2(trans)},P_{PPh3})$= 238 and $^2J(P_{PPh2},P_{PPh2})$= 70 Hz). The resonances at 54.02 and 30.37 ppm correspond respectively to the PPh_2 in cis to PPh_3 and PPh_3.

Monitoring the evolution of **7** in acetone with ^{11}B-NMR and ^{31}P-NMR spectroscopy showed [PdCl(**2**)(acetone)] (**8**) to be the major product after four days. Besides, only traces of unconverted **7** together with some minor unidentified phosphorus-containing products were detected. The ^{31}P-NMR spectrum of **8** displays two doublets at 64.48 ppm and 54.04 ppm with $^2J(P,P)$= 72 Hz.

Discussion

Ligand [**2**]$^-$ displays similarities with both 1,1'-bis(diphenylphosphino)ferrocene (**dppf**) and BINAP represented in figure 1. All of them have the possibility of various coordination modes reflecting their ability to match the steric demands of the coordinated metal, through axial rotation via a C-C bond (BINAP) or a centroid···metal···centroid axis in **dppf** or [**2**]$^-$. There are, however, important differences among these similar ligands. The most relevant are: i) while [**2**]$^-$ is anionic, BINAP and **dppf** are neutral, and ii) while

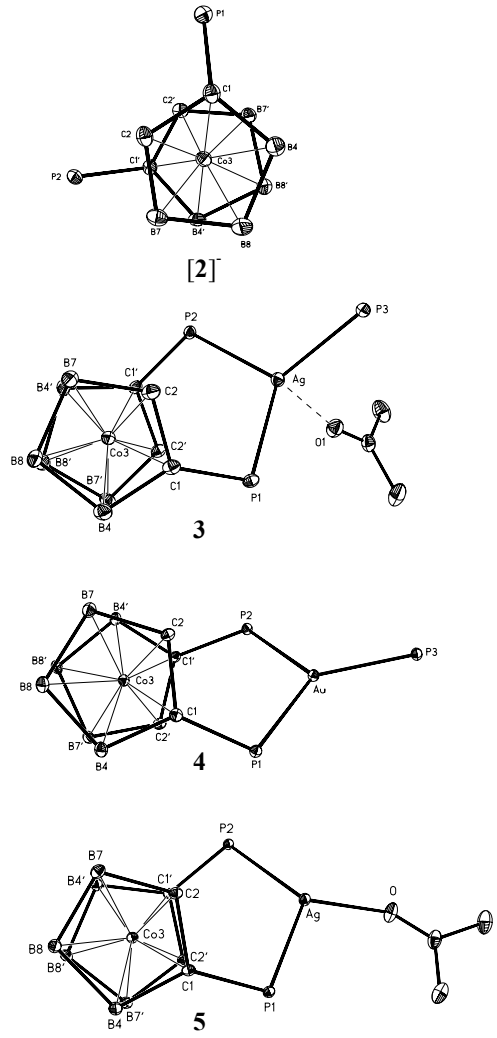

Figura 11. Top view of [**2**]$^-$, **3**·$OCMe_2$, **4** and **5** focusing on the influence of the metal in the cobaltabisdicarbollide rotamer produced.

[**2**]$^-$ and BINAP are produced in racemic form, therefore subjected to be separated into their enantiomers, **dppf** requires the introduction of a stereogenic center to produce a chiral ligand. In this sense [**2**]$^-$ is more similar to BINAP. Additionally, PPh_2 units in BINAP originate radially from the aromatic ring centroids being tilted towards the C-C axis. This is the origin of the atropisomerism. The possible optical isomerism is also originated this way in [**2**]$^-$, although in this case the reason of the racemic mixture has its origin in the C_2B_3 coordinating face with its prochiral carbon atoms. These axial ligands can be regarded as hinges, see figure 13, in which the leaves are each movable fragment, e.g. the antracenyl in BINAP, or the dicarbollide in [**2**]$^-$. This view helps to explain the great differences among them. If the P···Ag···P coordinating motif is taken as a reference it is found that the P···P distance in most diphosphine Ag complexes is practically constant ranging from 3.8 to 4.0 Å.[16] Therefore Ag demands the two P's to be geometrically separated by this value.

If we look at the hinge shown in figure 13 it is possible to notice that the distance between the holes (-PR_2) is maintained constant in a)-c). This has been possible varying the hole distances in the initial (D_0) position, shown in figure 13a), and swinging one of the leaves to the right **ω** value. Therefore with the hinge ligands BINAP, **dppf**, and [**2**]$^-$, practically any required P···P distance can be matched. In figure 13 hinge situation a) would be representative of **dppf**, hinge situation b) of [**2**]$^-$, and hinge situation c) could be representative of BINAP. Therefore the plane defined by the "P_2M" moiety will be more aligned with the hinge axis in **dppf** complexes than in BINAP, in which case the "P_2M" plane will be practically orthogonal to the axis. An intermediate situation, although closer to BINAP, would be with [**2**]$^-$. All this can be intuitively visualized just looking at the representations of BINAP, **dppf**, and [**2**]$^-$ in figure 12, and estimating the D_0 values. It would be expected that D_0 (**dppf**) > D_0 ([**2**]$^-$) > D_0 (BINAP).

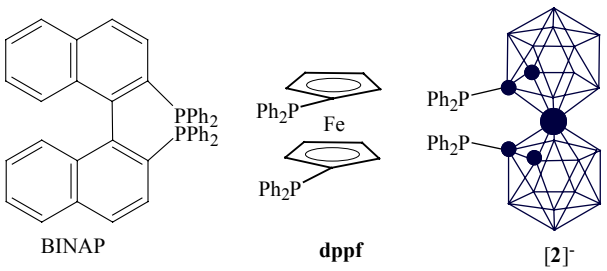

Figure 12. Comparison of BINAP, **dppf** and [**2**]$^-$, all representing initial eclipsed disposition, with **ω** = 0.

It is possible and of interest to provide a quantitative value that can define a hinge ligand. A good indication comes from the minimum possible P···P distance (D_0). This would be achieved when the two phosphorus are in an eclipsed disposition. As this hypothetical situation is virtually impossible to be obtained, and to account for the metal influence, we have developed equation 1 to get the D_0 value. This value should be taken with caution as it depends on the metal, the coordination, and other factors but it is orientative of the ligand characteristics.

$$D_\omega^2 = D_0^2 + 4R^2 \cos^2(90\text{-}0.5\omega) \quad \text{(equation 1)}$$

D_ω = P···P distance at the **ω** torsional value.
D_0 = P···P distance at the eclipsed position (**ω** = 0)
R = Distance of P to the hinge axis.
ω = Torsional angle from the eclipsed position.

Calculations based on equation 1 have been performed on data available from crystal structures[17] and these reported in this paper. The computed values average 3.8 Å, 1.1 Å and 0 Å for **dppf**, [**2**]$^-$ and BINAP, respectively, which are in perfect agreement with these intuitively given above. These three values mean that **dppf** will have to swing very little, small **ω** value, to fit a 4 Å (P···P) demand, for instance. To fit this value ligand [**2**]$^-$ will have to turn a larger **ω** angle, while BINAP will be the one with the P···M···P plane orthogonal to the hinge axis. The result is, then, very different geometrical figures with very similar ligands.

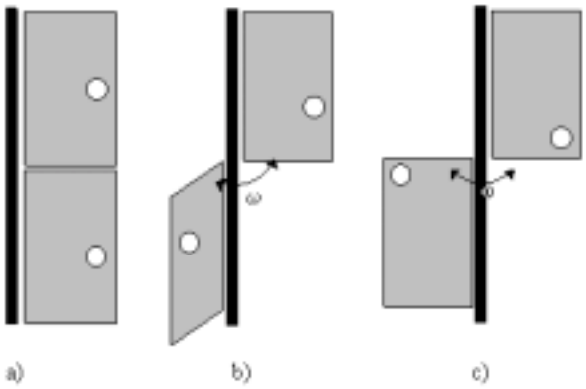

Figure 13. Hole-hole distance preservation by altering D_0 and **ω**.

Conclusions

In this paper the ligand [3,3'-Co(1-PPh_2-1,2-$C_2B_9H_{10})_2]^-$ ([**2**$]^-$) has been synthesized in one pot reaction from [3,3'-Co(1,2-$C_2B_9H_{11})_2]^-$ in very good yield and with an easy isolation process. Its two dicarbollide halves swing about one axis in the same way as 1,1'-binaphtyl or ferrocene derivatives. We consider these ligands to work as hinges, with the important property of being adjustable to any metal distance demand. Although the [3,3'-Co(1,2-$C_2B_9H_{11})_2]^-$, 1,1'-binaphtyl and ferrocene backbones have a similar torsional behavior their diphosphino derivatives will meet the metal's requirements very differently. This is due to the spatial origin and disposition of the $-PR_2$ units. The two $-PR_2$ units in the eclipsed disposition are more separated in the ferrocene than in the cobaltabisdicarbollide and, in the latter more than in the binaphyl derivatives. Therefore the "P_2M" plane generated will have a relative orientation with regard to the hinge axis very different. Furthermore the cobaltabisdicarbollide diphosphine derivative brings the novelty of being an intrinsically negative ligand, which apports interesting new possibilities for enhanced coordination and for optional metal site vacancies that otherwise would be fulfilled by a possible anionic monodentate ligand. Ligand [**2**$]^-$ should be separable into its enantiomers and therefore the possibility to study intrinsically anionic enantiomerically pure diphosphine ligands in catalysis. Finally, the easy synthesis of [**2**$]^-$ opens the opportunity to use carborane derivatives as real alternatives to conventional organic ligands.

Experimental Section

General Considerations. Elemental analyses were performed using a Carlo Erba EA1108 microanalyzer. IR spectra were recorded from KBr pellets on a Shimadzu FTIR-8300 spectrophotometer. The mass spectra were recorded in the negative ion mode using a Bruker Biflex MALDI-TOF-MS [N_2 laser; λ_{exc} 337 nm (0.5 ns pulses); voltage ion source 20.00 kV (Uis1) and 17.50 kV (Uis2)]. ^{1}H- and ^{1}H{^{11}B}-NMR (300.13 MHz), ^{13}C{^{1}H}-NMR (75.47 MHz), and ^{11}B-NMR (96.29 MHz) spectra were recorded with a Bruker ARX 300 instrument equipped with the appropriate decoupling accessories. All NMR spectra were recorded from CD_3COCD_3 solutions. Chemical shift values for ^{11}B-NMR spectra were referenced to external $BF_3{\cdot}OEt_2$, and those for ^{1}H-, ^{1}H{^{11}B}-, and ^{13}C{^{1}H}-NMR spectra were referenced to $Si(CH_3)_4$. Chemical shifts are reported in units of parts per million downfield from reference, and all coupling constants are reported in hertz.

All manipulations were carried out under a dry dinitrogen atmosphere with common Schlenk techniques. 1,2-Dimethoxyethane was distilled from sodium benzophenone prior to use. Ethanol and methylene chloride were dried over molecular sieves and deoxygenated prior to use. Cesium salt of compound [**1**$]^-$ was supplied by Katchem Ltd. (Prague) and used as received. Reagents were obtained commercially and used as purchased. Bis-(triphenylphosphine)palladium dichloride[18] was synthesized according to the literature.

Synthesis of [Li(DME)$_2$][3,3'-Co(1-PPh_2-1,2-$C_2B_9H_{10})_2$] ([Li(DME)$_2$][2]). Under inert atmosphere, *n*-butyllithium (3.4 mL, 5.48 mmol) (1.6 M in hexanes) was added dropwise to a stirred solution of Cs[3,3'-Co(1,2-$C_2B_9H_{11})_2$] (1.25 g, 2.74 mmol) in 120 mL of anhydrous 1,2-dimethoxyethane at -40ºC. The resulting purple solution was stirred for 30 min at low temperature. Then chlorodiphenylphosphine (1.0 mL, 5.48 mmol) was added causing a rapid color change to red and precipitation of a red solid. After stirring the mixture for an hour at room temperature, the solid was collected by filtration and washed with water and petroleum ether and, finally, was dried in vacuo. Yield: 2.3 g (96%). Anal. Calcd for $C_{36}H_{60}B_{18}CoLiO_4P_2$: C: 49.18, H: 6.88 %. Found: C: 48.95, H: 7.00 %. IR: ν (cm^{-1}) = 3049 (C_c-H), 2927, 2898 (C_{aryl}-H), 2548 (B-H), 1433, 1084, 746, 698, 499. ^{1}H NMR: δ = 7.76, 7.54, 7.46, 7.31 (m, 20H, *Ph*), 4.37 (br s, 2H, C_c-*H*), 3.46 (s, 8H, C*H*$_2$(DME)), 3.28 (s, 12H, C*H*$_3$(DME)), 4.14-1.25 (br m, 18H, B-*H*). ^{1}H{^{11}B} NMR**:** δ = 7.76, 7.54, 7.46, 7.31 (m, 20H, *Ph*), 4.37 (br s, 2H, C_c-*H*), 3.46 (s, 8H, C*H*$_2$(DME)), 3.28 (s, 12H, C*H*$_3$(DME)), 4.14 (br s, 2H, B-*H*), 3.21 (br s, 2H, B-*H*), 2.89 (br s, 4H, B-*H*), 2.21 (br s, 2H, B-*H*), 1.92 (br s, 4H, B-*H*), 1.47 (br s, 2H, B-*H*), 1.25 (br s, 2H, B-*H*). ^{13}C{^{1}H} NMR: δ = 139.05 (d, ^{1}J(P,C)= 22 Hz, P-*C*(Ph)), 137.05 (d, ^{1}J(P,C)= 17 Hz, P-*C*(Ph)), 135.23 (d, ^{2}J(P,C)= 29 Hz, *o*-*C*(Ph)), 134.27 (d, ^{2}J(P,C)= 26 Hz, *o*-*C*(Ph)), 129.54 (s, *p*-*C*(Ph)), 128.51 (s, *p*-*C*(Ph)), 128.18 (d, ^{3}J(P,C)= 8 Hz, *m*-*C*(Ph)), 127.31 (d, ^{3}J(P,C)= 8 Hz, *m*-*C*(Ph)), 71.64 (s, *C*H$_2$(DME)), 61.41 (d, ^{1}J(P,C)= 81 Hz, P-*C*$_c$), 60.22 (dd, ^{2}J(P,C)= 47 Hz, ^{3}J(P,C)= 14 Hz, *C*$_c$-H), 57.50 (s, *C*H$_3$(DME)). ^{11}B NMR: δ = 9.1 (d, ^{1}J(B,H)= 127 Hz, 2B), 2.3 (d, ^{1}J(B,H)= 137 Hz, 2B), -3.3 (d, ^{1}J(B,H)= 106 Hz, 4B), -4.2 (d, ^{1}J(B,H)= 98 Hz, 4B), -13.7 (d, ^{1}J(B,H)= 183 Hz, 2B) -15.9 (d, ^{1}J(B,H)= 163 Hz, 2B), -20.0 (d, ^{1}J(B,H)= 137 Hz, 2B). ^{31}P{^{1}H} NMR: δ = 23.48 (s, C_c-*P*Ph_2). MALDI-TOF-MS: (m/z) = 691.43 (M, 9%), 507.33 (M-PPh_2, 73%) i 323.32 (M-2PPh_2, 100%).

Synthesis of [Ag{3,3'-Co(1-PPh_2-1,2-$C_2B_9H_{10})_2$}(PPh_3)]·$OCMe_2$ (3). To a suspension of [NMe_4][3,3'-Co(1-PPh_2-1,2-$C_2B_9H_{10})_2$] (0.06 g, 0.08 mmol) in EtOH (10 mL) [AgClPPh_3] (0.034 g, 0.08 mmol) was added. The suspension was refluxed 30 min.. Then the resulting maroon solid was filtered off and wahed with ethanol and water. Yield: 59 mg (71 %). Anal. Calcd for $C_{49}H_{61}AgB_{18}CoOP_3$: C: 52.53, H: 5.49 %. Found: C: 52.79, H: 5.34 %. IR: ν (cm^{-1}) = 3058 (C_c-H), 2557 (B-H), 1359 (C-O), 1436, 1096, 743, 691, 502. ^{1}H NMR: δ = 8.30, 7.35, 6.37 (m, 35H, *Ph*), 4.83 (br s, 2H, C_c-*H*), 2.09 (s, 6H, C*H*$_3$), 4.41-0.88 (br m, 18H, B-*H*). ^{13}C{^{1}H} NMR: δ = 205.12 (s, *C*O), 137.55 (s, *Ph*), 135.82 (s, *Ph*), 133.69 (d, J(P,C)= 17, *Ph*), 130.01 (s, *Ph*), 128.94 (d, J(P,C)= 8, *Ph*), 127.95 (s, *Ph*), 126.35 (s, *Ph*), 61.14 (s, *C*$_c$), 28.99 (s, *C*H$_3$). ^{11}B NMR: δ = 9.9 (d, ^{1}J(B,H)= 105, 2B), 3.2 (d, ^{1}J(B,H)= 107, 2B), -3.1 (d, ^{1}J(B,H)= 110, 8B), -13.1 (d, ^{1}J(B,H)= 175, 2B) -15.0 (d, ^{1}J(B,H)= 145, 2B), -19.1 (d, 2B). ^{31}P{^{1}H} NMR (-60ºC): δ = 43.50 (2d, ^{1}J(^{109}Ag, P)= 330, ^{1}J(^{107}Ag, P)= 286, 1P, PPh_2), 42.81 (2d, ^{1}J(^{109}Ag, P)= 330, ^{1}J(^{107}Ag, P)= 286, 1P, PPh_2), 32.89 (2d, ^{1}J(^{109}Ag, P)= 392, ^{1}J(^{107}Ag, P)= 366, 1P, PPh_3).

Synthesis of [Au{3,3'-Co(1-PPh_2-1,2-$C_2B_9H_{10})_2$}(PPh_3)] (4). To a solution of Cs[3,3'-Co(1-PPh_2-1,2-$C_2B_9H_{10})_2$] (0.06 g, 0.07 mmol) in EtOH (10 mL) [AuClPPh_3] (0.034 g, 0.07 mmol) was

added. The complex, as a red solid, was obtained by filtration after 30 min of reflux. Yield: 89 mg (98 %). Anal. Calcd for $C_{46}H_{55}AuB_{18}CoP_3$: C: 47.99, H: 4.81 %. Found: C: 47.95, H: 4.63 %. IR: ν (cm^{-1}) = 3069 (C_c-H), 2573, 2550 (B-H), 1435, 1094, 746, 692. ^{1}H NMR: δ = 7.83, 7.61, 7.44, 7.36 (m, 35H, *Ph*), 4.42 (br s, 2H, C_c-*H*), 4.17-0.89 (br m, 18H, B-*H*). ^{1}H{^{11}B} NMR: δ = 7.83, 7.61, 7.44, 7.36 (m, 35H, *Ph*), 4.42 (br s, 2H, C_c-*H*), 4.17 (br s, 2H, B-*H*), 3.30 (br s, 2H, B-*H*), 2.81 (br s, 4H, B-*H*), 2.19 (br s, 2H, B-*H*), 1.93 (br s, 4H, B-*H*), 1.31 (br s, 2H, B-*H*), 0.89 (br s, 2H, B-*H*). ^{13}C{^{1}H} NMR: δ = 135.90 (d, J(P,C)= 26, *Ph*), 134.79 (d, J(P,C)= 25, *Ph*), 134.02 (d, J(P,C)= 14, *Ph*), 132.07 (s, *Ph*), 130.16 (s, *Ph*), 129.48 (d, J(P,C)= 11, *Ph*), 128.20 (d, J(P,C)= 34, *Ph*), 60.77 (s, C_c-H). ^{11}B NMR: δ = 10.0 (d, ^{1}J(B,H)= 116, 2B), 3.0 (d, ^{1}J(B,H)= 152, 2B), -3.0 (d, ^{1}J(B,H)= 135, 4B), -5.1 (d, ^{1}J(B,H)= 174, 4B), -13.1 (d, ^{1}J(B,H)= 147, 2B) -15.4 (d, ^{1}J(B,H)= 144, 2B), -19.4 (d, ^{1}J(B,H)= 152, 2B). ^{31}P{^{1}H} NMR (-60ºC): δ = 73.61 (d, ^{2}J(P_{PPh2},P_{PPh3})= 146, 2P, PPh_2), 45.06 (t, ^{2}J(P_{PPh2},P_{PPh3})= 146, 1P, PPh_3).

Synthesis of [Ag{3,3'-Co(1-PPh_2-1,2-$C_2B_9H_{10}$)$_2$}(OCMe$_2$)] (5). To a solution of [NMe_4][3,3'-Co(1-PPh_2-1,2-$C_2B_9H_{10}$)$_2$] (0.06 g, 0.08 mmol) in EtOH/acetone (10 mL/3 mL) a solution of [$AgClO_4$] (0.016 g, 0.08 mmol) in acetone (1 mL) was added. The mixture was stirred at room temperature overnight. Concentration of the mixture produced the precipitation of a pink solid. This was filtered off, washed with water and petroleum ether, and dried in vacuo. Yield: 59.2 mg (88 %). Anal. Calcd for $C_{31}H_{46}AgB_{18}CoOP_2$: C: 43.39, H: 5.40 %. Found: C: 43.20, H: 5.31 %. IR: ν (cm^{-1}) = 3058 (C_c-H), 2563, 2509 (B-H), 1310 (C-O), 1436, 1088, 741, 687. ^{1}H NMR: δ = 8.21 (br s, 5H, *Ph*), 8.09 (br s, 5H, *Ph*), 7.53, 7.45 (m, 10H, *Ph*), 4.73 (br s, 2H, C_c-*H*), 2.09 (s, 6H, C*H*$_3$), 4.47-0.88 (br m, 18H, B-*H*). ^{13}C{^{1}H} NMR: δ = 205.17 (s, *C*O), 137.23 (s, *Ph*), 135.38 (s, *Ph*), 132.46 (s, *Ph*), 131.81 (s, *Ph*), 131.24 (s, *Ph*), 128.83 (s, *Ph*), 128.06 (s, *Ph*), 62.26 (s, C_c-H), 28.90 (s, *C*H$_3$). ^{11}B NMR: δ = 12.7 (d, 2B), 3.8 (d, ^{1}J(B,H)= 132, 2B), -0.2 (d, ^{1}J(B,H)= 134, 2B), -4.0 (d, ^{1}J(B,H)= 118, 4B), -7.0 (d, 2B), -12.7 (d, 2B), -15.2 (d, 2B), -20.4 (d, ^{1}J(B,H)= 141, 2B). ^{31}P{^{1}H} NMR: δ = 46.01 (2d, ^{1}J(^{109}Ag, P)= 463, ^{1}J(^{107}Ag, P)= 403, 2P, PPh_2).

Synthesis of [NMe_4][Rh{3,3'-Co(1-PPh_2-1,2-$C_2B_9H_{10}$)$_2$}$_2$] (6). Starting from [Rh(μ-Cl)(cod)]$_2$: [Rh(μ-Cl)(cod)]$_2$ (0.032 g, 0.065 mmol) was added to 10 mL of a solution of [NMe_4][**2**] (0.2 g, 0.26 mmol), in deoxygenated methylene chloride, and the solution was stirred at room temperature overnight. A brown solid was separated by filtering and then washed with ethanol (10 mL) and water, giving **6**. Yield: 174 mg (85%). **Starting from [RhCl(PPh_3)$_3$]:** [RhCl(PPh_3)$_3$] (0.120 g, 0.13 mmol) was added to 10 mL of a solution of [NMe_4][**2**] (0.2 g, 0.26 mmol), in deoxygenated ehanol, and the mixture was refluxed for 1 h. A brown solid was separated by filtering and then washed with ethanol (10 mL) and water, giving **6**. Yield: 172 mg (87%). Anal. Calcd for $C_{60}H_{92}B_{36}Co_2NP_4Rh$: C: 46.16, H: 5.94, N: 0.90 %. Found: C: 45.97, H: 5.72, N: 1.10 %. IR: ν (cm^{-1}) = 3059 (C_c-H), 2558 (B-H), 1481, 1435, 1080, 943, 745, 694. ^{1}H NMR: δ = 8.53, 8.05-7.01 (m, 40H, *Ph*), 4.28 (br s, 4H, C_c-*H*), 3.40 (s, 12H, N*Me*$_4$). ^{11}B NMR: δ = 7.5, 3.6, -2.8, -6.5, -13.6, -19.5 (36B). ^{31}P{^{1}H} NMR: δ = 85.16 (d, ^{1}J(^{31}P,^{103}Rh)= 205, PPh_2).

Synthesis of [PdCl{3,3'-Co(1-PPh_2-1,2-$C_2B_9H_{10}$)$_2$}(PPh_3)] (7). [$PdCl_2(PPh_3)_2$] (0.183 g, 0.26 mmol) was added to 10 mL of a solution of [NMe_4][**2**] (0.2 g, 0.26 mmol), in deoxygenated ehanol, and the mixture was refluxed for 1 h. A brown solid was separated by filtering and then washed with ethanol (10 mL) and water, giving **7**. Yield: 270 mg (94%). Anal. Calcd for $C_{46}H_{55}B_{36}ClCoP_3Pd$: C: 50.40, H: 5.06 %. Found: C: 50.76, H: 4.93 %. IR: ν (cm^{-1}) = 3060 (C_c-H), 2563 (B-H), 1435, 1099, 745, 692. ^{1}H NMR: δ = 8.25-7.39 (m, 35H, *Ph*), 4.51 (br s, 1H, C_c-*H*), 4.31 (br s, 1H, C_c-*H*). ^{11}B NMR: δ = 9.7, 5.7, -0.05, -2.1, -3.8, -13.1, -20.9 (18B). ^{31}P{^{1}H} NMR: δ = 60.39 (dd, ^{2}J($P_{PPh2(trans)}$,P_{PPh3})= 238, ^{2}J(P_{PPh2},P_{PPh2})= 70, 1P, PPh_2 in trans to PPh_3), 54.02 (d, ^{2}J(P_{PPh2},P_{PPh2})= 70, 1P, PPh_2 in cis to PPh_3), 30.37 (d, ^{2}J($P_{PPh2(trans)}$,P_{PPh3})= 238, 1P, PPh_3).

Acknowledgment. We thank CICYT for MAT01-1575, Generalitat de Catalunya for 2001/SGR/00337 and CIEMAT for supporting this research.

Supporting information available: Full crystallographic data for the structures of [NMe_4][**2**], **3**·$OCMe_2$, **4** and **5** have been deposited with the Cambridge Crystallographic Data Centre as supplementary publication nos. CCDC-xxx, CCDC-yyy and CCDC-zzz, respectively. Copies of the data can be obtained free of charge on application to CCDC, 12 Union Road, Cambridge CB2 1EZ, UK (fax: (+44)1223-336-033; e-mail: deposit@ccdc.cam.ac.uk).

Notes and references

[1] a) W. S. Knowles, M. J. Sabacky, *Chem. Commun.* **1968**, 1445. b) W. S. Knowles, *Angew. Chem. Int. Ed.* **2002**, *41*, 1998.
[2] L. Horner, H. Siegel, H. Büthe, *Angew. Chem. Int. Ed.* **1968**, *7*, 942.
[3] T. P. Dang, H. B. Kagan, *J. Chem. Soc. Chem. Commun.* **1971**, 481.
[4] a) R. Noyori, *Acc. Chem. Res.* **1990**, *23*, 345. b) R. Noyori, *Tetrahedron* **1994**, *50*, 4259. c) R. Noyori, *Angew. Chem. Int. Ed.* **2002**, *41*, 2008.
[5] H. Brunner, W. Ed. Zettlmeier, *Handbook of Enantioselective Catalysis*, VCH: New York, **1993**.
[6] a) R. Noyori, H. Takaya, *Acc. Chem. Res.* **1990**, *23*, 345. b) H. Takaya, T. Ohta, R. Noyori, In *Catalytic Asymmetric Synthesis*; I. Ed. Ojima, VCH: New York, **1993**. c) R. Noyori, *Asymmetric Catalysis in Organic Synthesis*, Wiley: New York, **1994**.
[7] a) R. Schmid, M. Cereghetti, B. Heiser, P. Schonholzer, H.-J. Hansen, *Helv. Chim. Acta* **1988**, *71*, 897. b) R. Schmid, J. Foricher, M. Cereghetti, P. Schonhoizer, *Helv. Chim. Acta* **1991**, *74*, 370. c) R. Schmid, E. A. Broger, M. Cereghetti, Y. Crameri, J. Foricehr, M. Lalonde, R. K. Muller, M. Scalone, G. Schoettel, U. Zutter, *Pure Appl. Chem.* **1996**, *68*, 131.
[8] Z. Zhang, H. Qian, J. Longmire, X. Zhang *J. Org. Chem.* **2000**, *65(19)*, 6223.
[9] a) P. Lustenberger, E. Martinborough, T. M. Denti, F. Diederich, *J. Chem. Soc., Perkin. Trans. II* **1998**, 747. b) T. Harada, M. Takeuchi, M. Hatsuda, S. Ueda, A. Oku, *Tetrahedron*: *Asymmetry* **1996**, *7*, 2479. c) Lipshutz, B. H.; Shin, Y.-J. *Tetrahedron Lett.* **1998**, 7017.
[10] S. A. Raynor, J. M. Thomas, R. Raja, B. F. G. Johnson, R. G. Bell, M. D. Mantle, *Chem. Commun.* **2000**, 1925.
[11] I. B. Sivaev, V. I. Bregadze, *Collect. Czech. Chem. Commun.* **1999**, *64*, 783.
[12] a) K. T. Wan, M. E. Davis, *J. Catal.* **1994**, *148*, 1. b) Q.-H. Fan, Y.-M. Li, A. S. C. Chan, *Chem. Rev.* **2002**, *102*, 3385.
[13] Sheldrick, G. M. SHELX97. University of Göttingen, Germany, **1997.**
[14] O. Crespo, C. Gimeno, A. Laguna, *J. Chem. Educ.* **2000**, *77*, 86.
[15] Sheldrick, G. M. SHELX97. University of Göttingen, Germany, **1997.**
[16] G. Bandoli, A. Dolmella, *Coord. Chem. Rev.* **2000**, *209*, 161.
[17] a) M. C. Gimeno, P. G. Jones, A. Laguna, C. Sarroca, *J. Chem. Soc. Dalton Trans.* **1995**, 1473. b) A. Miyashita, A. Yasuda, H. Takaya, K. Toriumi, T. Ito, T. Souchi, R. Noyori, *J. Am. Chem. Soc.* **1980**, *201*, 7932. c) A. J. Deeming, D. M. Speel, M. Stchedroff, *Organometallics* **1997**, *16*, 6004.
[18] J. R. Blackburn, R. Nordberg, F. Stevie, R. G. Albrigde, M. M. Jones, *Inorg. Chem.* **1970**, *9*, 2374.

Oxidation and Partial degradation of *closo*-carboranyldiphosphines by using hydrogen peroxide.

Isabel Rojo,[a] Francesc Teixidor,[a] Clara Viñas,[a] Raikko Kivekäs,[b] Reijo Sillanpää[c]

[a]*Institut de Ciència de Materials de Barcelona (ICMAB/CSIC), Campus de la UAB, 08193 Bellaterra, Spain;* [b]*Department of Chemistry, P.O. Box 55, University of Helsinki, FIN-00014, Finland;* [c]*Department of Chemistry, University of Jyväskylä, FIN-40351, Jyväskylä, Finland.*

RECEIVED DATE (automatically inserted by publisher); E-mail:

Introduction

The *o*-carborane 1,2-$C_2B_{10}H_{12}$ is an icosahedral cluster with the two carbon atoms in adjacent positions. One way to comprehend the orbital set of *o*-carborane is to consider that each participating atom contributes with two **sp** and two $\mathbf{p_t}$ (tangential orbital on cluster carbon) orbitals. This situation is very similar to the atomic orbitals participating in the molecular orbitals of acetylene. In the same way, then, the hydrogen atom connected to the cage carbon (C_c) in *o*-carborane is acidic and may be removed by strong bases. Moreover, the *o*-carborane cluster is electron-withdrawing for the C_c substituents. During our research[1,2,3,4,5] we have observed many structural features, as well as reactivity behaviour, that make the *o*-carboranyl fragment unique in organic chemistry. Bidentate ligands have played an important role in the development of catalytic applications of metal organic complexes since 1959.[6] Our group has reported the synthesis of *closo* diphosphines 1,2-$(PR_2)_2$-1,2-$C_2B_{10}H_{10}$ that incorporate the *closo* 1,2-$C_2B_{10}H_{12}$ cluster,[1e] their partial degradation that produces the anionic diphosphine *nido* [7,8-$(PR_2)_2$-7,8-$C_2B_9H_{10}]^-$ ligands[1e] and the coordinating capability towards metals of both *closo* 1,2-$(PR_2)_2$-1,2-$C_2B_{10}H_{10}$ and *nido* [7,8-$(PR_2)_2$-7,8-$C_2B_9H_{10}]^-$ ligands.[7]

Additionally, diphosphine ligands or their chelating Au(I) complexes are active in several tumoral models in mice.[8] Oxidation and protonation reactions are of particular importance in understanding the anticancer activity of diphosphines.[9]

Despite the well-known affinity of trivalent phosphorous for oxygen and the frustrating destruction of metal catalysts via oxidation of phosphorus-containing ligands, there is a lack of kinetic data and mechanistic studies done on this reaction. In this paper, we report the forced oxidation reaction of *closo* 1,2-$(PR_2)_2$-1,2-$C_2B_{10}H_{10}$ (R= Ph, **1**; ^{i}Pr, **2**) compounds to *closo* 1,2-$(OPR_2)_2$-1,2-$C_2B_{10}H_{10}$ and the partial degradation process of these ligands to the anionic *nido* [7,8-$(OPR_2)_2$-7,8-$C_2B_9H_{10}]^-$ ones. The reactions have been monitoring by ^{31}P-NMR and ^{11}B-NMR spectroscopies. The sequence of the reactions has been proven by the crystal resolution of the *nido* [7,8-$(OP^iPr_2)_2$-7,8-$C_2B_9H_{10}]^-$ ligand as well as this for an intermediate. The phosphine oxide formation rate constant for compound **1** has also been calculated.

Results and discussion

I. Forced Oxidation of *closo*-carboranyldiphosphines, 1,2-$(PR_2)_2$-1,2-$C_2B_{10}H_{10}$. Synthesis and characterization of *closo*-1,2-$(OPR_2)_2$-1,2-$C_2B_{10}H_{10}$.

We had observed that, in contrast to other common phosphines, the *closo*-monophosphinocarborane 1-PR_2-2-R'-$C_2B_{10}H_{10}$ (R' = H, Me, Ph; R = Ph, Et, ^{i}Pr) derivatives present a high stability both in solid state and in solution, even under air, in the presence of mild oxidizing agents, alcohols and some acids.[1a] The behaviour of the *closo*-diphosphinocarboranes towards partial degradation,[1e] their high chemical stability both in solution and solid state and the difficulty to coordinate to metal[7g-i] seems to evidence the notable influence of the cluster *closo* on the P atoms. So, *closo*-carboranyldiphosphines have been forced to be oxidized to their corresponding *closo*-carboranyldiphosphine oxides by using hydrogen peroxide in acetone[10] (Scheme 1, i). In the oxidized species, the phosphorus oxidation state has changed from P(III) to P(V).

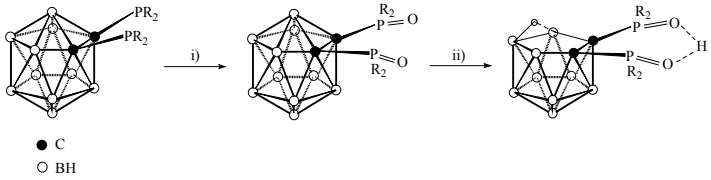

Scheme 1. Reaction of 1,2-$(PPh_2)_2$-1,2-$C_2B_{10}H_{10}$ with H_2O_2 in acetone. i) Phosphines oxidation. ii) *Closo* cluster partial degradation and zwitterion formation. R= Ph, ^{i}Pr.

The *closo* 1,2-$(OPR_2)_2$-1,2-$C_2B_{10}H_{10}$ (R= Ph, **3**; R= ^{i}Pr, **4**) diphosphine dioxide species have been synthesized and characterized by IR, ^{1}H-, ^{13}C-, ^{31}P- and ^{11}B-NMR spectroscopies. Only one singlet resonance at lower field than the corresponding diphosphine one in the starting (see Table 1) was observed in the ^{31}P-NMR spectra for **3** and **4**.

Table 1. ^{31}P{^{1}H}-NMR chemical shifts (ppm) for the carboranyldiphosphines.

1,2-$(PPh_2)_2$-1,2-$C_2B_{10}H_{10}$	8.22[11]
1,2-$(OPPh_2)_2$-1,2-$C_2B_{10}H_{10}$	23.67
1,2-$(P^iPr_2)_2$-1,2-$C_2B_{10}H_{10}$	32.79[1e]
1,2-$(OP^iPr_2)_2$-1,2-$C_2B_{10}H_{10}$	59.08
$[NMe_4][7,8\text{-}(PPh_2)_2\text{-}7,8\text{-}C_2B_9H_{10}]$	7.13[1e]
$[NMe_4][7,8\text{-}(OPPh_2)_2\text{-}7,8\text{-}C_2B_9H_{10}]$	29.33
$H[7,8\text{-}(OPPh_2)_2\text{-}7,8\text{-}C_2B_9H_{10}]$	47.09
$H[7,8\text{-}(P^iPr_2)_2\text{-}7,8\text{-}C_2B_9H_{10}]$	31.04
$H[7,8\text{-}(OP^iPr_2)_2\text{-}7,8\text{-}C_2B_9H_{10}]$	77.31

The ν(B-H) in the IR spectrum at 2555 cm^{-1} for **3** and at 2644, 2622, 2596, 2575, 2550 cm^{-1} for **4** are in agreement with a *closo* structure for the cluster fragment. The vibration at 1214 cm^{-1} for **3** and at 1192 cm^{-1} for **4** confirm the presence of P=O group in

the molecules. The ^{11}B-NMR spectra for compounds **3** and **4**, with a 2:2:6 pattern in the range +2.8 / –9.1 ppm, fully supports a *closo* structure. Just minor differences with regard to the *closo* 1,2-$(PR_2)_2$-1,2-$C_2B_{10}H_{10}$ precursors (see Figure 1) have been observed in the ^{11}B-NMR spectra of the new diphosphine dioxides 1,2-$(OPR_2)_2$-1,2-$C_2B_{10}H_{10}$. It is worth noticing, though, that the resonance corresponding to the antipodal boron atoms (B9 and B12) in **3** and **4** has been shifted to lower field with regard to the non oxidized starting ones. The ^{1}H-NMR spectrum of **3** shows two different multiplet resonances at 7.52 and 8.03 ppm which indicate two phenyl rings in each $–PPh_2$ group. The two doublets of doublets in the ^{1}H-NMR spectrum of **4** evidence two non-equivalent methyl groups in each isopropyl unit. The coupling between ^{31}P and ^{13}C nuclei is clearly observed in the ^{13}C{^{1}H}-NMR spectrum of **4**. This shows two different resonances at 17.4 and 18.4 ppm, in agreement with two different methyl groups in each isopropyl unit. The –CH resonance appears as a doublet (^{1}J(P,C)= 61 Hz) at 30.5 ppm and the doublet (^{1}J(P,C)= 19 Hz) at 81.6 ppm corresponds to the carbon cluster atoms (C_c).

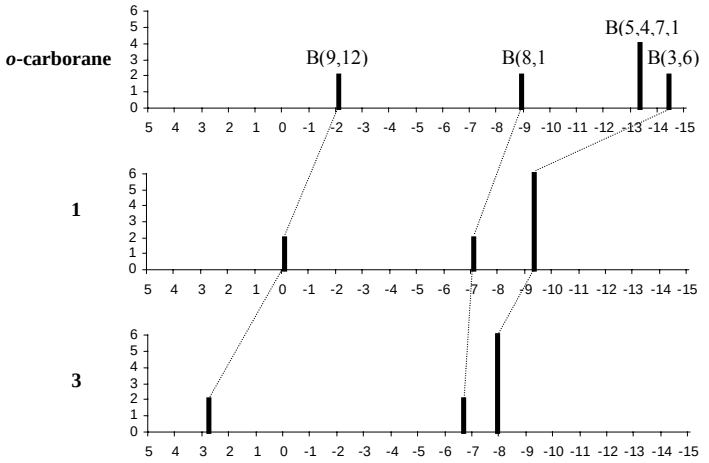

Figure 1. Stick representation of the chemical shifts and relative intensities in the ^{11}B{^{1}H}-NMR spectra of compounds *closo* 1,2-$C_2B_{10}H_{12}$ (*o*-carborane); *closo* 1,2-$(PPh_2)_2$-1,2-$C_2B_{10}H_{10}$ (**1**) and *closo* 1,2-$(OPPh_2)_2$-1,2-$C_2B_{10}H_{10}$ (**3**). Lines join equivalent positions in the three compounds.

II. Partial cluster degradation of the *closo*-carboranyldiphosphine dioxides, 1,2-$(OPR_2)_2$-1,2-$C_2B_{10}H_{10}$. Synthesis and characterization of *nido* [7,8-$(OPR_2)_2$-7,8-$C_2B_9H_{10}]^-$ ligands.

Partial degradation of *closo*-diphosphinocarboranes using the well established procedure[12] with alkoxyde did not produce the expected new *nido* species, instead it yielded 7,8-dicarba-*nido*-undecaborate(1-) by C-P bond cleavage. On the other hand, the reaction carried out in refluxing ethanol in the absence of alkoxyde yielded the *closo*-diphosphinocarboranes unaltered, as it was also the case with piperidine-toluene[13] in 1:4 ratio of *closo*-diphosphinocarboranes to piperidine at 20 ºC. Boron removal to yield the *nido* species while preserving the C_c-P bond was successfuly obtained in a 99% yield by reaction of 1,2-$(PR_2)_2$-1,2-$C_2B_{10}H_{10}$ with piperidine in ethanol in a ratio 1:10.[1e]

We later demonstrated that proton can induce partial degradation, thence conversion of the *closo*-C_2B_{10} to the *nido*-C_2B_9 species given the necessary chemical and geometrical arrangements to produce proton chelation.[14] For this purpose, an *o*-carborane adequately C-disubstituted with H^+ scavenger elements, such as oxygen was used. The *closo* 1,2-$(OPR_2)_2$-1,2-$C_2B_{10}H_{10}$ species (**3**, **4**) did fulfill these requirements as are chelating agents and contain oxygen atoms. Hydrogen peroxide which has recently[15] been used to produce *closo*-$[B_{12}(OH)_{12}]^{2-}$ was a suitable oxidizing agent, and a source of H^+. Thus it was expected that upon oxidation of the phosphorus atoms, and the availability of protons, the *closo* cluster would progress to the anionic *nido* cluster [7,8-$(OPR_2)_2$-7,8-$C_2B_9H_{10}]^-$ (R= Ph, [**5**]$^-$, R= ^{i}Pr, [**6**]$^-$) liberating one boron atom and overall producing a neutral species. Indeed this is what happened. The reaction is schematically represented in Scheme 1 ii).

The *nido* nature of the cluster was clearly demonstrated in the ^{1}H-NMR by the apical proton resonance at δ –2.05 and –2.56 ppm for compounds H[**5**] and H[**6**] respectively, and by the ^{11}B-NMR, 2:2:1:2:1:1 pattern (low field to high field) observed in the range δ –5.6/-33.9 typical for *nido*-C_2B_9 derivatives.[16] The resonances were separated enough to permit their unambiguous assignment by means of ^{11}B{^{1}H} -^{11}B{^{1}H} COSY (see Figure 2). The peak at –29.1 ppm is easily assigned to B(10) since it appears as a doublet of doublets in the ^{11}B-NMR spectrum due to coupling with the H bridge as well as the *exo*-H. The peak at –31.8 ppm, which is at highest field, corresponds to B(1), the antipodal position to the open face. The spectrum also exhibits a singlet at –14.0 ppm that do not show any cross peak and correspond to B(3) which is adjacent to both cluster carbon atoms.[17] With the resonances due to B(1), B(3) and B(10) thus established, analysis of the cross peaks easily allowed the assignment of the 2:2:1:2:1:1 pattern to B(9,11): B(5,6): B(3): B(2,4): B(10): B(1), respectively.

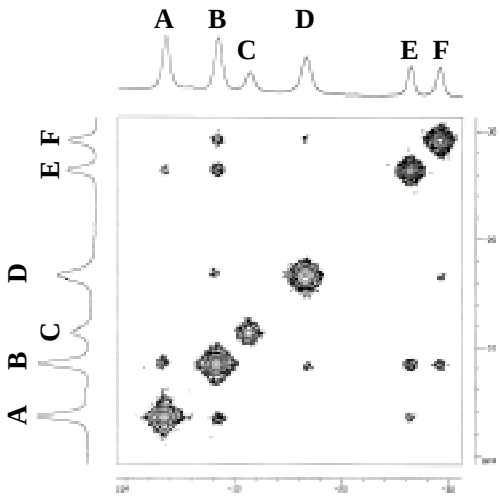

Figure 2. The ^{11}B{^{1}H}-^{11}B{^{1}H} 2D-COSY NMR spectrum of H[**6**]. The resonance marked **A** corresponds to B(9, 11), **B** to B(5, 6), **C** to B(3), **D** to B(2, 4), **E** to B(10), **F** to B(1).

Although the negative charge of the *nido* cluster is maintained in the oxidized species, the phosphorus oxidation state has changed from P(III) to P(V). This is clearly reflected on the ^{31}P{^{1}H}-NMR spectra (Table 1) in which the chemical shifts for the oxidized species have shifted to lower field as much as 46 ppm.

The ν(B-H) in the IR spectra at 2605, 2584, 2526 cm^{-1} for H[**5**] and at 2629-2608 cm^{-1} for H[**6**] are in agreement with a *nido* structure of the *o*-carboranyl fragment and the vibration at 1184 and 1081 cm^{-1} respectively confirm the presence of P=O groups.

To ensure that H_2O_2 was the sole agent causing the *closo* to *nido* conversion, an alternative sequential process was developed, which is indicated in Scheme 2. Oxidation of [NMe_4][7,8-

$(PPh_2)_2$-7,8-$C_2B_9H_{10}$], ([NMe_4][**7**]),[14] with H_2O_2 was performed in acetone at 0ºC to yield after stirring for 4 h a white solid that corresponds to [NMe_4][7,8-$(OPPh_2)_2$-7,8-$C_2B_9H_{10}$], [NMe_4][**8**].

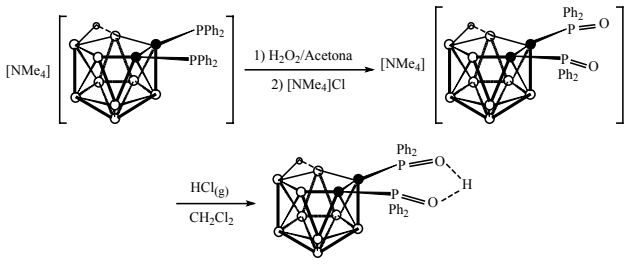

Scheme 2. Synthesis of H[7,8-$(OPPh_2)_2$-7,8-$C_2B_9H_{10}$] starting from [NMe_4][7,8-$(PPh_2)_2$-7,8-$C_2B_9H_{10}$].

III. Identification of the removed Boron vertex.

The partial degradation of **1** with hydrogen peroxide in THF and at room temperature for 24 hours was carried out to identify the nature of the removed B^+ containing species. The H[**5**] species was isolated by filtration. The $^{11}B\{^1H\}$ spectrum of the remaining aquous solution shows a resonance at +19.3 ppm corresponding to a boron atom with no B-H bond. According to the literature, the chemical shift for $B(OH)_3$ appears at +19.3 ppm,[18] confirming that the removed B^+ stays in solution as $B(OH)_3$.

IV. Forced protonation of the *nido*-carboranyldiphosphine dioxides.

As it is well known, phosphines react with perchloric acid in ethanol to give the corresponding phosphonium salts.[19] Acidification of [NMe_4][**8**] in CH_2Cl_2 with HCl gas produces a white solid corresponding to [NMe_4]Cl. Subsequent evaporation of the CH_2Cl_2 yields a H[**5**].

The ν(O-H) in the IR spectra at 3082 and 3059 cm^{-1} confirmed the formation of the protonated zwitterionic species. This IR data could not be further supported by the observation of a resonance attributed to the chelated proton neither in the ^1H-NMR spectra of H[**5**] nor H[**6**]. To get a precise structure determination, crystals were grown from an acetone solution of H[**6**] after slow evaporation.

V. Molecular and crystal structure of H[6]

Good quality crystals for X-Ray diffraction studies were grown by slow evaporation of compound H[**5**] in EtOH solutions and by slow evaporation of H[**6**] in acetone (Figure 3).

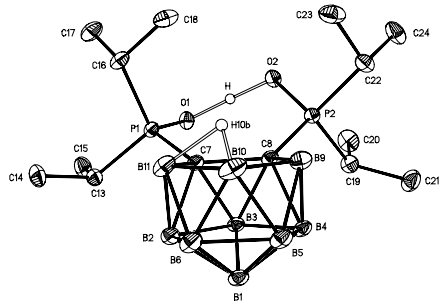

Figure 3. Perspective drawings of H[7,8-$(OP^iPr_2)_2$-7,8-$C_2B_9H_{10}$] grown from compound **6** in acetone.

VI. Mechanistic considerations

The reaction of *closo*-carboranyldiphosphines 1,2-$(PR_2)_2$-1,2-$C_2B_{10}H_{10}$ (R= Ph and ^{i}Pr) with H_2O_2 implies two processes: the partial degradation of the *closo* cluster and the oxidation of the phosphorus atoms. The progress of the reaction has been studied as a function of time to determine which process takes place first. In this sense, the progress of the reaction of both *closo* species **1** and **2** with H_2O_2 was monitored by $^{31}P\{^1H\}$(see Figure 4 for **1** and Figure 5 for **2**) and $^{11}B\{^1H\}$-NMR (see Figure 6 for **1**) spectroscopies. The study provides useful information about the structure of the compounds in solution. The resonance at 8.22 ppm in the $^{31}P\{^1H\}$-NMR spectrum that corresponds to non-altered **1** decreases with time while a new peak at 23.67 ppm increases (See Figure 4). In four hours there is no starting compound left while only the peak at 23.67 ppm is observed. The latter resonance also decreases with time while a new one at 47.09 ppm emerges. This final resonance persists indefinitely. The $^{11}B\{^1H\}$-NMR spectra also shows the process of conversion of the starting *closo* material into a *nido* species (See Figure 6) but is not as informative as the $^{31}P\{^1H\}$-NMR. The peak at 47.09 ppm in the $^{31}P\{^1H\}$-NMR spectrum corresponds to the end species H[7,8-$(OPPh_2)_2$-7,8-$C_2B_9H_{10}$]. Definitive proof of the proton containing P-O-H-O-P moiety has been confirmed by X-ray diffraction.

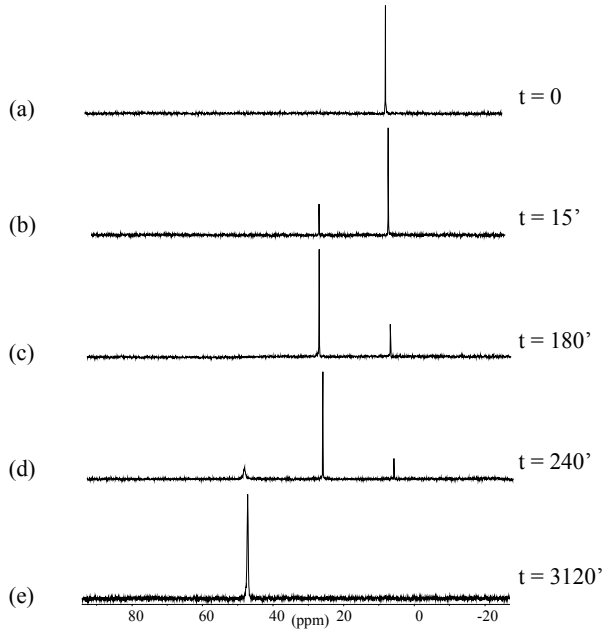

Figure 4. $^{31}P\{^1H\}$ spectra of the *closo* 1,2-$(PPh_2)_2$-1,2-$C_2B_{10}H_{10}$ showing its conversion to *nido* H[7,8-$(OPPh_2)_2$-7,8-$C_2B_9H_{10}$] after *closo* 1,2-$(OPPh_2)_2$-1,2-$C_2B_{10}H_{10}$ formation.

If the reaction is quenched when the peak at 23.67 ppm in the $^{31}P\{^1H\}$-NMR is the dominant one important information about the nature of the intermediate species is obtained. The $^{11}B\{^1H\}$-NMR spectrum indicates that the cluster is *closo*, which is also supported by the lack of hydrogen bridge in the $^{11}H\{^1B\}$-NMR spectrum. The elemental analysis is in agreement with a *closo* species with two P(O) units. All these data demonstrate that the first step of the reaction is the phosphorus oxidation with cluster preservation and the second one is cluster decapitation at it is shown in Scheme 1.

This mechanistic study allows accurate determination of the time to complete the two steps of the reaction: phosphorus

oxidation and cluster partial degradation. In the case of 1,2-$(PPh_2)_2$-1,2-$C_2B_{10}H_{10}$ 4 hours are necessary to accomplish the formation of both P-O bonds while the cluster partial degradation of 1,2-$(OPPh_2)_2$-1,2-$C_2B_{10}H_{10}$ into H[7,8-$(OPPh_2)_2$-7,8-$C_2B_9H_{10}$] is essentially done after 52 hours. It is then clear that the slow step of the total process is the cluster partial degradation.

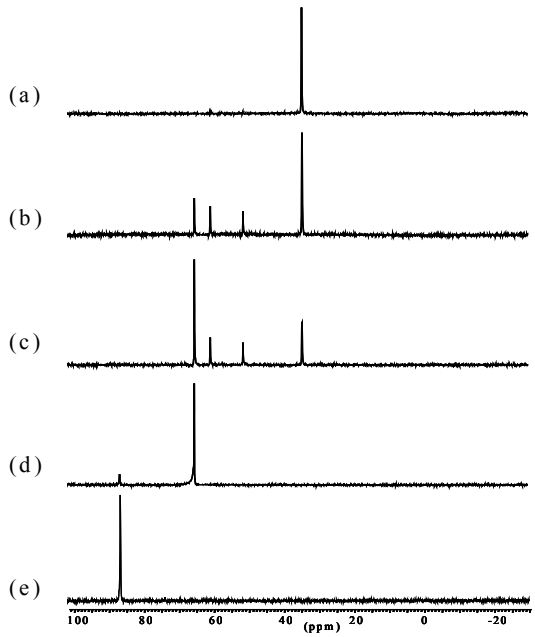

Figure 5. $^{31}P\{^1H\}$ spectra of the *closo* 1,2-$(P^iPr_2)_2$-1,2-$C_2B_{10}H_{10}$ showing its conversion to *nido* H[7,8-$(OP^iPr_2)_2$-7,8-$C_2B_9H_{10}$] after *closo* 1,2-$(OP^iPr_2)_2$-1,2-$C_2B_{10}H_{10}$ formation.

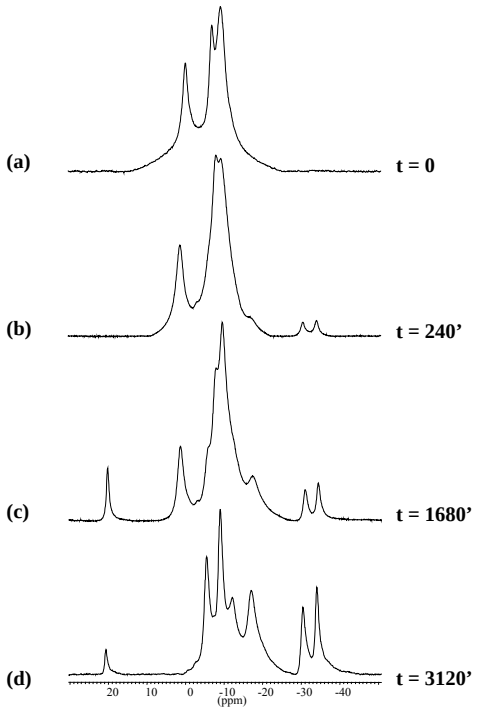

Figure 6. $^{11}B\{^1H\}$ spectra of the *closo* 1,2-$(OPPh_2)_2$-1,2-$C_2B_{10}H_{10}$ showing its partial degradation to *nido* H[7,8-$(OPPh_2)_2$-7,8-$C_2B_9H_{10}$].

When the H_2O_2 reaction study was done on 1,2-$(P^iPr_2)_2$-1,2-$C_2B_{10}H_{10}$, resonances at 33.27, 47.20, 55.08, 59.08, 65.48 and 77.31 ppm were observed in the $^{31}P\{^1H\}$-NMR spectra. There were three additional resonances on top of the awaited ones. The resonance at 33.27 corresponds to the starting *closo* compound **2**, the one at 59.08 corresponds to the *closo* compound **4** and the one at 77.31 to the *nido* compound **6**. Therefore it seems that the extra resonances at 47.20, 55.08 and 65.48 ppm, might be attributed to other intermediate species. One interpretation is that the two phosphorus atoms are not oxidized at the same time and a *closo* species containing a P(III) atom and P(V) is obtained which would possibly account for the resonances at 55.08 and 47.20 ppm. The additional resonance could correspond to the equivalent phosphorus in the H^+ bonded P-O-H-O-P *closo* species, just the previous step to B^+ removal and zwitterions. The crystal structure shown in Figure 7 fully supports this theory.

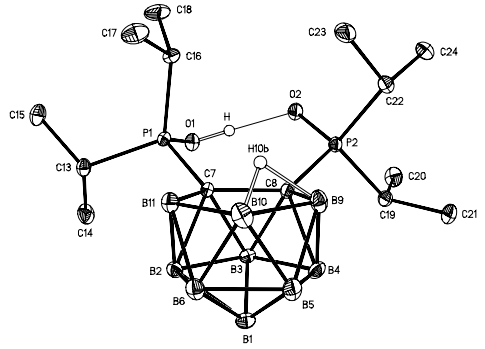

Figure 7. Perspective drawings of H[7,8-$(OP^iPr_2)_2$-7,8-$C_2B_9H_{10}$] grown in $OCMe_2$.

The mechanistic study shows that **2** is fully oxidized to compound **4** after 15 minutes. So, *closo* 1,2-$(P^iPr_2)_2$-1,2-$C_2B_{10}H_{10}$ is more susceptible to oxidation than *closo* 1,2-$(PPh_2)_2$-1,2-$C_2B_{10}H_{10}$ which is foreseeable considering the greater donating character of the isopropyl group.

VII. Kinetics of formation of 1,2-$(OPPh_2)_2$-1,2-$C_2B_{10}H_{10}$

The P(III) to P(V) oxidation reaction study on both *closo* specie **1** and **2** by using H_2O_2 in acetone or tetrahydrofurane at 23°C was monitored by $^{31}P\{^1H\}$ (see Figure 4 for **1** and Figure 5 for **2**) and $^{11}B\{^1H\}$-NMR (see Figure 6 for **1**) spectroscopies. The reaction was found to be first-order rate constant with respect to concentration of 1,2-$(PPh_2)_2$-1,2-$C_2B_{10}H_{10}$. The calculated rate constant is $(1.23 \pm 0.09) \times 10^{-4}$ s^{-1} (Figure 8, 9).

Conclusions

The carborane influence into the directly connected phosphorus atom is not only perceived in the chemical shift but also in the chemical properties. The electron-acceptor character of the cluster induces a lower charge density in the phosphorus atom which causes the P resonance to be shifted at lower field in the ^{31}P-NMR spectra. In addition, it makes the ligand to have a lower coordinating capacity towards transition metals and a higher stability in solid state and in solution, even under air. An influence of the R group in *closo* 1,2-$(PR_2)_2$-1,2-$C_2B_{10}H_{10}$ compounds has also been recognized. In this sense, an electron donating group (^{i}Pr) facilitates the oxidation reaction more than an electron withdrawing group (Ph).

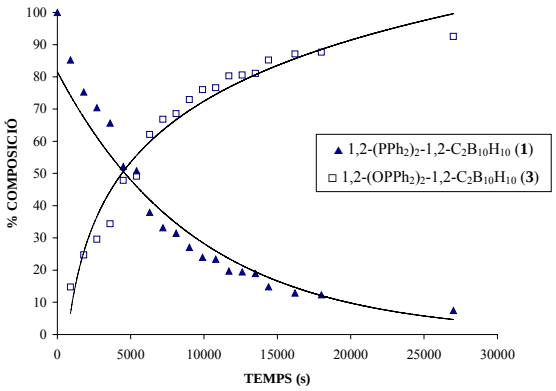

Figure 8. Plot of material balance vs. time for the reaction between *closo* 1,2-$(PPh_2)_2$-1,2-$C_2B_{10}H_{10}$ and *closo* 1,2-$(OPPh_2)_2$-1,2-$C_2B_{10}H_{10}$.

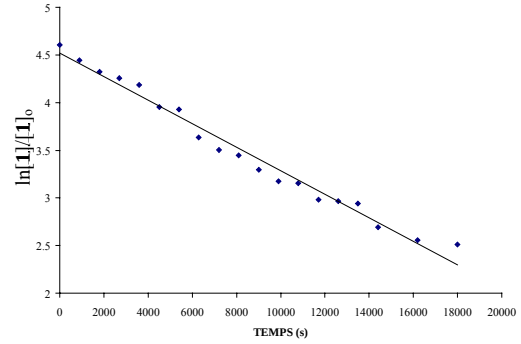

Figure 9. First-order kinetic plot for the reaction between *closo* 1,2-$(PPh_2)_2$-1,2-$C_2B_{10}H_{10}$ and *closo* 1,2-$(OPPh_2)_2$-1,2-$C_2B_{10}H_{10}$.

Experimental Section

Instrumentation. Elemental analyses were performed in our laboratory using a Carlo Erba EA1108 microanalyzer. IR spectra (ν, cm^{-1}; KBr pellets) were obtained on a Shimadzu FTIR-8300 spectrophotometer. The ^{1}H- and $^1H\{^{11}B\}$-NMR (300.13 MHz), $^{13}C\{^1H\}$-NMR (75.47 MHz), ^{11}B-NMR (96.29 MHz) and $^{31}P\{^1H\}$-NMR (121.48 MHz) spectra were recorded on a Bruker ARX 300 instrument equipped with the appropriate decoupling accessories. All NMR spectra were performed in deuterated solvents at 22 ºC. The ^{11}B-NMR shifts were referenced to external $BF_3{\cdot}OEt_2$, while the ^{1}H, $^1H\{^{11}B\}$, and $^{13}C\{^1H\}$-NMR shifts were referenced to $SiMe_4$ and the $^{31}P\{^1H\}$-NMR to external 85% H_3PO_4. Chemical shifts are reported in units of parts per million downfield from reference, and all coupling constants in Hz.

Materials. All manipulations were carried out under atmosphere. THF was distilled from sodium benzophenone prior to use. EtOH was dried over molecular sieves and deoxygenated prior to use. Reagents were obtained commercially and used as purchased. 1,2-Bis(diphenylphosphino)-1,2-dicarba-*closo*-dodecaborane[20] and 1,2-bis(diisopropylphosphino)-1,2-dicarba-*closo*-dodecaborane[1e] were prepared from *o*-carborane according to the literature.

Synthesis of 1,2-$(OPPh_2)_2$-1,2-$C_2B_{10}H_{10}$ (3). To a round bottom flask (25 mL) containing 1,2-bis(difenilfosfino)-1,2-dicarba-*closo*-dodecaborà (50 mg, 0.10 mmol) was added tetrahydrofuran (5 mL). The mixture was cooled (ice-water) during the dropwise addition of a 0.2 M solution of H_2O_2 (1.5 mL, 0.40 mmol). After stirring for 3h and 25 min at room temperature the solvent was removed. The evaporation of the solvent yield a white solid. Yield: 48 mg (98 %). Anal. Calcd for $C_{26}H_{30}B_{10}O_2P_2$: C: 57.34, H: 5.55 %. Found: C: 57.12, H: 5.80 %. FTIR: 3048, 2962 (C_{aryl}-H), 2555 (B-H), 1214, 1191 (P=O). ^{1}H NMR ($CDCl_3$) δ: 8.03 (m, 10H, Ph), 7.52 (m, 10H, Ph), 2.68-2.09 (br m, 10H, B-H). $^1H\{^{11}B\}$ NMR ($CDCl_3$): 8.03 (m, 10H, Ph), 7.52 (m, 10H, Ph), 2.68 (br s, 2H, B-H), 2.49 (br s, 1H, B-H), 2.35 (br s, 2H, B-H), 2.30 (br s, 3H, B-H), 2.09 (br s, 2H, B-H). $^{13}C\{^1H\}$ NMR ($CDCl_3$) δ: 132.58 (d, ^{2}J(C,P)= 8, Ph), 132.27, 130.80, 129.33 (s, Ph), 128.25 (d, ^{2}J(C,P)= 14, Ph). ^{11}B-NMR ($CDCl_3$) δ: 2.8 (d, ^{1}J(B,H)= 88, 2B), -6.7 (4B), -7.9 (4B). $^{31}P\{^1H\}$-NMR ($CDCl_3$) δ: 23.67 (s, $OPPh_2$).

Synthesis of 1,2-$(OP^iPr_2)_2$-1,2-$C_2B_{10}H_{10}$ (4). To a round bottom flask (25 mL) containing 1,2-bis(diisopropilfosfino)-1,2-dicarba-*closo*-dodecaborà (50 mg, 0.13 mmol) was added tetrahydrofuran (5 mL). The mixture was cooled (ice-water) during the dropwise addition of a 0.2 M solution of H_2O_2 (2.0 mL, 0.40 mmol). After stirring for 40 min at room temperature the solvent was removed. The evaporation of the solvent yield a white solid. Yield: 54 mg (99 %). Anal. Calcd for $C_{14}H_{38}B_{10}O_2P_2$= C: 41.16, H: 9.38 %. Found: C: 41.04, H: 9.25 %. FTIR: 2996, 2970, 2933, 2878 (C-H_{alkyl}), 2644, 2622, 2596, 2575, 2550 (B-H), 1192 (P=O). ^{1}H NMR ($CDCl_3$) δ: 3.10 (br s), 2.02 (m, 4H, CH), 1.41 (dd, ^{3}J(P,H)= 11, ^{3}J(H,H)= 7, 12H, Me), 1.35 (dd, ^{3}J(P,H)= 13, ^{3}J(H,H)= 7, 12H, Me). $^{13}C\{^1H\}$ NMR ($CDCl_3$) δ: 81.61 (d, ^{1}J(C,P)= 19, C_c), 30.53 (d, ^{1}J(C,P)= 61, CH), 17.4 (s, Me), 18.4 (s, Me). ^{11}B NMR ($CDCl_3$) δ: 2.8 (d, ^{1}J(B,H)= 140, 2B, B(9,12)), -6.5 (d, ^{1}J(B,H)= 211, 2B, B(8,10)), -9.1 (d, ^{1}J(B,H)= 138, 6B, B(3,4,5,6,7,11)). ^{31}P NMR ($CDCl_3$) δ: 59.08 (d, ^{3}J(P,H)= 16, OP^iPr_2).

Synthesis of H[7,8-$(OPPh_2)_2$-7,8-$C_2B_9H_{10}$] (5). Procedure a: A solution of [NMe_4][7,8-$(OPPh_2)_2$-7,8-$C_2B_9H_{10}$] (1.0 g, 1.64 mmol) in CH_2Cl_2 (50 mL) was bubbled with a HCl stream for 15 min. A precipitate of [NMe_4]Cl was separated, and the solution was evaporated in vacuo. A white solid was obtained. Yield: 0.86 g (98 %). **Procedure b**: To a solution of [1,2-$(PPh_2)_2$-1,2-$C_2B_{10}H_{10}$] (0.1 g, 0.20 mmol) in THF at 0ºC was added 5.56 mL (0.56 mmol) of a solution of 0.1 M H_2O_2. The mixture was stirred for 24 hours, and a precipitate was formed. The solid was filtered off, washed with water, and dried in vacuo. Yield: 0.10 g (94 %). Anal. Calcd for $C_{26}H_{31}B_9O_2P_2$: C: 58.40, H: 5.84 %. Found: C: 58.22, H: 5.78 %. FTIR: 3082, 3059 (O-H), 3016, 2961, 2918 (C-H_{aryl}), 2605, 2584, 2526 (B-H), 1184 (P=O). ^{1}H NMR ($CDCl_3$): 7.91 (m, 5H, Ph), 7.51 (m, 5H, Ph), 7.38 (m, 5H, Ph), 7.20 (m, 5H, Ph), 3.10-0.74 (br s, 9H, B-H), -2.05 (br s, 1H, BHB). $^1H\{^{11}B\}$ NMR ($CDCl_3$) δ: 7.91 (m, 5H, Ph), 7.51 (m, 5H, Ph), 7.38 (m, 5H, Ph), 7.20 (m, 5H, Ph), 3.10 (br s, 1H, B-H), 2.65 (br s, 1H, B-H), 1.84 (br s, 3H, B-H), 1.07 (br s, 3H, B-H), 0.74 (br s, 1H, B-H), -2.10 (br s, 1H, BHB). $^{13}C\{^1H\}$ NMR ($CDCl_3$) δ: 133.95, 133.82 (s, Ph), 133.05 (d, ^{1}J(P,C)= 21, Ph), 129.18 (d, ^{2}J(P,C)= 41, Ph). ^{11}B NMR ($CDCl_3$) δ: -5.6 (d, ^{1}J(B,H)= 128, 2B), -8.9 (d, ^{1}J(B,H)= 133, 2B), -12.1 (1B), -17.0 (2B), -30.4 (d, ^{1}J(B,H)= 123, 1B), -33.9 (d, ^{1}J(B,H)= 147, 1B). $^{31}P\{^1H\}$ NMR ($CDCl_3$) δ: 47.09 (s, $OPPh_2$).

Synthesis of H[7,8-$(OP^iPr_2)_2$-7,8-$C_2B_9H_{10}$] (6). To a solution of 1,2-bis(diisopropilfosfino)-1,2-dicarba-*closo*-dodecaborà (50 mg, 0.13 mmol) in THF at 0ºC was added 2.0 mL (0.40 mmol) of a solution of 0.2 M H_2O_2. The mixture was stirred during a weekend. Acetone (8mL) was added to the white solid and 2.4 mL (0.96 mmol) of a solution of 0.4 M H_2O_2 were added at room temperature. The solution was stirred for another weekend. Then this was concentrated until a white solid precipitated. The solid was filtered off and dried in vacuo. Yield: 38 mg (71 %). Anal. Calcd for $C_{14}H_{39}B_9O_2P_2$: C: 42.17, H: 9.86 %. Found: C: 41.82, H: 10.04 %. FTIR: 2995, 2973, 2936, 2877 (O-H, C-

H_{alkyl}), 2629, 2596, 2587, 2581, 2543, 2552, 2536, 2526, 2608 (B-H), 1081 (P=O). ^{1}H NMR (CD_3COCD_3) δ: 2.82 (m, 2H, CH), 2.59 (m, 2H, CH), 1.47 (dd, ^{3}J(P,H)= 11, ^{3}J(H,H)= 7, 6H, Me), 1.42 (dd, ^{3}J(P,H)= 11, ^{3}J(H,H)= 7, 6H, Me), 1.37 (dd, ^{3}J(P,H)= 17, ^{3}J(H,H)= 7, 6H, Me), 1.31 (dd, ^{3}J(P,H)= 15, ^{3}J(H,H)= 7, 6H, Me), 2.49-0.68 (br s, 9H, B-H), -2.56 (br s, 1H, BHB). ^{1}H{^{11}B} NMR (CD_3COCD_3) δ: 2.82 (m, 2H, CH), 2.59 (m, 2H, CH), 2.49 (br s, 1H, B-H), 2.42 (br s, 1H, B-H), 1.77 (br s, 2H, B-H), 1.61 (br s, 3H, B-H), 1.47 (dd, ^{3}J(P,H)= 11, ^{3}J(H,H)= 7, 6H, Me), 1.42 (dd, ^{3}J(P,H)= 11, ^{3}J(H,H)= 7, 6H, Me), 1.37 (dd, ^{3}J(P,H)= 17, ^{3}J(H,H)= 7, 6H, Me), 1.31 (dd, ^{3}J(P,H)= 15, ^{3}J(H,H)= 7, 6H, Me), 0.68 (br s, 2H, B-H), -2.56 (br s, 1H, BHB). ^{13}C{^{1}H} NMR (CD_3COCD_3) δ: 16.78, 16.71, 16.67, 16.31, 16.21 (s, CH, Me). ^{11}B NMR (CD_3COCD_3): -6.2 (d, ^{1}J(B,H)= 138, 2B, B(9,11)), -11.1 (d, ^{1}J(B,H)= 142, 2B, B(5,6)), -14.0 (d, ^{1}J(B,H)= 169, 1B, B(3)), -19.4 (d, ^{1}J(B,H)= 155, 2B, B(2,4)), -29.1 (dd, ^{1}J(B,H)= 138, ^{1}J(B,H)= 30, 1B, B(10)), -31.8 (d, ^{1}J(B,H)= 143, 1B, B(1)). ^{31}P{^{1}H} NMR (CD_3COCD_3) δ: 77.31 (s, OP^{i}Pr$_2$).

Synthesis of [NMe_4][7,8-($OPPh_2$)$_2$-7,8-$C_2B_9H_{10}$] (8). To a solution of [NMe_4][7,8-(PPh_2)$_2$-7,8-$C_2B_9H_{10}$] (0.5 g, 0.87 mmol) in acetone (15 mL) at 0ºC was added dropwise 17.4 mL (1.74 mmol) of a solution of 0.1 M in H_2O_2. The mixture was stirred for 4 hours at room temperature and then an aqueous solution with an excess of [NMe_4]Cl was added to precipitate the white product. This was filtered off, washed with water (3x10 mL) and dried in vacuo. Yield: 0.39 g (74 %). Anal. Calcd for $C_{30}H_{42}B_9NO_2P_2$: C: 59.27, H: 6.96, N: 2.30 %. Found: C: 58.95, H: 7.00, N: 2.45 %. FTIR: 3019 (C-H_{aryl}), 2959 (C-H_{alkyl}), 2535 (B-H), 1183 (P=O). ^{1}H NMR (CD_3COCD_3) δ: 7.91-7.23 (m, 20H, Ph), 3.43 (s, 12H, NMe_4), 2.84-0.42 (br m, 9H, B-H), -1.95 (br s, 1H, BHB). ^{1}H{^{11}B}-NMR (CD_3COCD_3) δ: 7.91-7.23 (m, 20H, Ph), 3.43 (s, 12H, NMe_4), 2.84 (br s, 2H, B-H), 2.33 (br s, 1H, B-H), 1.59 (br s, 2H, B-H), 1.20 (br s, 2H, B-H), 0.88 (br s, 1H, B-H), 0.42 (br s, 1H, B-H), -1.95 (br s, 1H, BHB). ^{13}C{^{1}H} NMR (CD_3COCD_3) δ: 137.72 (d, ^{1}J(C,P)= 87, Ph), 136.34 (d, ^{1}J(C,P)= 88, Ph), 132.53 (s, *p*-Ph), 132.01 (s, *p*-Ph), 129.63 (d, ^{2}J(C,P)= 25, *o*-Ph), 126.82 (s, *m*-Ph), 126.21 (s, *m*-Ph), 54.89 (s, NMe_4). ^{11}B NMR (CD_3COCD_3) δ: -5.6 (d, ^{1}J(B,H)= 119, 2B), -11.1 (d, ^{1}J(B,H)= 133, 3B), -19.0 (d, ^{1}J(B,H)= 111, 2B), -32.2 (d, ^{1}J(B,H)= 142, 1B), -34.0 (d, ^{1}J(B,H)= 150, 1B). ^{31}P{^{1}H} NMR (CD_3COCD_3): 29.33 (s, $OPPh_2$).

Acknowlegment. We thank ENRESA for the partial support of this research and MCyT (MAT01-1575), and Generalitat de Catalunya 2001/SGR/00337.

Notes and references

(1) (a) Núñez, R.; Viñas, C.; Teixidor, F.; Sillanpää, R.; Kivekäs, R. *J. Organomet. Chem.* **1999**, *592*, 22. (b) McWhannell, M. A.; Rosair, G. M.; Welch, A. J.; Teixidor, F.; Viñas, C. *Acta Cryst. C52* **1996**, 3135. (c) Kivekäs, R.; Teixidor, F.; Viñas, C.; Núñez, R. *Acta Cryst. C51* **1995**, 1868. (d) Kivekäs, R.; Sillanpää, R.; Teixidor, F.; Viñas, C.; Núñez, R.; Abad, M. *Acta Cryst. C51* **1995**, 1864. (e) Teixidor, F.; Viñas, C.; Abad, M. M.; Núñez, R.; Kivekäs, R.; Sillanpää, R. *J. Organomet. Chem.* **1995**, *503*, 193. (f) Kivekäs, R.; Sillanpää, R.; Teixidor, F.; Viñas, C.; Núñez, R. *Acta Cryst. C50* **1994**, 2027. (g) Sillanpää, R.; Kivekäs, R.; Teixidor, F.; Viñas, C.; Núñez, R. *Acta Cryst. C52* **1996**, 2223.

(2) (a) Viñas, C.; Abad, M. M.; Teixidor, F.; Sillanpää, R.; Kivekäs, R. *J. Organomet. Chem.* **1998**, *555*, 17. (b) Teixidor, F.; Viñas, C.; Abad, M. M.; Kivekäs, R.; Sillanpää, R. *J. Organomet. Chem.* **1996**, *509*, 139. (c) Kivekäs, R.; Sillanpää, R.; Teixidor, F.; Viñas, C.; Abad, M. M. *Acta Chem. Scand.* **1996**, *50*, 499.

(3) (a) Teixidor, F.; Viñas, C.; Benakki, R.; Kivekäs, R.; Sillanpää, R. *Inorg. Chem.* **1997**, *36*, 1719. (b) Viñas, C.; Cirera, M. R.; Teixidor, F.; Kivekäs, R.; Sillanpää, R.; Llibre, J. *Inorg. Chem.* **1998**, *37*, 6746. (c) Teixidor, F.; Rius, J.; Romerosa, A. M.; Miravitlles, C.; Escriche, L.; Sánchez, E.; Viñas, C.; Casabó, J. *Inorg. Chim. Acta* **1990**, *176*, 287. (d) Teixidor, F.; Viñas, C.; Casabó, J.; Romerosa, A. M.; Rius, J.; Miravitlles, C. *Organometallics* **1994**, *139*,14.

(4) (a) Teixidor, F.; Romerosa, A. M.; Rius, J.; Miravitlles, C.; Casabó, J.; Viñas, C.; Sánchez, E. *J. Chem. Soc., Dalton Trans.* **1990**, 525. (b) Teixidor, F.; Viñas, C.; Sillanpää, R.; Kivekäs, R.; Casabó, J. *Inorg. Chem.* **1994**, *33*, 2645. (c) Viñas, C.; Cirera, M. R.; Teixidor, F.; Sillanpää, R.; Kivekäs, R. *J. Organomet. Chem.* **1997**, *530*, 89.

(5) Teixidor, F.; Núñez, R.; Viñas, C.; Sillanpää, R.; Kivekäs, R. *Angew. Chem. Int. Ed.* **2000**, *39*, 4290.

(6) (a) Van Leeuwen, P. W. N. M; Kamer, P. C. J.; Reek, J. N. H.; Dierkes, P. *Chem. Rev.* **2000**, *100*, 2741. (b) Ittel, S. D.; Johnson, L. K.; Brookhart, M. *Chem. Rev.* **2000**, *100* 1169. (c) Issleib, K.; Müller, D. *Chem. Ber.* **1959**, *92*, 3175.

(7) (a) Teixidor, F.; Viñas, C.; Abad, M. M.; López, M.; Casabó, J. *Organometallics* **1993**, *12*, 3766. (b) Teixidor, F.; Viñas, C.; Abad, M. M.; Kivekäs, R.; Sillanpää, R. *J. Organomet. Chem.* **1996**, *509*, 139. (c) Kivekäs, R.; Sillanpää, R.; Teixidor, F.; Viñas, C.; Abad, M. M. *Acta Chem. Scand.* **1996**, *50*, 499. (d) Teixidor, F.; Viñas, C.; Abad, M. M.; Whitaker, C.; Rius, J. *Organometallics* **1996**, *15/14*, 3154. (e) Viñas, C.; Abad, M. M.; Teixidor, F.; Sillanpää, R.; Kivekas, R. *J. Organomet. Chem.* **1998**, *555*, 17. (f) Núñez, R.; Viñas, C.; Teixidor, F.; Abad M. M. *Appl. Organomet. Chem.* **2003**, *17*, 509. (g) Paavola, S.; Kivekäs, R.; Teixidor, F.; Viñas, C. *J. Organomet. Chem.* **2000**, *606*, 183. (h) Paavola, S.; Teixidor, F.; Viñas, C.; Kivekäs, R. *J. Organomet. Chem.* **2002**, *645*, 39. (i) Paavola, S.; Teixidor, F.; Viñas, C.; Kivekäs. R. *J. Organomet. Chem.* **2002**, *657*, 187.

(8) (a) Berners-Price, S. J.; Mirabelli, C. K.; Johnson, R. K.; Mattern, M. R.; McCabe, F. L.; Faucette, L. F.; Sung, C.-M-; Mong, S.-M.; Sadler, P. J.; Crooke, S. T. *Cancer Research* **1986**, *46*, 5486. (b) Johnson, R. K.; Mirabelli, C. K.; Faucette, L. F.; McCabe, F. L.; Sutton, B. M.; Bryan, D. L.; Girad, G. R.; Hill, D. T. *Proc. Amer. Assoc, Cancer Res.* **1985**, *26*, 254.

(9) (a) Buckler, S. A. *J. Am. Chem. Soc.* **1962**, *84*, 3093. (b) Floyd, M. B.; Boozer, C. E. *J. Am. Chem. Soc.* **1963**, *85*, 984. (c) Ogata, Y.; Yamashita, M. *J. Chem. Soc., Perkin Trans II* **1972**, 730.

(10) Malone, J. F.; Marrs, D. J.; Mckervey, M. A.; O'Hagan, P.; Thompson, N.; Walker, A.; Arnaud-Neu, F.; Mauprivez, O.; Schwing-Weill, M. J.; Dozol, J. F.; Rouquette, H.; Simon, N. *J. Chem. Soc., Chem. Commun.* **1995**, 2151.

(11) M. Abad, Doctoral thesys, UAB **1995**.

(12) (a) Wiesboeck, R. A.; Hawthorne, M. F. *J. Am. Chem. Soc.* **1964**, *86*, 1642. (b) Garret, P. M.; Tebbe, F. N.; Hawthorne, M. F. *J. Am. Chem. Soc.* **1964**, *86*, 5016. (c) Hawthorne, M. F.; Young, D. C.; Garret, P. M.; Owen, D. A.; Schwerin, S. G.; Tebbe, F. N.; Wegner, P. M. *J. Am. Chem Soc.* **1968**, *90*, 862.

(13) Zakharkin, L. I.; Kalinin, V. N. *Tetrahedron Letters* **1965**, 407.

(14) Viñas, C.; Núñez, R.; Rojo, I.; Teixidor, F.; Kivekäs, R.; Sillanpää, R. *Inorg. Chem.* **2001**, *14*, 3259.

(15) Peymann, T.; Herzog, A.; Knobler, C. B.; Hawthorne, M. F. *Angew. Chem. Int. Ed. Engl.* **1999**, *38*, 1062.

(16) Buchanan, J.; Hamilton, E. J. M.; Reed, D.; Welch, A. J. *J. Chem. Soc., Dalton Trans.* **1990**, 677.

(17) (a) M. Bown, J. Plesek, K. Base, B. Stibr *Mag. Reson, Chem.* **1989**, *27*, 947. (b) X. L. R. Fontaine, N. N. Greenwood, J. D. Kennedy, K. Nestor, M. Thornton-Pett *J. Chem. Soc., Dalton Trans.* **1990**, 681. (c) G. G. Hlatlky, R. R. Eckman, H. W. Turner *Organometallics* **1992**, *11*, 1413. (d) R. Uhrhammer, Y. S. Su, D. C. Swenson, R. F. Jordan *Inorg. Chem.*, **1994**, *33*, 43978.

(18) (a) Dewar, M.J.S.; Jones, R., *J. Amer. Chem. Soc.* **1967**, *89*, 4251. (b) H. Nöth, B. Wrackmeyer, *Magnetic Nuclear Resonance Spectroscopy of Boron Compounds*. Ed. P. Diehl, E. Fluck, R. Kosfeld. Spring-Verlag, Berlin heildelberg **1978**.

(19) Wanda, M.; Higashizaki, S.; Tsuboi, A. *J. Chem. Research* **1985**, 38.

(20) Alexander R.P., Schroeder H. A.: *Inorg. Chem.* **1963**, *2*, 1107.